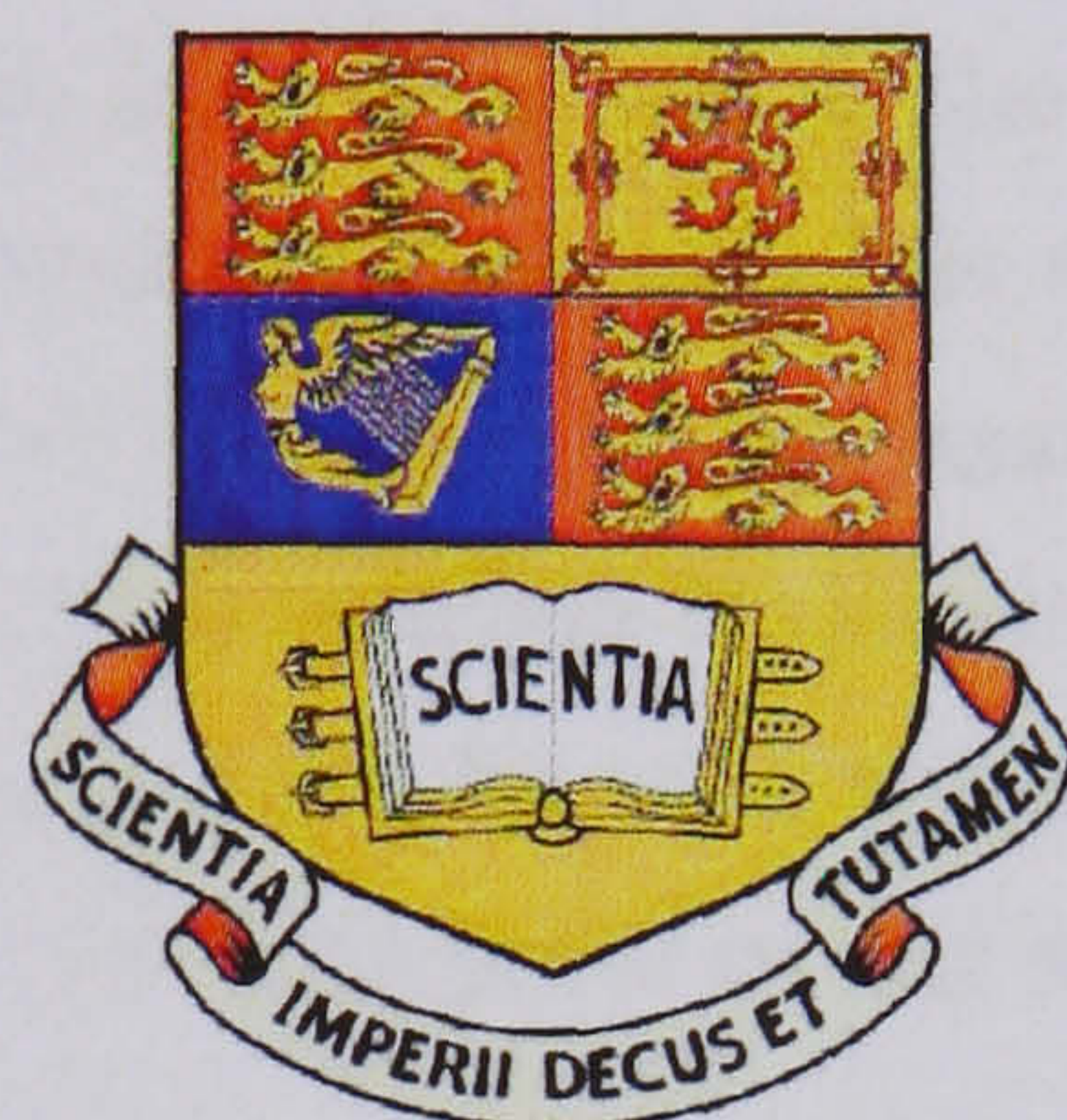


Network analysis of complex biological systems: Boundedness of weakly reversible chemical reaction networks and conditions for synchronisation of coupled oscillators



Elias August

Supervisor: Mauricio Barahona
Department of Bioengineering
Imperial College
University of London

A thesis submitted in partial fulfillment of the requirements for the degree of
Doctor of Philosophy

October 2007

Abstract

The broad aim of this thesis is to systematically investigate the interdependence of dynamical behaviour and network architecture in biological networks that consist of interconnected nonlinear elements. We use a series of mathematical tools from graph theory, dynamical systems, Lyapunov stability theory and semi-definite programming to prove and implement our results.

In the first part, we use Chemical Reaction Network Theory to investigate how the structure of the un-weighted graph of the underlying reaction network influences the dynamical properties of the system. This theory does not rely on the values associated with the different reaction rates. In particular, we provide a proof that a weakly reversible chemical reaction network (that is, one in which the digraph of the reaction complexes is the union of strongly connected components) has a bounded absorbing set. Thus, by checking structural properties of the graph of the reaction network, this result provides a qualitative criterion to establish that solution trajectories of the dynamical system will not diverge. Moreover, this information can be used to characterise certain bifurcations from stationary to oscillatory behaviour. The proof of our result is based on Lyapunov stability theory and graph theory.

In the second part, we first establish sufficient conditions that guarantee entrainment of a dynamical system to a periodic drive. We then establish sufficient conditions that guarantee synchronised behaviour of networks of coupled biological oscillatory systems. We treat the cases when they are identical (complete synchronisation) and when there is parameter mismatch (frequency synchronisation). We reformulate previously established conditions which are based on Lyapunov stability theory and contraction theory in order to make them computationally implementable. To this end, we use semidefinite programming techniques and can not only obtain certificates for synchronisability but also optimise associated cost functions. Along these lines, we also establish new and less strict conditions for complete synchronisation based on the Bendixson's Criterion for higher dimensional systems. All conditions are obtained by analysing the connection network and the model of the individual biological system only.

We provide illustrative examples from physics, chemistry and biology for the applicability of our work. The examples include the van der Pol oscillator, simple biochemical systems, synthetic genetic oscillators like the Repressilator, and models of the circadian clock.

Contents

1	Introduction	12
1.1	Motivation	13
1.2	Organisation of the thesis	21
1.3	Original contribution	23
2	Chemical reaction network theory	25
2.1	Chemical reaction networks obeying mass action kinetics	25
2.2	Martin Feinberg's chemical reaction network theory	31
2.3	Chemical reaction networks under dimensionally-restricted conditions	39
2.4	Boundedness of weakly reversible chemical reaction networks	42
2.4.1	Examples from biology and chemistry	48
2.5	Conclusion	55
3	Positivity conditions related to the stability of a dynamical system and their computational implementation	57
3.1	Dynamical systems with a certain contraction property	57
3.2	Bendixson's Criterion for higher dimensions	63
3.3	Interior-point methods and semidefinite programming	65
3.3.1	The Newton method	66
3.3.2	Interior-point methods	68
3.3.3	Semidefinite programming	72
3.4	The sum of squares decomposition	73
4	Finding invariant sets and proving exponential stability of limit cycles using sum of squares decompositions	76

4.1	Invariant sets	76
4.2	Finding invariant sets	78
4.3	Applications	79
4.4	Proving exponential stability of limit cycles	88
4.4.1	Application to the van der Pol oscillator	90
4.5	Conclusion	92
5	Entrainment and synchronisation of biological systems	93
5.1	Conditions for the entrainment of a dynamical system	95
5.1.1	A gene regulation model	95
5.1.2	A pacemaker model	99
5.2	Global complete synchronisation of identical oscillators with symmetric but otherwise arbitrary coupling	101
5.2.1	The master stability function	103
5.2.2	Sufficient conditions for global complete synchronisation of identical oscillators	104
5.2.3	Computational methods to obtain certificates for global complete synchronisation with applications	110
5.3	Constructing an observer	118
5.4	Frequency synchronisation of coupled nonidentical oscillators	120
5.5	Incomplete synchronisation of coupled identical oscillators	126
5.6	Global complete synchronisation of identical oscillators with all-to-all coupling	128
5.6.1	Sufficient conditions based on contraction theory	128
5.6.2	Sufficient conditions based on the Bendixson's Criterion for higher dimensions	133
5.7	Conclusion	137
6	Conclusions	139
6.1	Summary	139
6.2	Discussion and future research	141
A		143
B		146

List of Figures

1.1	Approaches to the mathematical modelling of biological networks.	14
1.2	The typical structure of an eukaryotic cells containing organelles.	16
1.3	Obstacles to small-molecule mixing and the volume exclusion effect.	17
1.4	Synchronisation and entrainment of biological systems.	18
1.5	The circadian clock.	20
2.1	The law of mass action.	26
2.2	Michaelis-Menten reaction.	28
2.3	A sample mass action system.	30
2.4	A model of the EnvZ/OmpR two-component circuit.	35
2.5	Manifestations of power-law kinetics.	39
2.6	A kinetic proofreading scheme.	42
2.7	Ultimately bounded system.	43
2.8	A sample mass action system.	49
2.9	Active membrane transport model.	50
2.10	Two valid chemical reaction network representations of (2.32). . .	53
2.11	A chemical oscillator.	54
2.12	Time series and limit cycle of (2.33).	55
3.1	A sufficient condition for two trajectories to approach each other.	62
3.2	The logarithmic barrier function.	70
3.3	Dimension of matrix Q as a function of the number of variables and degree of the polynomial.	75
4.1	The Lorenz attractor.	77
4.2	Finding invariant sets.	79

4.3	Solution trajectory of the van der Pol oscillator in \mathcal{B}	84
4.4	Regions of attractions for the equilibrium points of a neocortical model.	87
4.5	Two invariant sets for the Lorenz system.	88
4.6	The L_M Landscape.	92
5.1	Schematic control system for the production of an enzyme.	96
5.2	Gene regulatory system with external forcing I.	97
5.3	Gene regulatory system with external forcing II.	99
5.4	The van der Pol oscillator with an external drive.	101
5.5	A network of coupled oscillators.	102
5.6	Four different coupling configurations.	109
5.7	Two coupled identical Lorenz systems.	114
5.8	The Repressilator.	115
5.9	Two coupled identical Repressilator.	117
5.10	A schematic view of an observer.	118
5.11	Estimation error.	120
5.12	Two coupled nonidentical van der Pol oscillators.	122
5.13	Repressilator network.	123
5.14	Ten coupled nonidentical Repressilators.	125
5.15	Two coupled identical van der Pol oscillators.	132
5.16	Two coupled identical biological oscillators.	136

List of Tables

5.1	Coupling cost depending on configuration.	109
5.2	Comparison of values of κ^* obtained with and without the application of semidefinite programming.	114
5.3	Incomplete synchronisation.	127
5.4	Comparison between the different approaches to obtain the minimal value of κ that guarantees complete synchronisation.	137

Acknowledgements

I would like to express deep gratitude to my supervisor Mauricio Barahona for giving me the opportunity to work as a research assistant at Imperial College London on an EPSRC funded project. I am thankful to him and to Kim Parker for their academic and personal support. I would also like to thank J. Krishnan and particularly Ali Jadbabaie, who works in the United States, for agreeing to be my thesis examiners. While at Imperial, I benefited socially and intellectually from interaction with my fellow graduate students Martin Hemberg, Jazmin Aguado, Kathryn Cooper, and especially Fernando Montani. I also want to thank my parents for their constant support, encouragement and love, and my sister for the good times. My father made sure I will not have two left hands, my mother that I study English and both that I read books and never magazines. I dedicate this thesis to my parents, to my grandmother, my late grandfather and Ricardo, to them for giving me sweets and warmth, and to Juliane, who knows why.

Notation

$\mathbb{R}, \mathbb{R}^{m \times n}$	real numbers, $m \times n$ real matrices
x_i	i th entry of vector $x \in \mathbb{R}^n$
e	$[1, \dots, 1]^T$
E	the positive matrix: ee^T
$A_{(i,j)}$	(i, j) th entry of matrix $A \in \mathbb{R}^{m \times n}$
$A \geq \geq 0$ ($A \gg 0$)	$A_{(i,j)} \geq 0$ ($A_{(i,j)} > 0$) for all i and j
$A \geq 0$ ($A > 0$)	nonnegative (positive) definite matrix
$\mathbb{R}_+^n, \overline{\mathbb{R}}_+^n$	$\{x \in \mathbb{R}^n : x \gg 0\}, \{x \in \mathbb{R}^n : x \geq \geq 0\}$
$\text{rank}(A)$	rank of matrix $A \in \mathbb{R}^{m \times n}$
$\dim A$	dimension of matrix $A \in \mathbb{R}^{n \times n}$; that is, $\dim A = n$
I (I_n)	the identity matrix (of dimension n)
$\text{diag}(A), A \in \mathbb{R}^{n \times n}$	a vector of length n , where $\text{diag}(A)_i = A_{(i,i)}$
$\text{diag}(x), x \in \mathbb{R}^n$	a matrix $\in \mathbb{R}^{n \times n}$, where $\text{diag}(x)_{(i,i)} = x_i$ and $\text{diag}(x)_{(i,j \neq i)} = 0$
A^T	transpose of $A \in \mathbb{R}^{m \times n}$
$\mathcal{N}(A)$	null space of $A \in \mathbb{R}^{m \times n}$
\dot{x}	derivative of x with respect to the time variable t
$A \otimes B, A \in \mathbb{C}^{m \times n}, B \in \mathbb{C}^{p \times q}$	The Kronecker product: $\begin{bmatrix} A_{(1,1)}B & A_{(1,2)}B & \cdots & A_{(1,n)}B \\ A_{(2,1)}B & A_{(2,2)}B & \cdots & A_{(2,n)}B \\ \vdots & \vdots & & \vdots \\ A_{(m,1)}B & A_{(m,2)}B & \cdots & A_{(m,n)}B \end{bmatrix}$
$\nabla f(x)$	del operator: $[\frac{\partial f(x)}{\partial x_1} \ \dots \ \frac{\partial f(x)}{\partial x_n}]^T, x \in \mathbb{R}^n, f : \mathbb{R}^n \rightarrow \mathbb{R}$

Some mathematical definitions

set	A set is a finite or infinite collection of objects. $\alpha \in \mathcal{A}$ denotes that α is an element of a set \mathcal{A} .
subset	A subset is a portion of a set.
intersection	The intersection of two sets \mathcal{A} and \mathcal{B} is the set of elements common to \mathcal{A} and \mathcal{B} .
union	The union of two sets \mathcal{A} and \mathcal{B} is the set obtained by combining the members of each.
empty set	A set containing no elements.
open set	An open set of radius $r > 0$ and centre x_0 is the set of all points x such that $ x - x_0 < r$.
complement set	The subset \mathcal{F}' of some set \mathcal{S} which excludes a given subset \mathcal{F} .
closed set	A set \mathcal{S} is closed if the complement of \mathcal{S} is an open set.
set closure	The unique smallest closed set containing the given set, or the complement of the interior of the complement of the set.
connected set	A connected set is a set which cannot be partitioned into two nonempty open subsets.
simply connected	A path-connected domain is said to be simply connected if any simple closed curve can be shrunk to a point continuously in the set.

boundary The set of points, denoted by $\partial\mathcal{S}$, known as boundary points, which are members of the set closure of a given set \mathcal{S} and the set closure of its complement set.

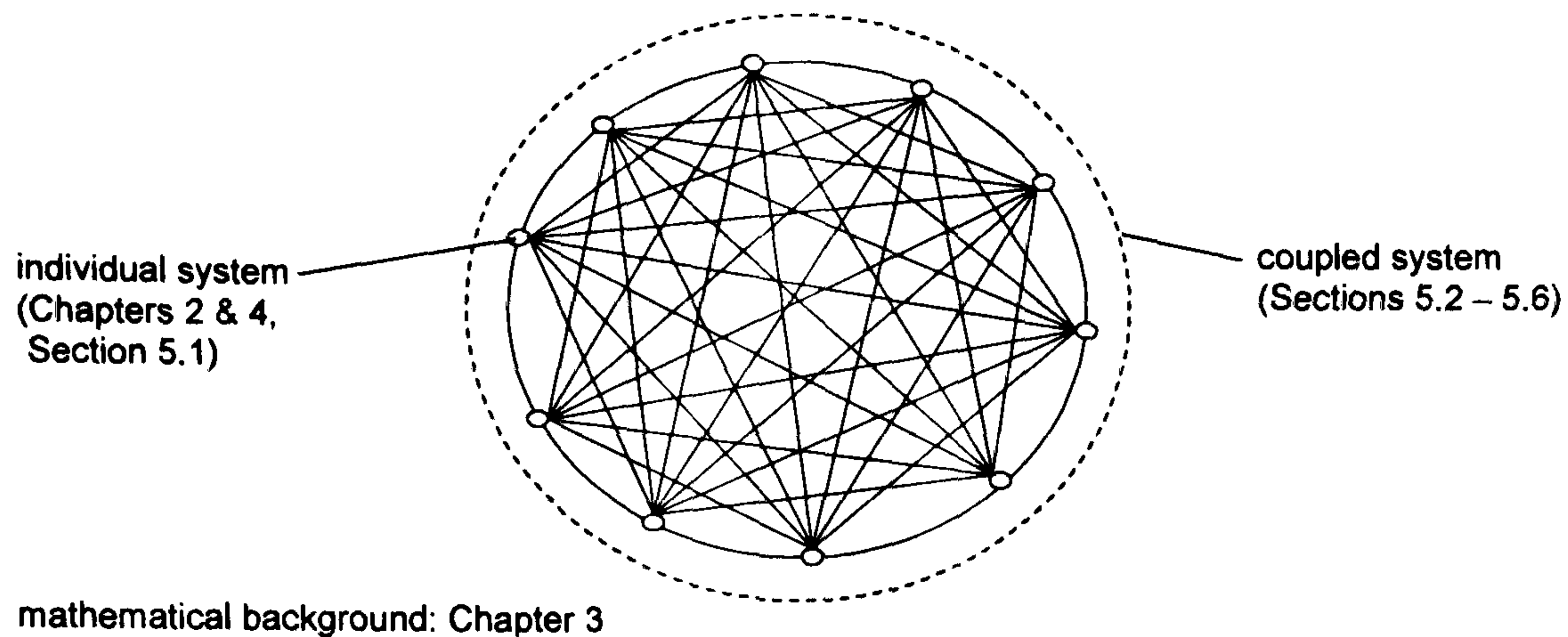
compact set Compact sets are closed and bounded.

Chapter 1

Introduction

The broad aim of this thesis is to systematically investigate the interdependence of dynamical behaviour and network architecture in biological networks that consist of interconnected nonlinear elements. On two levels, we seek to explain the behaviour of large and complex *biological systems* through the underlying network structure. First, we consider *Chemical Reaction Networks*. We investigate the unweighted graph underlying the network. We recapitulate previous important results by Martin Feinberg and establish new results on how the network structure governs the dynamical behaviour of the system; that is, independently of the values associated with the different reaction rates. Second, we establish mathematical conditions that guarantee synchronised behaviour (of a large number) of coupled biological system that are either identical or with parameter mismatch. The conditions are obtained by analysing the connection network and the model of the individual biological system only. (Additionally, we provide tools to investigate existence and stability of periodic behaviour of the individual system.)

One unifying goal in the work presented here is that we provide means to identify robustness of a biological system to changes in parameters; that is, in this thesis, we establish parameter ranges, in which a system is guaranteed to have bounded solution trajectories, to entrain to external periodic drives or, when consisting of coupled subsystems, to exhibit synchronised behaviour. The following diagram summarises the relationship of the different chapters:



1.1 Motivation

Recent years have seen the application of mathematical modelling to an increasing number of problems in the biological and medical sciences [1–4]. A mathematical model can represent an ecosystem, an organ, a cell, or the kinetic reaction between molecules. In short, it is a simplified representation of a biological system. A biological system has to be simplified because even the ‘simplest’ building block of higher organisms, the cell, is so highly complex that we will have to wait for many years before a complete description might be available. Furthermore, not only is the interaction within and between cells complex but also many interactions between proteins, lipids, and enzymes are not well known or understood. However, mathematical models can provide useful insights into the dynamics of biological systems and guide the scientists who might be overwhelmed by the complexity of their research objects. Many of these processes involve crosstalk and feedback loops generating complex networks rather than simple linear pathways. Dynamical system theory and graph theory are powerful tools for the analysis of such systems [5–7].

Biology with no parameters

In his 2001 paper (see reference [8]), the late James E. Bailey, Professor at the Institute of Biotechnology, ETH Zurich, stressed that in the field of modelling biological systems very often parameter values are unattainable. On the other hand, he acknowledged that for certain types of biological systems, and their mathematical counterparts, many results are available through analysis methods that do not require information on the quantitative values of system parameters [8]. Clearly, these results have a certain robustness associated with them which can greatly aid the task of model invalidation. The choice for many years

now has been to focus on the information obtainable from the structure of the *biological network*, which is an abstract representation of a biological system capturing many of its important characteristics [9–11]. For example, a typical biological network for an intracellular reaction scheme represents molecules by nodes, and their interactions by edges (or arrows). There are at least three major types of biological networks representing the processes within the cell: the protein-protein, the protein-DNA, and the protein-metabolite interaction networks [12]. However, this description remains a suppression of detail. For example, many different mechanisms of transcription regulation may be described by a single type of arrow. Figure 1.1 shows in increasing order of complexity (that is, from (a) to (c)) the relation between three elements $\{A, B, C\}$ of a biological network. Note that the representations and the corresponding mathematical models of the network in (a) and (b) do not require information on the quantitative values of parameters.

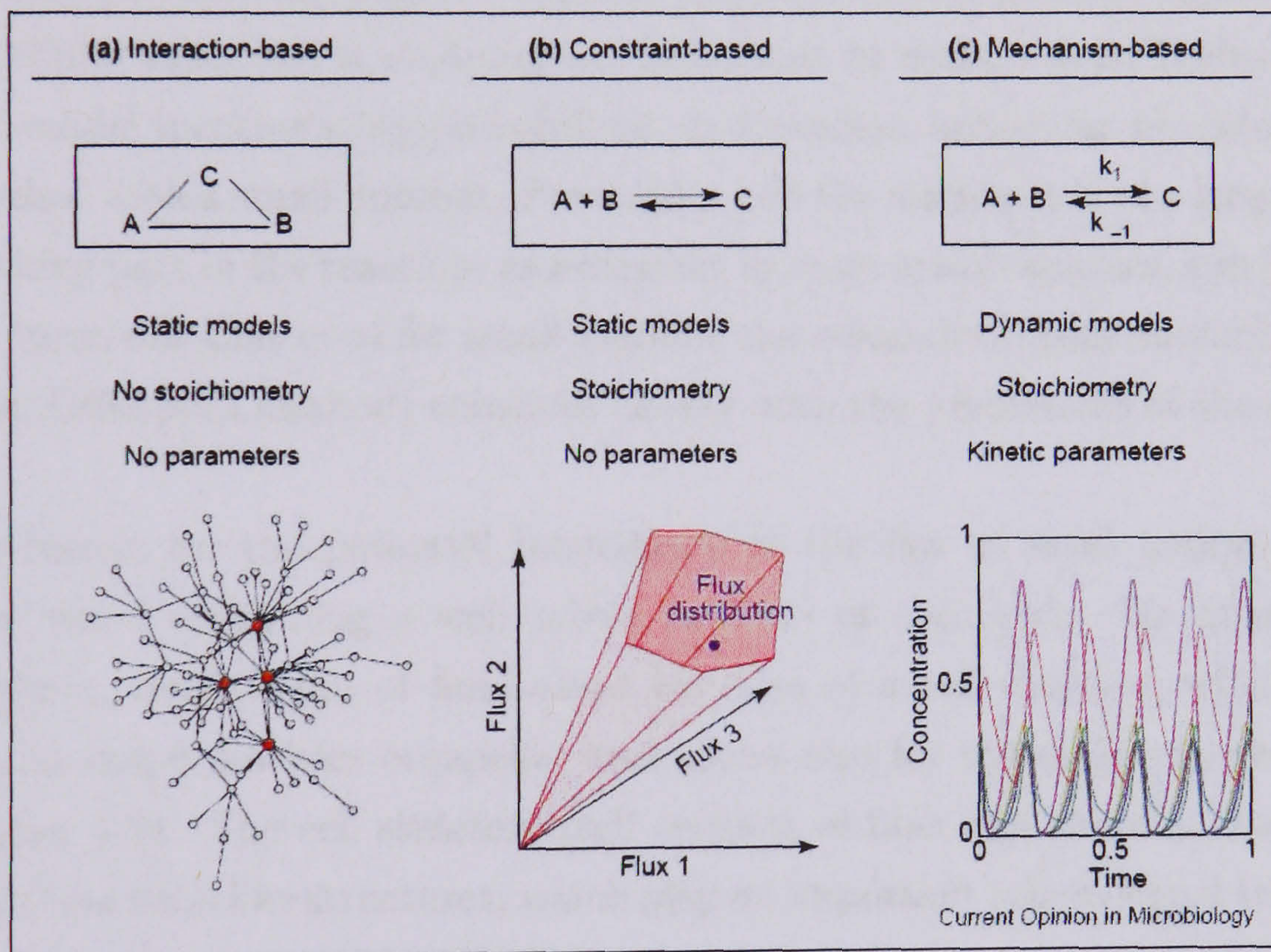


Figure 1.1: Approaches to the mathematical modelling of biological networks (taken from reference [13]). Mathematical models of biological networks can be based on (a) interactions, (b) constraints such as network topology and stoichiometries, or (c) reaction mechanisms.

Martin Feinberg's *Chemical Reaction Network Theory (CRNT)* investigates the be-

behaviour of biochemical models without requiring information about parameter values (reaction rates). It allows to derive statements directly from the network structure, which corresponds to a type (b) model analysis in Figure 1.1. Particularly, he has developed theorems that guarantee uniqueness and, under stronger assumptions, also stability of solutions (deficiency zero theorem). Martin Feinberg's results are for a specific class of nonlinear *ordinary differential equations (ODEs)* which describe the behaviour of chemical reactions in reactor vessels used in chemical engineering [9, 14]. These systems obey the *law of mass action*. The law of mass action assumes that if reactions take place at constant temperature in a homogenous and well mixed solution then the probability of a collision between molecules is proportional to the product of their concentrations. This assumption is probably less adequate in biology than it is in chemical engineering and it is therefore unclear to what extent CRNT is directly applicable to settings in biological systems. Nevertheless, for many reasons, it is widely used [15–17]. For instance, a more realistic approach to modelling intracellular reactions is studying the behaviour of molecules individually through a stochastic model incorporating probabilistic and random behaviour of molecules. This allows us to deal with a small number of reactants and the assumption of a large number of molecules taking part in the reaction, as necessary in mass action kinetics, can be dropped. However, it turns out that even for small systems the mean data from numerical methods (for example, Gillespie's method) coincides closely with the predictions of the law of mass action [18].

Another reason for the potential inadequacy of the law of mass action is that the cell is not a vessel containing a well mixed solution of chemicals. Its interior, the so called *cytoplasm*, consists not of fluid alone but also of a cell skeleton, which helps the cell to keep its shape, anchors organelles and allows also for molecule movements within the cell (Figure 1.2). The cell skeleton itself consists of fiber like proteins, some forming *microtubules*, tiny tube like structures, which play an important role in signal transduction.

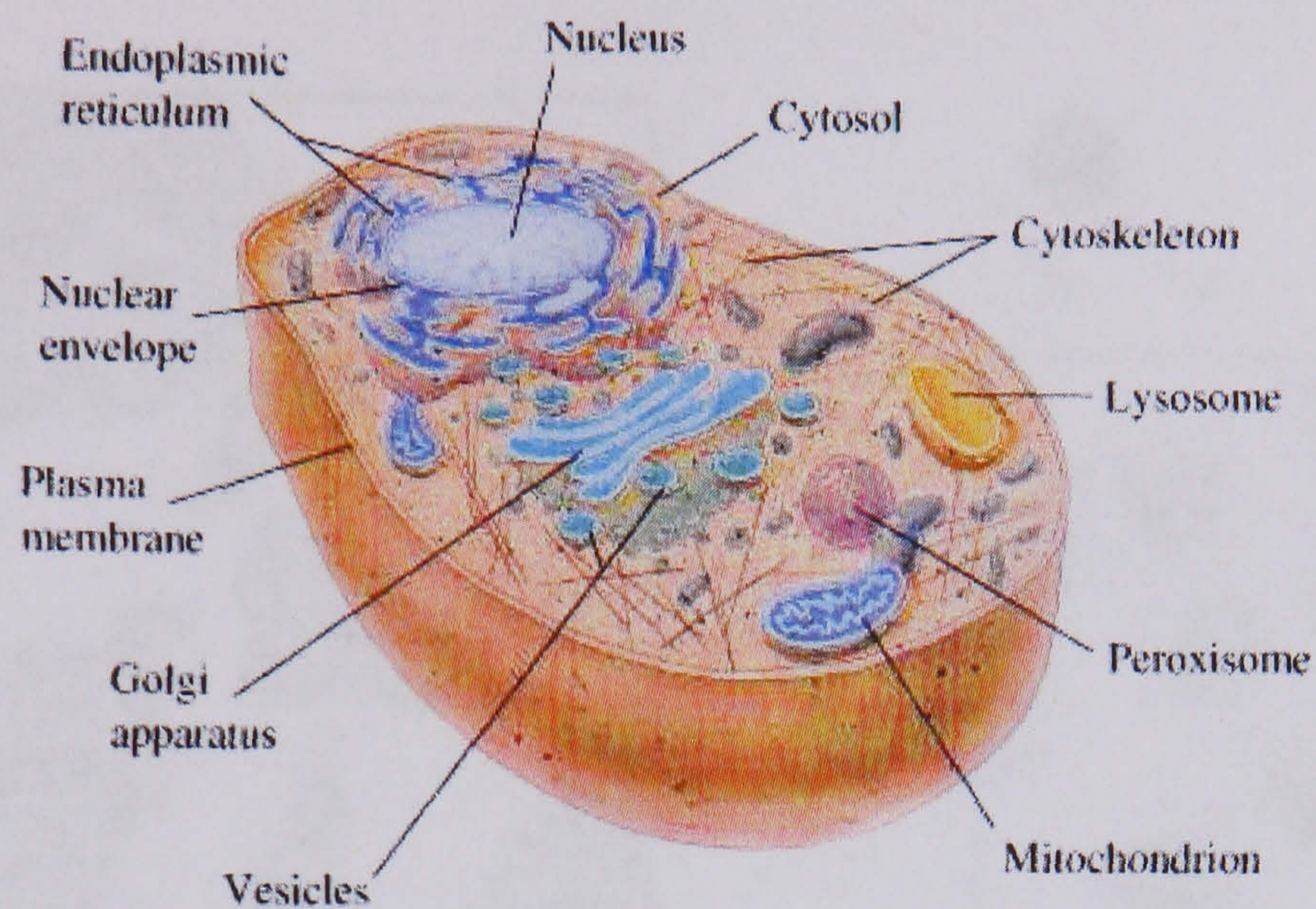


Figure 1.2: The typical structure of an eukaryotic cells containing organelles (taken from reference [19]).

Moreover, many vital reactions happen between extracellular ligands such as signal molecules and hormones and receptors on the membrane of the cell and between intracellular molecules and receptors on the membrane of organelles within the cell. Additionally, nutrients have to enter the cell by passing through the membrane and interact with structural proteins and lipids. In summary, the mixing of molecules can be often obstructed (Figure 1.3.a)).

Molecular reactions can also greatly depend on the availability of reaction volume. If a molecule, which participates in the reaction, is much smaller than the background molecules then they have no or only weak influence on the reaction rate as the molecule can freely diffuse between them. On the other hand, the diffusion of molecules of similar size would be greatly hindered. This effect is called the *volume exclusion effect* (Figure 1.3.b)).

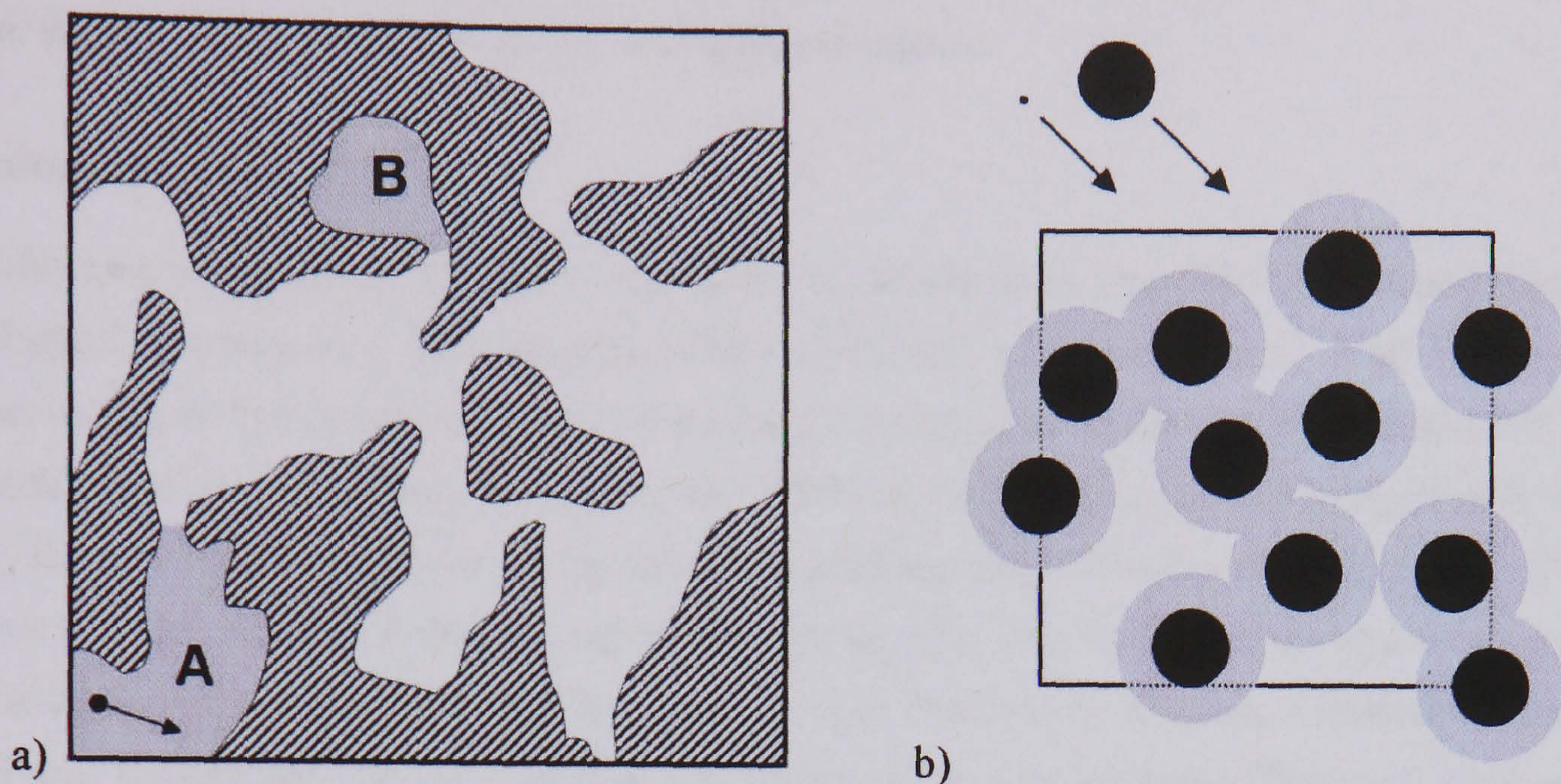


Figure 1.3: **Obstacles to small-molecule mixing and the volume exclusion effect (taken from reference [18]).** (a) Slow moving obstacles hinder the free movement of small molecules as, for example, molecules from region A might take along time to reach region B. (b) A small molecule can easily occupy the volume (white and gray areas) in between obstacles. The volume a molecule can occupy, whose size is of order of the obstacles, is greatly limited.

Michael A. Savageau developed a phenomenological approach to describe reactions following non-ideal kinetics in crowded environments such as the cell. It is called the *power-law approximation*. In Chapter 2 of this thesis, we first provide a theorem based on the network structure of the chemical reaction network that guarantees the uniqueness and local asymptotic stability of a positive equilibrium point for reactions under dimensionally-restricted conditions as experienced in the cellular environment. This theorem is related to Martin Feinberg's so called deficiency zero theorem, which requires the assumption of the mass action kinetics.

We then provide a proof that solution trajectories of the dynamical system representing certain chemical reaction networks will not diverge to infinity. It is based on the structural properties of the graph underlying the reaction network. Thus, this result provides a qualitative criterion to establish boundedness of solution. Moreover, the information can be used to characterise certain bifurcations from stationary to oscillatory behaviour (periodic,

quasi-periodic or chaotic). For the proof, we assume the law of mass action but conjecture that it also holds under the power-law approximation.

Biology in sync

In the last years much attention was given to research in the field of synchronisation of biological systems and their entrainment to external periodic inputs. The first reported observation of the synchronisation of coupled biological systems can be traced back to the Dutch physician Engelbert Kaempfer. In 1680, he visited Siam and described how a large population of fireflies slowly synchronised its flashing after it had settled on the branches of a tree (Figure 1.4.a)). A famous report on entrainment of a biological system to an external periodic input was given in 1729 by Jean-Jacques Dortous de Mairan, a French astronomer and mathematician. He noticed that the leaves of the haricot bean (Figure 1.4.b)) reacted to daylight changes by moving up during the day and down by night [20, 21].



Figure 1.4: Synchronisation and entrainment of biological systems (taken from references [22, 23]). (a) Synchronised flashing of fireflies in a tree in Malaysia [22]. (b) The haricot bean [23].

It was repeatedly shown that anticipating environmental changes has measurable fitness advantages for all organisms. Thus, many bodily functions in mammals are entrained

to the day-night cycle and achieve the anticipation of daily environmental changes through internal circadian clocks. This requires the synchronisation of the circadian clock of all cells [24, 25]. The lack of entrainment or synchronisation leads to loss of circadian rhythm (see Figure 1.5.a)). Individuals who suffer from ‘dys-entrainment’ of the circadian rhythm have an enhanced risk of errors and accidents at work, and of different health problems [24]. For example, this condition is common under shift worker, because of lack of entrainment to the diurnal cycle, and is also known to world travelers as the so called jet-lag. Quick recovery from jet-lag depends on the ability of body cells to synchronise their behaviour. Neurological defects can also lead to ‘dys-entrainment’, because of the lack of synchronisation between cells (see Figure 1.5.b)). Among the prokaryotes, cyanobacteria are the only ones known to follow a circadian rhythm. Importantly, they constitute a simple living model to study the circadian clock [26]. During the late 1970s and 1980s, it was discovered that the high sea environment is dominated by single-celled cyanobacteria [27]. For a long time, whether adaptation to the night and day cycle has any benefits to cyanobacteria remained unidentified. In 1998, it was shown that in a mixture of different mutants, the cyanobacteria strain whose clock period was closest to the artificially applied light and dark cycle performed best [28]. One aim of this thesis is to establish conditions that guarantee entrainment and synchronisation in a mathematical model of coupled biological oscillators. Providing certificates for entrainment and synchronisation, which depend on the different reaction rates in a biochemical system, could help to specify those rates to target through medication in cases of circadian ‘dys-entrainment’.

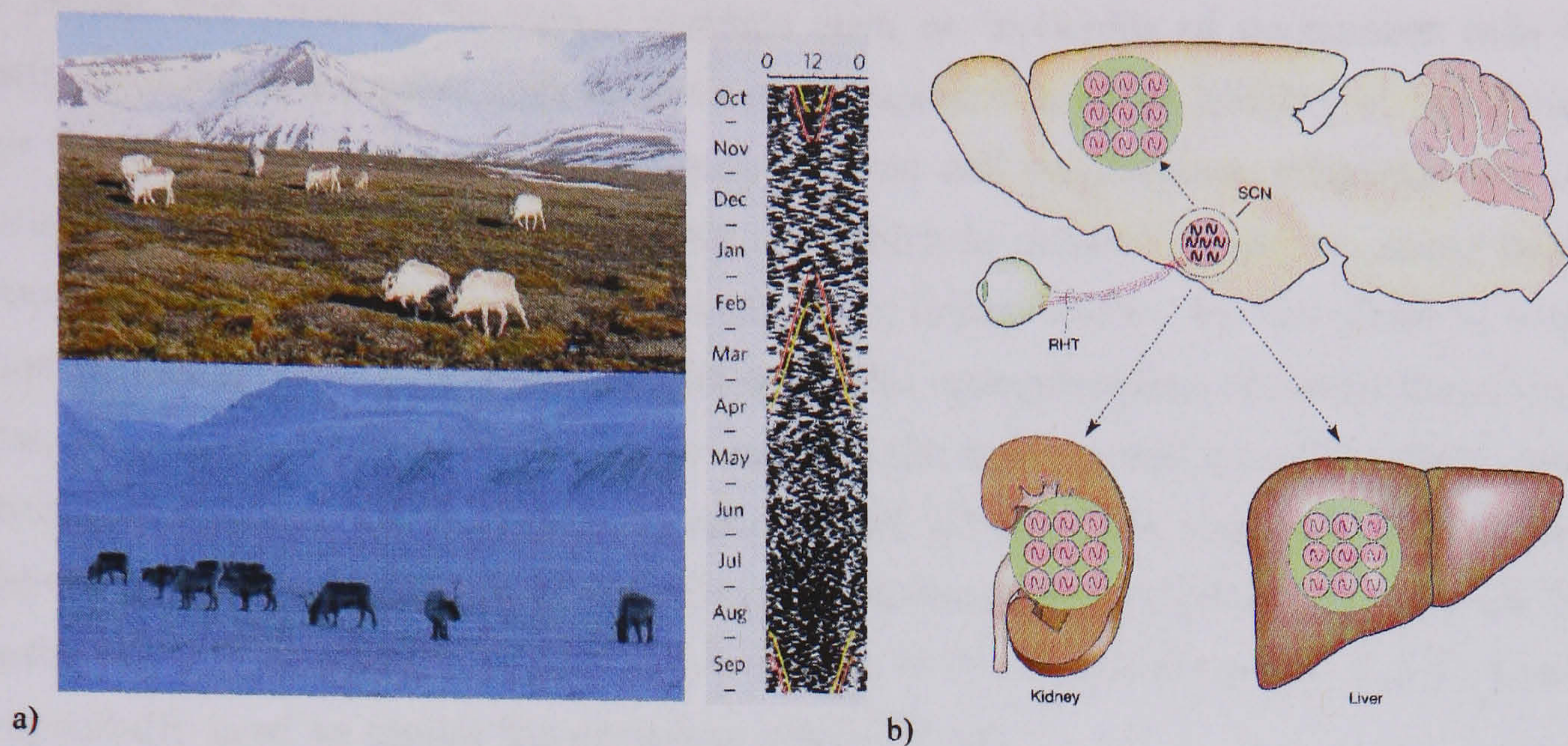


Figure 1.5: **The circadian clock** (taken from references [25, 29]). (a) Small data-loggers recorded activity pattern in reindeer on Svalbard, Norway, for the duration of one year. Each row in the actograms represents one day. Black dots indicate activity while inactivity is shown through white spaces [29]. The circadian rhythm is clearly lost during the months when both the polar day and the polar night are advancing. (b) Light entrains the master clock in the SCN. It is composed of many clock cells and is responsible for synchronising slave oscillators in other brain areas (for example, cortex) and in the organs (for example, kidney and liver) [25].

The circadian rhythm is not the only oscillator of physiological significance. An organ that shows constant periodicity is of course the heart. The normal cardiac rhythm is produced by the collective of many heart cells. Investigating conditions for synchrony between them is of major importance as it is believed that cardiac dysrhythmia, a life threatening heart disease, are caused by poor synchronisation between these autonomous pacemakers. A popular phenomenological model for the heartbeat is a system of coupled van der Pol oscillators. The choice is justifiable on the basis of the similarity with the qualitative features of the heart dynamics or ECG wave [30, 31]. Moreover, the model exhibits some relevant biological features such as complex periodicity and entrainment [30].

Another widely used mathematical model of coupled oscillators is the Kuramoto Model. In 1975, Yoshiki Kuramoto presented a model of coupled phase oscillators running at arbitrary individual frequencies. In his wonderful review paper on the Kuramoto model and the contributions to its analysis [32], Steven H. Strogatz makes the connection between

the model and different biological systems such as ‘networks of pacemaker cells in the heart; circadian pacemaker cells in the suprachiasmatic nucleus [(SCN)] of the brain [...] [(see Figure 1.5.b)]; metabolic synchrony in yeast cell suspensions; congregations of synchronously flashing fireflies; and crickets that chirp in unison’. However, many biological systems are not defined – or it is not suitable to define them – by the phase of a certain property and its time evolution but rather by the concentrations of substrates or species. Thus, in Chapter 5 of this thesis, we investigate the synchronisation of coupled dynamical systems which depart from the Kuramoto model [33–36]. We apply our results to three different and relevant models of biological for biochemical oscillators, the van der Pol oscillator [30], the Repressilator [37] and a variant of the Goodwin model [5, 38]. The latter is repeatedly used to model the circadian clock [39–41].

An important issue for our analysis is also finding invariants sets, because they decompose the state space into subsets whose boundaries trap solution trajectories. Thus, we can restrict our analysis to the dynamics in each invariant set. Moreover, often an analysis of the entire state space would not yield any result. In this thesis, we also show how the search for these sets can be implemented computationally.

1.2 Organisation of the thesis

In Chapter 2, we provide an overview on Martin Feinberg’s CRNT and his main theorems. Importantly, we extend his result and show the applicability of these novel results to systems in biology and biochemistry. In Section 2.1, we introduce chemical reaction networks which obey the law of mass action and in Section 2.2, Martin Feinberg’s CRNT. In section 2.3 and Section 2.4, we provide extensions to the theory. First, we consider reaction networks that do not obey the law of mass action and provide a deficiency-zero-like theorem for these networks. Second, we provide a result on the boundedness of solutions which depends only on the structure of the network and not on the deficiency. We demonstrate the applicability of our results with examples from biology and chemistry.

Chapter 3 gives the mathematical background necessary for the second part of the thesis. In Section 3.1, we give a brief literature review on results on dynamical systems with a certain contraction property. In Section 3.2, we present the so called Bendixson’s Criterion for higher dimensions. These results are based on extensions of Lyapunov theory and require positivity/negativity. They are a powerful framework for the analysis biological

systems, particularly, because they can be implemented computationally. To this end we use *semidefinite programming* and the *sum of squares decomposition*. Section 3.3 provides a brief introduction to both.

Chapter 4 consists of some preliminary applications of the results presented in Chapter 3. In Sections 4.1 – 4.3, we show how to obtain invariant sets of dynamical systems using semidefinite programming and the sum of squares decomposition. These results are important by themselves for the analysis of mathematical models in biology. However, we also use them in Chapter 5 in order to obtain lower bounds on the coupling strength that guarantees synchronisation of coupled systems. In Section 4.4, we computationally implement results by Peter Giesl [42–44] to prove existence, uniqueness and exponential stability of a limit cycle.

In Chapter 5, we use the results presented in the previous two chapters to obtain conditions for the entrainment (Section 5.1) of a dynamical system to an external input (for example, the heart driven by an external pacemaker) and for the synchronisation (Sections 5.2 – 5.6) of coupled dynamical systems (for example, coupled circadian clocks). Section 5.2.1 introduces Louis M. Pecora’s and Thomas L. Carroll’s *master stability function* which provides local results on the stability of the *completely synchronised* state of coupled identical oscillators [33]. Section 5.2.2 provides sufficient results for its global stability [34, 35, 45]. Certificates are hard to obtain; in a few instances, they can be obtained analytically. In this thesis, we show how they can be obtained computationally and how this can improve the bounds on the minimal coupling strength that guarantees synchronisation even for cases for which certificates were obtained analytically (Section 5.2.3 and Section 5.6.1). In Section 5.3, we draw connections between the synchronisation of dynamical systems and the construction of an observer. In Section 5.4, we extend the results on global *complete synchronisation* of coupled identical oscillators to *frequency synchronisation* of coupled nonidentical oscillators. In Section 5.5, we provide conditions that are weaker than the previous and that guarantee that the differences of solution trajectories between different oscillators remain small when they are coupled (*incomplete synchronisation*). In Section 5.6, we show that in the special case of a system of coupled identical oscillators with all-to-all coupling, it is possible to extend the results of Section 5.2. In Section 5.6.1, we provide a lemma which is equivalent to Theorem 5.2.3 but work also with a nonconstant matrix. We then extend this result to obtain conditions that guarantee global complete synchronisation for coupled identical discrete-time dynamical systems. In Section 5.6.2,

we provide novel sufficient conditions for global complete synchronisation of coupled identical oscillators as an alternative to the ones presented in Section 5.6.1. They are based on the so called Bendixson's Criterion for higher dimensions which we have presented in Section 3.2. They signify a move away from the, at times, strict requirements derived from contraction theory. This novel approach, which can be also implemented computationally via semidefinite programming, leads to major improvements on the lower bound of the coupling constant that guarantees global complete synchronisation. Furthermore, it is also applicable to systems which could not be analysed using the methods of Section 5.2. We show this through several examples that compare the two approaches. All sections are accompanied with examples from physics and biology. Finally, we draw conclusions and make suggestion for future research in Chapter 6.

1.3 Original contribution

Section 2.3 and Section 2.4 consist entirely of novel results that provide an extension of Martin Feinberg's CRNT and thus, of an analysis framework for chemical reaction networks which is independent of parameter values. First, we provide a deficiency-zero-like theorem for networks that do not obey the law of mass action. Second, we show that by checking structural properties of the graph of certain reaction networks, we can guarantee that they have a bounded absorbing set. This result provides a qualitative criterion, which is completely independent of reaction rate values and the deficiency of the network, to establish that a biochemical network will not diverge. Moreover, the result can also be used to characterise certain bifurcations from stationary to oscillatory behaviour.

In Section 4.2, we provide a technique to obtain invariant sets of dynamical systems using `SOSTOOLS`, a free `MATLAB` toolbox that checks for sum of square decompositions and is based on semidefinite programming. The existence and structure of invariant sets convey important information for the analysis of dynamical systems and thus, mathematical models of biological systems (Section 4.3). In Section 4.4, we reformulate Peter Giesl's results in [42–44] in order to make them computationally implementable. By doing so, we can prove existence, uniqueness and exponential stability of limit cycles (Section 4.4.1).

In Section 5.1, we propose an algorithm based on semidefinite programming that allows us to establish sufficient conditions under which a exponentially stable system will entrain to the external input. In Section 5.2.3 and Section 5.6.1, we show how to search

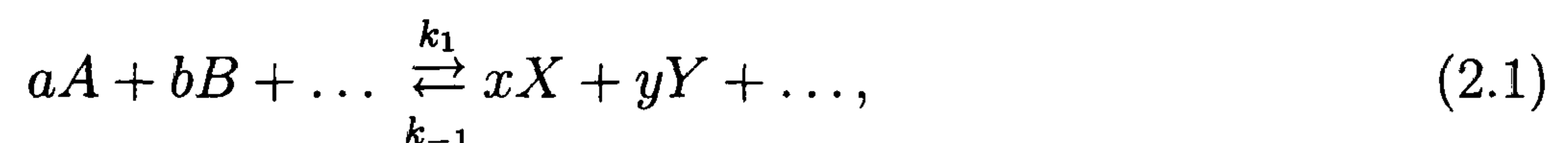
computationally, for the first time to our knowledge, for certificates for global complete synchronisation of coupled identical oscillators. We show the applicability of our technique through popular models of biological oscillators. We extend this approach to frequency synchronisation of coupled nonidentical oscillators in Section 5.4. The results of Section 5.6.2 consist of a novel approach to guarantee synchronisation of coupled oscillators. They are based on the so called Bendixson's criterion for higher dimensional dynamical systems. Their computational implementation shows that they can improve the results obtained in Section 5.6.1 tremendously.

Chapter 2

Chemical reaction network theory

2.1 Chemical reaction networks obeying mass action kinetics

Chemical reaction networks are used to describe and understand processes in biology and biochemistry. The general form for a chemical reaction is given by



where $[A]$, $[B]$, $[X]$, and $[Y]$ denote the concentrations of the chemicals or *species*: A , B , X and Y . The objects that appear before and after the reaction arrows in (2.1) are the so called *complexes*. Note that complexes are made up of species [46]. Furthermore, $k_1[A]^a[B]^b \dots$, and $k_{-1}[X]^x[Y]^y \dots$, are the *forward reaction rate* and *reverse reaction rate* respectively, where a , b , x , and y are the multiplicities (positive integers) of the respective chemicals, and k_1 and k_{-1} positive *rate constants*.

The law of mass action assumes that if reactions take place at constant temperature in a homogenous and well mixed solution (Figure 2.1) then the probability of a collision between molecules is proportional to the product of their concentrations. Now, consider the simple chemical reaction of the form



Then, it follows from the law of mass action that

$$\frac{d[C]}{dt} = k[A][B]. \quad (2.3)$$

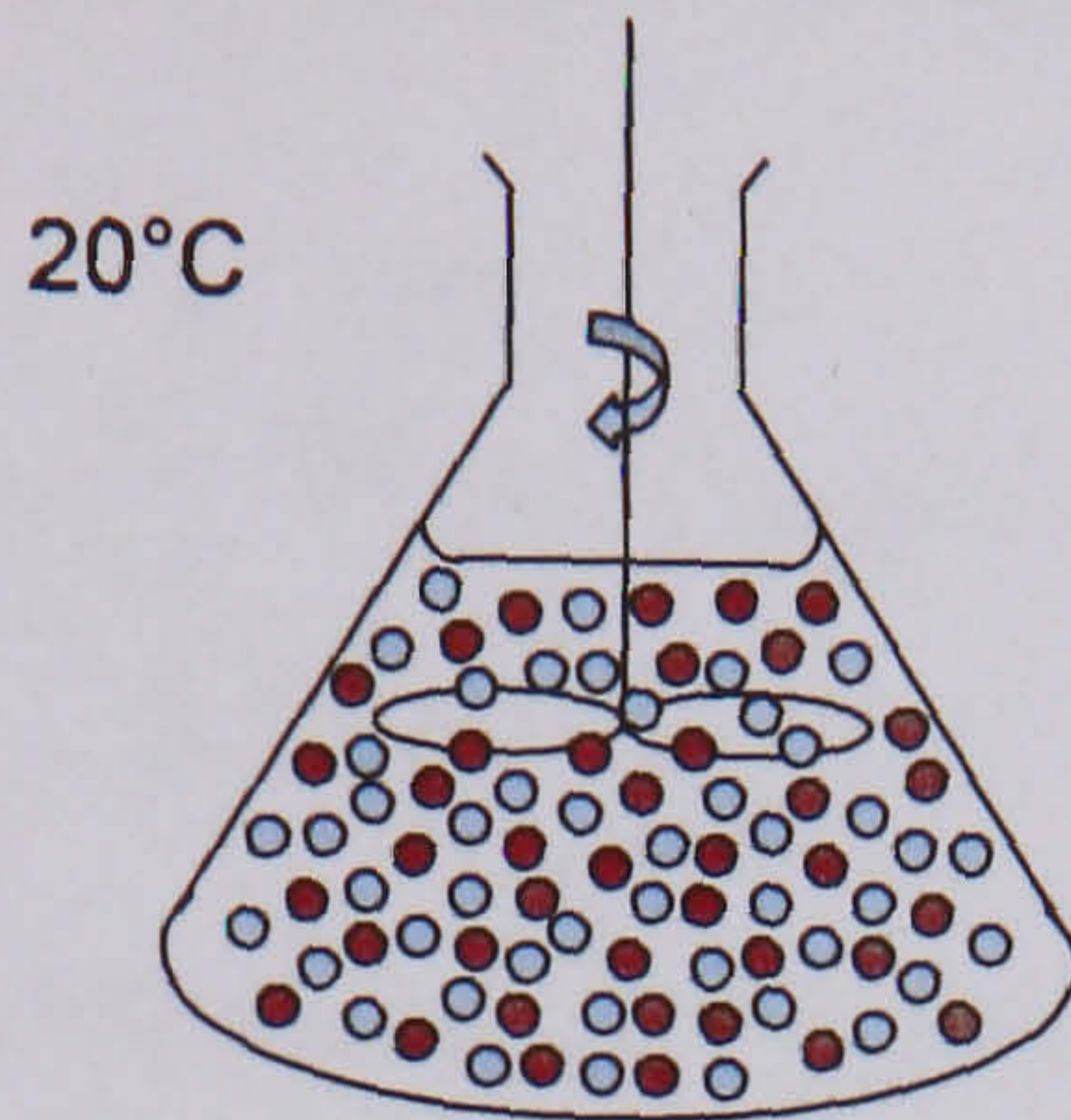


Figure 2.1: The law of mass action.

Moreover, chemical reactions do not proceed in one direction only and we have to include the reverse reactions. In this case, equation (2.2) becomes



and equation (2.3)

$$\frac{d[C]}{dt} = -k_-[C] + k_+[A][B]. \quad (2.5)$$

However, the reverse reaction could be so small that it can be considered negligible.

An illustrative example is the following reaction scheme proposed by Michaelis and Menten in the beginning of the last century for chemical reactions involving enzymes,



where S denotes the substrate, E the enzyme, P_1 the intermediate product formed by the reaction of S and E , and P_2 the final product. An enzyme is both a protein and catalyst. Most biological catalysts are enzymes. A catalyst is a molecule, whose function is to accelerate a chemical reaction (up to a billion times); that is, the particular reaction would occur even if the catalyst was not present but at a much slower rate. Furthermore, a catalyst is not altered by the reaction and can participate in subsequent reactions.

In the chemical reaction network given by (2.6), *edges* represent chemical reactions and *vertices* represent complexes. (In general, the symbol \emptyset represents the *null-complex*, which functions as a source and a sink for the system.) We denote the concentration vector of the different complexes by $\Psi(x)$, where x is the concentration vector of the different species.

For the Michaelis-Menten reaction, the vector of complexes and species are given by

$$\Psi(x) = \begin{bmatrix} [E][S] \\ [P_1] \\ [E][P_2] \end{bmatrix} \text{ and } x = \begin{bmatrix} [E] \\ [S] \\ [P_1] \\ [P_2] \end{bmatrix}$$

respectively ($[\cdot]$ denotes a concentration). Now, the so called *bookkeeping matrix* Y maps the space of complexes into the space of species. Its entries are nonnegative integers. The entries to the i th column of Y tell us in which complexes species i appears; or, equivalently, the entries to the j th row tell us of which species complex j is made of. For (2.6),

$$Y = \begin{bmatrix} 1 & 0 & 1 \\ 1 & 0 & 0 \\ 0 & 1 & 0 \\ 0 & 0 & 1 \end{bmatrix}.$$

Let $K \in \overline{\mathbb{R}}_+^m$ be the transpose of the *weighted adjacency matrix* of the weighted *digraph* representing the chemical reaction network. The entry $K_{(i,j)}$ corresponds to the rate constant associated with the reaction from complex j to i . Thus, for (2.6),

$$K = \begin{bmatrix} 0 & k_{-1} & 0 \\ k_1 & 0 & k_{-2} \\ 0 & k_2 & 0 \end{bmatrix}.$$

The transpose of the *weighted Laplacian matrix* is given by

$$L = \text{diag}(K^T e) - K,$$

where $e = [1, \dots, 1]^T$. The matrix $A_\kappa = -L$ is the so called the *kinetic matrix*. For (2.6),

$$A_\kappa = \begin{bmatrix} -k_1 & k_{-1} & 0 \\ k_1 & -(k_{-1} + k_2) & k_{-2} \\ 0 & k_2 & -k_{-2} \end{bmatrix}.$$

If we assume that the chemical system given by (2.6) obeys the law of mass action then its time evolution is given through the following set of nonlinear ODEs [16]:

$$\dot{x} = f(x) = Y A_\kappa \Psi(x), \quad \ln \Psi(x) = Y^T \ln x. \quad (2.7)$$

For clarity, we also provide the expanded ODE representation of the Michaelis-Menten reaction:

$$\begin{aligned}
 \dot{[E]} &= -k_1[E][S] + (k_{-1} + k_2)[P_1] - k_{-2}[E][P_2], \\
 \dot{[S]} &= -k_1[E][S] + k_{-1}[P_1], \\
 \dot{[P_1]} &= k_1[E][S] - (k_{-1} + k_2)[P_1] + k_{-2}[E][P_2], \\
 \dot{[P_2]} &= k_2[P_1] - k_{-2}[E][P_2].
 \end{aligned} \tag{2.8}$$

The figure below (Figure 2.2) depicts the time evolution of (2.8).

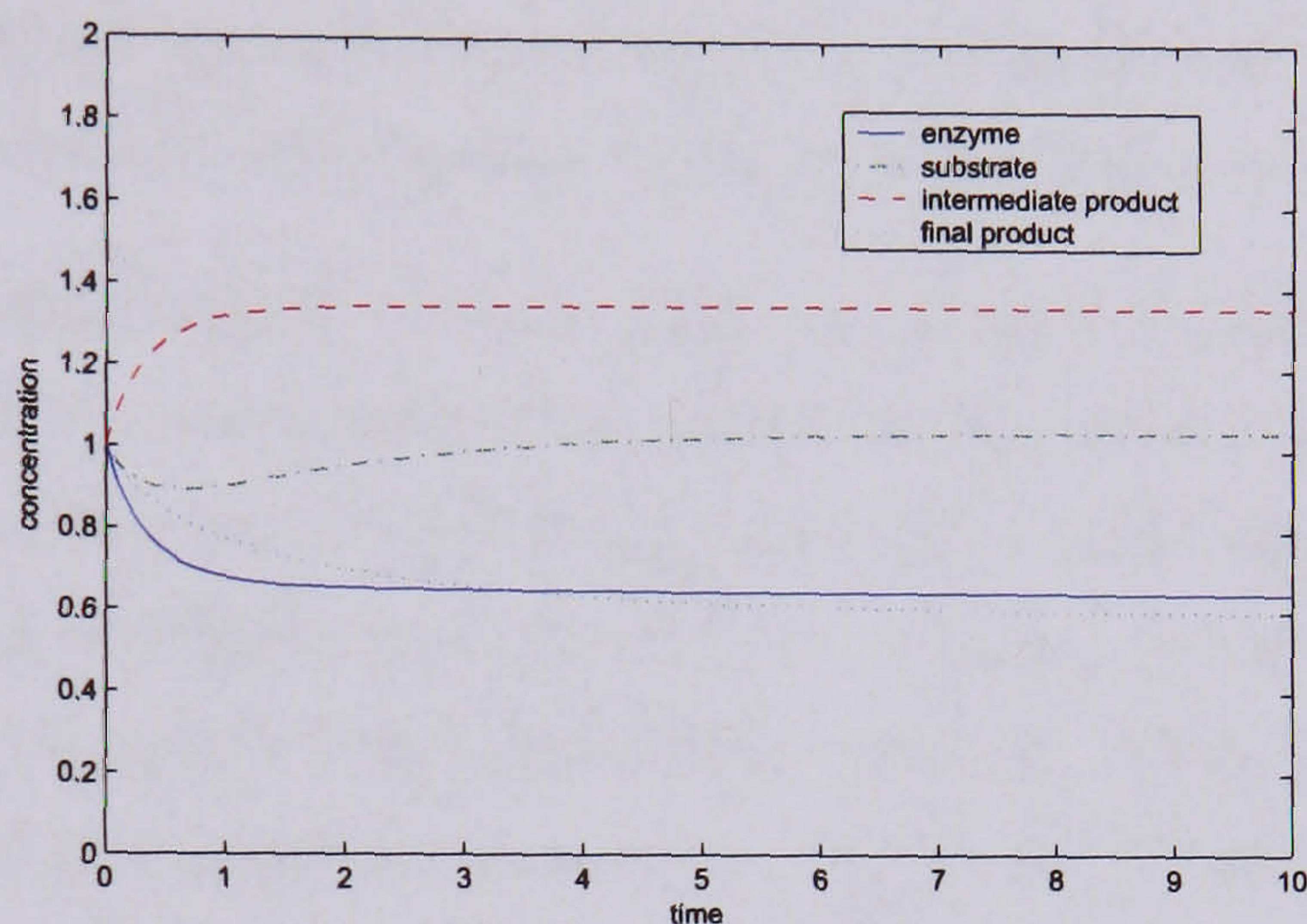


Figure 2.2: **Michaelis-Menten reaction.** The parameters have arbitrary concentration and time units and are $k_1 = 1$, $k_{-1} = 0.5$, $k_2 = 0.2$, and $k_{-2} = 0.7$.

In general, we assume that a chemical reaction network has n species and m complexes. Thus, in (2.7): $x \in \overline{\mathbb{R}}_+^n$, $\Psi(x) \in \overline{\mathbb{R}}_+^m$, $A_\kappa \in \mathbb{R}^{m \times m}$, and $Y \in \overline{\mathbb{R}}_+^{n \times m}$. In the following, we will highlight certain properties of (2.7), which we will exploit in order to prove the main theorem of this chapter (Theorem 2.4.3). Recall that

$$A_\kappa = K - \text{diag}(K^T e).$$

Let us denote $\text{diag}(K^T e)$ by D . Then, with $\sum_{l=1}^m K_{(l,j)} = D_{(j,j)}$, this leads to:

$$\dot{x}_i = \sum_{j=1}^m \Psi_j(x) \left(\sum_{l=1}^m Y_{(i,l)} K_{(l,j)} - Y_{(i,j)} D_{(j,j)} \right) = \sum_{j=1}^m \sum_{l=1}^m K_{(l,j)} \Psi_j(x) (Y_{(i,l)} - Y_{(i,j)}), \tag{2.9}$$

Let us denote the reaction rate of the reaction that transforms complex j into complex l by $k_{j \rightarrow l}$, $j, l = \{1, \dots, m\}$. Then, $K_{(l,j)} = k_{j \rightarrow l}$ (see [47]) and

$$\dot{x}_i = \sum_{\mathfrak{R}} k_{j \rightarrow l} \Psi_j(x) (Y_{(i,l)} - Y_{(i,j)}). \tag{2.10}$$

‘The symbol \mathfrak{R} denotes the set of reactions in the underlying network, and its presence under the summation sign is intended to indicate that the sum is taken over all reactions’ [9]. Note also that

$$\Psi_j(x) = \prod_{\wp=1}^n x_{\wp}^{Y_{(\wp,j)}}.$$

The following lemma introduces an important property of chemical reaction networks taken with mass action kinetics. It implies that we can restrict our analysis to the non-negative orthant, the space of realistic solution trajectories.

Lemma 2.1.1. *If a dynamical system represents a chemical reaction network, $\dot{x}_i|_{x_i=0} \geq 0$, $\forall i$. Then, solutions remain nonnegative if the initial conditions are nonnegative.*

Proof. The first statement follows directly from (2.7), since $x \in \overline{\mathbb{R}}_+^n$, $Y \in \overline{\mathbb{R}}_+^{n \times m}$ and the off-diagonal elements of A_{κ} are nonnegative, which implies that $\dot{x}_i|_{x_i=0} \geq 0$, $\forall i$. To prove the second statement, define $d(x, \overline{\mathbb{R}}_+^n) \triangleq \inf_{y \in \overline{\mathbb{R}}_+^n} \|x - y\|$, $x \in \mathbb{R}^n$. Since $\dot{x}_i|_{x_i=0} \geq 0$, $\forall i$, for every i such that $x_i = 0$, it follows that $x_i + hf_i(x) = hf_i(x) \geq 0$ for $h \geq 0$ while for every i such that $x_i > 0$, $x_i + hf_i(x) > 0$ for sufficiently small $|h|$. Thus, $x + hf(x) \in \overline{\mathbb{R}}_+^n$ for all sufficiently small $h > 0$ and hence $\lim_{h \rightarrow 0^+} d(x + hf(x), \overline{\mathbb{R}}_+^n)/h = 0$. It now follows from Theorem 4.1.26 of [48], with $x(0) = x$, that $x(t) \in \overline{\mathbb{R}}_+^n$ for all $t \geq 0$. \square

The following definitions of a *linkage class* and *weak reversibility* are central to CRNT.

Definition 2.1.2. A *linkage class* is a closed set of complexes that are linked through reactions. We denote the number of linkage classes by ℓ .

Remark 2.1.3. Note that Definition 2.1.2 implies that the linkage class of the chemical reaction network is what is called an *indecomposable* subgraph in graph theory. Furthermore, if $\ell > 1$ then A_{κ} can be block-diagonalised and each block-diagonal submatrix corresponds to a linkage class.

For example, the Michaelis-Menten reaction (2.6) has one linkage class ($\ell = 1$). The chemical reaction network in Figure 2.3 has three linkage classes ($\ell = 3$).

Definition 2.1.4. A chemical reaction network is *weakly reversible* if there is a directed reaction path from any complex to any other within the same linkage class.

Remark 2.1.5. Note that weak reversibility means that each indecomposable subgraph, G_{ℓ} , of the chemical reaction network is *strongly connected*; that is, ‘any two points are

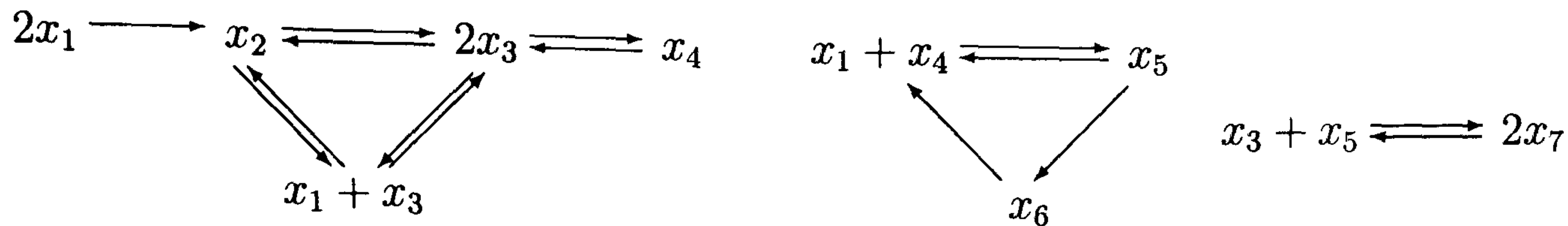


Figure 2.3: A sample mass action system.

mutually reachable by means of directed paths' [49]. This implies that in all linkage classes any individual reaction is always part of a reaction cycle. Furthermore, weak reversibility implies that every block-diagonal submatrix of A_κ associated with a linkage class is *irreducible*. A square matrix is irreducible if it is not reducible. It is reducible if and only if it can be made block upper-triangular by simultaneous row/column permutations.

For example, all individual reactions in the Michaelis-Menten system (2.6) are reversible and thus (2.6) is weakly reversible. In Figure 2.3, the reaction network in the first linkage class is not weakly reversible, because complex $2x_1$ is not reachable from all complexes in the class via a directed reaction path; the networks in the second and third linkage class are weakly reversible. It follows that this chemical reaction network is not weakly reversible.

Definition 2.1.6. The rank of the *stoichiometric subspace* of a chemical reaction network is given by $q = \text{rank}(YA_\kappa)$.

Definition 2.1.7. The *deficiency* of a chemical reaction network is given by

$$\delta = \dim A_\kappa - q - \ell = m - q - \ell \geq 0.$$

For the Michaelis-Menten reaction (2.6), $\dim A_\kappa = 3$,

$$YA_\kappa = \begin{bmatrix} -k_1 & k_{-1} + k_2 & -k_{-2} \\ -k_1 & k_{-1} & 0 \\ k_1 & -(k_{-1} + k_2) & k_{-2} \\ 0 & k_2 & -k_{-2} \end{bmatrix} \text{ and thus, } q = \text{rank}(YA_\kappa) = 2.$$

It follows, that $\delta = 3 - 2 - 1 = 0$. The Michaelis-Menten reaction is of deficiency zero. Note also that, in general, if Y has full column rank then the respective chemical reaction network is of deficiency zero. However, the reverse conclusion is not necessarily true.

Definition 2.1.8. If $q < n$, where n is the dimension of the *species subspace*, then each set of $n - q$ linearly independent vectors p_i , $i = 1, \dots, n - q$, together with the following set of constraints

$$p_i^T \dot{x} = 0 \Rightarrow p_i^T x = \gamma, \quad x \in \mathbb{R}_+^n, \gamma \in \mathbb{R}, p_i \in \mathbb{R}^n, p_i \neq 0, \quad (2.11)$$

defines an affine space of \mathbb{R}^n which is the *stoichiometric compatibility class* of the chemical reaction network. If $q = n$ then the stoichiometric compatibility class of the chemical reaction network is \mathbb{R}^n .

In the next section, we present Martin Feinberg's CRNT.

2.2 Martin Feinberg's chemical reaction network theory

Martin Feinberg's CRNT is based solely on the structure of the chemical reaction network and not the actual values of the reaction rates. Martin Feinberg describes the central premise of CRNT as follows: 'Although the governing differential equations vary markedly from one chemical system to another, the equations themselves are determined in a rather precise way by the underlying network of chemical reactions. Thus, one can hope to draw firm connections between aspects of reaction network structure and the variety of dynamics that might be admitted by the corresponding system of differential equations' [9]. Before stating Martin Feinberg's main results, we have to introduce Lyapunov's stability theorem of which we make extensive use in this thesis. We show the theorem as it appears in [50], Hassan H. Khalil's excellent book on nonlinear systems in general and Lyapunov theory in particular. The following formal definition is often used in dynamical system theory for Lyapunov stability, asymptotic stability, and instability [50].

Definition 2.2.1. The equilibrium point $x = 0$ of

$$\dot{x} = f(x) \quad (2.12)$$

is

- Lyapunov stable if, for each $\varepsilon > 0$, there is $\delta = \delta(\varepsilon) > 0$ such that $\|x(0)\| < \delta \Rightarrow \|x(t)\| < \varepsilon$, for all $t \geq 0$,

- unstable if it is not Lyapunov stable,
- asymptotically stable if it is Lyapunov stable and δ can be chosen such that

$$\|x(0)\| < \delta \Rightarrow \lim_{t \rightarrow \infty} x(t) = 0.$$

Theorem 2.2.2. (Lyapunov's stability theorem) *Let $x = 0$ be an equilibrium point for (2.12) and $\mathcal{D} \subseteq \mathbb{R}^n$ be a domain containing $x = 0$. Let $V : \mathbb{R} \rightarrow \mathbb{R}_+$ be a continuously differentiable function such that*

$$V(0) = 0 \text{ and } V(x) > 0 \text{ in } \mathcal{D} - \{0\} \quad (2.13)$$

$$\dot{V}(x) \leq 0 \text{ in } \mathcal{D} \quad (2.14)$$

Then $x = 0$ is Lyapunov stable. Moreover, if

$$\dot{V}(x) < 0 \text{ in } \mathcal{D} - \{0\} \quad (2.15)$$

then $x = 0$ is asymptotically stable

Now, the following two theorems from reference [16] represent one of the main results of CRNT: the deficiency zero theorem. In this thesis, we provide only the proof of statement 4 of Theorem 2.2.3. (The proofs for both theorems can be found in [16].) The proof uses a specific Lyapunov function

$$V(x(t)) = e^T(x_{\text{eq}} - x) + x^T(\ln x - \ln x_{\text{eq}}), \quad x \in \overline{\mathbb{R}}_+^n, \quad e^T = [1 \ \dots \ 1], \quad \ln x \triangleq [\ln x_1 \ \dots \ \ln x_n]^T, \quad (2.16)$$

which is closely related to the function

$$H(t) = \int f \ln f dc,$$

which was used by Ludwig Boltzmann in 1872 for his *H-theorem* to describe the increase of *entropy* in an *ideal gas*. Here, $f(r, c, t)$ is the so called *distribution function* and is defined such that $f(r, c, t)drdc$ is the number of molecules at time t between positions r and $r + dr$ and which have velocities between c and $c + dc$ (see reference [51] for a more detailed description). Moreover,

$$H(t) = -k_B S(t),$$

where k_B is the Boltzmann constant and $S(t)$ the entropy of the system [51]. Ludwig Boltzmann proved that $\dot{H}(t) \leq 0$. In [52], it was shown that (2.16) can be interpreted as the

thermodynamic state function (or *Gibbs free energy function*) $\psi(t)$ at constant temperature and constant pressure. Moreover, $\psi(t) \cong RTH(t)$, where T is the absolute temperature and R is the molar gas constant. Hermann von Helmholtz defined the (thermodynamic) free energy as

$$A(t) = U(t) - TS(t),$$

where $U(t)$ is the internal energy of the chemical system. When keeping temperature, pressure and volume constant, $A(t) = \psi(t)$. For this reason, F. Horn and R. Jackson named (2.16) the *pseudo-Helmholtz function* in [53].

Theorem 2.2.3. *In any chemical reaction network, suppose there exists a fixed point $x_{\text{eq}} \in \mathbb{R}_+^n$ for which $A_\kappa \Psi(x_{\text{eq}}) = 0$, then the following statements hold.*

1. *The network is weakly reversible.*
2. *Every fixed point, $x^* \in \mathbb{R}_+^n$ with $f(x^*) = 0$, satisfies $A_\kappa \Psi(x^*) = 0$.*
3. *There is one, and only one, fixed point in each stoichiometric compatibility class.*
4. *Each fixed point has a strict Lyapunov function defined on its stoichiometric compatibility class and is asymptotically stable relative to that class.*

Proof. Proof of statement 4: Consider the Lyapunov function

$$V(x) = e^T(x_{\text{eq}} - x) + x^T(\ln x - \ln x_{\text{eq}}), \quad e^T = [1 \ \dots \ 1], \quad V(x) > 0 \text{ if } x \in \overline{\mathbb{R}_+^n} - \{x_{\text{eq}}\}.$$

Here, $\ln x \triangleq [\ln x_1 \ \dots \ \ln x_n]^T$ and $\exp(x) \triangleq [\exp(x_1) \ \dots \ \exp(x_n)]^T$. To see that $V(x) > 0$ for all $x \in \overline{\mathbb{R}_+^n} - \{x_{\text{eq}}\}$, note that for all $y \in \mathbb{R}$,

$$\exp(y) > 1 + y \text{ if } y \neq 0,$$

thus,

$$\frac{\exp(\bar{y})}{\exp(y)} = \exp(\bar{y} - y) > 1 + \bar{y} - y \iff \exp(\bar{y}) - \exp(y) > \exp(y)(\bar{y} - y)$$

if $\bar{y} \neq y$, which implies that

$$e^T(\exp(\ln x_{\text{eq}}) - \exp(\ln x)) > \exp(\ln x)^T(\ln x_{\text{eq}} - \ln x) \iff e^T(x_{\text{eq}} - x) > x^T(\ln x_{\text{eq}} - \ln x)$$

if $x \neq x_{\text{eq}}$. Let $\mu_i = \ln x_i - \ln x_{i_{\text{eq}}}$. Then,

$$\begin{aligned}
\dot{V}(x) &= \frac{\partial V(x)}{\partial x} f(x) = f(x)^T (-e + \ln x - \ln x_{\text{eq}} + e) = f(x)^T (\ln x - \ln x_{\text{eq}}) \\
&= \Psi(x)^T A_\kappa^T Y^T (\ln x - \ln x_{\text{eq}}) = \sum_{i=1}^n \sum_{j=1}^m \sum_{l=1}^m K_{(l,j)} \Psi_j(x) (Y_{(i,l)} - Y_{(i,j)}) (\ln x_i - \ln x_{i_{\text{eq}}}) \\
&= \sum_{j=1}^m \sum_{l=1}^m K_{(l,j)} \prod_{\varphi=1}^n x_\varphi^{Y_{(\varphi,j)}} \sum_{i=1}^n (\mu_i Y_{(i,l)} - \mu_i Y_{(i,j)}) \\
&= \sum_{j=1}^m \sum_{l=1}^m K_{(l,j)} \prod_{\varphi=1}^n \left(x_{\varphi_{\text{eq}}}^{Y_{(\varphi,j)}} \exp(\mu_\varphi Y_{(\varphi,j)}) \right) \sum_{i=1}^n (\mu_i Y_{(i,l)} - \mu_i Y_{(i,j)}) \\
&= \sum_{j=1}^m \sum_{l=1}^m K_{(l,j)} \prod_{\varphi=1}^n x_{\varphi_{\text{eq}}}^{Y_{(\varphi,j)}} \exp \left(\sum_{i=1}^n \mu_i Y_{(i,j)} \right) \left(\sum_{i=1}^n \mu_i Y_{(i,l)} - \sum_{i=1}^n \mu_i Y_{(i,j)} \right) \\
&< \sum_{j=1}^m \sum_{l=1}^m K_{(l,j)} \prod_{\varphi=1}^n x_{\varphi_{\text{eq}}}^{Y_{(\varphi,j)}} \left(\exp \left(\sum_{i=1}^n \mu_i Y_{(i,l)} \right) - \exp \left(\sum_{i=1}^n \mu_i Y_{(i,j)} \right) \right) \\
&= \sum_{j=1}^m \sum_{l=1}^m K_{(l,j)} \Psi_j(x_{\text{eq}}) \prod_{i=1}^n (\exp(\mu_i Y_{(i,l)}) - \exp(\mu_i Y_{(i,j)})) \\
&= \sum_{j=1}^m \sum_{l=1}^m K_{(j,l)} \Psi_l(x_{\text{eq}}) \prod_{i=1}^n \exp(\mu_i Y_{(i,j)}) - \sum_{j=1}^m \sum_{l=1}^m K_{(l,j)} \Psi_j(x_{\text{eq}}) \prod_{i=1}^n \exp(\mu_i Y_{(i,j)}) \\
&= \sum_{j=1}^m \prod_{i=1}^n \exp(\mu_i Y_{(i,j)}) \sum_{l=1}^m (K_{(j,l)} \Psi_l(x_{\text{eq}}) - K_{(l,j)} \Psi_j(x_{\text{eq}})) = 0. \tag{2.17}
\end{aligned}$$

To see this, recall that $A_\kappa \Psi(x_{\text{eq}}) = 0$ and

$$A_\kappa = K - \text{diag}(K^T e) = K - D.$$

Then, with $\sum_{l=1}^m K_{(l,j)} = D_{(j,j)}$, for all j , $j = 1, \dots, m$,

$$(A_\kappa \Psi(x_{\text{eq}}))_j = \sum_{l=1}^m (K_{(j,l)} \Psi_l(x_{\text{eq}}) - D_{(j,j)} \Psi_j(x_{\text{eq}})) = \sum_{l=1}^m (K_{(j,l)} \Psi_l(x_{\text{eq}}) - K_{(l,j)} \Psi_j(x_{\text{eq}})) = 0.$$

The inequality in (2.17) implies that the equilibrium point is unique and globally asymptotically stable within a stoichiometric compatibility class. \square

Theorem 2.2.4. *If a chemical reaction network has deficiency zero, then it has a fixed point $x_{\text{eq}} \in \mathbb{R}_+^n$ for which $A_\kappa \Psi(x_{\text{eq}}) = 0$ if and only if it is weakly reversible.*

Remark 2.2.5. The trajectories of the system can evolve in different stoichiometric compatibility classes depending on the choice of initial conditions. However, these classes are invariant sets. Hence, for any given set of initial conditions, Theorem 2.2.3 and Theorem 2.2.4 imply asymptotic stability and uniqueness of the fixed point of a weakly reversible chemical reaction network of deficiency zero, that periodic solutions do not exist, and that if a chemical reaction network of deficiency zero is not weakly reversible then a positive fixed point does not exist.

We wish to stress that chemical reaction networks of deficiency zero are more than a theoretical construct. Many models in biochemistry correspond to such network. We refer the interested reader to Reference [17], an excellent paper by Martin Feinberg. In the following, we present two examples of systems from biology and biochemistry that are of deficiency zero, another example is given in Section 2.3.

Figure 2.4 shows the two-component EnvZ/OmpR signaling system in *E. coli*. It regulates OmpR-P and the expression of porins OmpF and OmpC which form a part of the osmotaxis signalling pathway [54]. The chemical reaction network is of deficiency zero. Hence, the equilibrium point is locally asymptotically stable.

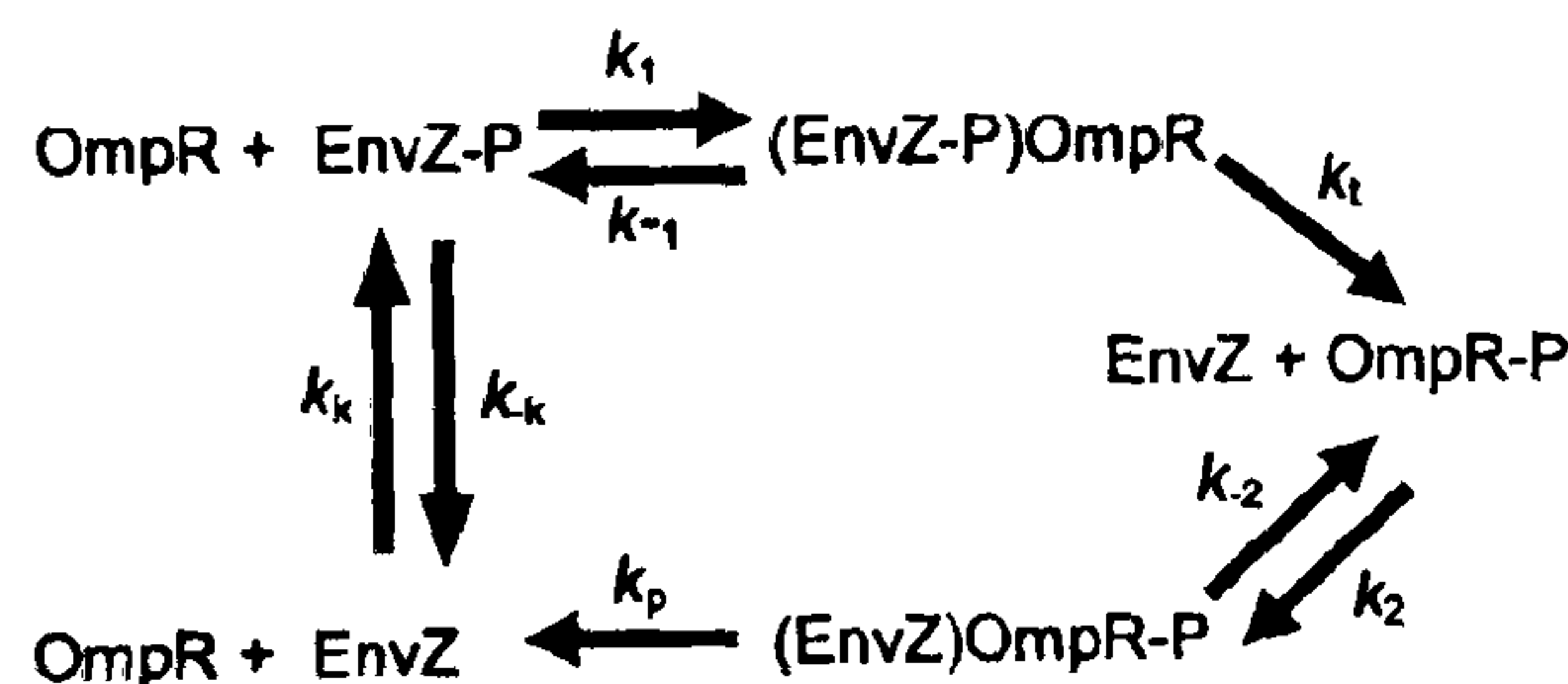
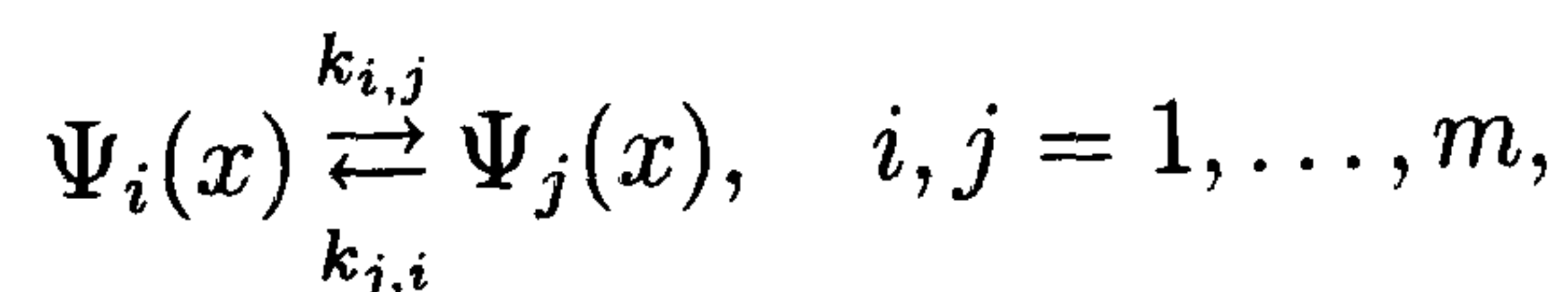


Figure 2.4: A model of the EnvZ/OmpR two-component circuit [54].

In [55], a long proof is presented to show that structurally stable closed orbits do not exist if there are no more (possibly reversible) reaction steps than reactants in the case of a closed reversible chemical system given by



with $\text{rank} Y = n$ and obeying mass action kinetics. (For example, such a system is the reversible Michaelis-Menten reaction given by (2.6).) This means that the system is weakly reversible, $n \geq m$ and $\text{rank} Y = n$ which implies that the system has deficiency zero and therefore a unique and stable fixed point and that periodic behaviour cannot exist. Hence,

we obtain the same result by applying CRNT. Now, we present Martin Feinberg's deficiency one theorem [9].

Theorem 2.2.6. *Consider a mass action system for which the underlying reaction network is weakly reversible and has ℓ linkage classes. Suppose that the deficiency of the network δ and the deficiencies of the individual linkage classes δ_θ satisfy the following conditions:*

1. $\delta_\theta \leq 1, \quad \theta = 1, 2, \dots, \ell$
2. $\sum_{\theta=1}^{\ell} \delta_\theta = \delta.$

Then, no matter what (positive) values the rate constants take, the corresponding differential equations admit precisely one steady state in each positive stoichiometric compatibility class.

The proof of this theorem is very involved and not of importance for the work presented in this thesis. We refer the interested reader to reference [56].

Remark 2.2.7. Note that Theorem 2.2.6 does not guarantee the stability of this unique positive equilibrium point. For example, for certain values of parameters the equilibrium solution for the chemical reaction network presented in last example of Section 2.4 is unstable and a stable periodic orbit appears.

For completeness, we should mention that Martin Feinberg has also showed that deficiency zero or one of a chemical reaction network rules out the possibility of multi-stationarity, the existence of several equilibria. For example, this is related to differentiation of cells [57]: *E. coli* can express two different phenotypes (Lac genes on or off) depending on whether it has been exposed to a high extracellular concentration of a specific chemical inducer or not. When concentrations are moderate, both types can coexist in the same culture as for some these concentration are just enough to push them in one direction while for others they are not. Recently, Martin Feinberg has developed together with Gheorghe Craciun a new method for distinguishing between chemical reaction networks that are capable of having multiple equilibria and those that are not [17].

The species-reaction graph

Martin Feinberg and Gheorghe Craciun have showed that if the system's Jacobian – that is, $\frac{\partial f(x)}{\partial x}$ – is nonsingular within each stoichiometric compatibility class then multi-stationarity

The graph of interaction

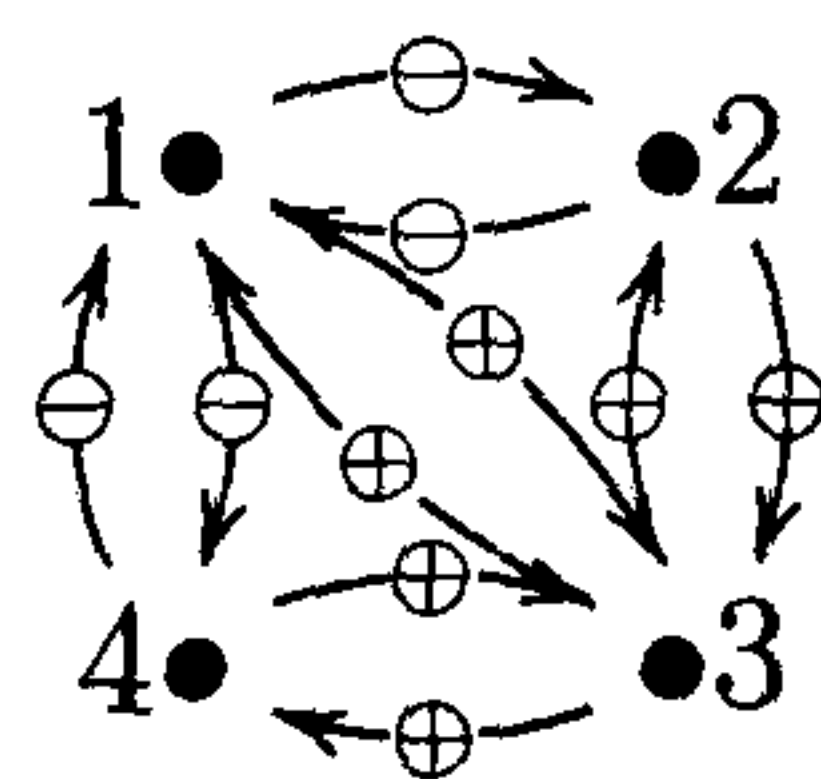
First, we introduce the following definition.

Definition 2.2.8. The *graph of interaction* is determined by the Jacobian of the dynamical system corresponding to a chemical reaction network. An off-diagonal entry $J_{(i,j)}$ in the Jacobian implies a directed edge (or arrow) from node i to node j in the graph of interaction of the system. The weight of the arrow, which can be either positive or negative, is given by the value of the entry.

We use the standard graph theoretical definition for the definition of circuits (or loops) in the graph of interaction. As implied in Definition 2.2.8 we do not consider self-loops. Furthermore, a circuit is positive or negative according to the product of the weights of its edges. For the Michaelis-Menten system (2.8) the Jacobian is

$$J = \begin{bmatrix} -(k_1[S] + k_{-2}[P_2]) & -k_1[E] & k_{-1} + k_2 & -k_{-2}[P_2] \\ -k_1[S] & -k_1[E] & k_{-1} & 0 \\ k_1[S] + k_{-2}[P_2] & k_1[E] & -(k_{-1} + k_2) & k_{-2}[P_2] \\ -k_{-2}[P_2] & 0 & k_2 & -k_{-2}[P_2] \end{bmatrix},$$

and the graph of interaction is as follows:



Here, we use \oplus and \ominus to indicate positive and negative weights respectively when we consider only positive values for the concentrations.

Lemma 2.2.9. (René Thomas's necessary conditions for multi-stationarity) *A positive directed loop in the graph of interaction of a dynamical system is necessary for multi-stationarity.*

From the graph of interaction, we can see that there exist several positive directed loops. Hence, for the Michaelis-Menten system, the lemma above does not rule out the possibility that there exist more than one equilibrium point with positive concentrations.

2.3 Chemical reaction networks under dimensionally-restricted conditions

The phenomenological approach developed by Michael A. Savageau to describe reactions following non-ideal kinetics in crowded environments such as the cell (mentioned in the Introduction) accounts for the fact that ‘the kinetic order of a reaction with respect to a given reactant is a function of the geometry within which the reaction takes place’ [60]. It is called the power-law approximation and introduces an additional asymmetry in the set of ODEs that describe the reaction network. In a three-dimensional homogeneous space, the kinetic order of a given reactant is identical to the number of its molecules that take part in the reaction. But studies have shown, that when reactions occur on a two-dimensional surface, the kinetic order is larger, and becomes even larger still in a one-dimensional channel (Figure 2.5). Moreover, this studies indicate that kinetic orders remain positive.

$$X + X \longrightarrow Y$$

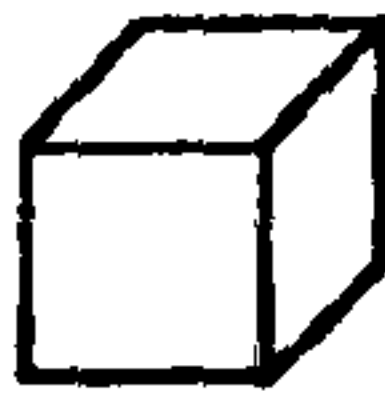
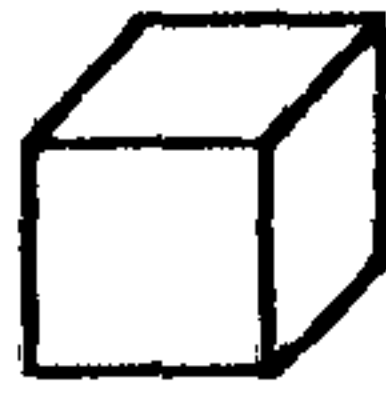
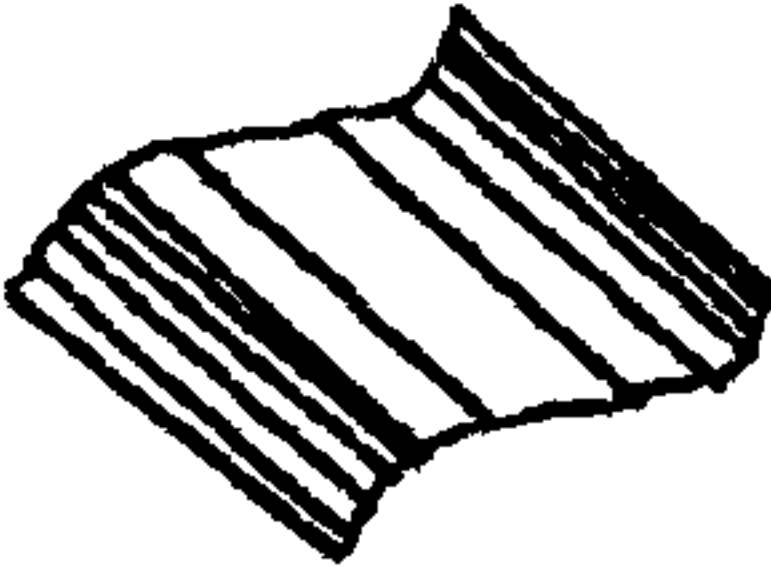

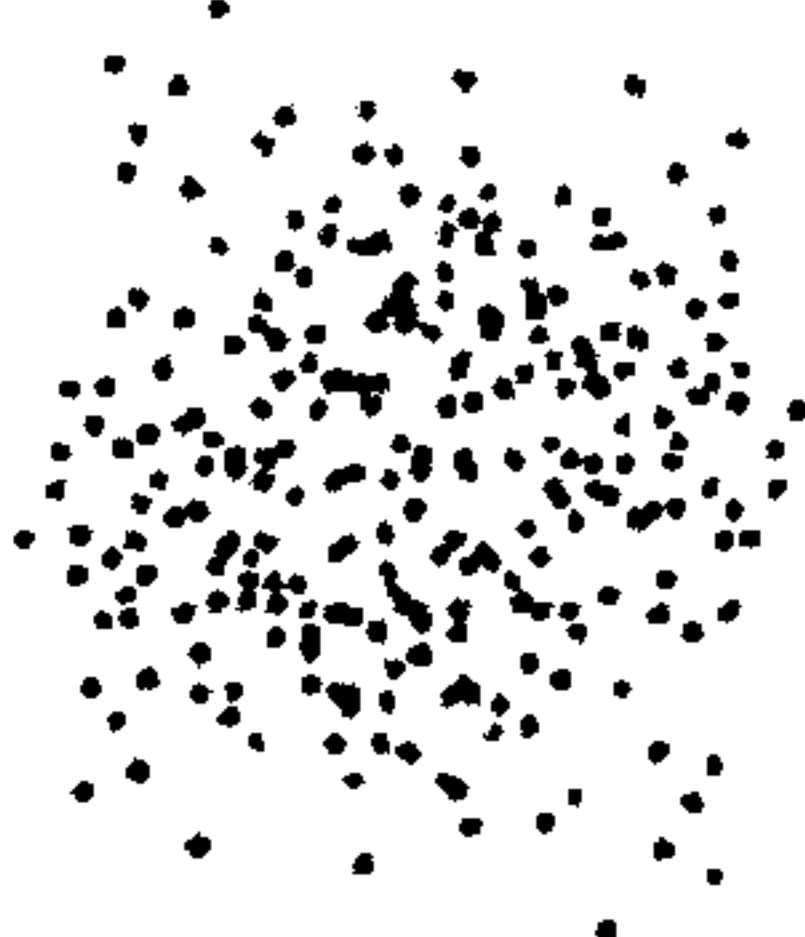
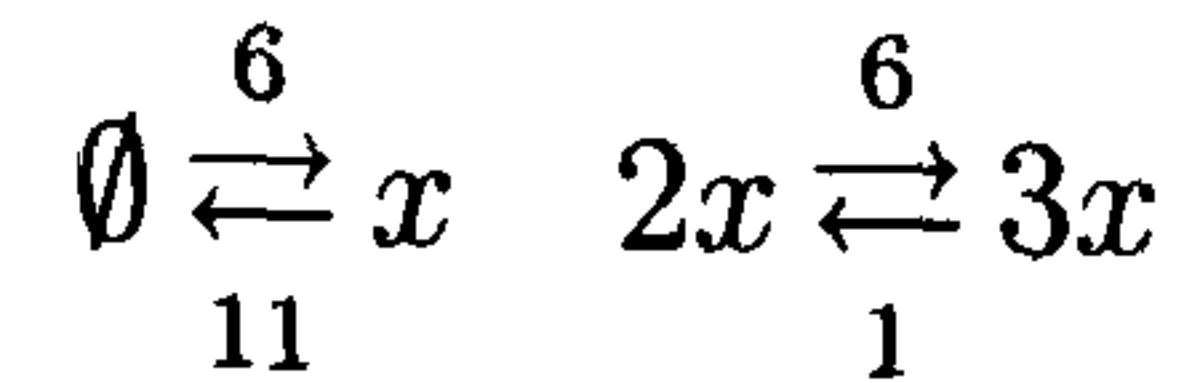
Traditional		Fractal		
3-D	3-D	2-D	1-D	1/n-D
				
$V=kX^2$	$V=kX^2$	$V=kX^{2.46}$	$V=kX^3$	$V=kX^{26.3}$

Figure 2.5: Manifestations of power-law kinetics (taken from reference [60]). Here, the kinetic order depends on the level of dimensional restriction. Experiments report the following: kinetic orders of 2 in homogeneous three-dimensional space, of 2.46 on two-dimensional surfaces, of 3 in a one-dimensional channel, and up to 50 in dispersed clusters or islands.

In the case of a chemical reaction network under the power-law approximation, the number of equilibrium solutions can be different from the number of equilibrium solutions of a chemical reaction network obeying the law of mass action and the same initial conditions might result in a different dynamical behaviour. For example, consider the following

chemical reaction network:



The corresponding differential equation is given by

$$\dot{x} = 6 - 11x + 6x^2 - x^3.$$

Then, the three equilibrium solutions are $x_{eq1} = 1$, $x_{eq2} = 2$ and $x_{eq3} = 3$. the equilibrium point $x_{eq2} = 2$ is unstable and the two others are stable. However, if a dimensional constraint changes the dynamics to

$$\dot{x} = 6 - 11x + 6x^{2.5} - x^5,$$

then there exists only one globally stable equilibrium solution $x_{eq} = 1$. Furthermore, periodic solutions can also appear or vanish because of changes in the differential equations (representing a chemical reaction network) under the power-law approximation.

A possible system of ODEs representing a chemical reaction network obeying Michael A. Savageau's power-law approximation is:

$$\dot{x} = Y A_{\kappa} \Psi(x), \quad \ln \Psi(x) = G^T \ln x, \quad (2.18)$$

where, we assume that

$$\text{there exists a diagonal matrix } D > 0 \text{ such that } G = DY. \quad (2.19)$$

The deficiency zero theorem guarantees that there exists a unique positive equilibrium point x_{eq} for

$$\dot{x} = DY A_{\kappa} \Psi(x) = G A_{\kappa} \Psi(x), \quad \ln \Psi(x) = G^T \ln x, \quad (2.20)$$

and that it satisfies $A_{\kappa} \Psi(x_{eq}) = 0$. This implies that if the chemical reaction network represented by (2.18) and (2.19) has deficiency zero then it has the same unique equilibrium point x_{eq} as (2.20), for which $A_{\kappa} \Psi(x_{eq}) = 0$. The following theorem proves local asymptotic stability of the equilibrium point x_{eq} of the chemical reaction network represented by (2.18) and (2.19).

Theorem 2.3.1. (A deficiency-zero-like theorem for reactions under dimensionally restricted conditions) *The fixed point $x_{eq} \in \mathbb{R}_+^n$ of a weakly reversible chemical reaction network with power-law kinetics, where x_{eq} is such that $A_{\kappa} \Psi(x_{eq}) = 0$ and there exists a diagonal matrix $D > 0$ such that $G = DY$, is locally asymptotically stable.*

Proof. The Jacobian at $x = x_{\text{eq}}$ is: $J = Y\tilde{A}_\kappa Y^T D[\text{diag}(x_{\text{eq}})]^{-1}$, where $\tilde{A}_\kappa = A_\kappa \text{diag}(\Psi(x_{\text{eq}}))$, $J \in \mathbb{R}^{n \times n}$, $Y \in \overline{\mathbb{R}}_+^{n \times m}$, $A_\kappa \in \mathbb{R}^{m \times m}$, and $\Psi(x_{\text{eq}}) \in \mathbb{R}^m$. It follows that \tilde{A}_κ is negative semidefinite, since it is block diagonalisable and each submatrix is irreducible and has zero row and zero column sum. Now, let

$$P = [\text{diag}(x_{\text{eq}})]D^{-1} = D^{-1}[\text{diag}(x_{\text{eq}})] > 0 \quad (2.21)$$

and $\xi = x - x_{\text{eq}}$, where $0 < |x - x_{\text{eq}}| \leq \varepsilon$, $x - x_{\text{eq}} \neq 0$, and $\varepsilon > 0$ is small. Consider the following (Lyapunov) inequality

$$\xi^T Y \tilde{A}_\kappa Y^T D[\text{diag}(x_{\text{eq}})]^{-1} P \xi + \xi^T P [\text{diag}(x_{\text{eq}})]^{-1} D Y \tilde{A}_\kappa^T Y^T \xi = 2\xi^T Y \tilde{A}_\kappa Y^T \xi. \quad (2.22)$$

Note that (2.22) ≤ 0 and that (2.22) < 0 implies local asymptotical stability of the fixed point.

It follows from $\delta = 0$ and weak reversibility that $q = \text{rank}(Y A_\kappa) = \text{rank}(A_\kappa)$. Thus, (2.22) = 0 only if $n > q$ and $\dim \mathcal{N}(Y A_\kappa) = n - q$. By (2.11), there exists $n - q$ linearly independent vectors $p \neq 0$ such that $p^T Y A_\kappa = 0$ and $p^T x = \gamma$. Therefore, (2.22) = 0 only if $\xi = p$ but then $\xi^T \xi = p^T(x - x_{\text{eq}}) = \gamma - \gamma = 0$, which is a contradiction. It follows that (2.22) < 0 for all ξ and thus, x_{eq} is locally asymptotically stable. \square

We have provided a deficiency-zero-like theorem for reactions under dimensionally-restricted conditions, as experienced in the cellular environment, where the law of mass action does not strictly apply. We now briefly illustrate this result with application to an important biological system.

Application to a kinetic proofreading scheme

Kinetic proofreading schemes, as the one depicted in Figure 2.6, have been proposed to model certain signalling cascades [61–63]. Particularly, let R correspond to the receptors of a T-cell which bind to antigens L . They consecutively form the complexes S_1 to S_N through several steps usually requiring phosphorylation. High concentrations at steady state of complexes further down the reaction chain imply the presence of a foreign antigen – as opposed to a ‘good’ self antigen – which triggers an immune response (not shown). This allows T-cells to discriminate between foreign and self antigens and to avoid signalling mistakes. Since the levels of the concentrations of complexes are determined by the dissociation constants d_i and transformation rates k_i , $i = 0, \dots, N$, in this model ‘good’ antigen have higher values of d_i and ‘bad’ antigens have higher values of k_i .

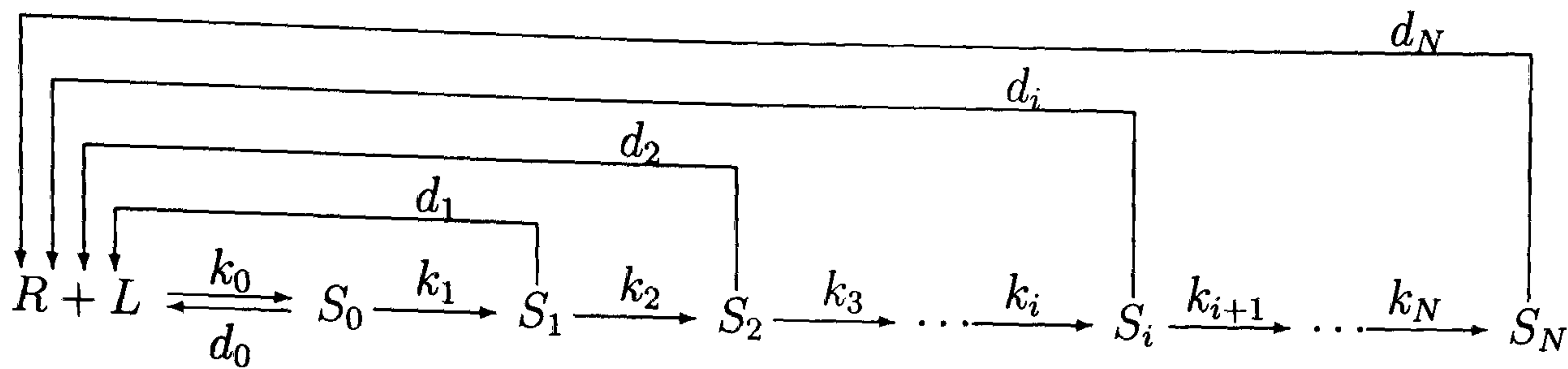


Figure 2.6: **A kinetic proofreading scheme** [62]. A signaling cascade where R is the receptor, L the ligand and the S_i are signal elements.

Note that this biochemical reaction network is weakly reversible and of deficiency zero. Thus, it has a unique stable equilibrium solution and periodic solutions can not exist under mass action kinetics. Now, independently of the kinetics, even if the reactions do not obey the law of mass action due to the volume exclusion effects or to macromolecular obstacles, Theorem 2.3.1 states that an equilibrium point of the chemical reaction network under power-law kinetics is locally asymptotically stable. This provides additional evidence that this system is a valid kinetic proofreading model of T-Cell receptor signal transduction.

2.4 Boundedness of weakly reversible chemical reaction networks

In this section, we give results on weakly reversible chemical reaction networks in general, since many relevant chemical reaction networks are weakly reversible [47], thereby going beyond Martin Feinberg's CRNT and hence, providing an extension to his network analysis framework. Importantly, the result is completely independent of the deficiency of the network. In the following, we assume that all chemical reaction networks are taken with mass action kinetics. First, we require the next two definitions of *conservative* and *ultimately bounded* chemical reaction networks.

Definition 2.4.1. If there exists a $p \gg 0$ such that $p^T Y A_\kappa = 0$, the chemical reaction network is conservative. Note that if a chemical reaction network is conservative, the origin is Lyapunov stable, since, for $x \neq 0$, the Lyapunov function $V = p^T x > 0$ and $\dot{V} = p^T Y A_\kappa \Psi(x) = 0$.

Note that this means that the sum of the concentrations of a conservative system

remains constant at all time

Definition 2.4.2. A dynamical system $f(x)$ is said to be ultimately bounded if it possesses a *bounded absorbing set*. The bounded set \mathcal{B}_0 is absorbing if for any bounded set $\mathcal{B} \in \mathbb{R}^n$ there exists a $t_0 = t_0(\mathcal{B})$ such that $x(\mathcal{B}) \in \mathcal{B}_0$ for $t > t_0$. Equivalently, there exists a scalar $\gamma \geq 0$ and a Lyapunov function $V(x)$ such that $\dot{V}(x) < 0$, if $\|x\| \geq \gamma$ (see Theorem 4.1 of [64]). The following figure is an illustration of the solution trajectory of an ultimately bounded system:

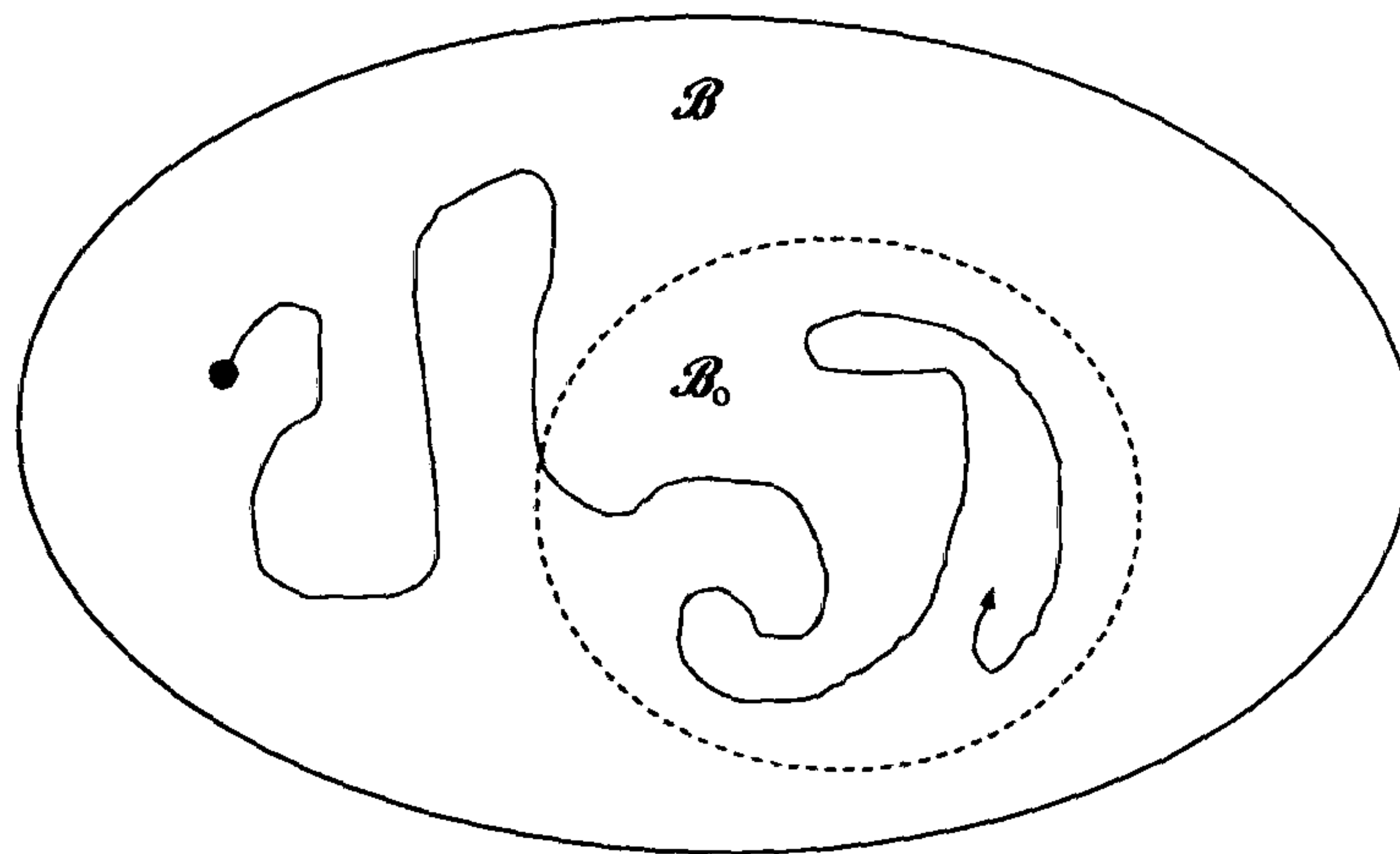
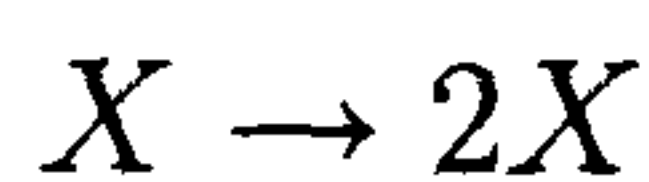


Figure 2.7: Ultimately bounded system.

A simple chemical reaction network whose solution trajectories diverge to infinity for any positive initial condition is:



This is an autocatalytic reaction. Another reaction network whose trajectories diverge to infinity is given by (2.29). Here, inputs (from the source) into the system are not balanced by outputs (into the sink). (See also references [65, 66].)

Theorem 2.4.3. *If a chemical reaction network is weakly reversible then $x_i \rightarrow \infty$, $\forall i$.*

Proof. First, recall that, by Lemma 2.1.1, solutions remain nonnegative if initial conditions are nonnegative. Furthermore, for all i , without loss of generality, we assume that $x_i \neq 0$ for all x . The idea behind the proof is the following:

In (I), we assume that for all j , $j \neq i$, $0 < x_j \leq x_{j\max}$, and show that $x_i \rightarrow \infty$. The polynomial function $p_i(x)$ that describes the time evolution of x_i (that is, $\dot{x}_i = p_i(x)$) can be written as

$$p_i(x) = \sum_{e_i=1}^{e_{i\max}} x_i^{e_i} m_{e_i}(x_j^{e_j}) + p_{i_2}(x_j^{e_j})$$

for a weakly reversible chemical reaction network, where $m_{e_i}(x_j^{e_j})$ are monomials and $p_{i_2}(x_j^{e_j})$ is a polynomial function, and both do not depend on x_i , $e_j = 0, 1, 2, \dots, e_{j_{\max}}$. We show that $m_{e_{i_{\max}}} < 0$, which implies that that solution trajectories x_i cannot diverge to infinity for a weakly reversible chemical reaction network.

In (II), we assume that for all j , $j \neq i, r$, $0 < x_j \leq x_{j_{\max}}$. We show that $m_{e_i^* e_r^*} < 0$, where

$$\dot{x}_i(x) + \dot{x}_r(x) = \sum_{e_i=1}^{e_{i_{\max}}} \sum_{e_r=1}^{e_{r_{\max}}} x_i^{e_i} x_r^{e_r} m_{e_i e_r}(x_j^{e_j}) + p_{ir_2}(x_j^{e_j})$$

and $m_{e_i^* e_r^*}$ is such that if $e_i^* + e_r^* < e_i^* + e_r^*$ then $m_{e_i^* e_r^*} = 0$. Here, $m_{e_i e_r}(x_j^{e_j})$ are monomials and $p_{ir_2}(x_j^{e_j})$ is a polynomial function and both do not depend on x_i or x_r . Thus, solutions of the pair $\{x_i, x_r\}$ are bounded. This argument can be extended to triplets, quadruples etc.

In (III), we show that even if some x_w tend towards zero solutions cannot diverge to infinity. By continuity, it is sufficient to show this for $x_w = 0$. We show that $x_w = 0$ implies that all complexes in the linkage classes that contain x_w are zero. For all other linkage classes (I) and (II) hold. Cases (I), (II) and (III) taken together imply that $x_i \rightarrow \infty$, $\forall i$, if the chemical reaction network is weakly reversible.

(I) By Remark 2.1.5, any individual reaction is always part of a reaction cycle. Thus, (2.10) can be written as the sum over all S reaction cycles, where each cycle s consists of a subset of reactions \mathfrak{R}_s , $s = \{1, \dots, S\}$:

$$\dot{x}_i = \sum_{s=1}^S \sum_{\mathfrak{R}_s} \frac{1}{\beta_{jl}} k_{j \rightarrow l} \Psi_j(x) (Y_{(i,l)} - Y_{(i,j)}). \quad (2.23)$$

The constant $\beta_{jl} \in \mathbb{N}$ is the multiplicity of $k_{j \rightarrow l}$ in $\{\mathfrak{R}_1, \dots, \mathfrak{R}_S\}$.

Remark 2.4.4. Note that $k_{j \rightarrow l} > 0$ for all j, l for which $k_{j \rightarrow l} \subset \mathfrak{R}$ and it follows that $k_{j \rightarrow l} \Psi_j(x) > 0$ for all j, l for which $k_{j \rightarrow l} \subset \mathfrak{R}$ if $x \gg 0$.

Now, analogously to Kirchhoff's second law, for each reaction cycle s ,

$$\sum_{\mathfrak{R}_s} \alpha_{jl}^i = 0, \quad \alpha_{jl}^i = Y_{(i,l)} - Y_{(i,j)}. \quad (2.24)$$

Thus,

- (i) either $\alpha_{jl}^i = 0$ for all j, l , which implies that $Y_{(i,j)} = Y_{(i,l)}$ for all j, l , where j, l are such that $k_{j \rightarrow l} \subset \mathfrak{R}_s$; furthermore, if this holds for all S reaction cycles then $\dot{x}_i = 0$ for all x and clearly $x_i \rightarrow \infty$ for all $i, i \in \{1, \dots, n\}$,
- (ii) or otherwise, for some m , $Y_{(i,m)}$ is such that $Y_{(i,m)} \geq Y_{(i,l)}$ holds for all l , where m, l are such that $k_{m \rightarrow l} \subset \mathfrak{R}_s$, which implies that for some M , $Y_{(i,M)}$ is such that $Y_{(i,M)} \geq Y_{(i,l)}$ holds for all l , where $k_{M \rightarrow l} \subset \mathfrak{R}$; it follows from (2.24) that $\alpha_{Ml}^i \leq 0$, and from Remark 2.4.4 that

$$\frac{1}{\beta_{Ml}} k_{M \rightarrow l} \Psi_M(x) \alpha_{Ml}^i < 0 \quad (2.25)$$

for at least one pair $\{M, l\}$. Recall that $\Psi_j(x) = \prod_{\varphi=1}^n x_{\varphi}^{Y_{(\varphi,j)}}$. Then, it follows from (2.25) that

$$\begin{aligned} \frac{\partial \dot{x}_i}{\partial x_i^{Y_{(i,M)}}} &= \frac{\partial \sum_{s=1}^S \sum_{\mathfrak{R}_s} \frac{1}{\beta_{jl}} k_{j \rightarrow l} \prod_{\varphi=1}^n x_{\varphi}^{Y_{(\varphi,j)}} (Y_{(i,l)} - Y_{(i,j)})}{\partial x_i^{Y_{(i,M)}}} \\ &= \frac{\partial \sum_{s=1}^S \sum_{\mathfrak{R}_s} \frac{1}{\beta_{Ml}} k_{M \rightarrow l} \prod_{\varphi=1}^n x_{\varphi}^{Y_{(\varphi,M)}} (Y_{(i,l)} - Y_{(i,M)})}{\partial x_i^{Y_{(i,M)}}} \\ &= \frac{\partial \sum_{s=1}^S \sum_{\mathfrak{R}_s} \frac{1}{\beta_{Ml}} k_{M \rightarrow l} \prod_{\varphi=1}^n x_{\varphi}^{Y_{(\varphi,M)}} \alpha_{Ml}^i}{\partial x_i^{Y_{(i,M)}}} < 0 \text{ if } x \gg 0. \end{aligned}$$

This implies that there exists a positive constant γ such that $\dot{x}_i < 0$ if $x_i > \gamma, x \gg 0$, and $x_j \rightarrow \infty$ for all $j \neq i, j \in \{1, \dots, n\}$.

Hence, for any $i, i = 1, \dots, n$, if $x \gg 0$ and solutions of x_j are bounded for all $j \neq i$ then solutions of x_i must also be bounded.

(II) Now, we let $x \gg 0$ and assume that solutions of x_i are unbounded. Then, $\dot{x}_i > 0$ as $x_i \rightarrow \infty$ and the previous result requires that there exists at least one x_r such that

$$\frac{\partial \dot{x}_i}{\partial x_r} > 0, \quad x_r \rightarrow \infty.$$

Assume that all other solutions are bounded. Then, either $(\alpha_{jl}^i + \alpha_{jl}^r) = 0$ for all S reaction cycles, or there exist a $Y_{(i,s)}$ and a $Y_{(r,s)}$ such $Y_{(i,s)} + Y_{(r,s)} \geq Y_{(i,l)} + Y_{(r,l)}$ holds for all l . (Note that $Y_{(i,s)} = Y_{(i,M)}$ or $Y_{(r,s)} = Y_{(r,M)}$ is not necessarily true.) It follows that

$$k_{s \rightarrow l} \left(\frac{1}{\beta_{sl}} \Psi_s(x) + \frac{1}{\beta_{sl}} \Psi_s(x) \right) (\alpha_{sl}^i + \alpha_{sl}^r) < 0$$

for at least one pair $\{s, l\}$. This implies that

$$\frac{\partial(\dot{x}_i + \dot{x}_r)}{\partial(x_i^{Y(i,s)} x_r^{Y(r,s)})} < 0 \text{ if } x \gg 0. \quad (2.26)$$

Note that (2.26) contradicts the assumption that $x_i, x_r \rightarrow \infty$. Repeating this argument, it follows that $x_i \rightarrow \infty$ for all i if $x \gg 0$.

(III) Finally, we will show by contradiction that it is also not possible that some $x_i \rightarrow \infty$, $i = 1, \dots, I < n$, while some $x_w \rightarrow 0$, $w = I, \dots, W < n$. For instance, assume that some $x_i \rightarrow \infty$ while some $x_w \rightarrow 0$, which implies that if $q > W$ then $0 < x_q < \infty$. Since $\frac{\partial \dot{x}_i}{\partial x_w}$ is continuous, which means that $\dot{x}_i(x_w) \rightarrow \dot{x}_i(0)$ whenever $x_w \rightarrow 0$, it is sufficient to investigate the behaviour of x_i at $x_w = 0$ and $\dot{x}_w = 0$.

Definition 2.4.5. We denote *the support of complex* $\Psi_i(x)$ by: $\text{supp}\Psi_i(x)$. ‘[T]he support of a complex is... the set of species “appearing in” that complex’ [9].

Let $x_w \subset \text{supp}\Psi_j(x)$, $w \in \{1, \dots, W\}$. Then, $\Psi_j(x) = 0$, since $x_w = 0$. This implies that $k_{k \rightarrow l} \Psi_k(x) \neq 0$ only if $k \neq j$. Since $Y_{(w,k)} = 0$ if $x_w \not\subset \text{supp}\Psi_k(x)$, it follows that for x_w :

$$\dot{x}_w = \sum_{s=1}^S \sum_{\mathfrak{R}_s} \frac{1}{\beta_{kl}} k_{k \rightarrow l} \Psi_k(x) Y_{(w,l)}, \quad (2.27)$$

which implies that $\Psi_k(x) = 0$ if $\dot{x}_w = 0$. Therefore, either our assumption that $x_w \not\subset \text{supp}\Psi_k(x)$ is violated or there exists at least one x_v such that $x_v \subset \text{supp}\Psi_k(x)$ and $x_v = 0$, that is $x_v \in \{1, \dots, W\}$. This implies that if $x_w \subset \text{supp}\Psi_j(x)$, $w \in \{1, \dots, W\}$ (that is, $x_w = 0$) then for each reaction cycle \mathfrak{R}_s , $s = 1, \dots, S$, if $k_{j \rightarrow l} \subset \mathfrak{R}_s$ then $x_a = 0$ and $x_b = 0$ for all a, b for which $k_{a \rightarrow b} \subset \mathfrak{R}_s$.

Now, if we ‘remove’ all reaction cycles for which $x_w \subset \text{supp}\Psi_j(x)$ holds then the attained network – of reactions between complexes that do not contain any x_w – remains weakly reversible (or is empty). However, we have shown in (I) and (II) that this implies that $x_i \rightarrow \infty$ for all i , since $x_c > 0$ if $c \neq w$. This contradicts our assumption that some $x_i \rightarrow \infty$ and concludes the proof. \square

Remark 2.4.6. Theorem 2.4.3 is completely independent of the deficiency of the network and implies that a weakly reversible network is either conservative or ultimately bounded.

Remark 2.4.7. Note that Theorem 2.4.3 together with the Brouwer Fixed Point Theorem implies that a weakly reversible chemical reaction network possesses at least one nonnegative equilibrium point.

Lemma 2.4.8. *Theorem 2.4.3 also applies to the weakly reversible chemical reaction networks when taken with the power-law approximation for which (2.19) holds.*

Remark 2.4.9. The significance of Theorem 2.4.3 and Remark 2.4.7 lies in the fact that existence of solutions and boundedness of solution trajectories are often an important requirements for the analysis of dynamical systems. Particularly, in the case of large systems checking for strong connectivity of the underlying graph can be performed automatically and efficiently as opposed to alternative means that establish boundedness of solution trajectories – for example, via Lyapunov stability theory.

Now, consider, for example, the following two chemical reaction networks and their respective representation through a dynamical system (Recall that the symbol \emptyset represents the null-complex, which functions as a source and a sink for the system.):

$$\emptyset \xrightleftharpoons[1]{1} x + y : \quad \begin{aligned} \dot{x} &= 1 - xy \\ \dot{y} &= 1 - xy \end{aligned} \quad (2.28)$$

$$y \xleftarrow{a>0} \emptyset \xrightleftharpoons[1]{1} x + y : \quad \begin{aligned} \dot{x} &= 1 - xy \\ \dot{y} &= 1 + a - xy \end{aligned} \quad (2.29)$$

The network presented in (2.28) is weakly reversible, while the network presented in (2.29) is not. Furthermore, the former has the unique asymptotically stable equilibrium point (1,1), while in the case of the latter $x \rightarrow 0$ and $y \rightarrow \infty$.

Remark 2.4.10. Since Theorem 2.4.3 guarantees boundedness of solutions, instability of all equilibria of a weakly reversible chemical reaction network guarantees oscillatory behaviour; that is, it guarantees periodic, quasi-periodic or chaotic behaviour.

Remark 2.4.11. (**‘Hidden’ weak reversibility**) Let $A_{\kappa,add} \in \mathcal{N}(Y)$ (that is, $Y A_{\kappa,add} = 0$) and $A_{\kappa,c} = A_{\kappa} + A_{\kappa,add}$. Then,

$$\dot{x} = Y A_{\kappa} \Psi(x) = Y A_{\kappa,c} \Psi(x).$$

If $-A_{\kappa,c}$ is an *M-matrix* with zero column sum and irreducible or can be block-diagonalised and each block-diagonal submatrix is irreducible (or empty) then the chemical reaction

network is weakly reversible. An M-matrix is a matrix with positive diagonal entries and non-positive off-diagonal entries. Moreover, all principal minors are nonnegative [67].

For illustration, consider the following chemical reaction network, which is not weakly reversible for all $a \geq 0$:



Now, let us add matrix $A_{\kappa,add} \in \mathcal{N}(Y)$ to A_{κ} , where

$$A_{\kappa} = \begin{bmatrix} -2-a & 1 & 0 & 0 \\ 0 & -1 & 0 & 0 \\ 1+a & 0 & 0 & 0 \\ 1 & 0 & 0 & 0 \end{bmatrix}, A_{\kappa,add} = \begin{bmatrix} 1 & 0 & 0 & 0 \\ 1 & 0 & 0 & 0 \\ -1 & 0 & 0 & 0 \\ -1 & 0 & 0 & 0 \end{bmatrix}, Y = \begin{bmatrix} 0 & 1 & 0 & 1 \\ 0 & 1 & 1 & 0 \end{bmatrix}, \Psi = \begin{bmatrix} 1 \\ xy \\ y \\ x \end{bmatrix}.$$

Thus,

$$A_{\kappa,c} = A_{\kappa} + A_{\kappa,add} = \begin{bmatrix} -1-a & 1 & 0 & 0 \\ 1 & -1 & 0 & 0 \\ a & 0 & 0 & 0 \\ 0 & 0 & 0 & 0 \end{bmatrix}.$$

Note that $A_{\kappa,c}$ is block diagonal. The new network correspond to (2.29) if $a \neq 0$. This implies that the dynamical system representations of (2.30) and of (2.29) are identical. If $a = 0$ then the upper block-diagonal submatrix is irreducible and thus, the corresponding chemical reaction network is weakly reversible (in fact, it is network (2.28)). In summary, certain dynamical systems arising from a chemical reaction network that is not weakly reversible can be represented through a weakly reversible one. In this case, Theorem 2.4.3 guarantees the boundedness of their solutions (for example, see Figure 2.10).

2.4.1 Examples from biology and chemistry

A sample mass action system

Consider the sample mass action system from [14, 47] given in Figure 2.8. Note that an *ad hoc* study of the corresponding dynamical system (2.31) requires an analysis of seven polynomial equations in seven variables with up to eighteen unspecified parameters, or reaction rates. On the other hand, it is easy to verify that the chemical reaction network

in Figure 2.8 is of deficiency one and weakly reversible. Thus, (2.31) admits a unique positive equilibrium point independently of parameter values.

$$\begin{aligned}
\dot{x}_1 &= -2k_{2,1}x_1^2 + (2k_{1,2} + k_{3,2})x_2 - (k_{2,3} + k_{4,3})x_1x_3 + k_{3,4}x_3^2 \\
&\quad - (k_{7,6} + k_{8,6})x_1x_4 + k_{6,7}x_5 + k_{6,8}x_6, \\
\dot{x}_2 &= k_{2,1}x_1^2 - (k_{1,2} + k_{3,2} + k_{4,2})x_2 + k_{2,3}x_1x_3 + k_{2,4}x_3^2, \\
\dot{x}_3 &= (k_{3,2} + 2k_{4,2})x_2 + (k_{4,3} - k_{2,3})x_1x_3 - (k_{3,4} + 2k_{2,4} + 2k_{5,4})x_3^2 \\
&\quad + 2k_{4,5}x_4 - k_{10,9}x_3x_5 + k_{9,10}x_7^2, \\
\dot{x}_4 &= k_{5,4}x_3^2 - k_{4,5}x_4 - (k_{7,6} + k_{8,6})x_1x_4 + k_{6,7}x_5 + k_{6,8}x_6, \\
\dot{x}_5 &= k_{7,6}x_1x_4 - (k_{6,7} + k_{8,7})x_5 + k_{7,8}x_6 - k_{10,9}x_3x_5 + k_{9,10}x_7^2, \\
\dot{x}_6 &= k_{8,6}x_1x_4 + k_{8,7}x_5 - (k_{6,8} + k_{7,8})x_6, \\
\dot{x}_7 &= 2k_{10,9}x_3x_5 - 2k_{9,10}x_7^2.
\end{aligned} \tag{2.31}$$

Moreover, applying Theorem 2.4.3 we can immediately guarantee that, independently of the values of reaction rates, solutions will not diverge for nonnegative initial conditions.

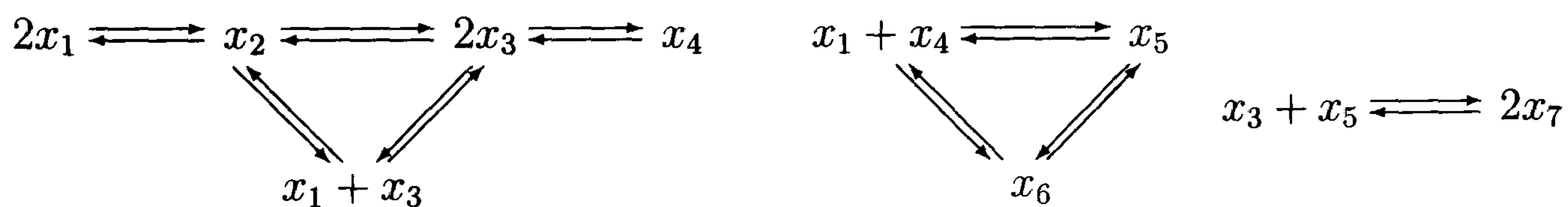


Figure 2.8: A sample mass action system.

An Active Membrane Transport Model

Figure 2.9 shows a simple model consisting of elementary steps for an active transport system that carries molecules across the cell membrane:

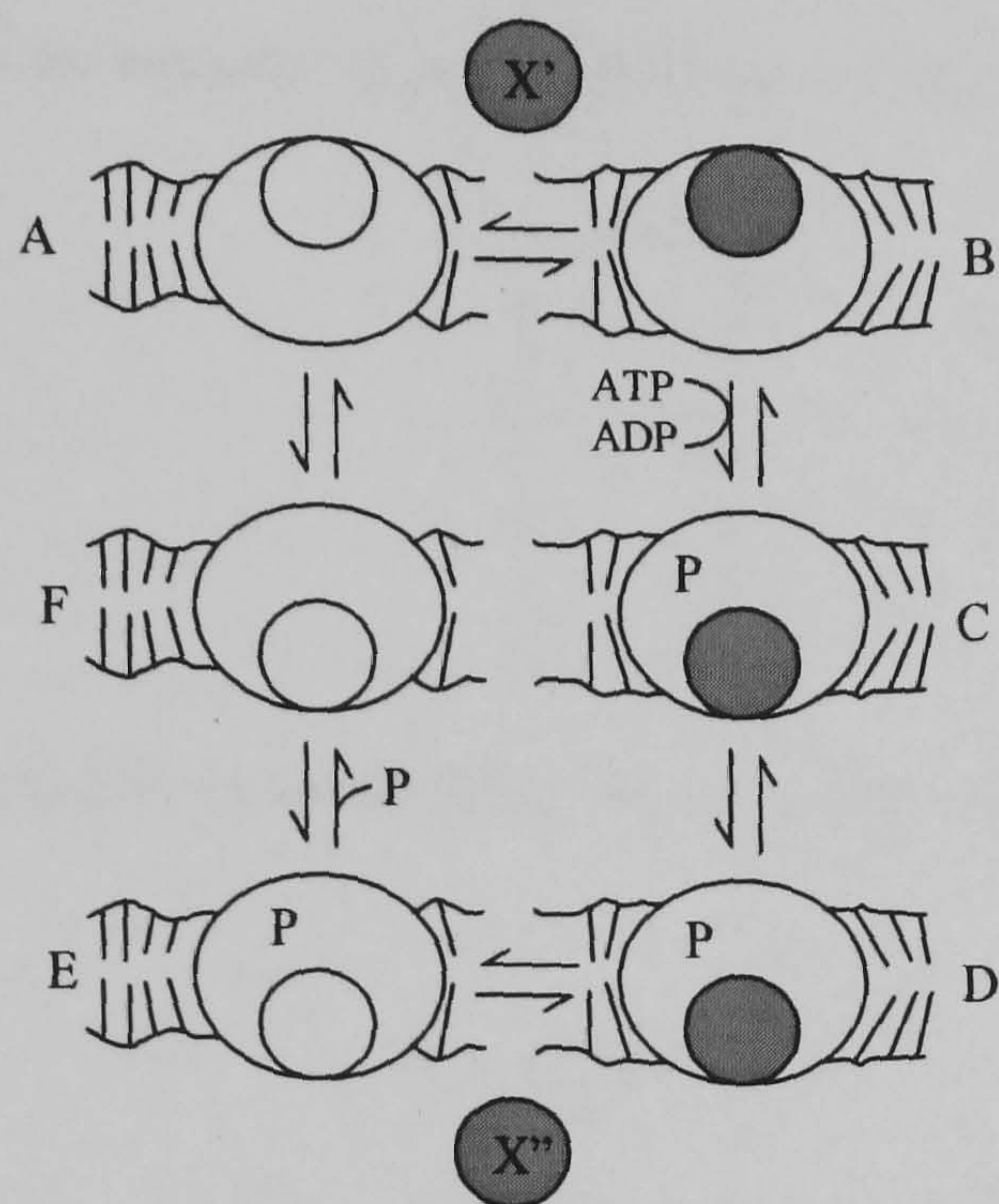
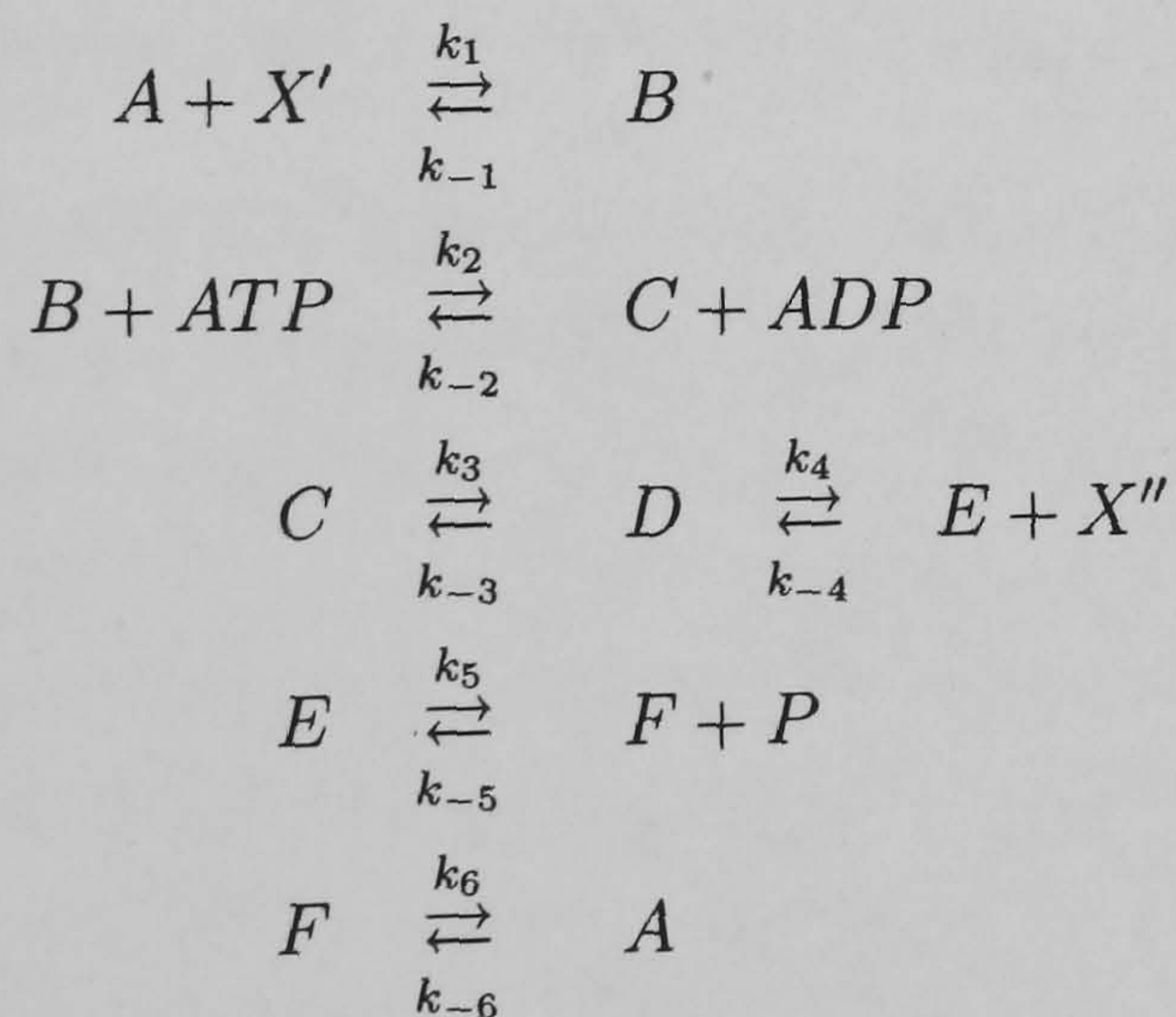


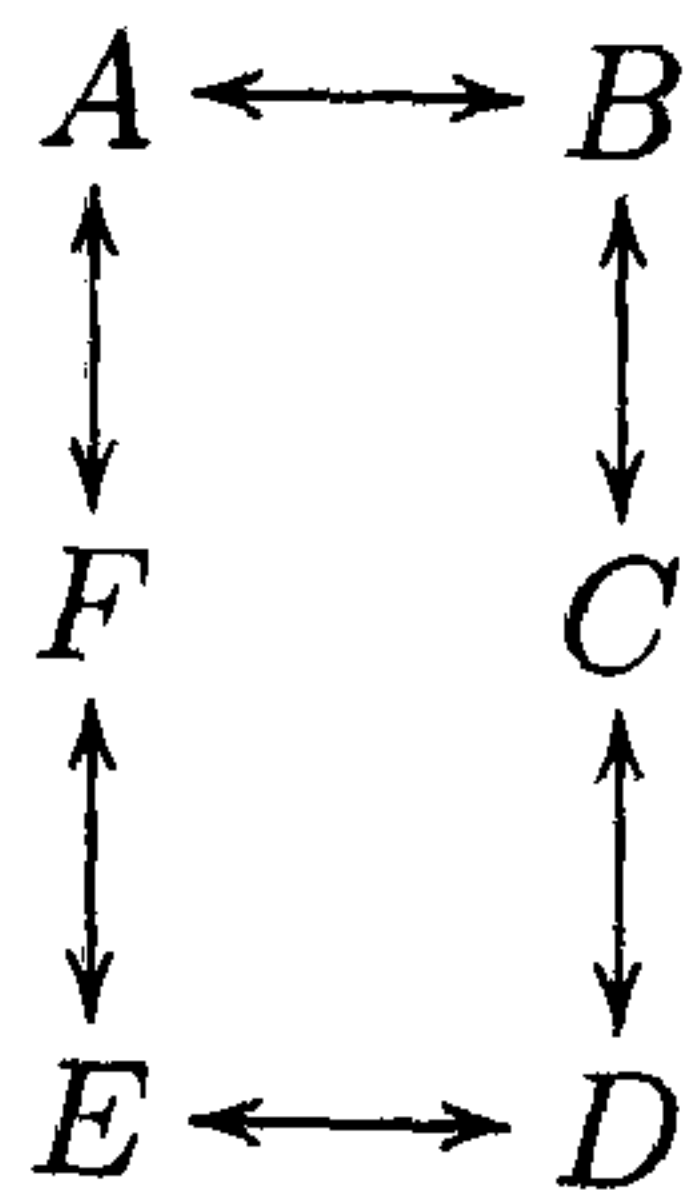
Figure 2.9: **Active membrane transport model** [68]. Molecules are actively carried across the cell membrane. An extracellular molecule, X' , binds to a free transporter molecule in the membrane: $A + X' \rightleftharpoons B$. ATP hydrolysis ($B + ATP \rightleftharpoons C + ADP$) then drives the transport of the molecule into the internal medium, where it is released (X''): $C \rightleftharpoons D \rightleftharpoons E + X''$. Thereafter, the empty binding site is prepared to repeat the cycle through the de/phosphorylation reaction $E \rightleftharpoons F + P$, and through the reaction $F \rightleftharpoons A$.

The chemical reaction network of the model in Figure 2.9 has the following form:

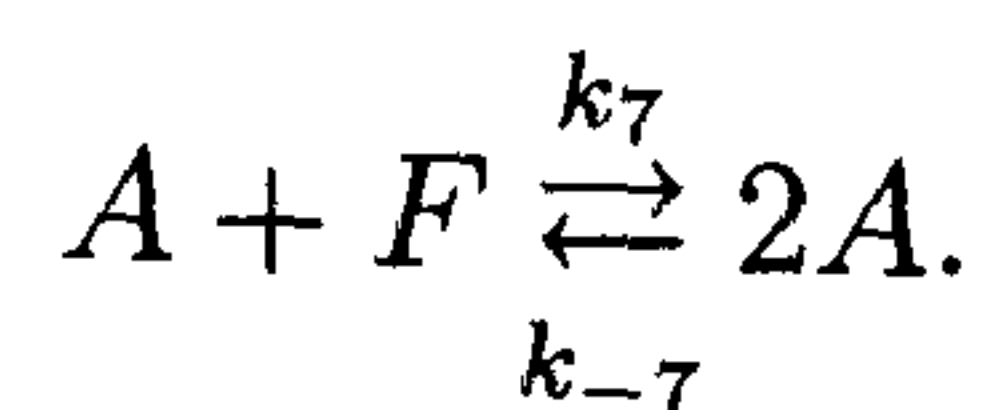


In [68], the concentrations of ligand molecules (X), of ATP, ADP (which drive the transport (pumping) through ATP hydrolysis) and P (inorganic phosphate involved in the phosphorylation-dephosphorylation reactions) are assumed to be externally controlled parameters. This leads to a chemical reaction network that is (weakly) reversible (and to a

mathematical model that consists of a set of linear ordinary differential equations):



In order to simulate dynamic cooperativity, an extra autocatalytic reaction of the following form is added:



This addition results in a mathematical model with a nonlinearity ($[\cdot]$ denote concentrations):

$$\begin{aligned}
 \dot{[A]} &= -(k_1 + k_{-6})[A] + k_{-1}[B] + k_6[F] + k_7[A][F] - k_{-7}[A]^2, \\
 \dot{[B]} &= -(k_2 + k_{-1})[B] + k_{-2}[C] + k_1[A], \\
 \dot{[C]} &= -(k_3 + k_{-2})[C] + k_{-3}[D] + k_2[B], \\
 \dot{[D]} &= -(k_4 + k_{-3})[D] + k_{-4}[E] + k_3[C], \\
 \dot{[E]} &= -(k_5 + k_{-4})[E] + k_{-5}[F] + k_4[D], \\
 \dot{[F]} &= -(k_6 + k_{-5})[F] + k_{-6}[A] + k_5[E] - k_7[A][F] + k_{-7}[A]^2.
 \end{aligned}$$

The chemical reaction network is of deficiency one. This implies that the corresponding dynamical system has a unique positive equilibrium point independently of parameter values. Moreover, one can easily verify that it is also the only nonnegative equilibrium point. In [68], the authors recognised that the system is conservative and thus, solution trajectories are bounded for nonnegative initial conditions. We reach the same conclusion by using Theorem 2.4.3, since the chemical reaction network is (weakly) reversible. Therefore, instability of the fixed point necessarily leads to oscillatory behaviour. In [68], the parameter regions in which the fixed point is unstable were found and characterised. Additionally, the authors used numerical methods to show that the oscillatory behaviour corresponds to a limit cycle.

Lotka-Volterra system

Lotka-Volterra equations, or the predator-prey equations, are generally used to describe the dynamics of biological systems in which different species interact, of which some are the prey of others. The simplest of their type is the following two dimensional first order system:

$$\begin{aligned}\dot{x} &= \alpha x - \beta xy \\ \dot{y} &= \delta xy - \gamma y.\end{aligned}$$

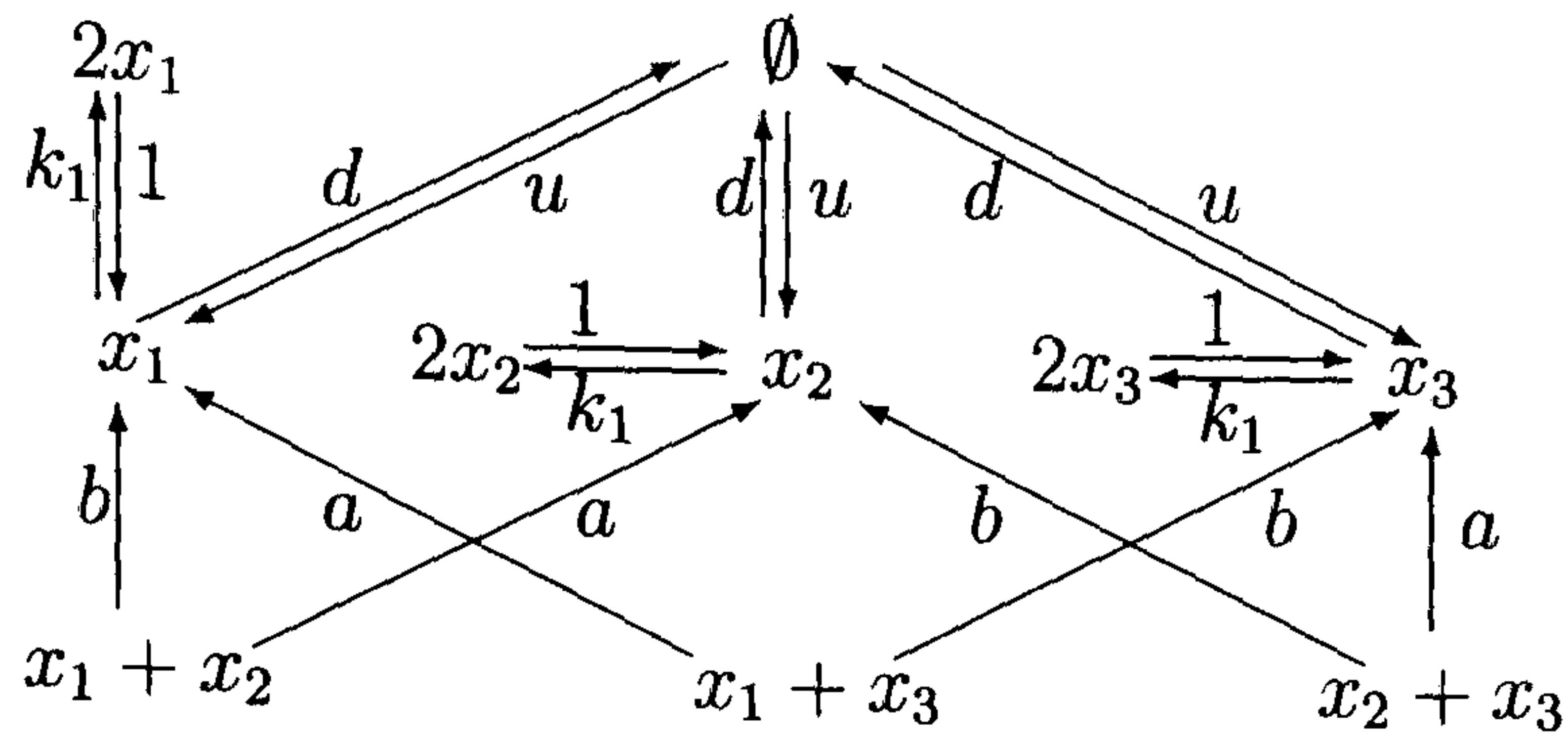
The first variable, x , represents the prey, who are assumed to have unrestricted food resources. Their reproduction rate is determined by parameter α and their death rate by β , where only death by predation is assumed. The reproduction rate of the predators, y , is determined by the amount of prey they catch and weighted by constant δ . Parameter γ influences their natural death rate.

Consider the three species Lotka-Volterra system in [69]. The ‘concentrations’ of the three species are denoted by x_i , $i = 1, 2, 3$. The terms $k_1 x_i$ and $k_2 x_i^2$ denote birth and death rate respectively. In accordance with [69], we set $k_1 - d = k_2 = 1$. Parameters $a > 0$ and $b > 0$ denote competition between the different species. Here, we add to this model a constant migration rate in to ($u > 0$) and a migration term out of the habitat ($d x_i$, $d > 0$) which is proportional to the population strength. The mathematical model of the system has now the following form:

$$\begin{aligned}\dot{x}_1 &= u + x_1(k_1 - d - k_2 x_1 - a x_2 - b x_3), \\ \dot{x}_2 &= u + x_2(k_1 - d - b x_1 - k_2 x_2 - a x_3), \\ \dot{x}_3 &= u + x_3(k_1 - d - a x_1 - b x_2 - k_2 x_3).\end{aligned}\tag{2.32}$$

In the following, we will construct a chemical reaction network that corresponds to (2.32). Note that there exists more than one valid representation. In Figure 2.10a, the ‘biologically sensible’ realisation is depicted; that is, migration of the different species is independent of each other. However, although this representation is not weakly reversible, the chemical reaction network has a ‘hidden’ weakly reversible structure (Remark 2.4.11). A weakly reversible chemical reaction network which corresponds to (2.32) is shown in Figure 2.10b. Here, we assume the some migration occurs in pairs, where the pairs consist of members from different species.

a)



b)

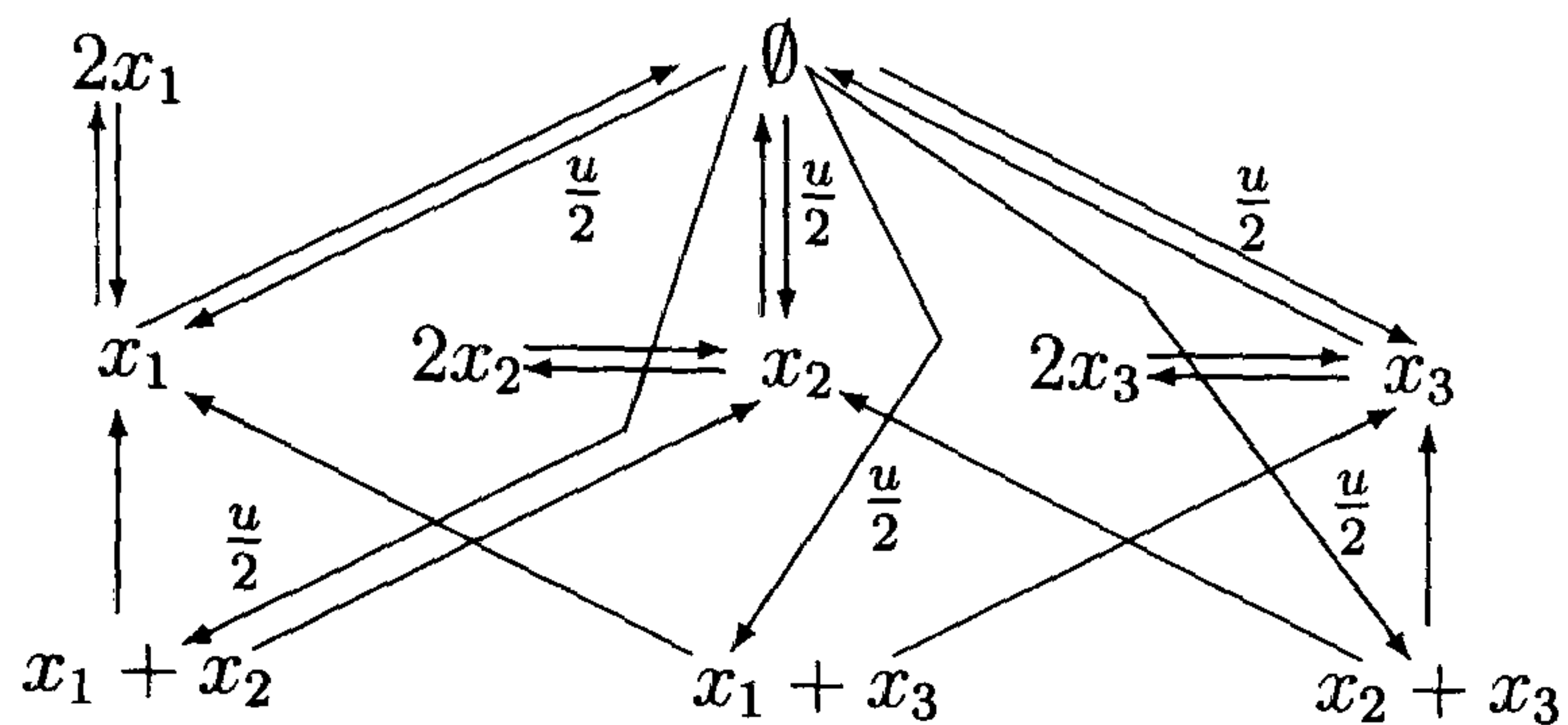


Figure 2.10: **Two valid chemical reaction network representations of (2.32).** For clarity, we omitted the reaction rates in (b) that remain identical to the rates in (a). Note that the network in (b) is weakly reversible.

By inspection, nonnegative equilibria of (2.32) are not feasible. Now, consider $\dot{x}_1 = 0$: Since $0 = u + x_1 - x_1^2 - ax_1x_2 - bx_1x_3$, Descartes' rule of signs implies that there exists a unique positive equilibrium point for x_1 (and analogously for x_2 and x_3). It is given by $x_{i_{\text{eq}}} = \frac{1 + \sqrt{1 + 4u(1 + a + b)}}{2(1 + a + b)}$, for all i . The Jacobian of (2.32) is a *circulant matrix*, its eigenvalues are $\lambda_1 = -\sqrt{1 + 4u(1 + a + b)}$ and $\lambda_{2,3} = 1 - (2 + 0.5a + 0.5b)x_{i_{\text{eq}}} \pm 0.5\sqrt{3}(a - b)x_{i_{\text{eq}}}$ (see [69] and the references therein). After some algebraic manipulations, we obtain that the Jacobian is unstable if

$$9 \left(\frac{a + b}{4 + a + b} \right)^2 > 1 + 4u(1 + a + b).$$

(Note that for $u = 0$ this simplifies to the condition $a + b > 2$ as in [69] (p. 246).) Now, since (2.32) has a weakly reversible chemical reaction network associated with it, instability of the unique fixed point necessarily leads to oscillatory behaviour. Using numerical methods, we find only limit cycles for different parameter values even for very small values of u while it was shown in [69] that for $u = 0$, $a = 0.8$ and $b = 1.3$ nonperiodic behaviour exists. This

gives rise to the question whether weakly reversible chemical reaction network can display nonperiodic behaviour.

Finally, note that ultimate boundedness of (2.32) can also be established via the Lyapunov function $V(x) = \sum_{i=1}^3 x_i$, since $\dot{V}(x) < 0$ for large values of $\sum_{i=1}^3 x_i$. (Recall that we consider only nonnegative values of x_i .) In the next example, we will provide an example of a relatively simple chemical reaction network that is weakly reversible but for which a Lyapunov function that proves ultimate boundedness cannot be readily found, which highlights the significance of Theorem 2.4.3.

A chemical oscillator

The chemical reaction network in Figure 2.11 (taken from reference [14]) is weakly reversible and of deficiency one. Thus, the corresponding dynamical system has a unique positive

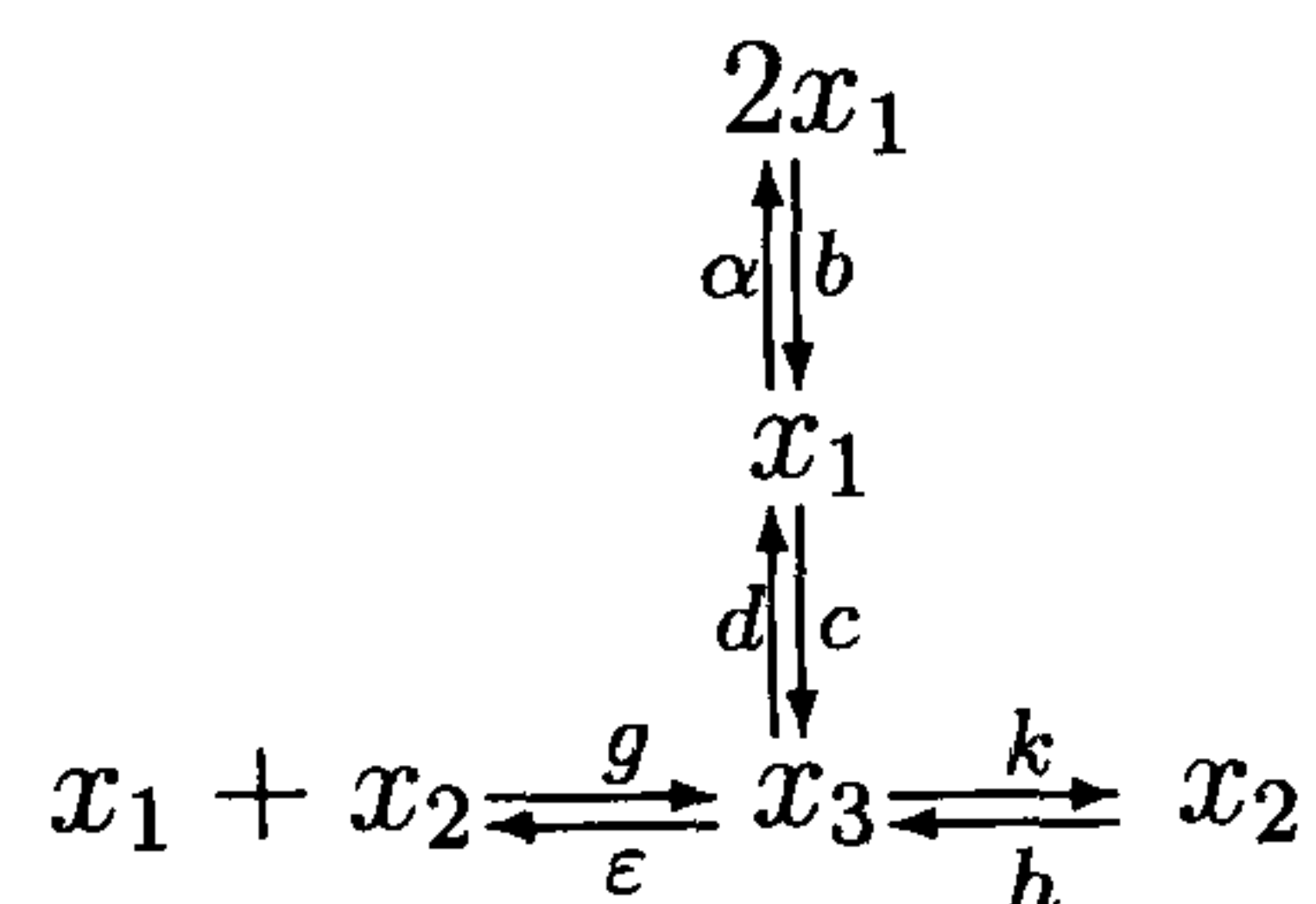


Figure 2.11: **A chemical oscillator.** The chemical reaction network presented here is weakly reversible and of deficiency one.

equilibrium point independently of parameter values. The set of ODEs describing the system is:

$$\begin{aligned}
 \dot{x}_1 &= \alpha x_1 - cx_1 - bx_1^2 + (d + \varepsilon)x_3 - gx_1x_2, \\
 \dot{x}_2 &= -hx_2 + (k + \varepsilon)x_3 - gx_1x_2, \\
 \dot{x}_3 &= -(d + k + \varepsilon)x_3 + hx_2 + cx_1 + gx_1x_2.
 \end{aligned} \tag{2.33}$$

By inspection, there is only one additional nonnegative equilibrium point, which is the origin and unstable for all parameter values. This follows from applying the Routh-Hurwitz criterion: Consider matrix $A \in \mathbb{R}^{3 \times 3}$. Its eigenvalues λ are the roots of the *characteristic polynomial*

$$|A - \lambda I_n| = \lambda^n + a_1 \lambda^{n-1} + \dots + a_n = 0, \tag{2.34}$$

where the coefficients a_i are all real, $i = 1, \dots, n$. The Routh-Hurwitz criterion (see [5]) says that necessary and sufficient condition for $\text{Re}\lambda < 0$ are

$$a_1 > 0, \quad a_3 > 0, \quad a_1 a_2 - a_3 > 0. \quad (2.35)$$

Note that a Lyapunov function that shows ultimate boundedness cannot be easily found for the dynamical system given by (2.33). However, it follows from Theorem 2.4.3 that (2.33) is ultimately bounded and thus, if the positive equilibrium is unstable then the system exhibits oscillatory behaviour. Now, using the Routh-Hurwitz criterion the parameter space can be easily explored. For example, if $\alpha = 100$, $b, c, d = 0.1$, $g = 1$, $h = 1$ and $k = 100$, we have oscillatory behaviour when $\varepsilon < 354$. In this case, we get a periodic limit cycle (Figure 2.12).

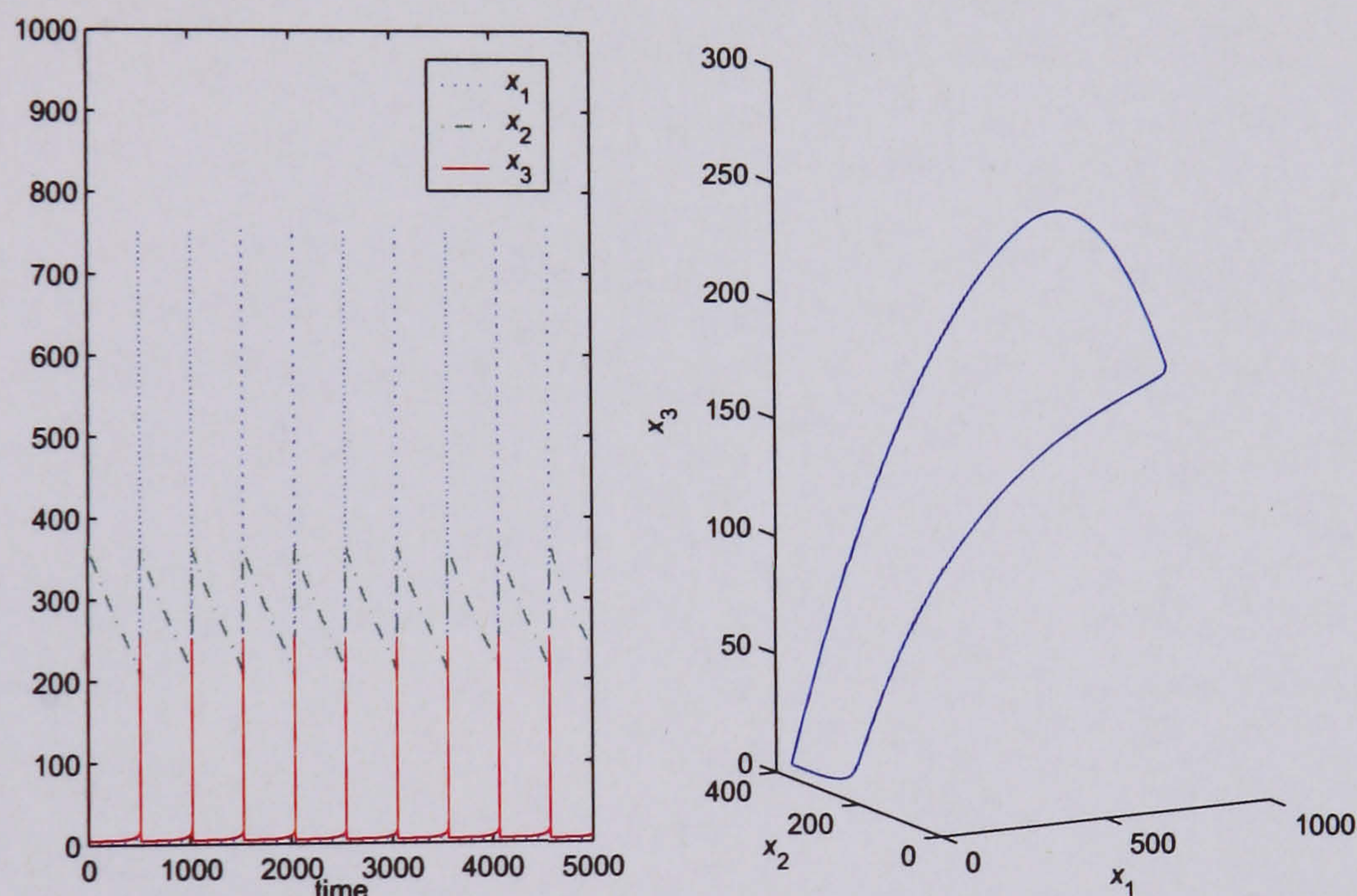


Figure 2.12: Time series and limit cycle of (2.33). $\varepsilon = 100$, all other parameter values are as in the text.

2.5 Conclusion

In this chapter, we have first presented a deficiency-zero-like theorem for chemical reaction networks that do not obey the law of mass action. We have then showed that a weakly reversible chemical reaction network has a bounded absorbing set. When dealing with

dynamical systems that have multiple equilibria, limit cycles, chaotic attractors, and combinations of these, it is often of great interest to find this set, provided it exists. By checking structural properties of the graph of the reaction network, our result provides a qualitative criterion, which is completely independent of reaction rate values, to establish that solution trajectories of a biochemical network will not diverge to infinity. Moreover, the result can also be used to characterise certain bifurcations from stationary to oscillatory behaviour as exemplified in Section 2.4. In the examples presented in this chapter, we have observed only periodic behaviour. Additionally, when we have introduced migration terms to the Lotka-Volterra model and thus, made the corresponding chemical reaction network weakly reversible previously nonperiodic behaviour of the system became periodic. Therefore, an interesting question is whether weak reversibility of a chemical reaction network excludes nonperiodic behaviour.

Chapter 3

Positivity conditions related to the stability of a dynamical system and their computational implementation

In this chapter, we give the mathematical background necessary for the second part of the thesis. In Section 3.1, we give a brief literature review on results on dynamical systems with a certain contraction property. In Section 3.2, we present the so called Bendixson's Criterion for higher dimensions. These results are based on extensions of Lyapunov theory and require positivity/negativity. They are a powerful framework for the analysis biological systems, particularly, because they can be implemented computationally. To this end we use *semidefinite programming* and the *sum of squares decomposition*. Section 3.3 provides a brief introduction to both.

3.1 Dynamical systems with a certain contraction property

In this chapter, we present dynamical systems with a certain contraction property. This property leads to stability of limit sets. In [70], D. C. Lewis studied autonomous dynamical systems with a certain local contraction property (condition (3.3)). Jean-Jacques E. Slotine [45] modernised D. C. Lewis's work and made it known to the wider audience under the name of *contraction theory* by applying it to problems in engineering. The idea behind

is that if trajectories remain in a bounded region and the distance between any two decreases with time then there exists a unique exponentially stable equilibrium point in that region. We refer the interested reader to the excellent review by Jérôme Jouffroy [71].

Bo. T. Stenström in [72] and Peter Giesl in [44] provide sufficient conditions for the existence of a unique and exponentially stable periodic orbit. Their concept is similar to the one mentioned above. The extension is possible by relaxing the requirement of contraction in the direction of the trajectory (condition (3.8)).

As we will show, the theory of dynamical systems with a certain local contraction property presents an extension of Lyapunov stability theory. Importantly, through SOSTOOLS it offers means to computationally perform a search for conditions that guarantee exponential stability of limit cycles. In this section, we provide a short overview on D. C. Lewis's, Jean-Jacques E. Slotine's and Peter Giesl's work, since we will use their results later in the thesis. In the following, we adopt Jérôme Jouffroy's notation which also corresponds to Peter Giesl's in [43, 44]. Consider the following system:

$$\dot{x} = f(x), \quad x \in \mathcal{B} \subseteq \mathbb{R}^n. \quad (3.1)$$

Importantly, in this section,

- \mathcal{B} is a compact, connected and positively invariant set of (3.1).

In his 1949 paper [70], D. C. Lewis provided all major results on what would be later known as 'contraction theory'. He used Finsler metrics for his proofs of which Riemannian metrics are a subset. For the purpose of this thesis, only conditions in the Riemannian space are of relevance and we will formulate all results in this space. First, we require the *mean value theorem* [50]:

Theorem 3.1.1. (Mean value theorem) *Assume that $f : \mathbb{R}^n \rightarrow \mathbb{R}$ is continuously differentiable at each point x of an open set $\mathcal{S} \subset \mathbb{R}^n$. Let x and y be two points of \mathcal{S} such that the line segment $L(x, y) \subset \mathcal{S}$. Then there exists a point z of $L(x, y)$ such that*

$$f(y) - f(x) = \left. \frac{\partial f}{\partial x} \right|_{x=z} (y - x). \quad (3.2)$$

It follows that if $f : \mathbb{R}^n \rightarrow \mathbb{R}^n$ then there exists a $z \in \mathbb{R}^n$ such that $z_i \in [x_i, y_i]$ for all i , $i = 1, \dots, n$, and (3.2) holds.

Now, consider the following definition:

Definition 3.1.2. (Giesl, Definition 4 of [44]) A matrix-valued C^1 -function M will be called a *Riemannian metric* if $M(x)$ is a symmetric and positive definite matrix for all $x \in \mathcal{B}$.

In this thesis, whenever we require $M(x) > 0$, we assume that is a Riemannian metric. The following theorem is a reformulation of D. C. Lewis's Theorem 9 from [70]. It establishes conditions under which asymptotic stability of solutions is guaranteed.

Theorem 3.1.3. (Lewis, Theorem 9 of [70]) *If there exists a matrix $M(x) > 0$, $x \in \mathcal{B}$, such that*

$$M(x) \frac{\partial f(x)}{\partial x} + \frac{1}{2} M'(x) < 0, \quad \forall x \in \mathcal{B}, \quad \text{with } M'(x)_{(i,j)} = \sum_{k=1}^n \frac{\partial M(x)_{(i,j)}}{\partial x_k} f_k \quad (3.3)$$

holds, then any two solutions x_1 and x_2 of (3.1) must approach each other asymptotically.

We briefly illustrate the idea behind Theorem 3.1.3. For simplicity, let $M(x) = I$. Consider any two trajectories at time t_0 , one that passes through p and one that passes $p + v$ which implies that the distance between the two is $v^T v$. Then, the distance between two trajectories after an infinitesimal time step is

$$\begin{aligned} & \left(v + \int f(p+v) - \int f(p) \right)^T \left(v + \int f(p+v) - \int f(p) \right) \\ &= \left(v + \int \frac{\partial f(p)}{\partial p} \Big|_{p=z} v \right)^T \left(v + \int \frac{\partial f(p)}{\partial p} \Big|_{p=z} v \right) \approx v^T v + 2v^T \int \frac{\partial f(p)}{\partial p} \Big|_{p=z} v < v^T v, \end{aligned}$$

where the equality holds by Theorem 3.1.1 with $z_i \in [p_i, p_i + v_i]$ for all i , the approximation since we consider an infinitesimal time interval, and the inequality follows from (3.3) for $M(x) = I$. Thus, the two trajectories approach each other. Now, the next theorem is an immediate consequence of Theorem 3.1.3. The proof is based on Lyapunov stability theory and constitutes an extension of the standard proof of Krasovskii's Theorem [45, 50].

Theorem 3.1.4. *If \mathcal{B} is a compact, convex and positively invariant set of (3.1) and there exists a matrix $M(x) > 0$ such that (3.3) holds for all $x \in \mathcal{B}$ then (3.1) has a unique asymptotically stable equilibrium point in \mathcal{B} . Additionally, if $M(x)$ is bounded in \mathcal{B} then the equilibrium point is exponentially stable.*

Proof. First, since \mathcal{B} is a compact, convex and positively invariant set of (3.1), by the Brouwer fixed point theorem, there exists at least one equilibrium point in \mathcal{B} . We denote

it by x_{eq} . Without loss of generality, let $x_{\text{eq}} = 0$, for otherwise the equilibrium point can be shifted to the origin through a change of a variables. Now, let there exists a matrix $M(x)$ such that (3.3) holds. Then, consider the Lyapunov function $V(x) = \frac{1}{2}x^T M(x)x$.

Note that \mathcal{B} is convex; recall that this means that the straight path that connects a pair of points in \mathcal{B} also lies in \mathcal{B} . Thus, it follows from Theorem 3.1.1 that there exists a z such that $z_i \in [x_i, y_i]$ for all $i, i = 1, \dots, n$, and

$$\begin{aligned} \dot{V}(x) &= x^T M(x) f(x) + \frac{1}{2} x^T M'(x) x = x^T M(x) (f(x) - f(x_{\text{eq}})) + \frac{1}{2} x^T M'(x) x \\ &= x^T \left(M(x) \frac{\partial f(x)}{\partial x} \Big|_{x=z} + \frac{1}{2} M'(x) \right) x < 0. \end{aligned}$$

This implies that x_{eq} is unique and asymptotically stable. Exponential stability follows from Theorem 4.10 in [50] if $M(x)$ is bounded, because there exist positive constants k_1, k_2, k_3 such that $k_1 x^T x < V(x) < k_2 x^T x$ and $\dot{V}(x) < -k_3 x^T x$. \square

Here, we give the discrete-time version of Theorem 3.1.4, which is proved via Lyapunov second method applied to discrete-time systems [50]. Corollary 3.1.5 is equivalent to Theorem 3 in [45]. Consider a discrete-time dynamical system given by

$$x(k+1) = f(x(k)), \quad x \in \mathbb{R}^n, \quad k = 1, 2, \dots, \quad (3.4)$$

where $f(\cdot)$ is a continuous function. Moreover, let \mathcal{B} be a compact, convex and positive invariant set for solutions of (3.4).

Corollary 3.1.5. *If there exists a matrix $M(x) > 0$ such that*

$$\frac{\partial f(x)}{\partial x}^T M(x) \frac{\partial f(x)}{\partial x} - M(x) < 0 \quad (3.5)$$

holds for all $x \in \mathcal{B}$ then (3.5) has a unique asymptotically stable equilibrium point in \mathcal{B} . Additionally, if $M(x)$ is bounded in \mathcal{B} then the equilibrium point is exponentially stable.

Proof. Note that Lyapunov second method applied to discrete-time systems guarantees asymptotic stability of x_{fix} if there exists a continuous Lyapunov function $V(x) > 0, x \neq x_{\text{fix}}$ such that

$$\Delta V = V(f(x)) - V(x) < 0, \quad x \neq x_{\text{fix}}.$$

Now, the proof is similar to the proof of Theorem 3.1.4 and hence is omitted. \square

Remark 3.1.6. Possibly inspired by D. C. Lewis's work, Larry Markus and Hidehiko Yamabe made the following conjecture about the global behaviour of a dynamical system in their 1960 paper [73]:

Conjecture 3.1.7. (Markus-Yamabe conjecture) Consider the dynamical system

$$\dot{x}(t) = f(x(t)), \quad (3.6)$$

where the vector field $f : \mathbb{R}^n \rightarrow \mathbb{R}^n$ is C^1 , and let x_{cp} be a critical point of the system, $f(x_{cp}) = 0$. If the eigenvalues of the Jacobian matrix $J(x)$ have negative real parts for all $x \in \mathbb{R}^n$, then x_{cp} is a global attractor of (3.6).

A discrete version of Conjecture 3.1.7 was given by J. P. La Salle in [74]. While the conjecture is true for one and two dimensional dynamical systems a polynomial counterexample (both continuous and discrete) was given in 1997 for all dimensions ≥ 3 [75].

The following theorem considers the case of non-autonomous dynamical systems; that is, when

$$\dot{x} = h(x, t) = f(x) + u(t), \quad x \in \mathcal{B} \subseteq \mathbb{R}^n. \quad (3.7)$$

Theorem 3.1.8. *Under the assumptions of Theorem 3.1.3, if (3.7) has no fixed points in \mathcal{B} and $u(t)$ is T -periodic then (3.7) has a unique and exponentially stable T -periodic solution in \mathcal{B} .*

Theorem 3.1.8 is similar to Theorem 10 of [70], Remark (vi) in Section 3.7 of [45], and can be also derived from the work presented in [43]. The proof in [43] is the only satisfactory one but highly involved. We therefore provide only a brief sketch: First, Peter Giesl showed that the distance between two trajectories with initial conditions (t_0, x_0) and (t_0, x_1) is exponentially decreasing, which follows from Theorem 3.1.3, and that their ω -limit sets are equal. He then proved that the ω -limit sets of two adjacent points (t_0, x_0) and (t_1, x_1) are also equal and that the ω -limit set of all points in \mathcal{B} is actually the same. Finally, he concluded the proof by showing that this ω -limit set is an exponentially stable T -periodic orbit.

Note that this theorem implies that an autonomous dynamical system with a T -periodic input $u(t)$ for which (3.3) holds will entrain to the input's period. Furthermore, D. C. Lewis showed that if (3.3) holds and $f(x)$ does not depend explicitly on t then it is impossible to have a solution other than a stable equilibrium point in \mathcal{B} . Clearly, chaotic behaviour

is also excluded. In the following, we present an important result by Peter Giesl on the exponential stability of the periodic solution of autonomous dynamical systems.

Theorem 3.1.9. (Giesl, Theorem 5 of [44]) *Let $M(x)$ be a Riemannian metric with its directional derivative $M'(x)$ given by:*

$$M'(x)_{(i,j)} = \sum_{k=1}^n \frac{\partial M(x)_{(i,j)}}{\partial x_k} f_k.$$

If for all $x \in \mathcal{B}$,

$$w^T \left(M(x) \frac{\partial f(x)}{\partial x} + \frac{1}{2} M'(x) \right) w < 0, \quad \forall w \text{ such that } w^T M(x) f(x) = 0, \quad (3.8)$$

then (3.1) has either a unique, exponentially stable periodic orbit or fixed point in \mathcal{B} .

We briefly illustrate the idea behind condition (3.8), which guarantees that the two trajectories approach each other. For simplicity, let $M(x) = I$. Consider any two trajectories at time t_0 , one that passes through p and one that passes $p + \delta w$. Then, we require that the distance between $f(p)$ and $f(p + \delta w)$ decreases in the normal direction of $f(p)$. Thus, a sufficient condition for the two trajectories to approach each other is that

$$\cos \varphi < 0, \quad (3.9)$$

where φ is defined as in Figure 3.1.

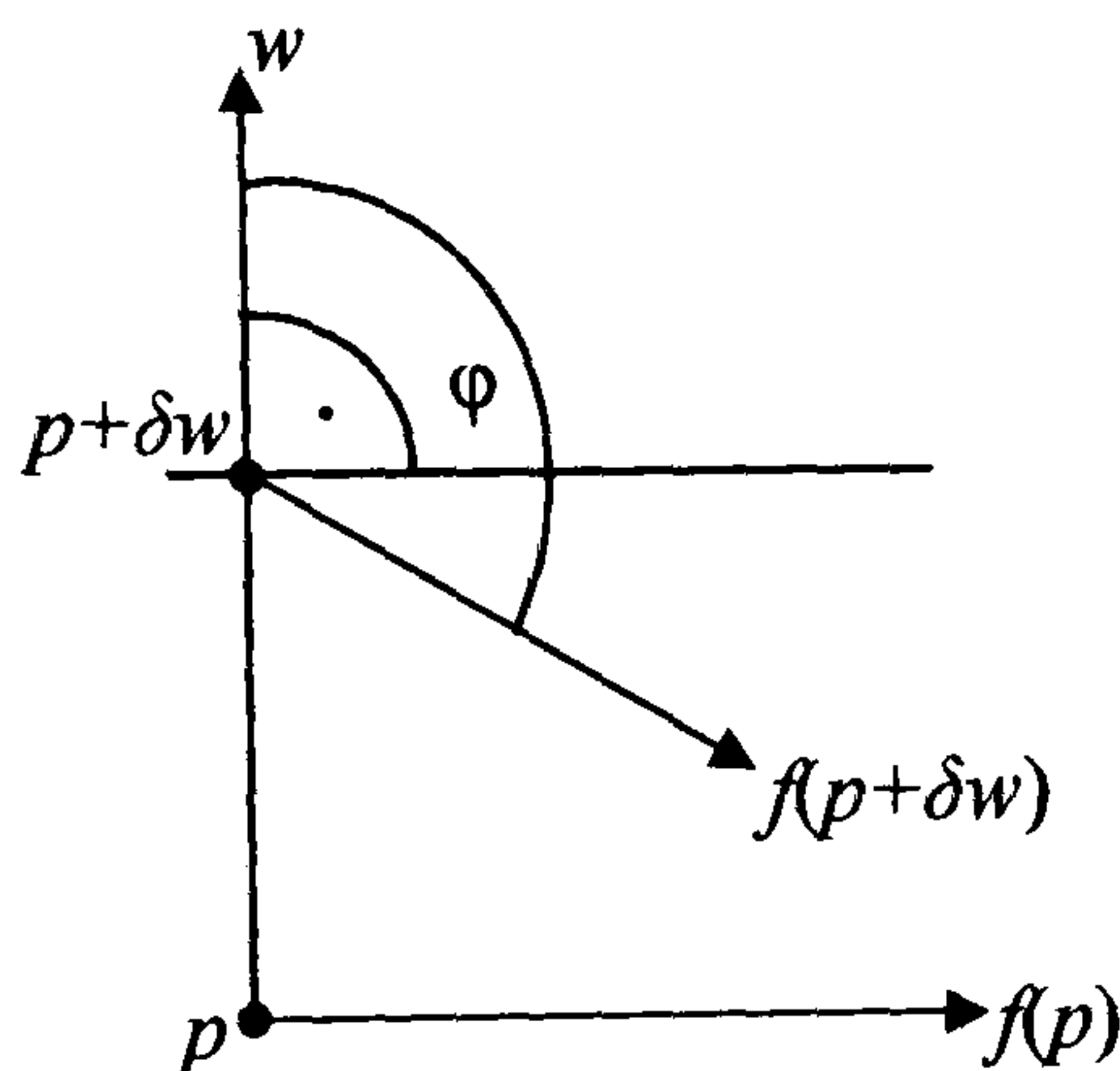


Figure 3.1: A sufficient condition for two trajectories to approach each other.

Since $\cos \varphi$ is formally defined as $\cos \varphi = \frac{f(p+\delta w)^T w}{|e^T f(p+\delta w) e^T w|}$, it follows that (3.9) holds if $f(p + \delta w)^T w < 0$. Now, let us consider the local behaviour of the two trajectories, that is, for small values of δ . Then,

$$f(p + \delta w)^T w \approx \left(f(p) + \delta \frac{\partial f(x)}{\partial x} \Big|_{x=p} w \right)^T w = \delta \left(\frac{\partial f(x)}{\partial x} \Big|_{x=p} w \right)^T w < 0.$$

The equality follows since $f^T(p)w = 0$ and the inequality from (3.8) for $M(x) = I$. Furthermore, Peter Giesl also proved that if there exists only one periodic orbit in \mathcal{B} and it is exponentially stable then (3.8) must hold. In [44], he extends his results to the case in which f depends explicitly on t and shows that the sufficient conditions are also necessary. For instance, consider the following definition and theorem:

Definition 3.1.10. (Giesl, Definition 2.3 of [43]) A matrix-valued C^1 -function M will be called a Riemannian metric if $M(x, t)$ is a symmetric and positive definite matrix for all $x \in \mathcal{B}$ and all t , and $M(x, t) = M(x, t + T)$ for all $x \in \mathcal{B}$ and all t .

Theorem 3.1.11. (Giesl, Theorem 5.1 of [43]) Assume that, in (3.7), $f(x, t)$ is a periodic function with period T , and all partial derivatives of order one with respect to x are continuous functions of t and x . Then, the following two conditions are equivalent:

- (i) The system has an exponentially asymptotically stable T -periodic orbit in \mathcal{B} .
- (ii) There is a Riemannian metric M such that

$$M(x, t)J(x) + \frac{1}{2}M'(x, t) < 0 \text{ with } M'_{(i,j)} = \frac{\partial M_{(i,j)}}{\partial t} + \sum_{k=1}^n \frac{\partial M_{(i,j)}}{\partial x_k} f_k, \quad \forall x \in \mathcal{B}, \forall t. \quad (3.10)$$

In fact, Theorem 3.1 of [43] establishes that (3.10) is strictly less than a constant $\beta < 0$.

3.2 Bendixson's Criterion for higher dimensions

In this section, we present the so called Bendixson's Criterion for higher dimensions [76, 77]. First, we require a definition from [77]. The *second additive compound* $A^{[2]}$ of matrix $A \in \mathbb{R}^{n \times n}$ is the $\binom{n}{2} \times \binom{n}{2}$ matrix defined as follows. For any integer $i = 1, \dots, \binom{n}{2}$, let $(i) = (i_1, i_2)$ be the i th member in the lexicographic ordering of integer pairs (i_1, i_2) such that $1 \leq i_1 < i_2 \leq n$. Then, the element of the i th row and j th column of $A^{[2]}$ is

$$\left\{ \begin{array}{ll} A_{(i_1, i_1)} + A_{(i_2, i_2)} & \text{if } (j) = (i), \\ (-1)^{r+s} A_{(i_r, j_s)} & \text{if exactly one entry } i_r \text{ of } (i) \text{ does not} \\ & \text{occur in } (j) \text{ and } j_s \text{ does not occur in } (i), \\ 0 & \text{if neither entry from } (i) \text{ occurs in } (j). \end{array} \right.$$

For example, if $n = 3$ then $(1) = (1, 2)$, $(2) = (1, 3)$, $(3) = (2, 3)$ and

$$A^{[2]} = \begin{bmatrix} A_{(1,1)} + A_{(2,2)} & A_{(2,3)} & -A_{(1,3)} \\ A_{(3,2)} & A_{(1,1)} + A_{(3,3)} & A_{(1,2)} \\ -A_{(3,1)} & A_{(2,1)} & A_{(2,2)} + A_{(3,3)} \end{bmatrix};$$

if $n = 4$ then $(1) = (1, 2)$, $(2) = (1, 3)$, $(3) = (1, 4)$, $(4) = (2, 3)$, $(5) = (2, 4)$, $(6) = (3, 4)$ and $A^{[2]} =$

$$\begin{bmatrix} A_{(1,1)} + A_{(2,2)} & A_{(2,3)} & A_{(2,4)} & -A_{(1,3)} & -A_{(1,4)} & 0 \\ A_{(3,2)} & A_{(1,1)} + A_{(3,3)} & A_{(3,4)} & A_{(1,2)} & 0 & -A_{(1,4)} \\ A_{(4,2)} & A_{(4,3)} & A_{(1,1)} + A_{(4,4)} & 0 & A_{(1,2)} & A_{(1,3)} \\ -A_{(3,1)} & A_{(2,1)} & 0 & A_{(2,2)} + A_{(3,3)} & A_{(3,4)} & -A_{(2,4)} \\ -A_{(4,1)} & 0 & A_{(2,1)} & A_{(4,3)} & A_{(2,2)} + A_{(4,4)} & A_{(2,3)} \\ 0 & -A_{(4,1)} & A_{(3,1)} & -A_{(4,2)} & A_{(3,2)} & A_{(3,3)} + A_{(4,4)} \end{bmatrix}.$$

Note that $(A + B)^{[2]} = A^{[2]} + B^{[2]}$ and that the eigenvalues of $\frac{1}{2}(A + A^T)^{[2]}$ are given by $\lambda_i + \lambda_j$, where λ_i, λ_j are the eigenvalues of $\frac{1}{2}(A + A^T)$, $1 \leq i < j \leq n$ [78].

Let $\mathcal{B} \subseteq \mathbb{R}^n$ be a compact, simply connected and positively invariant set of $\dot{x} = f(x)$, and $x \in \mathcal{B}$. Then, the following theorem by Michael Y. Li and James S. Muldowney proves global asymptotic stability (Theorem 2.5 in [79] with equality (2.6) and inequality (2.7) from [77]).

Theorem 3.2.1. (Li's and Muldowney's theorem on global asymptotic stability)

Let the origin be the unique equilibrium point of

$$\dot{x} = f(x), \quad x \in \mathcal{B}. \quad (3.11)$$

If there exists a $\binom{n}{2} \times \binom{n}{2}$ matrix $P(x)$ and

$$\frac{1}{2}P'(x) + P(x) \left(\frac{\partial f(x)}{\partial x} \right)^{[2]} < 0, \quad \forall x \in \mathcal{B}, \quad (3.12)$$

then the origin is globally asymptotically stable. Here,

$$P'_{(i,j)}(x) = \sum_{k=1}^n \frac{\partial P_{(i,j)}(x)}{\partial x_k} f_k(x).$$

Consider the variational equation

$$\dot{z} = \frac{\partial f(x)}{\partial x} \quad (3.13)$$

and let $\hat{z}(t)$ and $\tilde{z}(t)$ be solutions of (3.13). Let \wedge denote the exterior product. Then, the time evolution of $y(t) = \hat{z}(t) \wedge \tilde{z}(t)$ is given by

$$\dot{y} = \left(\frac{\partial f(x)}{\partial x} \right)^{[2]} y. \quad (3.14)$$

The proof of Theorem 3.2.1 uses the fact that (3.14) describes the local evolution in \mathcal{B} of measures of 2-dimensional surfaces under the dynamics of (3.11). In other words, (3.12) implies that the area of surfaces decrease under the dynamics of (3.11).

Note that Theorem 3.2.1 proves asymptotic stability of the equilibrium point and not exponential stability as contraction theory does (Section 3.1). Therefore, the following remark comes as no surprise.

Remark 3.2.2. Consider

$$\dot{x} = f(x) + u(t), \quad x \in \mathcal{B}, \quad (3.15)$$

where $u(t)$ is a bounded T -periodic input. It was shown in [76] that the fact that (3.12) holds does not imply that bounded solutions of (3.15) converge to a T -periodic solution.

Finally, note that Theorem 3.2.1 implies that if (3.12) holds then periodic solutions cannot exist. Moreover, this is also true if $\frac{1}{2}P'(x) + P(x) \left(\frac{\partial f(x)}{\partial x} \right)^{[2]} > 0, \forall x \in \mathcal{B}$ (see [76,77]). Thus, if any of the two conditions hold then periodic solutions cannot exist, which means that this is a higher dimensional version of Bendixson's Criterion (which is for $n = 2$).

3.3 Interior-point methods and semidefinite programming

In this section, we provide the mathematical tools that we use in the remainder of the thesis in order to computationally implement minimisation problems that arise in the field of biological systems modelling. Many optimisation problems can be solved using *semidefinite programmes* [80], which were shown to be solved efficiently both theoretically and practically via *interior-point methods* [81]. These methods were introduced in order to solve optimisation problems with nonlinear inequality constraints. In the following,

we provide only a brief introduction to the topic extracted from references [80, 81]. The interested reader is referred to the paper by Lieven Vandenberghe and Stephen Boyd [80] and the excellent text book by the same authors [81]. Before we introduce the concept of how to solve minimisation problems and how they relate to semidefinite programming, we need some definitions from [81].

Definition 3.3.1. A *cone* C is defined as follows: if $x \in C$ and $\theta \geq 0$ then $\theta x \in C$, where θ is a constant.

Definition 3.3.2. A set C is said to be *convex* if for any $x_1, x_2 \in C$ and any $\theta, 0 \leq \theta \leq 1$, we have $\theta x_1 + (1 - \theta)x_2 \in C$.

Roughly speaking, if, for all $x_1, x_2 \in C$, the straight path that connects x_1 and x_2 lies in C then the set is convex.

Definition 3.3.3. Let C be a cone. The set $C^* = \{y | x^T y \geq 0 \text{ for all } x \in C\}$ is called the *dual cone* of C . Moreover, if $C = C^*$ then it is called *self-dual*.

It follows that the set of symmetric positive semidefinite matrices S_+^n is a convex cone, since for $\theta_1, \theta_2 \geq 0$ and $A, B \in S_+^n$ it follows that $\theta_1 A + \theta_2 B \in S_+^n$. The latter follows from the fact that if $x \in \mathbb{R}^n$, $A \geq 0$ and $B \geq 0$ then

$$x^T(\theta_1 A + \theta_2 B)x = \theta_1 x^T A x + \theta_2 x^T B x \geq 0.$$

3.3.1 The Newton method

Consider the following unconstrained minimisation problem:

$$\text{minimise } f(x), \tag{3.16}$$

where $f(x)$ is convex and twice continuously differentiable, $x \in \mathbb{R}^n$. It is solved by producing a sequence $x^{(k)}$, where

$$x^{(k+1)} = x^{(k)} + s^{(k)} \Delta x^{(k)}, \quad k = 1, \dots \tag{3.17}$$

and the *step size* $s^{(k)} > 0$ if $x^{(k)}$ is non-optimal [81]. It follows from convexity that $\nabla f(x^{(k)})^T (y - x^{(k)}) \geq 0$ implies that $f(y) \geq f(x^{(k)})$ [81]. Thus, $\Delta x^{(k)}$ should satisfy

$$\nabla f(x^{(k)})^T \Delta x^{(k)} < 0.$$

In the *Newton method*,

$$\Delta x = \Delta x_{nt} = -\nabla^2 f(x)^{-1} \nabla f(x)$$

is called the *Newton step*. Note that the Newton step is *steepest descent direction* [81]. Since $\nabla^2 f(x)$ is positive definite (see §3.1.4 in [81]) it follows that

$$\nabla f(x)^T \Delta x_{nt} = -\nabla f(x)^T \nabla^2 f(x)^{-1} \nabla f(x) < 0$$

as long as $\nabla f(x) \neq 0$. The *Newton decrement* is given by

$$\lambda(x) = (\nabla f(x)^T \nabla^2 f(x)^{-1} \nabla f(x))^{1/2}.$$

This quantity is useful as a stopping criterion for sequence (3.17). For instance, if we denote the second-order Taylor approximation of f by \hat{f} then

$$f(x) - \hat{f}(x + \Delta x_{nt}) = \frac{1}{2} \lambda(x)^2.$$

Thus, if $\frac{1}{2} \lambda(x)^2$ is small then so are changes in the value of $f(x)$ in the direction of the Newton step, which implies that x is close to the optimal value x^* . The algorithm that solves (3.16) is called the *pure Newton method*¹ and is outlined below [81].

Algorithm 3.3.4.

given starting point x , tolerance ϵ .

repeat

1. Compute the Newton step Δx_{nt} and decrement $\lambda(x)$.
2. *Stopping criterion.* **quit** if $\frac{\lambda^2}{2} \leq \epsilon$.
3. *Update.* $x := x + \Delta x_{nt}$.

Now, consider the following equality constrained minimisation problem:

$$\begin{aligned} &\text{minimise} && f(x), \\ &\text{subject to} && Ax = b. \end{aligned} \tag{3.18}$$

The difference to (3.16) is that not every x and not every descent direction given by the Newton step Δx_{nt} is feasible.

¹The pure Newton method uses a fixed step size $s = 1$ as opposed to the *damped* or *guarded* Newton method, which updates s at each iteration via a *backtracking line search* (consult [81] on the topic).

To obtain a feasible Δx_{nt} , we have to solve the following minimisation problem which replaces the objective function in (3.18) with its second-order Taylor approximation near x [81]:

$$\begin{aligned} \text{minimise} \quad & \widehat{f}(x+v) = f(x) + \nabla f(x)^T v + \frac{1}{2} v^T \nabla^2 f(x) v, \\ \text{subject to} \quad & A(x+v) = b. \end{aligned} \tag{3.19}$$

This problem can be solved analytically by solving

$$\begin{bmatrix} \nabla^2 f(x) & A^T \\ A & 0 \end{bmatrix} \begin{bmatrix} \Delta x_{\text{nt}} \\ w \end{bmatrix} = \begin{bmatrix} -\nabla f(x) \\ 0 \end{bmatrix} \tag{3.20}$$

(see reference [81]). This guarantees that Δx_{nt} is a feasible direction; that is, $A\Delta x_{\text{nt}} = 0$. The matrix in (3.20) is the so called *Karush-Kuhn-Tucker (KKT)* matrix. The Newton step is defined only when this matrix is nonsingular. (In the next section, we will require w to substitute for ν the dual variable.) With the Δx_{nt} which is the solution of (3.20) we can now solve (3.18) by means of Algorithm 3.3.4.

Additionally, if a feasible starting point for x is unknown then the following equation must be solved in order to obtain a feasible one [81]:

$$\begin{bmatrix} \nabla^2 f(x) & A^T \\ A & 0 \end{bmatrix} \begin{bmatrix} \Delta x \\ w \end{bmatrix} = - \begin{bmatrix} \nabla f(x) \\ Ax - b \end{bmatrix}. \tag{3.21}$$

Then, a feasible starting point is given by $x + \Delta x$. In the following section, we show how to deal with minimisation problems that contain inequality constraints.

3.3.2 Interior-point methods

In this section, we discuss *interior-point methods* for solving semidefinite programmes. These methods were introduced in order to solve optimisation problems with nonlinear inequality constraints. We define the *Lagrangian* associated with (3.23) by [81]:

$$L(x, \lambda, \nu) = f_0(x) + \sum_{i=1}^m \lambda_i f_i(x) + \nu^T (Ax - b).$$

We call the vectors $\lambda \in \mathbb{R}^m$ and $\nu \in \mathbb{R}^p$ the *dual variables*. Let $x \in \mathcal{D} \subseteq \mathbb{R}^n$, the *Lagrange dual function* is given by [81]:

$$g(\lambda, \nu) = \inf_{x \in \mathcal{D}} L(x, \lambda, \nu) = \inf_{x \in \mathcal{D}} \left(f_0(x) + \sum_{i=1}^m \lambda_i f_i(x) + \nu^T (Ax - b) \right).$$

Let p^* denote the optimal value of (3.23). Then, $g(\lambda, \nu) \leq p^*$ for any $\lambda \geq 0$, since for any feasible point, denoted by \tilde{x} , of (3.23) the following holds $f_i(\tilde{x}) \leq 0, \forall i, A\tilde{x} - b = 0$ and thus, $\sum_{i=1}^m \lambda_i f_i(\tilde{x}) + \nu^T(A\tilde{x} - b) \leq 0$. This implies that

$$L(\tilde{x}, \lambda, \nu) = f_0(\tilde{x}) + \sum_{i=1}^m \lambda_i f_i(\tilde{x}) + \nu^T(A\tilde{x} - b) \leq f_0(\tilde{x})$$

and therefore,

$$g(\lambda, \nu) = \inf_{x \in \mathcal{D}} L(x, \lambda, \nu) \leq L(\tilde{x}, \lambda, \nu) \leq f_0(\tilde{x}).$$

This leads to the following *Lagrange dual problem* that is associated with (3.23):

$$\begin{aligned} & \text{maximise} && g(\lambda, \nu) \\ & \text{subject to} && \lambda \geq 0. \end{aligned} \tag{3.22}$$

The barrier method

Here, we present the *barrier method* [81]. Consider the following minimisation problem with inequality constraints

$$\begin{aligned} & \text{minimise} && f_0(x), \quad x \in \mathbb{R}^n \\ & \text{subject to} && f_i(x) \leq 0, \quad i = 1, \dots, m \\ & && Ax = b, \quad A \in \mathbb{R}^{p \times n} \end{aligned} \tag{3.23}$$

which we rewrite as

$$\begin{aligned} & \text{minimise} && f_0(x) + \sum_{i=1}^m I_-(f_i(x)), \\ & \text{subject to} && Ax = b. \end{aligned} \tag{3.24}$$

$I_-(\cdot)$ is the following *indicator function* [81]:

$$I_-(u) = \begin{cases} 0 & u \leq 0 \\ \infty & u > 0. \end{cases}$$

Since the objective function is not differentiable in general, we approximate the indicator function as follows [81]:

$$\hat{I}_-(u) = -\frac{1}{t} \log(-u).$$

Parameter $t > 0$ determines the quality of the approximation (see Figure 3.2). Substituting the barrier function in (3.24) by the *logarithmic barrier function* $\hat{I}_-(u)$ leads to the following problem:

$$\begin{aligned} &\text{minimise} && f_0(x) - \sum_{i=1}^m \frac{1}{t} \log(-f_i(x)), \\ &\text{subject to} && Ax = b, \end{aligned}$$

or equivalently:

$$\begin{aligned} &\text{minimise} && tf_0(x) - \sum_{i=1}^m \log(-f_i(x)), \\ &\text{subject to} && Ax = b. \end{aligned} \tag{3.25}$$

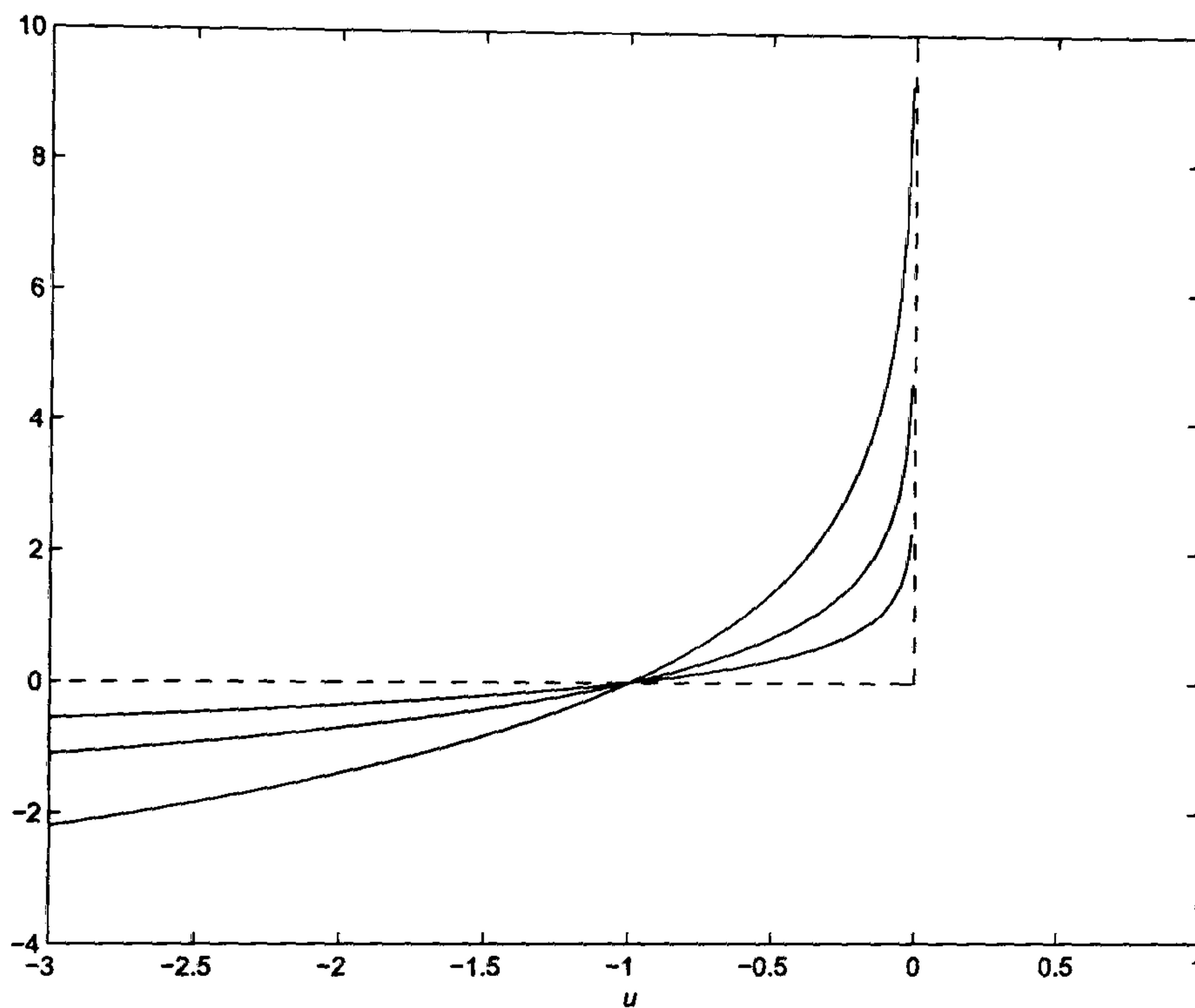


Figure 3.2: **The logarithmic barrier function.** The dashed lines show the function $I_-(u)$, and the solid curves show $\hat{I}_-(u) = -\frac{1}{t} \log(-u)$, for $t = 0.5, 1, 2$. The curve for $t = 2$ gives the best approximation [81].

The minimisation problem given by (3.25) can be solved via the Newton method. As apparent from Figure 3.2, a large t is necessary to ensure that the solution of (3.25) is close to the solution of the original problem (3.23). However, the Newton method runs into computational difficulties for large t [81]. It was shown that the problem can

be avoided by solving (3.25) stepwise, increasing t each time, and starting each Newton minimisation at the solution for the previous value of t , with stopping criterion $\frac{m}{t} < \epsilon$, where $\frac{m}{t} = f_0(x^*(t)) - g(\lambda^*(t), \nu^*(t))$ is the so called duality gap η for any feasible x^* [81]. The algorithm for the barrier method is outlined below [81].

Algorithm 3.3.5.

given strictly feasible x , $t := t^{(0)}$, $\mu > 1$, tolerance $\epsilon > 0$.

repeat

1. Compute $x^*(t)$ by solving (3.25), starting at x .
2. Update. $x := x^*(t)$.
3. Stopping criterion. quit if $\frac{m}{t} \leq \epsilon$.
3. Increase t . $t := \mu t$.

Note that the Algorithm 3.3.6 requires strict feasibility of x ; that is, $f_i(x) < 0$ must hold for all i . In order to obtain a strictly feasible starting point x if it exists, we have to solve the following minimisation problem [81]:

$$\begin{aligned} & \text{minimise} && s \\ & \text{subject to} && f_i(x) \leq s, \quad i = 1, \dots, m \\ & && Ax = b. \end{aligned} \tag{3.26}$$

Primal-dual interior-point method

In this section, we briefly explain a simple primal-dual interior-point method. It is similar to the barrier method but not quite. The main difference is that the search direction is derived from Newton's method, applied to modified KKT equations (3.27). This can lead to convergence that is better than linear convergence [81]. Thus, that primal-dual interior-point method often outperforms the barrier method, particularly, when solving problems in semidefinite programming. For instance, the primal-dual interior method solves both problems, (3.23) and (3.22), simultaneously. The search direction is given by $\Delta y_{pd} = (\Delta x_{pd}, \Delta \lambda_{pd}, \Delta \nu_{pd})$, which is the solution of

$$\begin{bmatrix} \nabla^2 f_0(x) + \sum_{i=1}^m \lambda_i \nabla^2 f_i(x) & Df(x)^T & A^T \\ -\text{diag}(\lambda) Df(x) & -\text{diag}(f(x)) & 0 \\ A & 0 & 0 \end{bmatrix} \begin{bmatrix} \Delta x \\ \Delta \lambda \\ \Delta \nu \end{bmatrix} = - \begin{bmatrix} r_{\text{dual}} \\ r_{\text{cent}} \\ r_{\text{pri}} \end{bmatrix}, \tag{3.27}$$

where

$$\begin{aligned}
 Df(x) &= \begin{bmatrix} \nabla f_1(x)^T \\ \vdots \\ \nabla f_m(x)^T \end{bmatrix}, \\
 r_{\text{dual}} &= \nabla f_0(x) + Df(x)^T \lambda = A^T \nu \\
 r_{\text{cent}} &= Ax - b \\
 r_{\text{pri}} &= -\text{diag}(\lambda) f(x) - \frac{1}{t} e, \quad e = [1 \dots 1]^T.
 \end{aligned}$$

In the primal-dual interior-point method, x, λ, ν are not necessarily feasible. Thus, we introduce the *surrogate duality gap* $\hat{\eta}(x, \lambda) = -f(x)^T \lambda$ for any x such that $f(x) \leq 0$ and any $\lambda \gg 0$. The algorithm for the primal-dual interior-point method is outlined below [81].

Algorithm 3.3.6.

given x that satisfies $f(x) \ll 0, \lambda \gg 0, \mu > 1, \epsilon_{\text{feas}} > 0, \epsilon > 0$.

repeat

1. *Determine* t . Set $t := \frac{\mu m}{\hat{\eta}}$
2. Compute primal-dual search direction Δy_{pd} .
3. *Update*. $y := y + \Delta y_{\text{pd}}$.

until $\|r_{\text{pri}}\|_2 \leq \epsilon_{\text{feas}}, \|r_{\text{dual}}\|_2 \leq \epsilon_{\text{feas}},$ and $\hat{\eta} \leq \epsilon$.

3.3.3 Semidefinite programming

In the following we provide a brief overview on semidefinite programming, particularly, on the parts related to the work presented in this thesis. In semidefinite programming, we replace the nonnegative orthant constraint of linear programming by the cone of positive semidefinite matrices and pose the following minimisation problem [80]:

$$\begin{aligned}
 &\text{minimise} && c^T x \\
 &\text{subject to} && F(x) \geq 0, \text{ where} \\
 &&& F(x) = F_0 + \sum_{i=1}^n x_i F_i.
 \end{aligned} \tag{3.28}$$

Here, $x \in \mathbb{R}^n$ is the free variable. The so called problem data, which are given, are the vector $c \in \mathbb{R}^n$ and the matrices $F_j \in \mathbb{R}^{m \times m}, j = 0, \dots, n$. Note that $F(x) \geq 0$

means that $F(x)$ is positive semidefinite; that is, $z^T F(x) z \geq 0$ for all $z \in \mathbb{R}^n$. Moreover, $z^T F(x) z = \frac{1}{2} z^T (F(x) + F(x)^T) z = z^T \hat{F}(x) z$. Thus, if $F(x)$ is not symmetric (or for that matter F_j) then we can replace it by $\hat{F}(x)$ ($\hat{F}_j(x)$, $j = 0, \dots, n$).

The *dual* problem associated with the semidefinite program given by (3.28) is [80]:

$$\begin{aligned} & \text{maximise} && -\text{trace}(F_0 Z) \\ & \text{subject to} && \text{trace}(F_i Z) = c_i, \quad i = 1, \dots, n \\ & && Z \geq 0. \end{aligned} \tag{3.29}$$

Here, the variable is the matrix $Z \in R^{m \times m}$. Note that solutions of the primal problem provides upper bounds on solution of the dual and vice versa. This is called *weak duality* and holds since

$$\begin{aligned} c^T x + \text{trace}(F_0 Z) &= \sum_{i=1}^n c_i x_i + \text{trace}(F_0 Z) = \sum_{i=1}^n \text{trace}(F_i Z) x_i + \text{trace}(F_0 Z) \\ &= \text{trace}\left(\sum_{i=1}^n F_i x_i + F_0\right) Z \geq 0. \end{aligned}$$

The inequality is true because of self-duality of the positive semidefinite cone [82]. If the inequality holds strictly then we speak of *strong duality*.

The results presented in this thesis that require the solution of a semidefinite program have been obtained by using YALMIP. YALMIP is a free, third-party MATLAB toolbox for solving semidefinite programs [83], which relies on the solver SeDuMi [84].

3.4 The sum of squares decomposition

In this section, we introduce the sum of squares decomposition. For problem data that consists of polynomials of any degree, it changes the requirement of positivity to the condition that the polynomial function is a sum of squares. This is of great advantage, since we can now consider nonlinear problem data. However, since this is only a sufficient condition for positivity it can at times be quite conservative. In other words, a function can be positive without being a sum of squares. David Hilbert proved that equivalence of nonnegativity and the sum of squares condition is true in general only for the following three cases [82]:

- for polynomials with only one variable,

- for the case of quadratic polynomials,
- and, somewhat surprising, for quartic polynomials in two variables.

In [85], it was shown that for all other cases if the degree of the polynomial is given then as the number of variables grows so does the number of nonnegative polynomials that are not sums of squares.

Consider the real-valued polynomial function $F(x)$ of degree $2d$, $x \in \mathbb{R}^n$. A sufficient condition for $F(x)$ to be nonnegative is that it can be decomposed into a *sum of squares* [82]:

$$F(x) = \sum_i f_i^2(x) \geq 0,$$

where f_i are polynomial functions. Now, $F(x)$ is a sum of squares if and only if there exists a positive semidefinite matrix Q and

$$F(x) = z^T Q z, \quad z = [1, x_1, x_2, \dots, x_n, x_1 x_2, \dots, x_n^d].$$

The length of vector z is $\ell = \binom{n+d}{d}$. Note that Q is not necessarily unique. However, $\sum_i f_i^2(x) = z^T Q z$ poses certain constraints on Q of the form $\text{trace}(A_j Q) = c_j$, where A_j and c_j are appropriate matrices and constants respectively. As an illustration consider the following polynomial function (Example 3.5 in [82]), where $z_1 = x_1^2$, $z_2 = x_2^2$, $z_3 = x_1 x_2$:

$$\begin{aligned} F(x) &= 2x_1^4 + 2x_1^3 x_2 - x_1^2 x_2^2 + 5x_2^4 \\ &= \begin{bmatrix} x_1^2 \\ x_2^2 \\ x_1 x_2 \end{bmatrix}^T \begin{bmatrix} q_{11} & q_{12} & q_{13} \\ q_{12} & q_{22} & q_{23} \\ q_{13} & q_{23} & q_{33} \end{bmatrix} \begin{bmatrix} x_1^2 \\ x_2^2 \\ x_1 x_2 \end{bmatrix} \\ &= q_{11} x_1^4 + q_{22} x_2^4 + (q_{33} + 2q_{12}) x_1^2 x_2^2 + 2q_{13} x_1^3 x_2 + 2q_{23} x_1 x_2^3. \end{aligned}$$

This leads to the following set of linear equalities:

$$q_{11} = 2, \quad q_{22} = 5, \quad q_{33} + 2q_{12} = -1, \quad 2q_{13} = 2, \quad 2q_{23} = 0.$$

Thus, $j = 1, \dots, 5$, and, for example, $c_1 = 2$, $c_3 = -1$,

$$A_1 = \begin{bmatrix} 1 & 0 & 0 \\ 0 & 0 & 0 \\ 0 & 0 & 0 \end{bmatrix}, \quad \text{and} \quad A_3 = \begin{bmatrix} 0 & 1 & 0 \\ 1 & 0 & 0 \\ 0 & 0 & 1 \end{bmatrix}.$$

In general, in order to find Q , we solve the optimisation problem associated with the following semidefinite program:

$$\begin{aligned}
& \text{minimise} && \text{trace}(A_0 Q) \\
& \text{subject to} && \text{trace}(A_j Q) = c_j, \quad j = 1, \dots, m \\
& && Q \geq 0.
\end{aligned} \tag{3.30}$$

Remark 3.4.1. Some additional issues:

- Consider a rational function $F(x)$; that is, $F(x) = \frac{f(x)}{g(x)}$, where $f(x)$ and $g(x)$ are polynomial functions. Then, $F(x) \geq 0$ if $g^2(x) > 0$ and (3.30) is feasible with $z^T Q z = F(x)g^2(x)$ or with $z^T Q z = F(x)g(x)$ if $g(x) > 0$.
- If

$$F(x) + p(x)h(x) = \sum_i g_i^2(x) \geq 0, \quad p(x) \geq 0, \quad h(x) = \begin{cases} \leq 0 & \text{if } a \geq x \geq b \\ > 0 & \text{otherwise} \end{cases},$$

then $F(x) \geq 0$ if $a \geq x \geq b$, where a, b are vectors. Later, we will use this fact to show that $F(x)$ is nonnegative in specific regions of the state space that are of interest.

In this thesis, to solve sum of squares programs, we have used SOSTOOLS [86], a free, third-party MATLAB toolbox, which also relies on the solver SeDuMi. Note, however, that the computational time necessary to solve to problems using SOSTOOLS scales badly with the size of the problem [82]:

$2d \setminus n$	1	3	5	7	9	11	13	15
2	2	4	6	8	10	12	14	16
4	3	10	21	36	55	78	105	136
6	4	20	56	120	220	364	560	816
8	5	35	126	330	715	1365	2380	3876
10	6	56	252	792	2002	4368	8568	15504
12	7	84	462	1716	5005	12376	27132	54264

Figure 3.3: Dimension of matrix Q as a function of the number of variables and degree of the polynomial (taken from [82]). Dimension of the matrix Q as a function of the number of variables n and the degree $2d$. The corresponding expression is $\binom{n+d}{d}$.

Chapter 4

Finding invariant sets and proving exponential stability of limit cycles using sum of squares decompositions

4.1 Invariant sets

When dealing with dynamical systems that have multiple equilibria, limit cycles, chaotic attractors, and combinations of these, it is often of interest to find a *invariant sets* for solution trajectories, provided they exist. (The following definitions are from [50].) If $x(t)$ is a solution of (4.1) then p is said to be a *positive limit point* of $x(t)$ if there is a sequence $\{t_n\}$, with $t_n \rightarrow \infty$ as $n \rightarrow \infty$, such that $x(t_n) \rightarrow p$ as $n \rightarrow \infty$. Furthermore, the set of all positive limit points of $x(t)$ is called a *positive limit set*. A set M is *invariant* with respect to $\dot{x} = f(x)$ if

$$x(0) \in M \Rightarrow x(t) \in M, \text{ for all } t \in \mathbb{R}$$

This means, that if a solution belongs to M at some time instant, then it belongs to M for all time. Furthermore, a set M is *positively invariant* if

$$x(0) \in M \Rightarrow x(t) \in M, \text{ for all } t \geq 0.$$

In Chapter 2, we have proved the existence of an absorbing set, which belongs to a subclass of invariant sets, for chemical reaction networks with a certain property. In this section, we present sufficient conditions for the existence of an invariant set \mathcal{B} of a

dynamical system

$$\dot{x} = f(x) \quad (4.1)$$

and show how to it can be found using SOSTOOLS. (A related procedure was presented in [87] (Chapter 3.3).) In Chapter 5, we will require the existence of a compact, convex and positively invariant set in order to find lower bounds for the coupling strength of interconnected system that guarantees their synchronisation.

A famous example of deterministic chaos is the work by the meteorologist Edward Lorenz. In 1963, while trying to understand the behaviour of a reduced model of circulation in the atmosphere, he established the following model [88]:

$$\begin{aligned} \dot{x} &= \sigma(y - x), \\ \dot{y} &= rx - y - xz, \\ \dot{z} &= xy - bz. \end{aligned} \quad (4.2)$$

He soon discovered that the system can exhibit nonperiodic, chaotic behaviour. A well known absorbing set for this system is given by

$$x^2 + y^2 + (z - \sigma - r)^2 < \frac{b^2(r + \sigma)^2}{4(b - 1)}. \quad (4.3)$$

Typically, the following system parameters are chosen: $\sigma = 10$, $b = \frac{8}{3}$, and $r = 28$. Figure 4.1a shows the Lorenz attractor and Figure 4.1b the absorbing set given by (4.3).

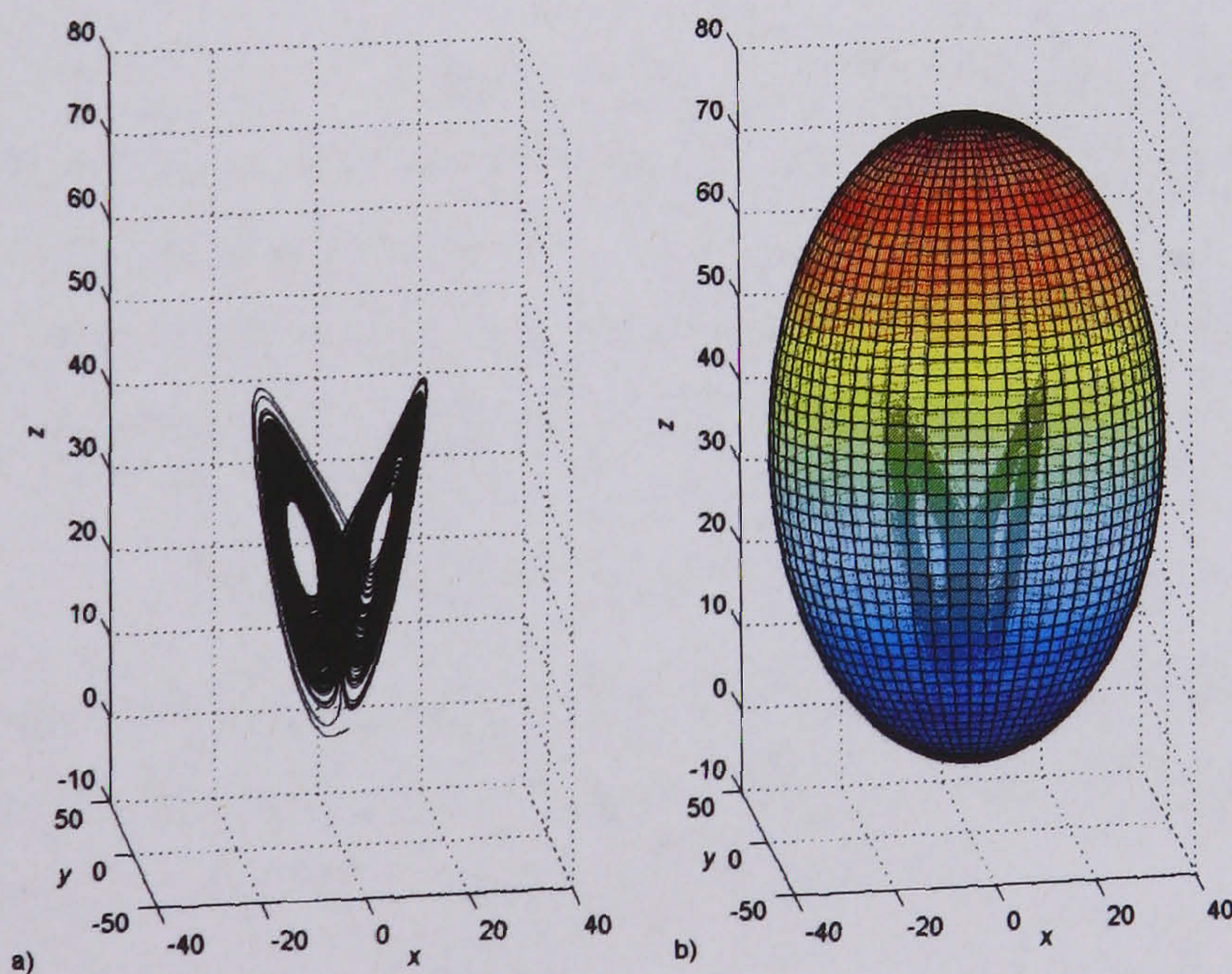


Figure 4.1: The Lorenz attractor.

4.2 Finding invariant sets

Now, the following corollary provides sufficient conditions that guarantee boundedness of solutions.

Lemma 4.2.1. *If there exist a positive constant β_u and sum of squares polynomials $V_u(x) > 0$ and $p_1(x)$ such that*

$$-f(x) \cdot \nabla V_u(x) - p_1(x)(\|x\|_2^2 - \beta_u) \text{ is a sum of squares} \quad (4.4)$$

then $\dot{V}_u(x) \leq 0$ if $\|x\|_2^2 \geq \beta_u$.

Note that we have to perform a search on (the desirably minimal) β_u for which (4.4) holds. Moreover, if there exists a positive constant γ_u such that $\|x\|_2^2 \geq \beta_u$ if $V_u(x) - \gamma_u = 0$ then the region bounded by $V_u(x) - \gamma_u = 0$ is an invariant set, since $f(x) \cdot \nabla V_u(x) \leq 0$ on the boundary. The following corollary provides sufficient conditions that guarantee the existence of such a γ_u .

Lemma 4.2.2. *If there exist a positive constant γ_u and a polynomial $p_2(x)$ (not necessarily positive) such that*

$$-(V_u(x) - \gamma_u) + p_2(x)(\|x\|_2^2 - \beta_u) \text{ is a sum of squares} \quad (4.5)$$

then $\|x\|_2^2 \geq \beta_u$ if $V_u(x) - \gamma_u = 0$.

Note that the search for γ_u can be posed as an optimisation problem, and thus, provides $\gamma_{u/\min}$, the minimal value of γ_u for which (4.5) holds. Figure 4.2 illustrates the different functions in Lemma 4.2.1 and Lemma 4.2.2.

Similarly, we can search for regions that will not be entered. If there exist a positive constant γ_ℓ and a sum of squares polynomial $V_\ell(x) > 0$ such that

$$f(x) \cdot \nabla V_\ell(x) \geq 0 \text{ if } V_\ell(x) - \gamma_\ell = 0$$

then solutions will not enter the region bounded by $V_\ell(x) - \gamma_\ell = 0$. To find such a region it is sufficient to show that there exist a (desirably large) positive constant β_ℓ a sum of squares polynomial $q_1(x)$ and a polynomial $q_2(x)$ such that

$$f(x) \cdot \nabla V_\ell(x) + q_1(x)(\|x\|_2^2 - \beta_\ell) \text{ is a sum of squares,} \quad (4.6)$$

$$(V_\ell(x) - \gamma_\ell) + q_2(x)(\|x\|_2^2 - \beta_\ell) \text{ is a sum of squares.} \quad (4.7)$$

Note that the region between the isolines $V_l(x) = \gamma_l$ and $V_u(x) = \gamma_u$ is positively invariant. In the following, we apply this procedure to find an invariant set for the van der Pol, FitzHugh-Nagumo model and the Lorenz system.

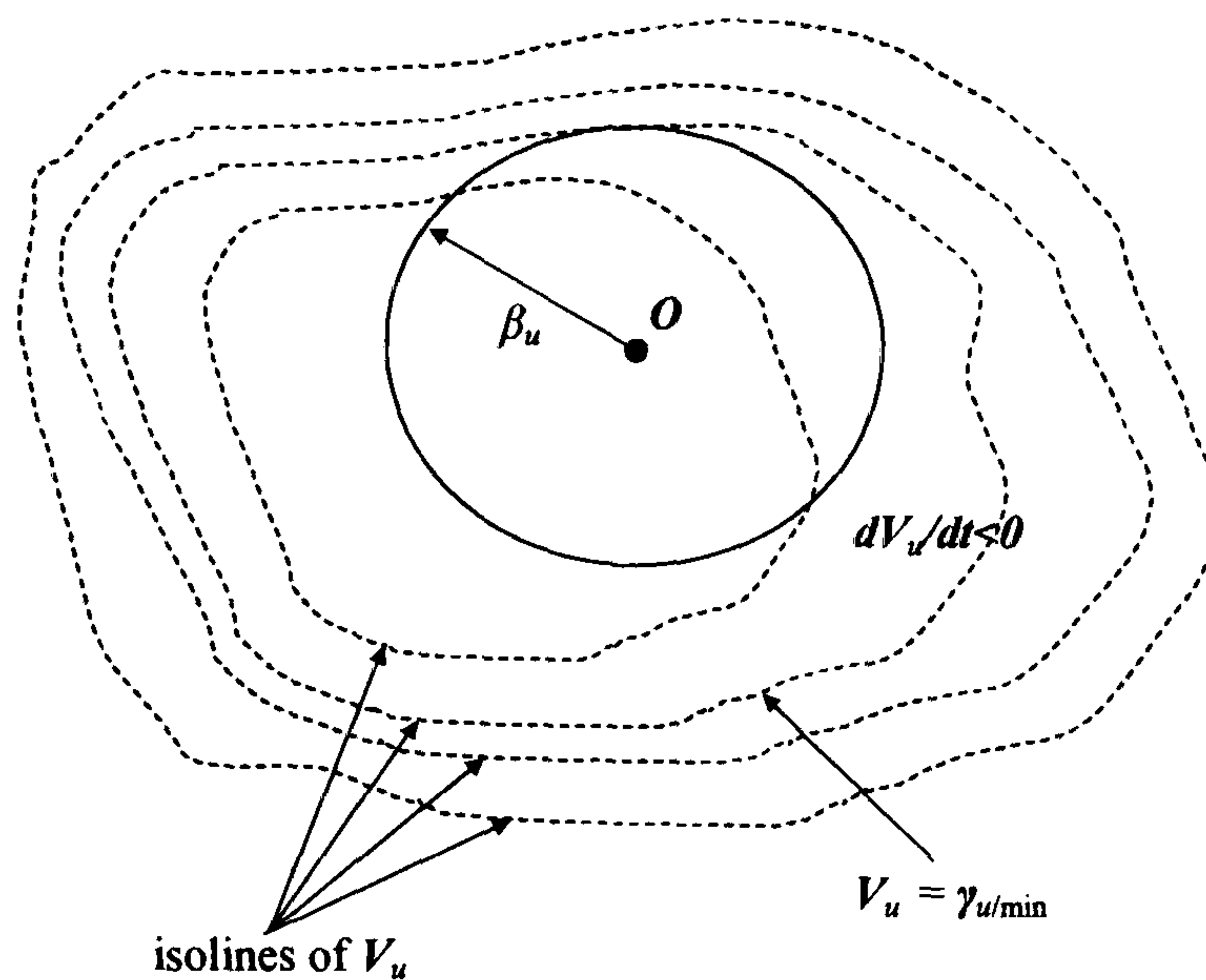


Figure 4.2: **Finding invariant sets.** The isoline $V_u = \gamma_{u/\min}$ bounds the smallest invariant set for the specific function V_u .

4.3 Applications

The van der Pol oscillator

Consider the van der Pol oscillator which is a widely used simple system to model oscillatory behaviour in biological systems [30, 89]

$$\begin{aligned} \dot{x}_1 &= x_2 \\ \dot{x}_2 &= -(k + x_1^2)x_2 - x_1. \end{aligned} \tag{4.8}$$

Here, $k \in \mathbb{R}$ is a parameter. Note that the origin is the only fixed point of (4.8). For $k > 0$, the origin is stable. For $k < 0$, the origin becomes unstable and there exists a unique stable limit cycle for this system. Its existence and stability can be proved using Liénard's theorem:

Theorem 4.3.1. (Liénard's theorem) [90] For $x \in \mathbb{R}$, the equation

$$\ddot{x} + f(x)\dot{x} + g(x) = 0$$

has a unique and asymptotically stable periodic solution if

- f, g are continuous
- f is an even function
- $F(x) < 0$ for $0 < x < a$, $F(x) > 0$ and is increasing for $x > 0$ (so, $F(x) = 0$ only at $x = 0, \pm a$), where F is defined by $F(x) := \int_0^x f(u)du$
- g is an odd function and $xg(x) > 0$ for all $x \neq 0$.

Now, let us apply the results of Section 4.1 in order to check whether we can find an invariant set for (4.8). As an example let $k = -1$. Requirement (4.4) is a feasibility problem and can be implemented as

$$\begin{array}{ll}
 \text{given} & f(x), \beta_u, \delta > 0 \\
 \text{search for} & V_u(x), p_1(x) \\
 \text{subject to} & V_u(x) - \delta(x_1^2 + x_2^2), p_1(x) \text{ are sum of squares} \\
 & -f(x) \cdot \nabla V_u(x) - p_1(x)(\|x\|_2^2 - \beta_u) \text{ is a sum of squares.} \quad (4.9)
 \end{array}$$

We find that reproducing the actual algorithm is quite useful and believe that the comments make clear the procedure. The implementation in MATLAB using the SOSTOOLS toolbox is as follows (We refer the reader to [86] for a detailed explanation of the different functions.):

```

% system's variables and initiation
syms x1 x2; vars=[x1;x2]; prog = sosprogram(vars);

% defining vector of monomials of order 2,4,6
VEC1 = monomials(vars,[2 4 6]);
% creating a polynomial with unknown coefficients
[prog,V_u] =sospolyvar(prog,VEC1,'wscoeff');

VEC2=monomials(vars,[0 2 4]); [prog,p1]=sospolyvar(prog,VEC2,'wscoeff');

% requiring p1>=0, V_u>0
prog = sosineq(prog,p1); prog = sosineq(prog,V_u-0.0001*(x1^2+x2^2));

% van der Pol equations
f1=x2; k=-1;
f2=-(k+x1^2)*x2-x1;

% requiring [diff(V_u,x1)*f1+diff(V_u,x2)*f2]+p1*(x1^2+x2^2-beta_u)]<=0
beta_u=3.7; prog = sosineq(prog, -(diff(V_u,x1)*f1+diff(V_u,x2)*f2)...
    -p1*(x1^2+x2^2-beta_u) );

% calling solver
prog=sossolve(prog);
% getting V_u
V_u = sosgetsol(prog,V_u)

```

We obtain with $\beta_u = 3.7$:

$$\begin{aligned}
V_u(x) = & 8.361x_1^2 - 11.679x_1x_2 + 4.925x_2^2 - 4.098x_1^4 + 3.240x_1^3x_2 + 0.710x_1^2x_2^2 \\
& -0.063x_1x_2^3 + 0.050x_2^4 + 0.781x_1^6 + 0.298x_1^4x_2^2 - 0.434x_1^3x_2^3 + 0.283x_1^2x_2^4 \\
& -0.089x_1x_2^5 + 0.012x_2^6.
\end{aligned} \tag{4.10}$$

We replace β_u, V_u, p_1 by β_ℓ, V_ℓ, q_1 and make the following change:

```

prog = sosineq(prog, diff(V_ell,x1)*f1+diff(V_ell,x2)*f2)...
      +q1*(x1^2+x2^2-beta_ell) );

```

Then, we obtain that (4.6) holds if $\beta_\ell = 5.8$ and

$$\begin{aligned}
V_\ell(x) = & (10.854x_1 - 1.942x_2 - 1.258x_1^3 + 0.517x_1^2x_2 - 0.244x_1x_2^2 - 0.105x_2^3)x_1 \\
& +(-1.942x_1 + 6.094x_2 + 0.315x_1^3 - 0.571x_1^2x_2 - 0.159x_1x_2^2 - 0.447x_2^3)x_2 \\
& +(-1.258x_1 + 0.315x_2 + 0.180x_1^3 - 0.093x_1^2x_2 - 0.030x_1x_2^2 + 0.017x_2^3)x_1^3 \\
& +(0.517x_1 - 0.570x_2 - 0.092x_1^3 + 0.107x_1^2x_2 + 0.021x_1x_2^2 + 0.007x_2^3)x_1^2x_2 \\
& +(-0.244x_1 - 0.159x_2 - 0.030x_1^3 + 0.021x_1^2x_2 + 0.149x_1x_2^2 + 0.003x_2^3)x_1x_2^2 \\
& +(-0.105x_1 - 0.447x_2 + 0.017x_1^3 + 0.007x_1^2x_2 + 0.003x_1x_2^2 + 0.085x_2^3)x_2^3.
\end{aligned} \tag{4.11}$$

(The computation time is on the scale of a few seconds on a standard PC.) Requirement (4.5) can be implemented as the following minimisation problem:

$$\begin{array}{ll}
\text{given} & \beta_u, V_u(x) \\
\text{minimise} & \gamma_u \\
\text{subject to} & \gamma_u, p_2(x) \text{ are sum of squares} \\
& -(V_u(x) - \gamma_u) + p_2(x)(x_1^2 + x_2^2 - \beta_u) \text{ is a sum of squares.}
\end{array} \tag{4.12}$$

The implementation in MATLAB using the SOSTOOLS toolbox is as follows:

```

syms x1 x2; vars=[x1;x2]; prog = sosprogram(vars);

beta_u = 3.7;
V_u = ...

VEC3 = monomials(vars,[0]);
[prog,gamma_u] = sospolyvar(prog,VEC3,'wscoeff');
VEC4 = monomials(vars,[0 2 4]);
[prog,p2] = sospolyvar(prog,VEC4,'wscoeff');

prog = sosineq(prog,gamma_u);
prog = sosineq(prog,-(V_u-gamma_u)+p2*(x1^2+x2^2-beta_u));

% gamma_u is the 'objective function' to be minimised
prog = sossetobj(prog,gamma_u);

[prog,info] = sossolve(prog); gamma_u = sosgetsol(prog,gamma_u);

```

We obtain that the minimal value of γ_u such that (4.5) holds is $\gamma_u = 41$. Let us replace β_u, V_u, p_2 by β_ℓ, V_ℓ, q_2 and make the following changes:

```

prog = sosineq(prog,(V_ell-gamma_ell)+q2*(x1^2+x2^2-beta_ell));
prog = sossetobj(prog,-gamma_ell);

```

Then, we obtain that the maximal value of γ_ℓ such that (4.7) holds is $\gamma_\ell = 12.4$. The region between the isolines $V_\ell(x) = \gamma_\ell$ and $V_u(x) = \gamma_u$ is the positively invariant set \mathcal{B} . It is shown in Figure 4.3.



Figure 4.3: Solution trajectory of the van der Pol oscillator in \mathcal{B} . The boundaries of the positively invariant set \mathcal{B} are given in blue; the gradient field on these is indicated by vectors (red); and the trajectory of the van der Pol Oscillator is in black.

Since \mathcal{B} does not contain fixed points, we can apply, as an alternative to Liénard's theorem, the Poincaré–Bendixson Criterion:

Lemma 4.3.2. (Poincaré–Bendixson Criterion) [50] *Consider the system (4.1) and let \mathcal{M} be a closed bounded subset of the plane such that*

- *\mathcal{M} contains no equilibrium points, or contains only one unstable equilibrium point.*
- *Every trajectory starting in \mathcal{M} stays in \mathcal{M} for all future time.*

Then, \mathcal{M} contains a periodic orbit of (4.1).

This implies that \mathcal{B} must contain an asymptotically stable limit cycle. The limit cycle is shown in Figure 4.3. Note that the criterion only holds in the case of a second–order system. In Section 4.4, we present results for systems of order ≥ 2 that guarantee existence of exponentially stable limit cycles in \mathcal{B} when it does not contain fixed points and prove exponential stability of the van der Pol limit cycle.

Neocortical model

The dynamics of neocortical neurons in humans and mammals are governed by roughly a dozen ion currents and their interplay. This leads to complex behaviour and thus, low-dimensional models have been developed in order to provide insight into the relationship between the core dynamical principles and biophysics. A popular model was proposed by the nobel laureates Alan Lloyd Hodgkin and Andrew Huxley, and further simplified by Richard FitzHugh and Jin-Ichi Nagumo to the following expression [5, 91]:

$$\begin{aligned} C\dot{v} &= m_\infty[v](v - E) - w + I, \\ \dot{w} &= bv - \gamma w, \end{aligned} \tag{4.13}$$

where $m_\infty[v] = v(a - v)$. The first equation describes the changes in membrane potential which depend on changes in membrane capacitance, ionic currents, and the stimulating current I (in nA). Constant E is the steady state ion potential. The term $m_\infty[v](v - E)$ is the current contribution from ionic movement and $m_\infty[v]$ is the ion activation function. The second equation is to fit results to data. Note that the time t is measured in ms and the voltage is measured in 10^{-2} mV. Parameter a is neuron-dependent and lead to different dynamical responses. Let the magnitude of the different system parameters be as follows: $C = E = b = \gamma = 1$, $I = 0$ and $a = 4$. Then, we describe (4.13) by

$$\begin{aligned} \dot{x}_1 &= -x_1^3 + 5x_1^2 - 4x_1 - x_2 \\ \dot{x}_2 &= x_1 - x_2. \end{aligned} \tag{4.14}$$

Note that (4.14) has switching behaviour. That is, it has two stable equilibria $\{0, 0\}$ and $\{3.618, 3.618\}$ and one unstable, which is $\{1.382, 1.382\}$.

Using SOSTOOLS, we can search for a set around the three equilibria that traps solution trajectory in the same manner as previously for the van der Pol oscillator. We then obtain the following:

$$\beta_u = 26.2, \quad \gamma_u = 88.183$$

$$V_u(x) = 0.109x_1^2 - 0.089x_1x_2 + 0.484x_2^2 + 0.028x_1^4 - 0.007x_1^3x_2 + 0.045x_1^2x_2^2 + 0.11x_2^4.$$

The boundary of the invariant set is given by $V_u(x) = \gamma_u$ and is shown Figure 4.4 (blue dashed line).

To find an estimate for the region of attraction for the two stable equilibria, it is sufficient to show that there exist a (desirably large) positive constant β_a , a sum of squares polynomial $r_1(x)$ and a polynomial $r_2(x)$ such that

$$-f(x) \cdot \nabla V_a(x) + r_1(x)(\|x\|_2^2 - \beta_a) \text{ is a sum of squares} \quad (4.15)$$

and a positive constant γ_a such that

$$(V_a(x) - \gamma_a) + r_2(x)(\|x\|_2^2 - \beta_a) \text{ is a sum of squares.} \quad (4.16)$$

Implementing (4.15)–(4.16) in SOSTOOLS, we obtain for the origin:

$$\beta_a = 1.56, \quad \gamma_a = 0.381$$

$$V_a(x) = 0.422x_1^2 - 0.552x_1x_2 + 0.609x_2^2 + 0.066x_1^4 - 0.023x_1^3x_2 + 0.224x_1^2x_2^2 + 0.063x_2^4. \quad (4.17)$$

The estimate for the region of attraction is then given by $V_a(x) \leq \gamma_a$. Before we implement (4.15)–(4.16) in SOSTOOLS for the equilibrium point given by $\{3.618, 3.618\}$, we shift it to the origin through a change of a variables: $y_1 = x_1 + 3.618$ and $y_2 = x_2 + 3.618$. This leads to the following result.

$$\beta_a = 3.6, \quad \gamma_a = 0.235$$

$$V_a(y) = 0.088y_1^2 - 0.093y_1y_2 + 0.159y_2^2. \quad (4.18)$$

The estimate for the region of attraction is then given by $V_a(y) \leq \gamma_a$. Both estimates, (4.17) and (4.18), are shown in Figure 4.4 (blue solid lines).

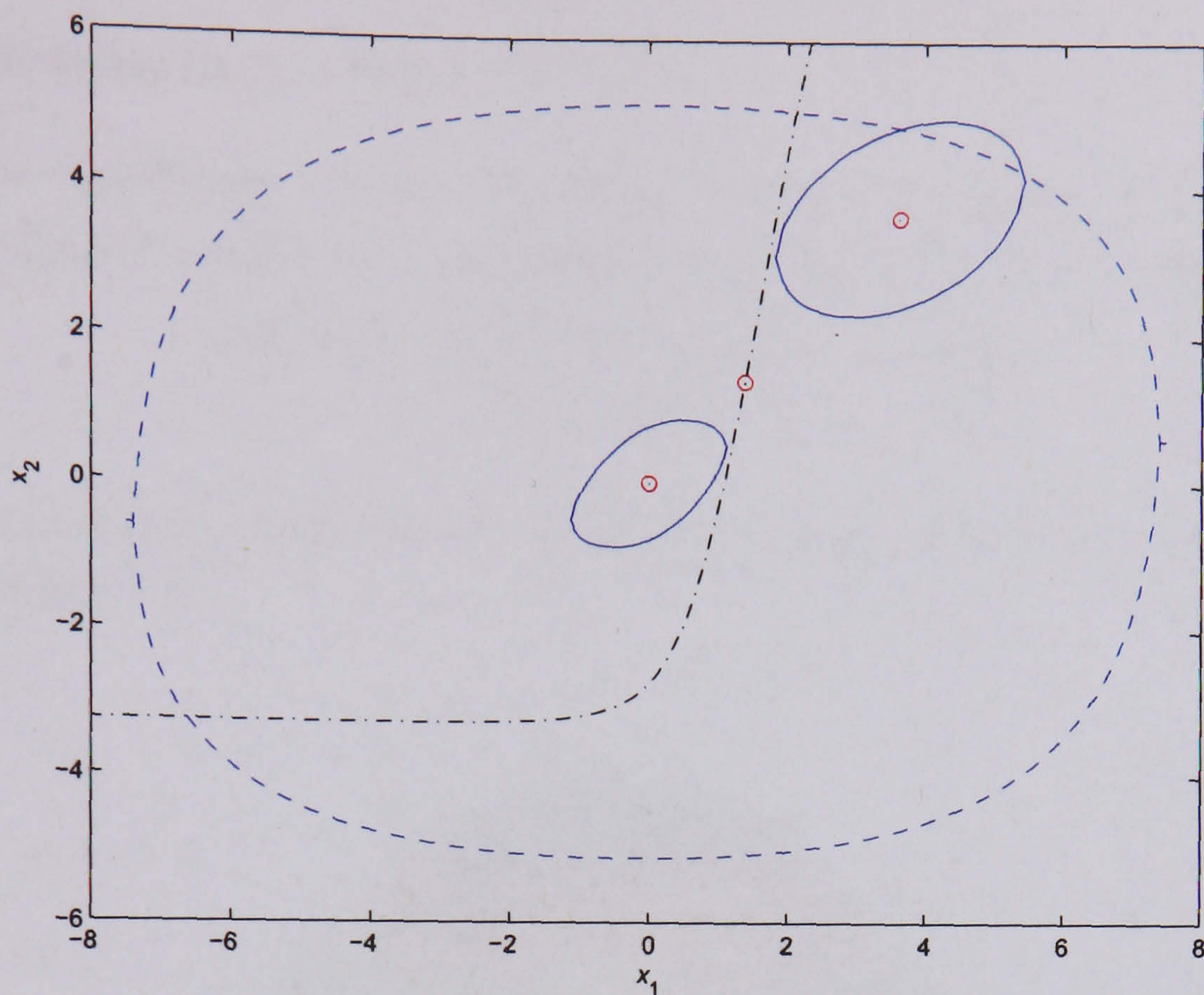


Figure 4.4: **Regions of attractions for the equilibrium points of a neocortical model.** The positively invariant set for system (4.14) is bounded by the blue dashed line. The region of attraction of the individual equilibrium points is bounded by solid blue lines. The black dash-dotted line was calculated numerically and shows the true border between the two regions of attraction.

It has been observed that the neural system is excitable. That is, if the system at equilibrium is sufficiently perturbed, the individual variables will display a considerable large excursion in phase space. This can be also understood as switching between two stable steady states. Our analysis, summarised in Figure 4.4, shows just how much perturbation is at least necessary before one can expect this behaviour.

The Lorenz system

Consider the Lorenz system. We apply Lemmas 4.2.1 and 4.2.2 in order to find an invariant set and to see how it compares with (4.3). Particularly, we search for a fourth order polynomial $V_u(x, y, z)$ for which $[\dot{x} \ \dot{y} \ \dot{z}] \nabla V_u(x, y, z) \leq 0$ if $x^2 + y^2 + (z - 38)^2 \geq \beta_u$. Using

SOSTOOLS, we obtain for $\beta_u = 1100$:

$$\begin{aligned}
 V_u(x, y, z) = & -0.00191xyz + 3.346z - 0.2989xy - 0.04723x^2z - 0.0667y^2z + 0.00043x^2y^2 \\
 & + 0.00043x^2z^2 + 0.00121y^2z^2 + 0.26991x^2 + 0.03172y^2 + 1.9105z^2 - 0.06689z^3 \\
 & + 0.00123x^4 + 0.00061y^4 + 0.00061z^4 + 8.8309, \\
 & \gamma_u = 1347.
 \end{aligned} \tag{4.19}$$

The computation time is on the scale of a minute on a standard PC. The set $V_u(x, y, z) = \gamma_u$ is shown in Figure 4.5.

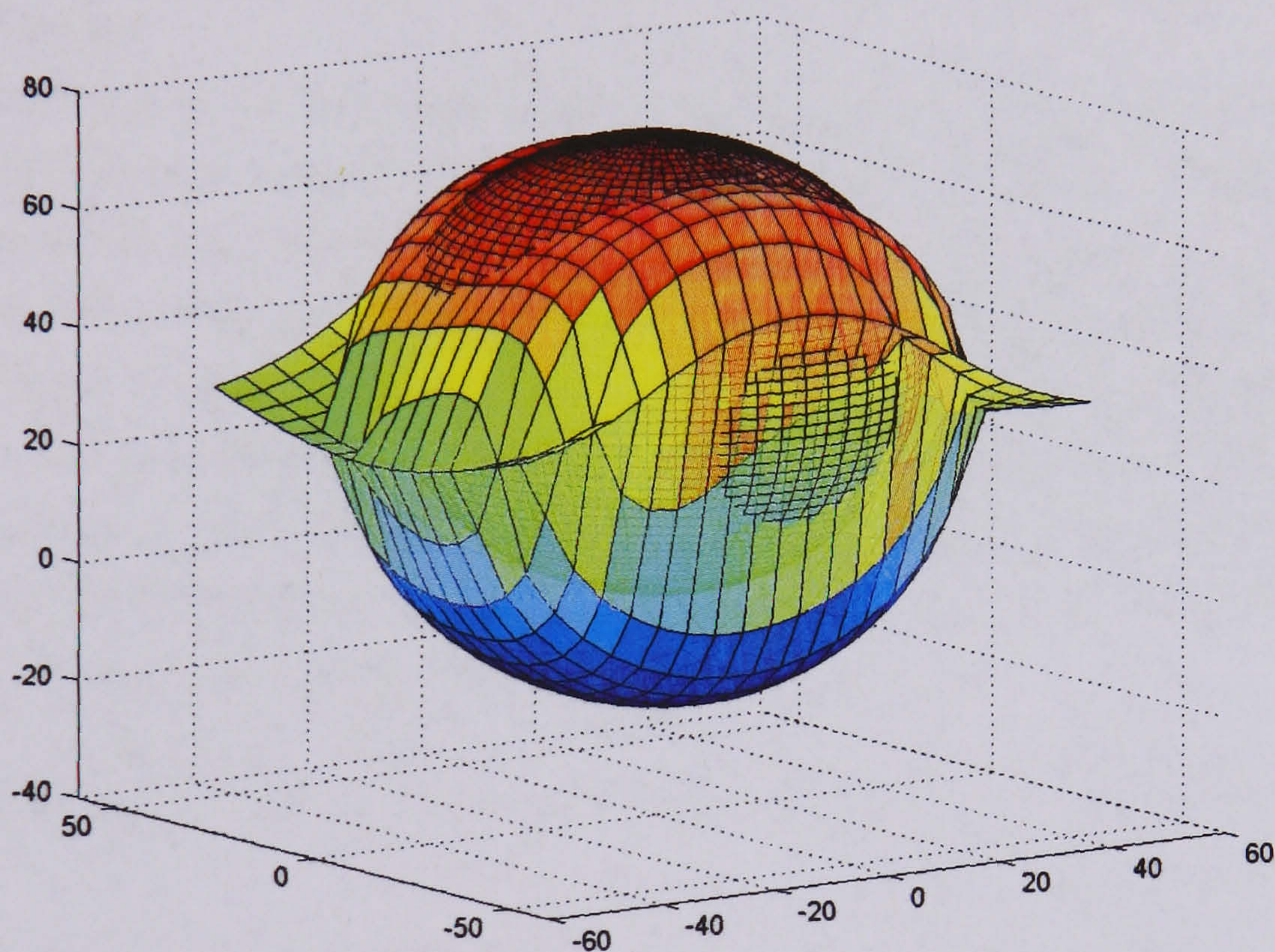


Figure 4.5: **Two invariant sets for the Lorenz system.** The ‘outer’ set boundary is given by $V_u = \gamma_u$. The embedded spherical shell is from Figure 4.1b and defined by (4.3).

4.4 Proving exponential stability of limit cycles

Based on the sufficient positivity condition established by Peter Giesl, in this section, we use sum of squares programs to search for a matrix function that guarantees existence, uniqueness and exponential stability of a limit cycle. We illustrate our results with the van

der Pol oscillator, which is a widely used model in physics and biology for a system that exhibits oscillations.

Consider the dynamical system

$$\dot{x} = f(x) \quad \text{where } x \in \mathbb{R}^n. \quad (4.20)$$

Theorem 3.1.9 by Peter Giesl provides a means to prove the existence of a unique, exponentially stable periodic orbit in a given region of the state space, \mathcal{B} . However, it requires conditions that are usually difficult to check. We have been able to relax them through a sum of squares decomposition [82]. Using SOSTOOLS, we prove exponential stability of van der Pol oscillations.

If the vector field (4.20) is polynomial or rational, (3.8) is a conditional positivity condition on multivariate polynomials. It is well known that such conditions are difficult to check in general. However, one can create a particular hierarchy of relaxations, by replacing the positivity conditions with sum of squares conditions, which can be implemented efficiently using semidefinite programming with the aid of the MATLAB toolbox SOSTOOLS [82, 86]. Moreover, we can use SOSTOOLS to search for polynomial functions which fulfill the sum of squares conditions, thus providing a sufficient condition ('certificate') for the existence of a limit cycle in \mathcal{B} . In order to use the sum of squares framework, we reformulate the original condition (3.8) as follows. First, we recall (3.8):

$$w^T \left(M(x) \frac{\partial f(x)}{\partial x} + \frac{1}{2} M'(x) \right) w < 0, \quad \forall w \text{ such that } w^T M(x) f(x) = 0, \quad \forall w, x \in \mathcal{B}.$$

Now, if

$$w^T \left(M(x) \frac{\partial f(x)}{\partial x} + \frac{1}{2} M'(x) \right) w - \alpha(x) (w^T M(x) f(x))^2 < 0, \quad \forall w, x \in \mathcal{B} \quad (4.21)$$

then (3.8) holds. If we define $v = M(x)w$, then (4.21) becomes:

$$v^T \left(\frac{\partial f(x)}{\partial x} M(x)^{-1} - \frac{1}{2} (M(x)^{-1})' - \alpha(x) f(x) f(x)^T \right) v < 0, \quad \forall v, x \in \mathcal{B}, \quad (4.22)$$

where we have used the fact that

$$(M(x)M(x)^{-1})' = 0 = M'(x)M(x)^{-1} + M(x)(M(x)^{-1})' \implies \\ -(M(x)^{-1})' = M(x)^{-1}M'(x)M(x)^{-1}.$$

Let $B_I(x) = 0$ be the inner boundary of \mathcal{B} and $B_O(x) = 0$ the outer boundary. If $f(x)$, $B_I(x)$ and $B_O(x)$ are given by polynomial functions, we can use SOSTOOLS to search for polynomial functions $M(x)$ and $\alpha(x)$ that fulfill sum of squares conditions derived from (4.22). This is a feasibility problem that can be implemented as

$$\begin{array}{ll}
\text{given} & f(x), B_I(x), B_O(x), \delta > 0 \\
\text{search for} & N_{(1,1)}(x), N_{(1,2)}(x), N_{(2,2)}(x), \alpha(x), p_1(v), p_2(v) \\
\text{subject to} & p_1(v), p_2(v), v^T (N(x) - \delta I) v \text{ are sum of squares} \\
& -v^T \left(\frac{\partial f(x)}{\partial x} N(x) - \frac{1}{2} N'(x) - \alpha(x) f(x) f(x)^T - \delta I \right) v \\
& -p_1(v) B_I(x) + p_2(v) B_O(x) \text{ is a sum of squares,} \quad (4.23)
\end{array}$$

where $N(x) = M^{-1}(x)$. If a solution is found in terms of sum of squares decompositions, this provides a sufficient condition for the existence of an exponentially stable limit cycle in \mathcal{B} . This certificate is therefore a proof of the existence of the limit cycle. Clearly, these are not necessary conditions and the absence of a solution says nothing about the existence of the limit cycle. We now illustrate the method establishing the existence and exponential stability of the limit cycle for the van der Pol oscillator.

4.4.1 Application to the van der Pol oscillator

Recall the set of equations for van der Pol oscillator:

$$\begin{aligned}
\dot{x}_1 &= x_2 \\
\dot{x}_2 &= -(k + x_1^2)x_2 - x_1, \quad (4.24)
\end{aligned}$$

Contraction analysis and SOSTOOLS were recently used to establish global exponential stability of the origin for $k > 0$ [92]. For $k < 0$, the existence and stability of the periodic orbit can be proved using Liénard's theorem or by obtaining a compact, connected and positively invariant set \mathcal{B} which contains no fixed point as in Section 4.2. Here, \mathcal{B} is the region between $B_I(x) = 0$ and $B_O(x) = 0$, where

$$\begin{aligned}
B_I(x) &= -4 - 4.281x_1x_2 + 4.93x_1^2 + 2.213x_2^2 - 1.578x_1^4 + 0.012x_2^4 + 0.202x_1^6 + 1.07x_1^3x_2 \\
&\quad - 0.048x_1^2x_2^2 - 0.483x_1x_2^3. \quad (4.25)
\end{aligned}$$

and

$$\begin{aligned}
B_O(x) = & -3.7 + 78.361x_1^2 - 11.679x_1x_2 + 4.925x_2^2 - 4.098x_1^4 + 3.240x_1^3x_2 + 0.710x_1^2x_2^2 \\
& -0.063x_1x_2^3 + 0.050x_2^4 + 0.781x_1^6 + 0.298x_1^4x_2^2 - 0.434x_1^3x_2^3 + 0.283x_1^2x_2^4 \\
& -0.089x_1x_2^5 + 0.012x_2^6.
\end{aligned} \tag{4.26}$$

Note that for computational reason, we chose to use (4.25), obtained by considering monomials of order 4, instead of (4.11), for which we considered monomials of order 6, because (4.25) is simpler (but also smaller).

However, the inner boundary of \mathcal{B} given (4.25) is smaller. We now use the above results to establish the existence and exponential stability of the periodic orbit of (4.24) for $k < 0$. Because $f(x)$ in (4.24) is a polynomial field, we can use SOSTOOLS in order to obtain polynomial functions $M(x)$, and $\alpha(x)$ such that (4.22) holds. The computational implementation is given in Appendix A. Then, for $k = -1$ we obtain, with $N(x) = M^{-1}(x)$,

$$\begin{aligned}
N_{(1,1)}(x) &= 2.759 + 1.080x_1^2 + 0.489x_1x_2 + 0.032x_2^2 + 0.514x_1^4 + 0.021x_1^3x_2 + 0.002x_1^2x_2^2 \\
&\quad -0.006x_1x_2^3 + 0.001x_2^4, \\
N_{(1,2)}(x) &= -0.746 - 0.933x_1^2 + 1.652x_1x_2 + 0.033x_2^2 - 0.266x_1^4 + 0.014x_1^3x_2 + 0.015x_1^2x_2^2 \\
&\quad -0.0002x_1x_2^3 - 0.001x_2^4, \\
N_{(2,2)}(x) &= 0.517 + 0.593x_1^2 + 0.717x_1x_2 + 3.900x_2^2 + 1.929x_1^4 - 0.184x_1^3x_2 + .304x_1^2x_2^2 \\
&\quad +0.139x_1x_2^3 + 0.028x_2^4, \\
\alpha(x) &= -1.592 - 2.310x_1^2 - 0.117x_1x_2 - 0.396x_2^2 - 0.977x_1^4 - 0.105x_1^3x_2 - 0.488x_1^2x_2^2 \\
&\quad -0.151x_1x_2^3 - 0.296x_2^4.
\end{aligned}$$

This result guarantees the existence and exponential stability of a periodic orbit for the van der Pol oscillator in \mathcal{B} (Figure 4.6). The computation time is on the scale of a few seconds on a standard PC. We have obtained similar results for several values of $k < 0$.

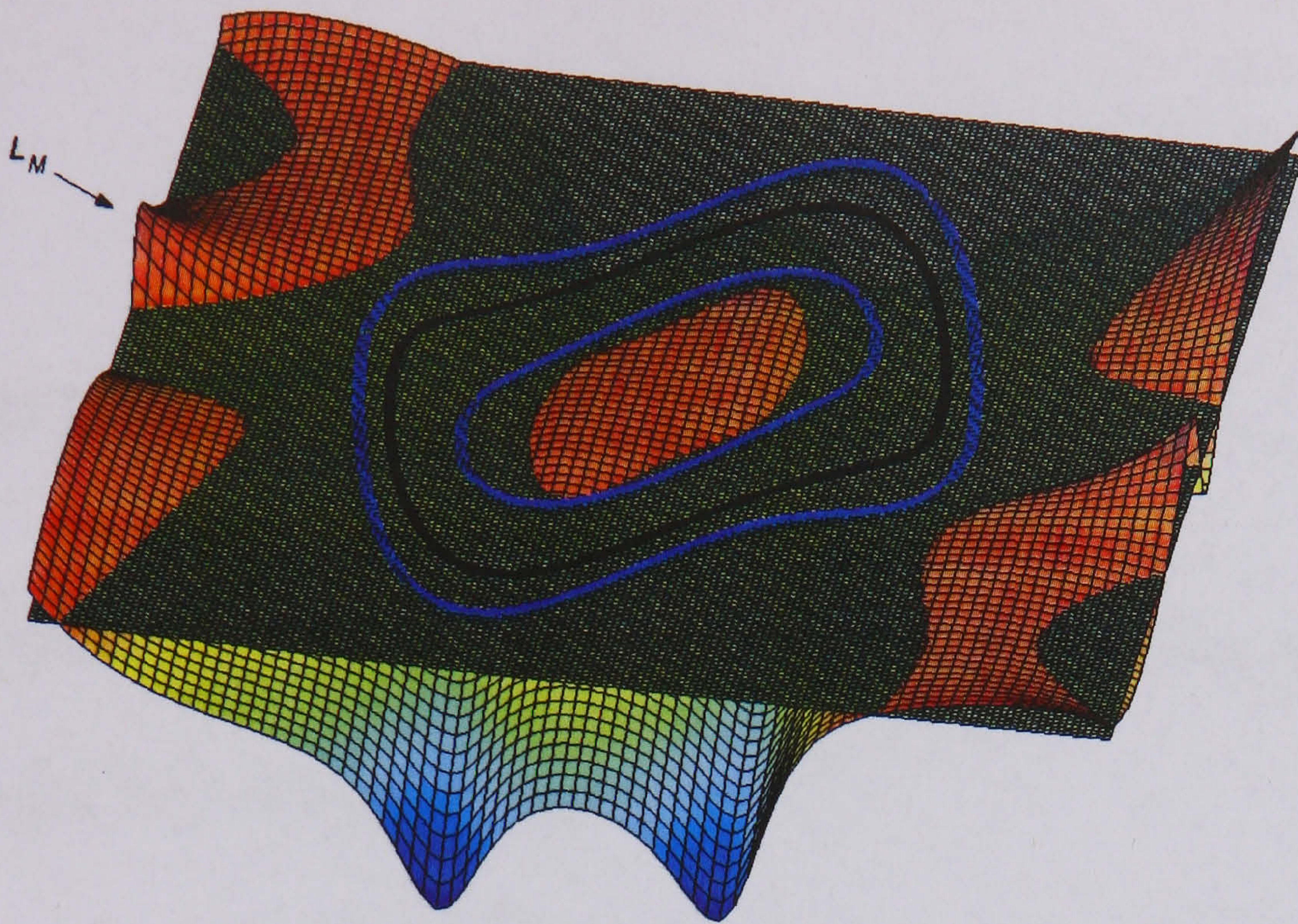


Figure 4.6: **The L_M Landscape.** The limit cycle of the van der Pol oscillators and set \mathcal{B} are shown (in black and blue respectively). Let (4.22) hold if $L_M(x) < 0$. The contour surface of $L_M(x)$ is shown (the plane corresponds to the zero level).

4.5 Conclusion

In this chapter, we have provided a practical means to prove the existence of exponentially stable periodic solutions of polynomial dynamical systems. Based on results by Peter Giesl, we have used SOSTOOLS to search for sum of squares decompositions that provide sufficient conditions for the existence of an exponentially stable limit cycle. We have applied the method to the van der Pol system.

Chapter 5

Entrainment and synchronisation of biological systems

The function of many biological systems is dependent on their ability to entrain to external periodic inputs. Moreover, when analysing a biological system, it is often not only important to know when it will entrain to an external input, but also when it will synchronise its period to the period of surrounding systems. For instance, as mentioned in the introduction, many bodily functions require entrainment to the day-night cycle and the synchronisation of the circadian clock of all cells. It is also of great importance that heart cells work in sync as it is believed that cardiac dysrhythmia, a life threatening heart disease, are caused by poor synchronisation between these autonomous pacemakers [30]. Additionally, experiments have shown that, because of high degrees of variability even between synthetic genetic oscillators, observing rhythmical behaviour becomes improbable [93]. This highlights the importance of mathematical analysis tools for models of coupled biological *nonidentical* oscillators.

In Section 5.1, we propose an algorithm based on semidefinite programming that allows us to establish sufficient conditions under which an exponentially stable system will entrain to the external input. In Section 5.2, we introduce known results on global *complete synchronisation* of coupled identical oscillators [33–35]. In Section 5.2.3, we show, for the first time to our knowledge, how to obtain these certificates for global complete synchronisation computationally. In Section 5.3, we draw connections between the notion of synchrony and the notion of observability. We then extend the results of Section 5.2 to obtain conditions for *frequency synchronisation* of nonidentical oscillators when coupled through a network

in Section 5.4. We apply our results to different important biological systems that consist of a network of coupled oscillators. In Section 5.5, we provide a relaxation of previous results by requiring *incomplete synchronisation* only; that is, we require that the differences between the coupled oscillators remain small as time goes on and not that they approach zero. In Section 5.6, we show that in the special case of a system of coupled identical oscillators with all-to-all, it is possible to extend previous results. In Section 5.6.1, we provide a lemma which is equivalent to Theorem 5.2.3 but works also with a nonconstant matrix. We then extend this result to obtain conditions that guarantee global complete synchronisation for coupled identical discrete-time dynamical systems. In Section 5.6.2, we provide novel sufficient conditions for global complete synchronisation of coupled identical oscillators as an alternative to the ones presented in Section 5.6.1. They are based on the so called Bendixson's Criterion for higher dimensions which we have presented in Section 3.2. They signify a move away from the, at times, strict requirements derived from contraction theory in Section 5.2. Section 5.7 summarises the results of Chapter 5.

As synchronisation of dynamical systems with unbounded and diverging solutions does not make much sense, in the applications, we shall either show or assume that solution trajectories are bounded. Finally, the following remark addresses an issue that is relevant to most results in this chapter and which is not satisfactorily addressed in the literature in our opinion.

Remark 5.0.1. Consider

$$\dot{x} = f(x). \quad (5.1)$$

Let the origin be the only equilibrium point of (5.1) and globally asymptotically stable. Let $D \geq 0$ be a diagonal matrix. Then, the origin is not necessarily a globally asymptotically stable equilibrium point of

$$\dot{x} = f(x) - Dx. \quad (5.2)$$

For instance, let

$$A = \begin{bmatrix} 0.5 & -1 & 1 \\ 2 & -4 & 1 \\ -1 & 1 & -10 \end{bmatrix}, \quad f(x) = Ax, \quad D = \text{diag}([0 \ 10 \ 0]).$$

Then all eigenvalues of A are negative and thus, the origin is a globally asymptotically stable equilibrium point of (5.1). However, one eigenvalue of $A - D$ is positive and thus,

the origin is an unstable equilibrium point of (5.2). Now, if there exists a (not necessarily symmetric) matrix $P > 0$ such that $x^T P f(x) < 0$ and $x^T P D x \geq 0$ then $x^T P f(x) - x^T P D x < 0$ and the origin is globally asymptotically stable equilibrium point of (5.2).

5.1 Conditions for the entrainment of a dynamical system

Consider a continuous dynamical system given by

$$\dot{x} = h(x, t) = f(x, u(t)), \quad f : \mathcal{D} \subset \mathbb{R}^n \rightarrow \mathbb{R}^n, \quad u(t) \in \mathcal{U} \subset \mathbb{R}^n. \quad (5.3)$$

Here, $u(t)$ is a continuous, T -periodic function with zero mean. Let

$$h(x, t) = f(x) + u(t).$$

Then, the following result is well known (see, for instance, Chapter 10.3 in [50]). If the autonomous system with $u(t) = 0$ associated with (5.3) has a stable equilibrium point and the Jacobian at the equilibrium point is Hurwitz then the system (5.3) has a stable T -periodic solution for sufficiently small amplitude. However, it is worth remarking that in order to obtain a bound on the amplitude the periodic orbit must be known. In this section, we present an algorithmic implementation of Theorem 3.1.8 based on semidefinite programming. This provides the necessary information to establish sufficient conditions under which the system will entrain to the external input. Before, we briefly repeat Theorem 3.1.8:

Theorem 5.1.1. *If*

$$M(x)J(x) + \frac{1}{2}M'(x) < 0 \text{ with } M'_{(i,j)} = \sum_{k=1}^n \frac{\partial M_{(i,j)}}{\partial x_k} f_k, \quad \forall x \in \mathcal{B}, \quad (5.4)$$

holds for (5.3), (5.3) has no fixed points in \mathcal{B} and $u(t)$ is T -periodic then (5.3) has a unique and exponentially stable T -periodic solution in \mathcal{B} .

5.1.1 A gene regulation model

In this section, we apply the results obtained in the previous section to a biological model. We consider a gene regulatory system that controls the production of an enzyme from reference [5] and examine the conditions that guarantee entrainment to an external drive. This

input could consist of the regular intake of medication, where entrainment is important. In Figure 5.1, x_1 denotes the concentration of mRNA, which is the template for the synthesis of an enzyme, whose concentration is given by x_2 . The enzyme combines with a substrate to produce a product, whose concentration given by x_3 , that inhibits the transcription of mRNA and also enhances its own depletion.

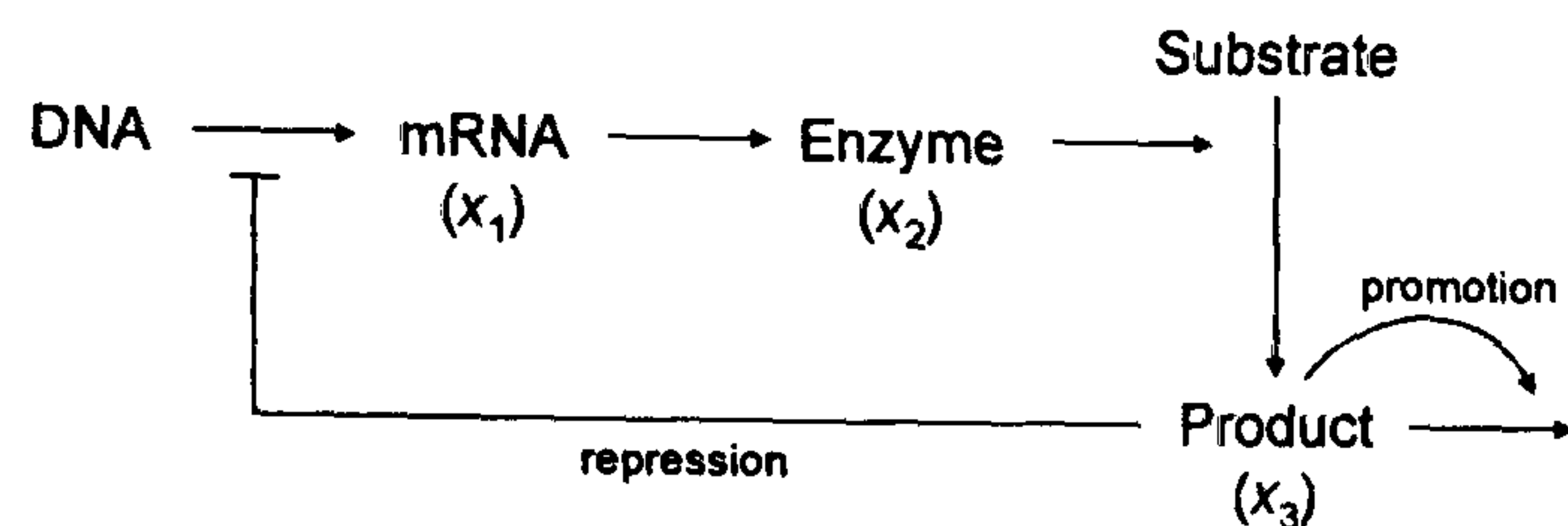


Figure 5.1: Schematic control system for the production of an enzyme [5].

The dynamics of this system can be represented by a system of differential equations with linear terms for the degradation and some of the saturated enzymatic reactions and nonlinear (Hill and Monod) terms for the regulation exerted by the product x_3 :

$$\begin{aligned} \dot{x}_1 &= \frac{k}{1+x_3} - ax_1, \\ \dot{x}_2 &= bx_1 - dx_2, \\ \dot{x}_3 &= dx_2 - \frac{kx_3}{1+x_3} - ex_3 + u_m + Au(t). \end{aligned} \quad (5.5)$$

In (5.5), we have also assumed a positive periodic influx of the product x_3 from other sources into the cell: $u_m + Au(t)$, where u_m corresponds to the mean of the input and A to the amplitude.

Note that for nonnegative initial conditions, the solutions of (5.5) remain in the non-negative orthant and their trajectories are bounded. The latter can be seen using the Lyapunov Function $V(x) = p^T x$, $p^T = [\frac{3b}{a} \ 2 \ 1]$, $x^T = [x_1 \ x_2 \ x_3]$, since there exists a positive scalar α such that $\dot{V}(x) < 0$ when $p^T x > \alpha$, which implies boundedness (see Definition 2.4.2). Let the periodic drive be pure sinusoidal: $Au(t) = A \sin(2\pi t/T)$. Figure 5.2 shows that the system does not necessarily entrain to the external input.

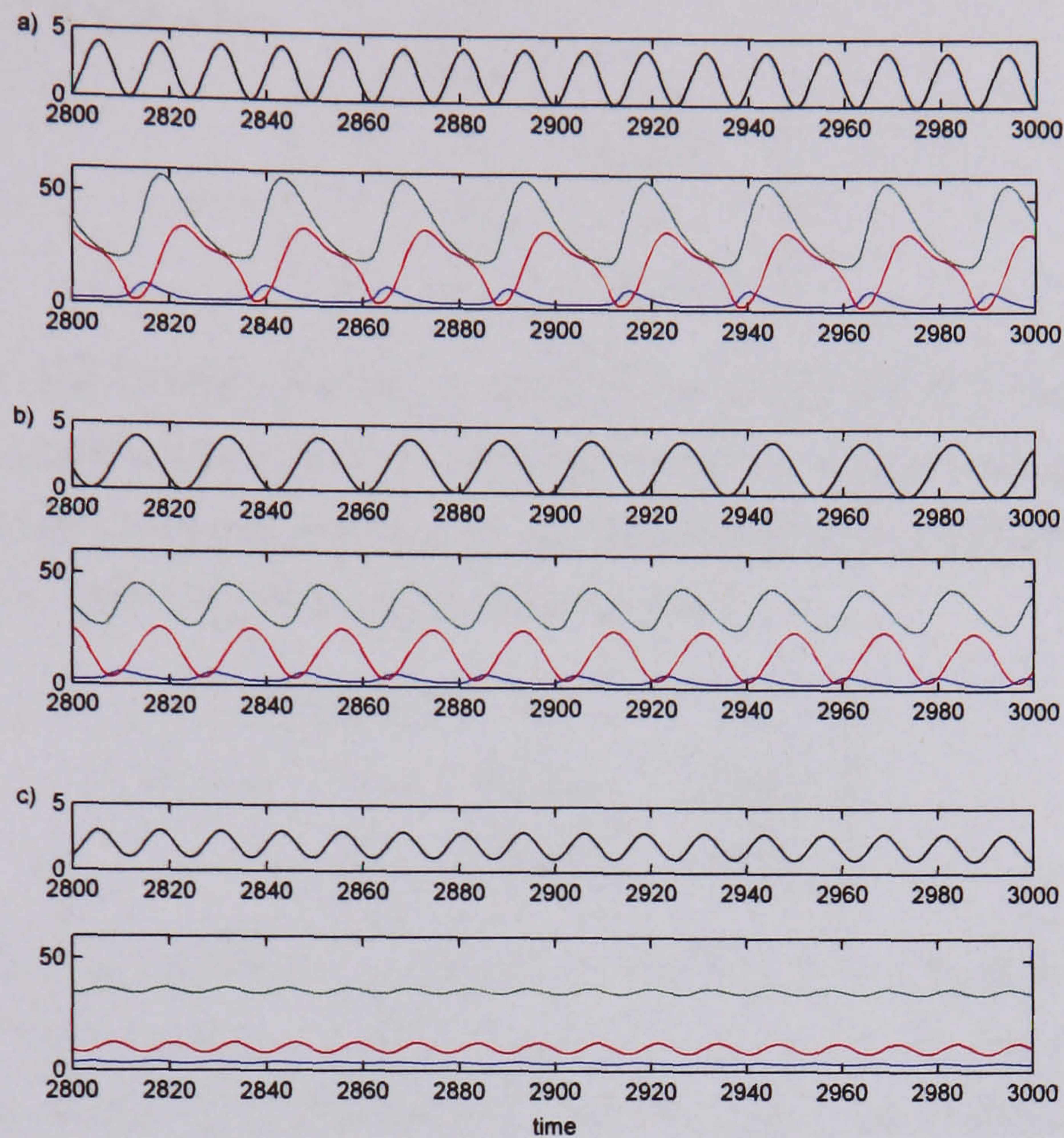


Figure 5.2: **Gene regulatory system with external forcing I.** The parameters of the system are $a = 0.25$, $d = 0.2$, $b = 2$, $e = 0.005$, $k = 10$ and $u_m = 2$. The three sub-figures represent the response of the system (bottom panel) to a sinusoidal drive of different amplitude and period (top panel): (a) $Au(t) = 2 \sin(\frac{1}{2}t)$, (b) $Au(t) = 2 \sin(\frac{1}{3}t)$, (c) $Au(t) = \sin(\frac{1}{2}t)$. Note that the system is not entrained in (a).

We apply Theorem 5.1.1 to establish conditions on parameters a and e of the system under which entrainment is guaranteed. Moreover, in accordance with Remark 5.0.1, we require that

$$M \text{diag}([a \ 0 \ 0]), \quad M \text{diag}([0 \ 0 \ e]), \quad \text{or} \quad M \text{diag}([a \ 0 \ e]) \geq 0. \quad (5.6)$$

To this end, we use YALMIP to solve the following feasibility problem:

$$\begin{array}{ll} \text{given} & a, e \\ \text{search for} & M \\ \text{subject to} & M > 0, \quad MJ(x) < 0, \quad \forall x_3 \in \overline{\mathbb{R}}_+ \\ & M \text{diag}([a \ 0 \ 0]), \quad M \text{diag}([0 \ 0 \ e]), \quad \text{or} \quad M \text{diag}([a \ 0 \ e]) \geq 0. \end{array} \quad (5.7)$$

Here, the Jacobian J is given by

$$J = \begin{bmatrix} -a & 0 & \frac{-10}{(1+x_3)^2} \\ 2 & -0.2 & 0 \\ 0 & 0.2 & \frac{-10}{(1+x_3)^2} - e \end{bmatrix}.$$

See Appendix B for the implementation in MATLAB using the YALMIP toolbox; note that YALMIP can handle uncertainties in $J(x)$. We use recursive sequencing to search for the lowest values a and the computation time is on the scale of a few seconds on a standard PC for each iteration. Our computations show that with

$$M = \begin{bmatrix} 0.1011 & 0 & 0 \\ 0 & 0.3272 & -0.0066 \\ 0 & -0.0066 & 0.0124 \end{bmatrix}$$

the system is guaranteed to entrain to all $u_m + Au(t) \geq 0$ if $a \geq 26.6$ (the inequality holds because of (5.6)), keeping all other parameter constants at the values shown in Figure 5.2. Similarly, $a, e \geq 1.3$ guarantee entrainment to any $u_m + Au(t) \geq 0$, if we keep all other parameters constants at those reference values (Figure 5.3). Note that if we drop requirement (5.6) then we find that synchronisation occurs already for lower parameter values; for instance, if $a = 21.8$, $e = 2.6$ or $a, e = 0.6$.

We have checked this sufficient condition numerically by testing for entrainment for random parameter values of a and e while keeping all other parameters constant. The numerical results indicate that entrainment is observed if $a \geq 0.4$ or, alternatively, if $e \geq 0.08$. As expected, our condition is conservative but it provides guarantees for entrainment and thus, could assist the process of drug design by identifying targets: changes in e , the depletion rate of the final product are easiest to change and will lead to entrainment as shown before. It is also less risky than introducing changes to the rate of loss and of recycling of mRNA given by a . However, a minor increase of the latter would mean that the changes to rate e could be reduced greatly. Moreover, the analysis provides a parameter regime $a, e \geq 1.3$ in which the gene regulatory system is robust to changes of a and e with respect to its ability to entrain.

Finally, note that this model is closely related to the Goodwin Model [38], which is often used to model the circadian clock [39–41]. Therefore, our analysis could provide means to help individuals who suffer from ‘dys-entrainment’ [24]. This condition is responsible

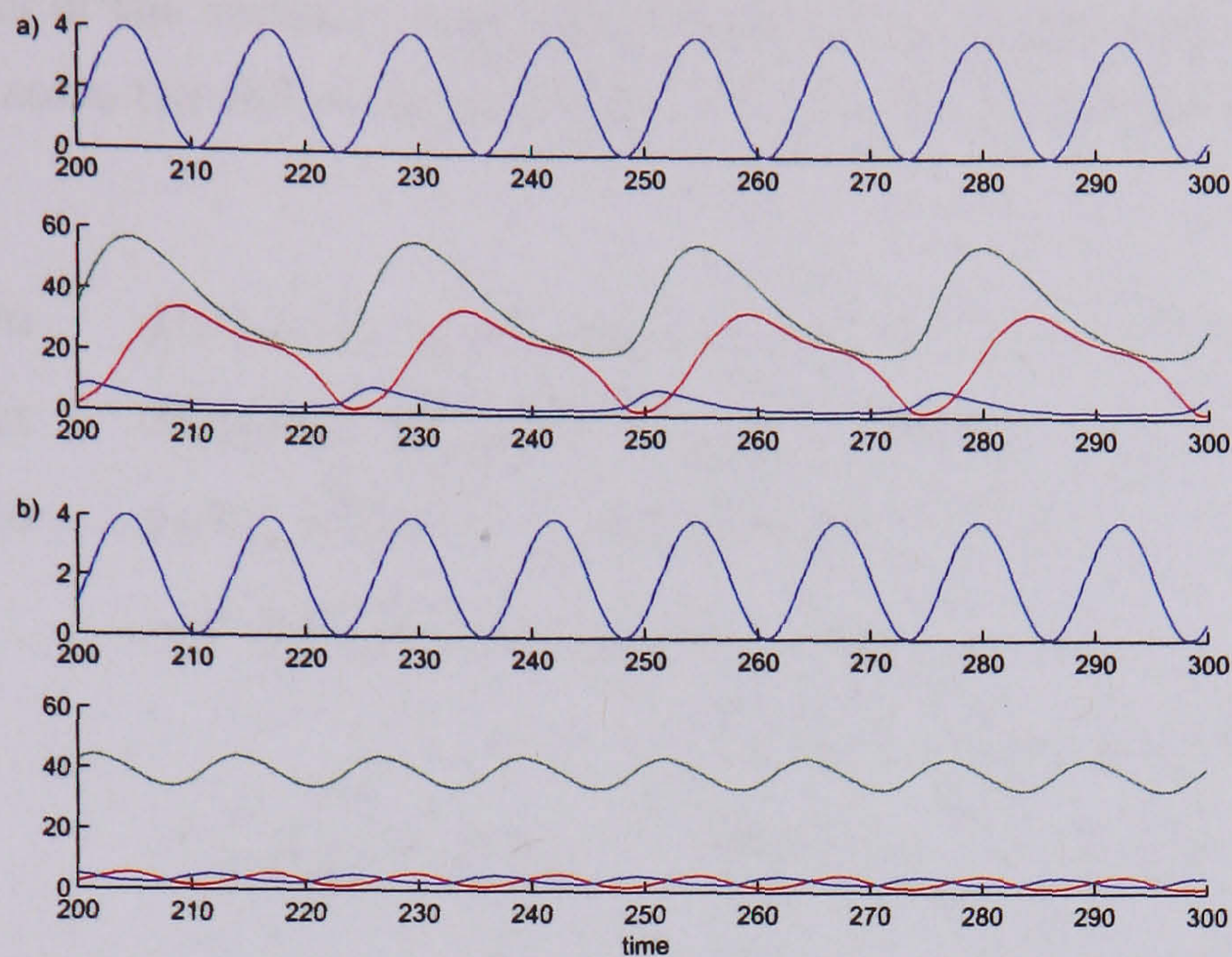


Figure 5.3: **Gene regulatory system with external forcing II.** The figure shows the response of the system to the sinusoidal drive $u(t) = 2 \sin \frac{t}{2}$ (top panels). (a) If $a = 0.25$ and $e = 0.005$ then the system does not entrain to the drive (bottom panel). (b) The system with $a, e = 0.6$ entrains (bottom panel).

for an enhanced risk of errors and accidents at work and different health problems. In this case, x_1 would denote the concentration of PER-mRNA. PER, whose concentration would be given by x_2 , is an oscillator gene, which drives the transcription of transcriptional inhibitor (x_3) that creates a feed back loop by blocking the activation of PER [94].

5.1.2 A pacemaker model

Entrainment is also important in models of the heart beat driven by a pacemaker in order to prevent cardiac dysrhythmia. As a phenomenological model of the heartbeat, the Van der Pol Oscillator is justifiable on the basis of the similarity with the qualitative features of the heart dynamics or ECG wave [30,31]. The driven Van der Pol Oscillator is given by:

$$\begin{aligned} \dot{x}_1 &= x_2 \\ \dot{x}_2 &= -(k + x_1^2)x_2 - x_1 + u(t), \end{aligned} \quad (5.8)$$

where $u(t)$ represents the external drive. Let $|u(t)|$ be bounded; that is, there exists a positive constant a such that $|u(t)| \leq a$. We apply Theorem 5.1.1 to establish conditions

on the parameters of the system under which entrainment is guaranteed. To this end, we use SOSTOOLS to solve the following feasibility problem, where we include the requirement of Remark 5.0.1:

$$\begin{array}{ll}
\text{given} & f(x) = [x_2 - (k + x_1^2)x_2 - x_1 + u]^T, \quad k, a, \delta > 0 \\
\text{search for} & M_{(1,1)}(x), M_{(1,2)}(x), M_{(2,2)}(x), p_1(v) \\
\text{subject to} & p_1(v), v^T (M(x) - \delta I) v \text{ are sum of squares} \\
& -v^T \left(M(x)J(x) + \frac{1}{2}M'(x) - \delta I \right) v \\
& \quad \quad \quad + p_1(x)(u^2 - a^2) \text{ is a sum of squares} \\
& v^T \left(M(x)\text{diag}([0 \ 1]) + \frac{1}{2} \frac{\partial M(x)}{\partial x_2} x_2 \right) v \text{ is a sum of squares.} \quad (5.9)
\end{array}$$

Note that $p_1(x)(u^2 - a^2) \leq 0$ for $|u(t)| \leq a$. Here, the Jacobian is given by

$$J = \begin{bmatrix} 0 & 1 \\ -(2x_1x_2 + 1) & k - x_1^2 \end{bmatrix}.$$

Now, let $|u(t)| \leq a = 1$. Then, we obtain with $k \geq 0.01$ and

$$\begin{aligned}
M_{(1,1)}(x) &= 7.535 + 1.971x_1^2 - 0.591x_1x_2 + 0.121x_2^2 + 7.147x_1^4 + 0.034x_1^2x_2^2 - 0.004x_1x_2^3 \\
M_{(1,2)}(x) &= 0.050 + 7.287x_1^2 + 0.012x_1x_2 - 0.003x_2^2 - 0.004x_1^3x_2 + 0.003x_1^2x_2^2 \\
M_{(2,2)}(x) &= 7.544 + 0.113x_1^2 - 0.042x_1x_2 + 0.006x_2^2 + 0.006x_1^4 - 0.001x_1^3x_2.
\end{aligned}$$

that the van der Pol oscillator entrains to time dependent inputs. Moreover, this result also holds for $a = 100$. For larger bounds on $u(t)$ we run into computational problems. However, we think that it is safe to conclude that in order to guarantee entrainment to an external drive the van der Pol system has to operate in the stable regime: $k > 0$ (see Figure 5.4).

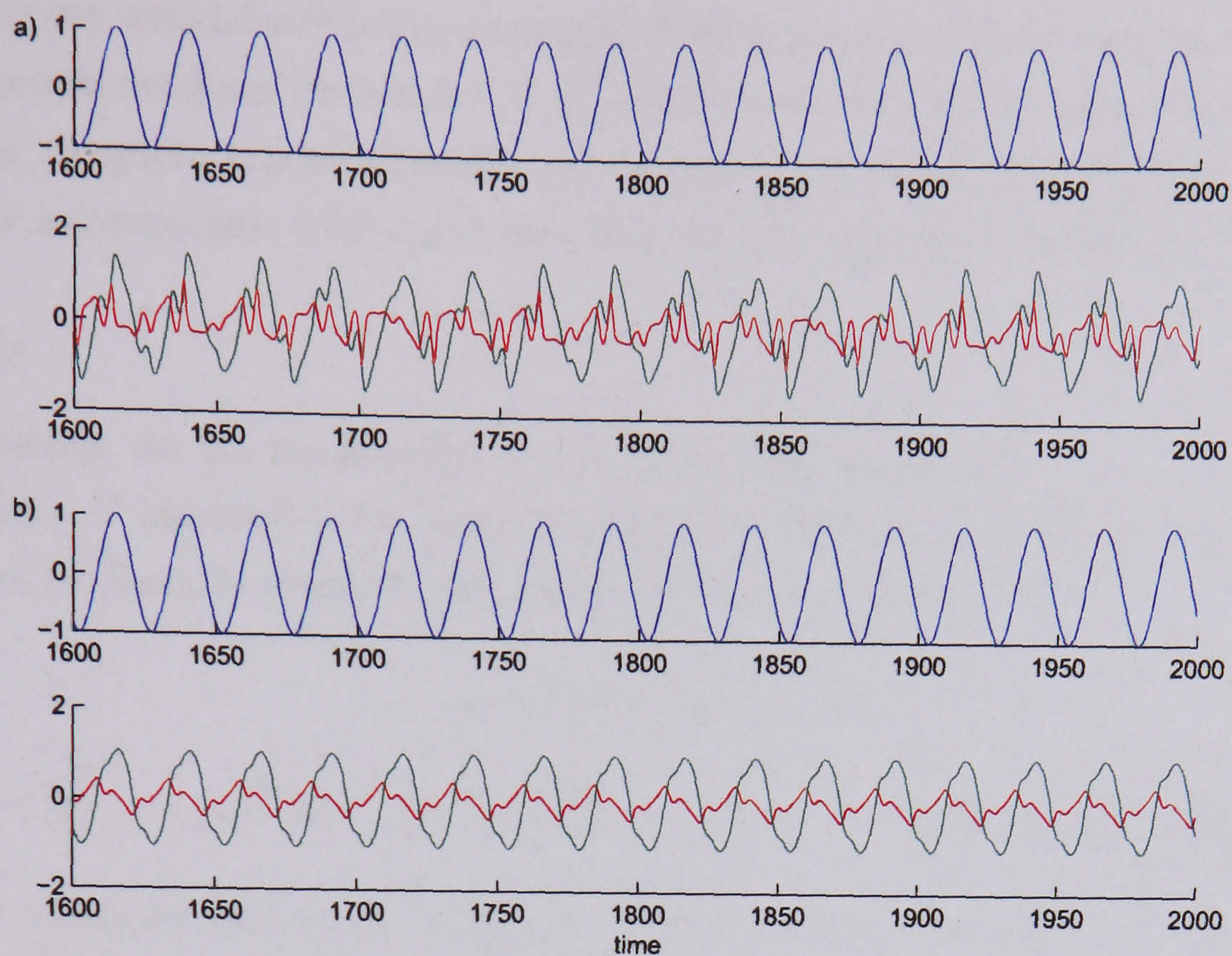


Figure 5.4: **The van der Pol oscillator with an external drive.** (a) For $k = -0.6$, The van der Pol oscillator (bottom panel) does not entrain to the periodic drive (top panel). (b) For $k = 0.01$, the van der Pol oscillator (bottom panel) entrains to the drive (top panel).

5.2 Global complete synchronisation of identical oscillators with symmetric but otherwise arbitrary coupling

In this section, we provide results on global complete synchronisation of coupled identical oscillators with a coupling graph that is symmetric and connected but otherwise arbitrary. Two dynamical systems x and y are completely synchronised if $x = y$ for all $t > t_0$. In Section 5.2.1, we briefly present known conditions on a system of coupled identical oscillators that guarantee the stability of the completely synchronised state locally [33]. In Section 5.2.2, we first present conditions on global stability of the complete synchronised state from references [34,35] and compare them. In Section 5.2.3, we exemplify the results through a network of coupled Repressilators and chaotic Lorenz systems. Importantly, as a

novelty we use semidefinite programming to make it possible to computationally implement the theoretical results of Section 5.2.2. We obtain numerical results that fulfil the conditions for global complete synchronisation and moreover, can search for their optimum, which allows for a comparison with cases, in which ‘simple’ analytical results exist.

Notation

In this section, we use the notation set by Chai Wah Wu in [35]:

Consider N identical n -dimensional oscillators given by $x_i \in \mathbb{R}^n$, $i = 1, \dots, N$. If the oscillators are linearly coupled, their dynamics can be described by:

$$\dot{x} = \tilde{f}(x) + \kappa(C \otimes D)x, \quad (5.10)$$

where $x = [x_1 \dots x_N]^T$ and $\tilde{f}(x) = [f(x_1) \dots f(x_N)]^T$. In the coupling term of (5.10)

- the positive constant κ corresponds to the coupling strength,
- $D \in \overline{\mathbb{R}}_+^{n \times n}$ denotes the output matrix for each oscillator of the variables that are used in the coupling,
- and the matrix $-C \in \mathbb{R}^{N \times N}$ is the Laplacian matrix of the coupling topology.

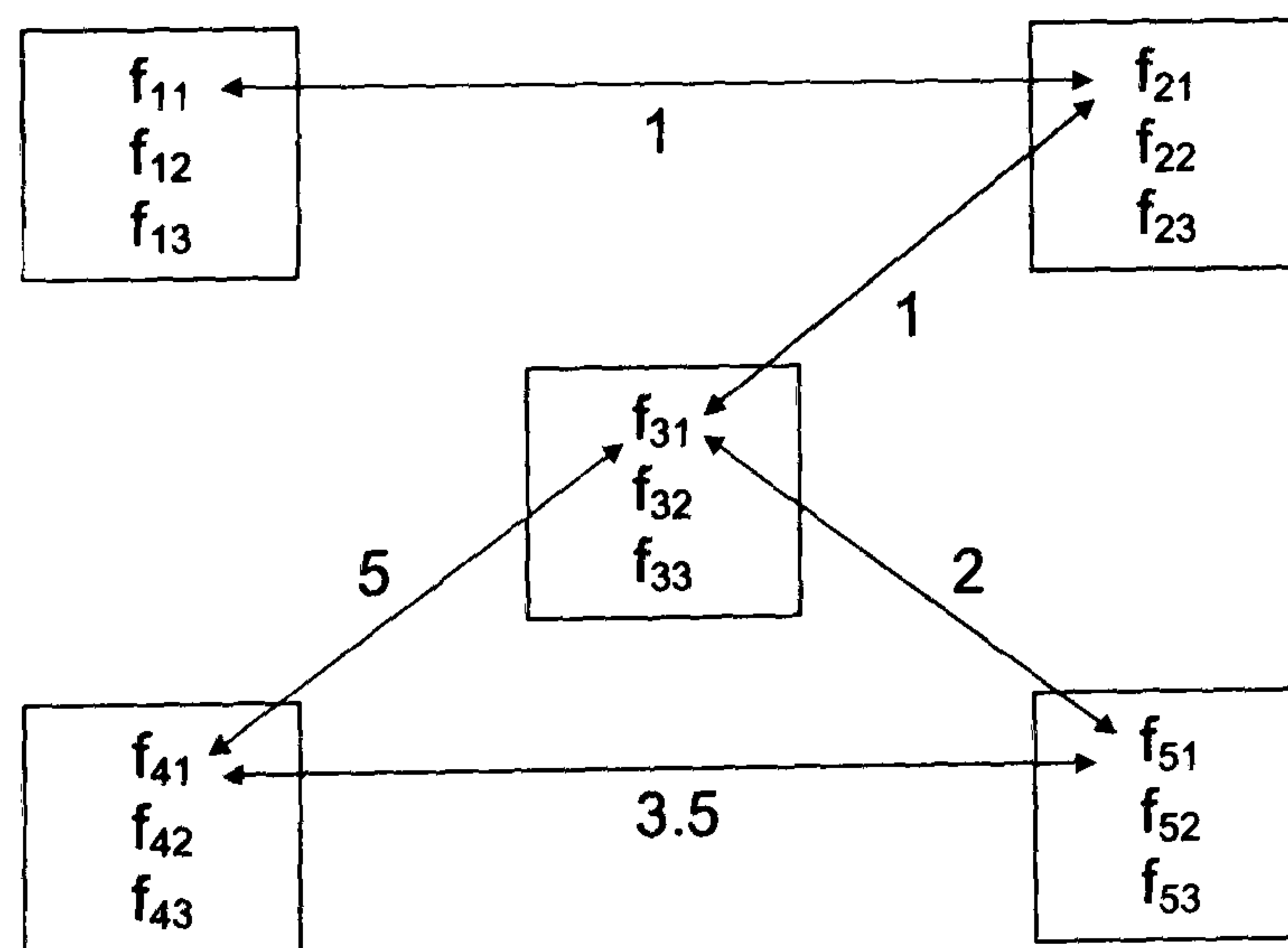


Figure 5.5: A network of coupled oscillators. Each square represents a three dimensional dynamical system. They are connected through a weighted network.

In Figure 5.5, $n = 3$, $N = 5$,

$$C = \begin{bmatrix} -1 & 1 & 0 & 0 & 0 \\ 1 & -2 & 1 & 0 & 0 \\ 0 & 1 & -8 & 5 & 2 \\ 0 & 0 & 5 & -8.5 & 3.5 \\ 0 & 0 & 2 & 3.5 & -5.5 \end{bmatrix}, \text{ and } D = \begin{bmatrix} 1 & 0 & 0 \\ 0 & 0 & 0 \\ 0 & 0 & 0 \end{bmatrix}.$$

Note that D is diagonal and an output counts 1, which we will assume to be the case throughout the thesis but which is not necessary. In this case, the connection is in f_1 and given through the exchange of x_{i_1} ; for example,

$$D = \begin{bmatrix} 0 & 1 & 0 \\ 0 & 0 & 0 \\ 0 & 0 & 0 \end{bmatrix}$$

would imply that the connection is also in f_1 but given through the exchange of x_{i_2} .

5.2.1 The master stability function

In [33], Louis M. Pecora and Thomas L. Carroll introduced the notion of the *Master Stability Function (MSF)* for coupled identical dynamical systems. Consider N identical n -dimensional linearly coupled oscillators:

$$\dot{x} = \tilde{f}(x) + \kappa(C \otimes D)x, \quad (5.11)$$

where $x = [x_1 \dots x_N]^T$, $\tilde{f}(x) = [f(x_1) \dots f(x_N)]^T$, κ is the coupling strength, and $D \in \overline{\mathbb{R}}_+^{n \times n}$ and $-C \in \mathbb{R}^{N \times N}$ are matrices encoding the coupling (see (5.10)).

Let $x_i = x_j$ for all $i, j = 1, \dots, N$. We denote this state of (5.11) by \bar{x} ; that is, $\bar{x}_1 = \bar{x}_2 = \dots = \bar{x}_N$. If the coupling matrix is a zero row sum matrix then $(C \otimes D)\bar{x} = 0$. The MSF approach locally investigates the stability of this state. If the individual uncoupled system has a (not necessarily constant) globally stable steady state then the synchronised state corresponds to the union of the individual (identical) steady states.

Now, consider the following linearised variational equation for the synchronised state of (5.11):

$$\dot{\xi} = \left[\frac{\partial \tilde{f}(x)}{\partial x} \Big|_{\bar{x}} + \kappa(C \otimes D) \right] \xi, \quad (5.12)$$

where $\xi = [\xi_1 \dots \xi_N]^T$. Let $\bar{J} = \left. \frac{\partial f(x_1)}{\partial x_1} \right|_{\bar{x}_1}$. Then,

$$\dot{\xi} = [I_N \otimes \bar{J} + \kappa(C \otimes D)] \xi. \quad (5.13)$$

Let $S\Lambda S^{-1} = C$, where Λ is a diagonal matrix containing the eigenvalues of C denoted by λ_i , $i = 1 \dots, N$. Let C be connected. Then, one eigenvalue is zero and all others are negative. Let $\lambda_1 = 0$ and $\xi = S \otimes I_n \vartheta$. Then,

$$\dot{\xi}(S \otimes I_n)^{-1} = \dot{\vartheta} = [SI_N S^{-1} \otimes \bar{J} + \kappa(SCS^{-1} \otimes D)] \vartheta = [I_N \otimes \bar{J} + \kappa(\Lambda \otimes D)] \vartheta. \quad (5.14)$$

Note that in (5.14) the different variational directions are separated. Thus,

$$\dot{\vartheta}_i = [\bar{J} + \lambda_i \kappa D] \vartheta_i, \quad i = 1, \dots, N. \quad (5.15)$$

Moreover, $i = 1$ corresponds to the synchronisation manifold ($\lambda_1 = 0$) and all other i 's to transverse variations. The *Master Stability Equation* is given by

$$\dot{\zeta} = [\bar{J} + \alpha \kappa D] \zeta, \quad \alpha \in \mathbb{C}. \quad (5.16)$$

By computing the maximal Lyapunov exponent of (5.16) along the trajectory of an individual uncoupled system for different values of $\alpha \in \mathbb{C}$, we can construct a map of the stability of (5.16) in the complex plane. Stable regions correspond to values of α which have negative exponents associated with, and unstable to those which have positive exponents associated with. Then, we can locate $\lambda_i \kappa$ in the complex plane for all i . If at least one is located within the unstable zone then the synchronised state is unstable at that κ ; which implies that a necessary condition for stability of the synchronised state is that, for all i , $\lambda_i \kappa$ is not located within the unstable zone. If they are all located within the stable zone then the synchronised state is locally stable for that κ .

5.2.2 Sufficient conditions for global complete synchronisation of identical oscillators

In the 1990s, Jack K. Hale published his work on sufficient conditions that guarantee global stability of the synchronised state of a system of coupled identical oscillators based on dissipation in the coupling [95]. The new millennium has seen extensions to this work by Chai Wah Wu [35,96] and Igor Belykh et al [34,97], who have developed independently

different but related approaches to obtain conditions that are based on graph theory and Lyapunov theory. In the following, we will present and compare them. In Section 5.2.3, we show how to computationally implement the conditions presented here.

We reformulate Theorem 2.1 of [35] on global complete synchronisation as Theorem 5.2.3 by using the result of our Lemma 5.2.2. (We have recently discovered that an equivalent requirement was already presented in [96].) First, we define the Laplacian matrix of the completely connected graph (recall that $E = ee^T$, $e^T = [1 \dots 1]$):

Definition 5.2.1. The Laplacian matrix of the completely connected graph is given by $-U \in \mathbb{R}^{N \times N}$, where

$$-U = NI_N - E \leq 0. \quad (5.17)$$

In what follows, $-C$ is the Laplacian matrix of the coupling topology, which is not required to be constant; that is, it can be of the form $C(x)$ or $C(t)$.

Lemma 5.2.2. Let $C, U \in \mathbb{R}^{N \times N}$ and U be given by (5.17). If $-C$ is a symmetric M -matrix (that is, it has zero row and column sum) of rank $(N - 1)$ then there exists a positive constant γ such that $-\gamma U \leq -C$ if

$$\gamma N = \lambda_{\min}(-C), \quad (5.18)$$

where $\lambda_{\min}(-C)$ denotes the smallest positive eigenvalue of the matrix $-C$.

Proof. First note that $C_{(i,j \neq i)} \geq 0$. Now, $UE = 0$ and $CE = 0$. Hence, $UU = -NU$ and $CU = -NC$. Let $-SCS^{-1} = \Lambda_{-C}$, where Λ_{-C} is the diagonal matrix containing the eigenvalues of $-C$; without loss of generality, let $\Lambda_{-C_{1,1}} = 0$. Moreover, $S^{-1} = S^T$, and since

$$SCUS^T = SCS^T S U S^T = -NSCS^T$$

it follows that $SUS^T = \Lambda_U$, where Λ_U is the diagonal matrix containing the eigenvalues of U and $\Lambda_{U_{1,1}} = 0$. Now, for all $y \in \mathbb{R}^N$,

$$-y^T \gamma U y = -y^T S^T \gamma \Lambda_U S y = -v^T \gamma \Lambda_U v \leq v^T \Lambda_{-C} v = y^T S^T \Lambda_{-C} S y = -y^T C y$$

holds if $\lambda_{\max}(-\gamma U) = \gamma N = \lambda_{\min}(-C)$. □

In the following, matrix D represents the coupling between any two dynamical systems, which is also not required to be constant; that is, it can be of the form $D(x)$ or $D(t)$.

Theorem 5.2.3. *Let C, U be as in Lemma 5.2.2, and*

$$\dot{x} = \tilde{f}(x) + \kappa(C \otimes D)x, \quad (5.19)$$

where $D \in \overline{\mathbb{R}}_+^{n \times n}$, $x = [x_1 \dots x_N]^T$, $\tilde{f}(x) = [f(x_1) \dots f(x_N)]^T$, $x_i \in \mathcal{D} \subseteq \mathbb{R}^n$, $i \in \{1, \dots, N\}$. Furthermore, let γ be such that $\gamma N = \lambda_{\min}(-C)$ and

$$g(x_i) = f(x_i) - \gamma N \kappa D x_i. \quad (5.20)$$

Then, if there exists a symmetric and positive matrix $P \in \mathbb{R}^{n \times n}$ such that for all x_i and all i

$$(x_i - x_j)^T P (g(x_i) - g(x_j)) < 0, \quad x_j \neq x_i, \quad (5.21)$$

the network of coupled dynamical systems given by (5.19) synchronises in the sense that $x_i - x_j \rightarrow 0$, $\forall i, j$, as $t \rightarrow \infty$.

Proof. Consider the following Lyapunov function from [35]:

$$V(x) = -x^T (U \otimes P) x = \frac{1}{2} \sum_{i < j} U_{(i,j)} (x_i - x_j)^T P (x_i - x_j) > 0 \text{ if } x_i \neq x_j, \quad \forall i, j,$$

and thus,

$$\dot{V}(x) = -\frac{1}{2} x^T (U \otimes P) \dot{x} - \frac{1}{2} \dot{x}^T (U \otimes P) x = -x^T (U \otimes P) \dot{x}.$$

The second equality follows from the symmetry of $U \otimes P$. Now, note that if $i < j$, for all i, j , then $U_{(i,j)} = 1$, and recall that $U^2 = -NU$. Since γ is such that $\gamma N = \lambda_{\min}(-C)$, it follows that

$$\begin{aligned} \dot{V}(x) &= -x^T (U \otimes P) \dot{x} = -x^T (U \otimes P) (\tilde{f}(x) + \kappa(C \otimes D)x) \\ &= -x^T (U \otimes P) \tilde{f}(x) - x^T \kappa(U C \otimes P D)x = -x^T (U \otimes P) \tilde{f}(x) + x^T N \kappa(C \otimes P D)x \\ &\leq -x^T (U \otimes P) \tilde{f}(x) + x^T \gamma N \kappa(U \otimes P D)x \\ &= \sum_{i < j} (x_i - x_j)^T P (f(x_i) - f(x_j)) - \gamma N \kappa \sum_{i < j} (x_i - x_j)^T P (D x_i - D x_j) \\ &= \sum_{i < j} (x_i - x_j)^T P (g(x_i) - g(x_j)) < 0, \quad x_i \neq x_j. \end{aligned} \quad (5.22)$$

The inequality in (5.22) implies that (5.19) synchronises in the sense that $x_i - x_j \rightarrow 0$, $\forall i, j$, as $t \rightarrow \infty$. \square

By the mean value theorem (Theorem 3.1.1), inequality (5.21) holds if

$$P \left(\frac{\partial g(y)}{\partial y} \right) < 0, \quad \forall y \in \mathcal{D}. \quad (5.23)$$

As opposed to the approach presented in the previous section, which investigates the stability of the synchronisation manifold locally through the analysis of the Lyapunov exponent, the result in this section guarantees global asymptotic stability. However, it is more conservative and requires a search for matrix P . In Section 5.2.3 of this thesis, we show how to computationally perform this search.

To see how the results of Igor Belykh et al. in [34] are related to the previously presented, we show in the following the ideas behind them. In [34], the difference

$$X_{ij} = x_i - x_j \quad (5.24)$$

was considered. However, synchronisation is also well defined in a system, where the different systems are compared to one reference system. Thus, for all i , consider the difference $x_i - x_1 \equiv X_i$ ($X_1 = 0$). Then,

$$X = \begin{bmatrix} X_1 \\ X_2 \\ X_3 \\ \vdots \\ X_N \end{bmatrix} = \left(\begin{bmatrix} 0 & 0 & 0 & \dots & 0 \\ -1 & 1 & 0 & \dots & 0 \\ -1 & 0 & 1 & \dots & 0 \\ \vdots & \vdots & \vdots & \ddots & \vdots \\ -1 & 0 & 0 & \dots & 1 \end{bmatrix} \otimes I_n \right) x = (F \otimes I_n)x, \quad (5.25)$$

and

$$\dot{X} = (F \otimes I_n)\dot{x}. \quad (5.26)$$

Let matrix P be such that $P > 0$ and consider the following Lyapunov function:

$$V(X) = \frac{1}{2} X^T (I_N \otimes P) X > 0, \quad X \neq 0.$$

Note that $C = CF$. Then,

$$\begin{aligned} \dot{V}(X) &= X^T (I_N \otimes P) \dot{X} = X^T (F \otimes P) \dot{x} \\ &= X^T (F \otimes P) (\tilde{f}(x) + \kappa(C \otimes D)x) \\ &= \sum_{i=2}^N X_i^T P (f(x_i) - f(x_1)) + X^T \kappa (FCF \otimes PD)x \\ &= \sum_{i=2}^N X_i^T P (f(x_i) - f(x_1)) + X^T \kappa (FC \otimes PD)X. \end{aligned}$$

By Theorem 3.1.1, there exists a z_i such that $z_{ij} \in [x_{ij}, x_{1j}]$ for all $j, j = 1, \dots, n$ and

$$f(x_i) - f(x_1) = J(x_i)|_{x_i=z_i} X_i,$$

where $\frac{\partial f(x_i)}{\partial x_i} \equiv J(x_i)$. Thus,

$$\dot{V}(X) = \sum_{1 < i}^N X_i^T P J(x_i)|_{x_i=z_i} X_i + X^T \kappa (FC \otimes PD) X = \sum_{1 < i}^N X_i^T P (J(x_i)|_{x_i=z_i} - \alpha \kappa ND) X_i,$$

where $\alpha N = \lambda_{\min}(-(FC)_{\text{gL}})$ and $(FC)_{\text{gL}}$ is the matrix obtained by deleting the first row and the first column. It is the so called *grounded Laplacian* [98, 99], where the deleted row and deleted column correspond to the grounded variable – in our case it is x_1 . A grounded Laplacian matrix is a principal sub-matrix of the Laplacian matrix. Now, this implies that $\dot{V}(x) < 0$ if

$$P(J(x_i)|_{x_i=z} - \alpha \kappa ND) < 0, \quad z \in \mathcal{D}, \quad (5.27)$$

The inequality $\dot{V}(x) < 0$ means that the difference $x_i - x_1$ tends to zero for all i as $t \rightarrow \infty$ and thus, that the system of coupled identical oscillators completely synchronises. Since $\text{eig}(FC) = \text{eig}(CF) = \text{eig}(C)$ ¹ and the first row of matrix FC is zero, it follows that $\lambda_{\min}(-(FC)_{\text{gL}}) = \lambda_{\min}(-C)$. Thus, (5.27) is equivalent to (5.23) with constant α replacing constant γ .

In summary, if solution trajectories of the coupled system are bounded and one can show that the origin is a globally asymptotically stable equilibrium point of (5.26) then the coupled system will exhibit synchronised behaviour that corresponds to the behaviour of an individual uncoupled system as $t \rightarrow \infty$.

Different coupling configurations

For illustration, we provide examples of $\lambda_{\min}(-C)$ of different unweighted coupling configurations; recall that $\alpha N = \gamma N = \lambda_{\min}(-C)$.

- a) All-to-all coupling ($C = U$): $\lambda_{\min}(-C) = N$.
- b) Star-configuration: $\lambda_{\min}(-C) = 1$.
- c) Ring of diffusively coupled oscillators: $\lambda_{\min}(-C) = 4 \sin^2 \frac{\pi}{N}$.

¹The fact that for square matrices A, B , $\text{eig}(A) = \text{eig}(B)$ is proven in [100].

- d) Ring of $2k$ -nearest neighbor coupled oscillators: $\lambda_{\min}(-C) \simeq 2\pi^2 k(k+1)(2k+1)/3N^2$ if $k \ll N$ (see [7]).

The different coupling configurations are illustrated in the figure below.

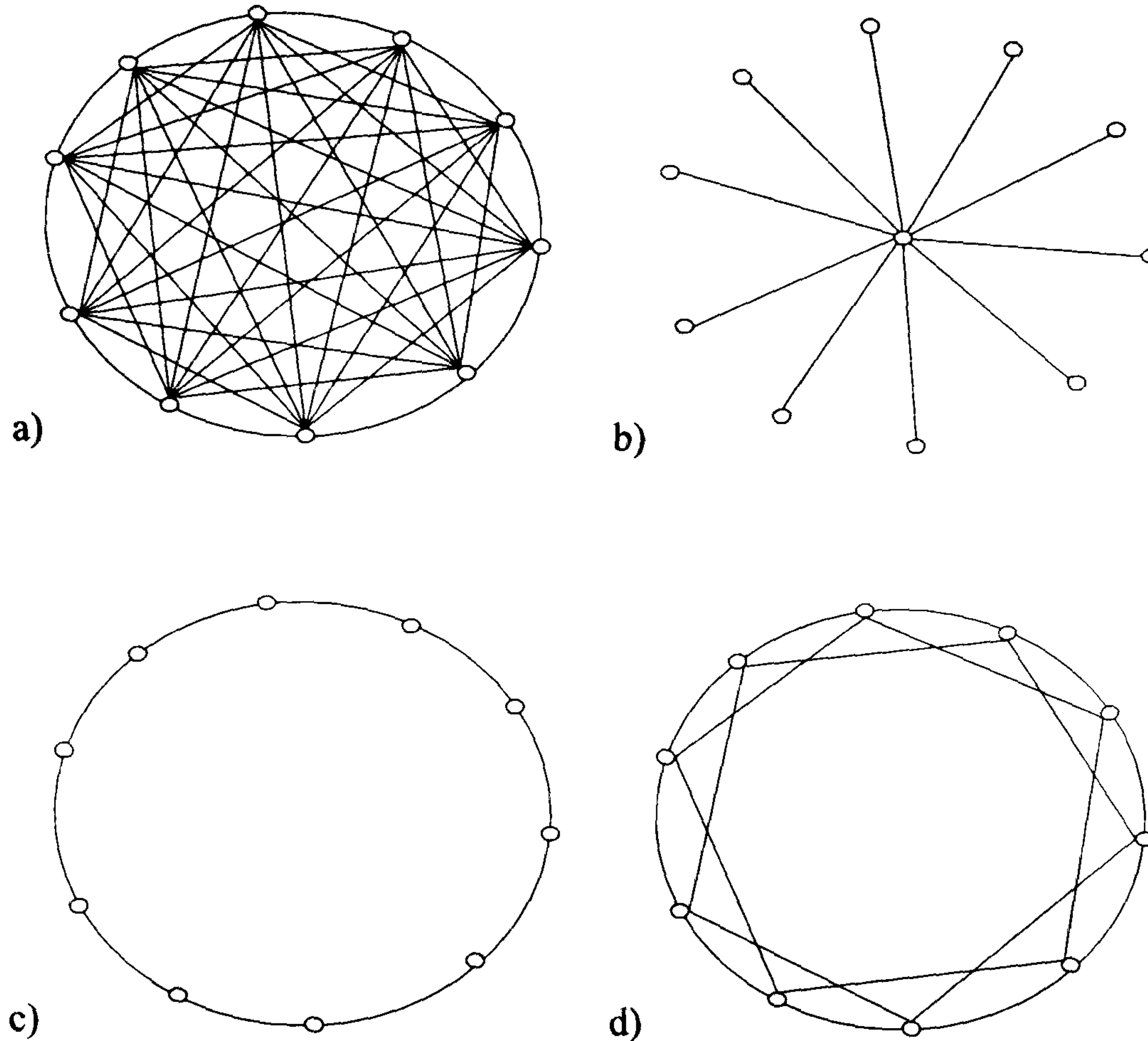


Figure 5.6: **Four different coupling configurations.** Here, $N = 10$ in (a), (c) and (d), $N = 11$ in (b), and $k = 2$ in (d).

It follows that for any given number N of coupled oscillators, the lower the value of γ is, the larger the value of κ must be in order for (5.27) to hold. If κ is associated with a cost function and larger values of κ are more costly then clearly configuration (a) is the most desirable. Let $\gamma\kappa N = 1$. Then, the following table compares the values of κ for configuration (a) – (c) when $N = 7, \dots, 10$:

N	7			8			9			10		
conf.	(a)	(b)	(c)	(a)	(b)	(c)	(a)	(b)	(c)	(a)	(b)	(c)
κ	0.143	1	0.19	0.125	1	0.213	0.111	1	0.238	0.1	1	0.262

Table 5.1: Coupling cost depending on configuration.

5.2.3 Computational methods to obtain certificates for global complete synchronisation with applications

In this section, we show how to implement the theoretical results presented previously in order to obtain computationally certificates that guarantee global complete synchronisation. First, note that condition (5.23) (which is equivalent to (5.27)) corresponds to a feasibility problem and can be implemented as:

$$\begin{array}{ll}
 \text{given} & f(x), \gamma, N, D, \kappa \\
 \text{search for} & P \\
 \text{subject to} & P > 0, PD \geq 0, P \left(\frac{\partial f(x)}{\partial x} - \gamma N \kappa D \right) < 0.
 \end{array} \tag{5.28}$$

Note that we have included the requirement of Remark 5.0.1. In the following, we provide applications to coupled Lorenz systems and a network of Repressilators (a synthetic biological circuit).

A network of coupled identical Lorenz systems

Consider a network of N coupled identical Lorenz systems. The set of equations for each individual system is given by ($i = 1, \dots, N$):

$$\begin{aligned}
 \dot{x}_{i_1} &= \sigma(y_{i_2} - x_{i_1}), \\
 \dot{x}_{i_2} &= rx_{i_1} - x_{i_2} - x_{i_1}x_{i_3}, \\
 \dot{x}_{i_3} &= x_{i_1}x_{i_2} - bx_{i_3}.
 \end{aligned} \tag{5.29}$$

The coupled system is given by (5.19):

$$\dot{x} = \tilde{f}(x) + \kappa(C \otimes D)x.$$

The Jacobian of each individual Lorenz system is given by

$$J_L = \begin{bmatrix} -\sigma & \sigma & 0 \\ r - x_{i_3} & -1 & -x_{i_1} \\ x_{i_2} & x_{i_1} & -b \end{bmatrix}.$$

Now, let $D = \text{diag}([1 \ 0 \ 0])$, where D is the output matrix of the variables that are used in the coupling. Let $\sigma > 1$ and $b > 2$.

Similarly to [101], the following analysis will establish a bound for (5.2.3). For instance, consider

$$V(x) = \frac{1}{2} \left(\sum_{i=1}^N x_{i_1}^2 + \sum_{i=1}^N x_{i_2}^2 + \sum_{i=1}^N (x_{i_3} - \sigma - r)^2 \right). \quad (5.30)$$

It follows that

$$\begin{aligned} \dot{V}(x) &= -\sigma \sum_{i=1}^N x_{i_1}^2 - \sum_{i=1}^N x_{i_2}^2 - b \sum_{i=1}^N (x_{i_3}^2 - (\sigma + r)x_{i_3}) + x^T \kappa(C \otimes D)x \\ &= -\sigma \sum_{i=1}^N x_{i_1}^2 - \sum_{i=1}^N x_{i_2}^2 - b \sum_{i=1}^N \left(x_{i_3} - \frac{\sigma + r}{2} \right)^2 + Nb \left(\frac{\sigma + r}{2} \right)^2 + x^T \kappa(C \otimes D)x. \end{aligned} \quad (5.31)$$

Let Γ be given by

$$\sigma \sum_{i=1}^N x_{i_1}^2 + \sum_{i=1}^N x_{i_2}^2 - b \sum_{i=1}^N \left(x_{i_3} + \frac{\sigma + r}{2} \right)^2 - x^T \kappa(C \otimes D)x = Nb \left(\frac{\sigma + r}{2} \right)^2.$$

Then, $\dot{V}(x) < 0$ outside Γ and $\dot{V}(x) > 0$ inside Γ . It follows that, for initial condition inside Γ , the upper bound \mathfrak{b} of $V(x)$ lies on Γ , on which $\dot{V}(x) = 0$ and thus,

$$\sum_{i=1}^N x_{i_2}^2 = -\sigma \sum_{i=1}^N x_{i_1}^2 - b \sum_{i=1}^N (x_{i_3}^2 - (\sigma + r)x_{i_3}) + x^T \kappa(C \otimes D)x$$

which leads to

$$\begin{aligned} V(x \in \Gamma) &= \frac{1}{2} \left((1 - \sigma) \sum_{i=1}^N x_{i_1}^2 + \sum_{i=1}^N (-bx_{i_3}^2 + b(\sigma + r)x_{i_3} + (x_{i_3} - \sigma - r)^2) + x^T \kappa(C \otimes D)x \right) \\ &\leq \tilde{V}(x \in \Gamma) = \frac{1}{2} \left((1 - \sigma) \sum_{i=1}^N x_{i_1}^2 + \sum_{i=1}^N (-bx_{i_3}^2 + b(\sigma + r)x_{i_3} + (x_{i_3} - \sigma - r)^2) \right). \end{aligned}$$

Thus, $\mathfrak{b} = \max\{V(x \in \Gamma)\} \leq \max\{\tilde{V}(x \in \Gamma)\}$. Now, for all i , the solutions to

$$\frac{\partial \tilde{V}(x \in \tilde{\Gamma})}{\partial x_{i_1}} = (1 - \sigma)x_{i_1} = 0, \quad \frac{\partial \tilde{V}(x \in \tilde{\Gamma})}{\partial x_{i_3}} = x_{i_3} - (\sigma + r) - b(x_{i_3} - \frac{\sigma + r}{2}) = 0,$$

are given by $\bar{x}_{i_1} = 0$ and $\bar{x}_{i_3} = \frac{b-2}{2(b-1)}(\sigma + r) = \rho$. Note that, for all i ,

$$\left. \frac{\partial^2 V(x \in \Gamma)}{\partial x_{i_1}^2} \right|_{x_{i_1}=\bar{x}_{i_1}, x_{i_3}=\bar{x}_{i_3}} < 0 \quad \text{and} \quad \left. \frac{\partial^2 V(x \in \Gamma)}{\partial x_{i_3}^2} \right|_{x_{i_1}=\bar{x}_{i_1}, x_{i_3}=\bar{x}_{i_3}} < 0.$$

It follows that

$$\mathbf{b} \leq \max\{\tilde{V}(x \in \Gamma)\} = \frac{N}{2}(-b\rho^2 + b(\sigma + r)\rho + (\rho - \sigma - r)^2) = \frac{N}{2} \frac{b^2(r + \sigma)^2}{4(b - 1)}.$$

Thus, for initial conditions inside Γ , the following bound holds:

$$\sum_{i=1}^N x_{i_1}^2 + x_{i_2}^2 + (\sigma + r - x_{i_3})^2 < N \frac{b^2(r + \sigma)^2}{4(b - 1)}. \quad (5.32)$$

Note that this set is compact and convex. In the following, we will assume that the dynamics of the coupled system evolve in or at most on Γ .

Similarly to [34], we let $P = I$, use (5.32) and obtain that

$$PJ_L + J_L^T P - 2\gamma N \kappa PD = J_L + J_L^T - 2\gamma N \kappa D < 0 \quad (5.33)$$

if

$$\kappa > \frac{b(1 + b)(r + \sigma)^2}{16\gamma(b - 1)} - \frac{\sigma}{\gamma N}, \quad (5.34)$$

where γ is as in Lemma 5.2.2. Condition (5.34) follows from the Routh-Hurwitz criterion. For instance, (5.34) guarantees that $a_3 > 0$ and $a_1 a_2 > a_3$, where

$$\begin{aligned} a_1 &= \sigma + \gamma N \kappa + 1 + b, \\ a_2 &= \sigma + \gamma N \kappa + b + (\sigma + \gamma N \kappa)b - 0.25((\sigma + r - x_{i_3})^2 + x_{i_2}^2) \\ \text{and } a_3 &= (\sigma + \gamma N \kappa)b - 0.25(b(\sigma + r - x_{i_3})^2 + x_{i_2}^2) \end{aligned}$$

are the coefficients of the characteristic equation of (5.33): $\lambda^3 + a_1 \lambda^2 + a_2 \lambda + a_3 = 0$.

Typically, the following system parameters are chosen for the Lorenz system: $\sigma = 10$, $b = \frac{8}{3}$, and $r = 28$. Thus, if we assume that $P = I$ as in [34] then (5.34) guarantees global complete synchronisation if $\kappa > 530 - \frac{10}{\gamma N}$. Figure 5.6 shows how γ changes according to different coupling topologies. For example, the coupled Lorenz system completely synchronises with all-to-all coupling if $\kappa \geq 525$ and $N = 2$, or if $\kappa \geq 529$ and $N = 10$.

By using semidefinite programming, the bound on κ can be improved significantly. Using YALMIP, we obtain that with

$$P = \begin{bmatrix} 4.929 & 0 & 0 \\ 0 & 0.877 & 0 \\ 0 & 0 & 0.877 \end{bmatrix} \quad (5.35)$$

the coupled Lorenz system completely synchronises if $\kappa \geq \frac{251}{\gamma}$ ($\kappa \geq 251$ with all-to-all coupling) and $N = 2$; and that with

$$P = \begin{bmatrix} 4.328 & 0 & 0 \\ 0 & 0.327 & 0 \\ 0 & 0 & 0.327 \end{bmatrix} \quad (5.36)$$

the system synchronises if $\kappa \geq \frac{125}{\gamma}$ ($\kappa \geq 125$ with all-to-all coupling) and $N = 10$.

Note, that the bound given by (5.32) was implemented in YALMIP as

$$x_{i_1}^2, x_{i_2}^2, (38 - x_{i_3})^2 < 1540.3N.$$

This is somewhat conservative. One great advantage of SOSTOOLS is that condition (5.32) can be posed as it is, however at greater computational effort:

$$\begin{array}{ll} \text{given} & x_i, f(x_i), \gamma, N, D, \kappa, \delta > 0 \\ \text{search for} & P, p(v) \\ \text{subject to} & v^T(P - \delta I)v, v^T P D v, p(v) \text{ are SOS } \forall v \in \mathbb{R}^n \\ & -v^T(J(x_i) - \gamma N \kappa D + \delta I)v + p(v)(x_{i_1}^2 + x_{i_2}^2 + (38 - x_{i_3})^2 - 1540.3N) \text{ is SOS} \\ & \forall v \in \mathbb{R}^n. \end{array} \quad (5.37)$$

Searching for a lower bound on κ using SOSTOOLS, we obtain that with

$$P = \begin{bmatrix} 17.077 & 0 & 0 \\ 0 & 3.777 & 0 \\ 0 & 0 & 3.782 \end{bmatrix} \quad (5.38)$$

the coupled Lorenz system completely synchronises if $\kappa \geq \frac{222.6}{\gamma}$ ($\kappa \geq 222.6$ with all-to-all coupling) and $N = 2$; and that with

$$P = \begin{bmatrix} 9.59 & 0 & 0 \\ 0 & 1.116 & 0 \\ 0 & 0 & 1.116 \end{bmatrix} \quad (5.39)$$

the system synchronises if $\kappa \geq \frac{117.9}{\gamma}$ ($\kappa \geq 117.9$ with all-to-all coupling) and $N = 10$. Numerics indicate that for $N = 2$ global complete synchronisation occurs if $\kappa \geq 4$ (Figure 5.7).

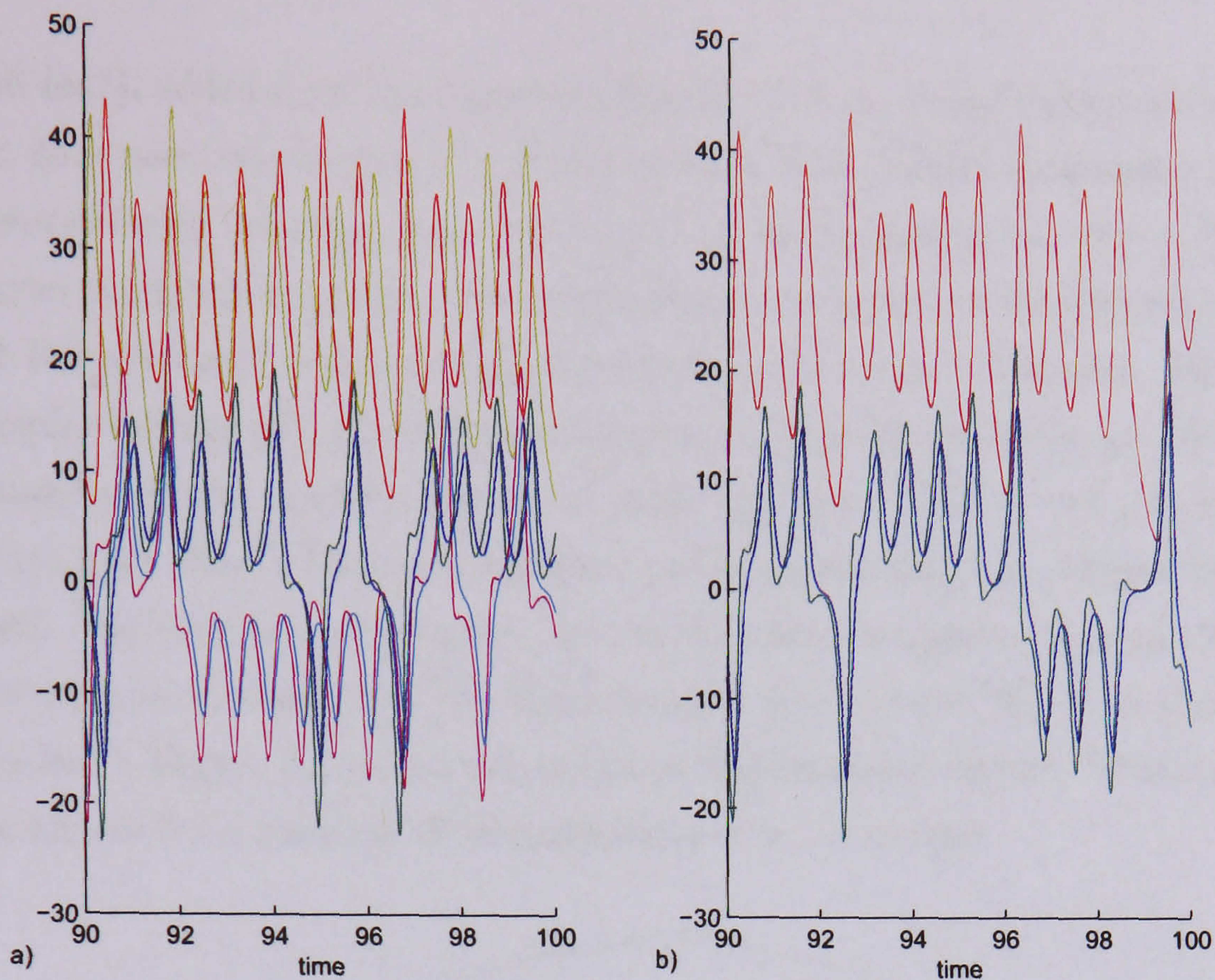


Figure 5.7: **Two coupled identical Lorenz systems.** (a) For $\kappa = 1$, the two coupled identical Lorenz systems do not synchronise. (b) For $\kappa = 4$, the two coupled identical Lorenz systems completely synchronise.

The following table summarises the results of this example and shows how using semidefinite programming lowers the value of the minimal κ that guarantees global complete synchronisation and which we denote by κ^* :

	$P = I$		SOSTOOLS	
N	2	10	2	10
κ^*	525	529	$222.6 \left(\frac{222.6}{525} \approx \frac{1}{2} \right)$	$117 \left(\frac{117.9}{529} = 0.22 \right)$

Table 5.2: Comparison of values of κ^* obtained with and without the application of semidefinite programming.

A network of coupled identical Repressilators

In a seminal paper [37], Michael B. Elowitz and Stanislas Leibler presented the so called *Repressilator*, a synthetic biological oscillator in *E. coli* which has been used to facilitate our understanding of genetic oscillatory circuits. The Repressilator consists of three genes

(*cI*, *tetR*, and *lacI*), which synthesise proteins that inhibit the transcription of each other in a cyclic way. In a more recent paper, a modified version of the Repressilator was proposed to enable inter-cellular coupling that can lead to synchronised behaviour [93]. Here, we study the issue of global complete synchronisation in networks of Repressilators. In [93], two coupled Repressilator circuits controlling each other were considered. We propose a different, simpler biologically plausible modification of the Repressilator circuit that allows for easier analysis of the synchronisation of these systems. Namely, we propose to swap gene *tetR* with gene *luxI*, which synthesises a protein (AI) that can diffuse freely in and out of the cell. Furthermore, we assume that AI can bind to another protein and that this complex inhibits the expression of the Repressilator gene *cI* (in [93], it is promoting the expression of *lacI*). Figure 5.8 shows the modified Repressilator circuit. This configuration provides the means for a network of ‘Repressilator cells’ to couple.

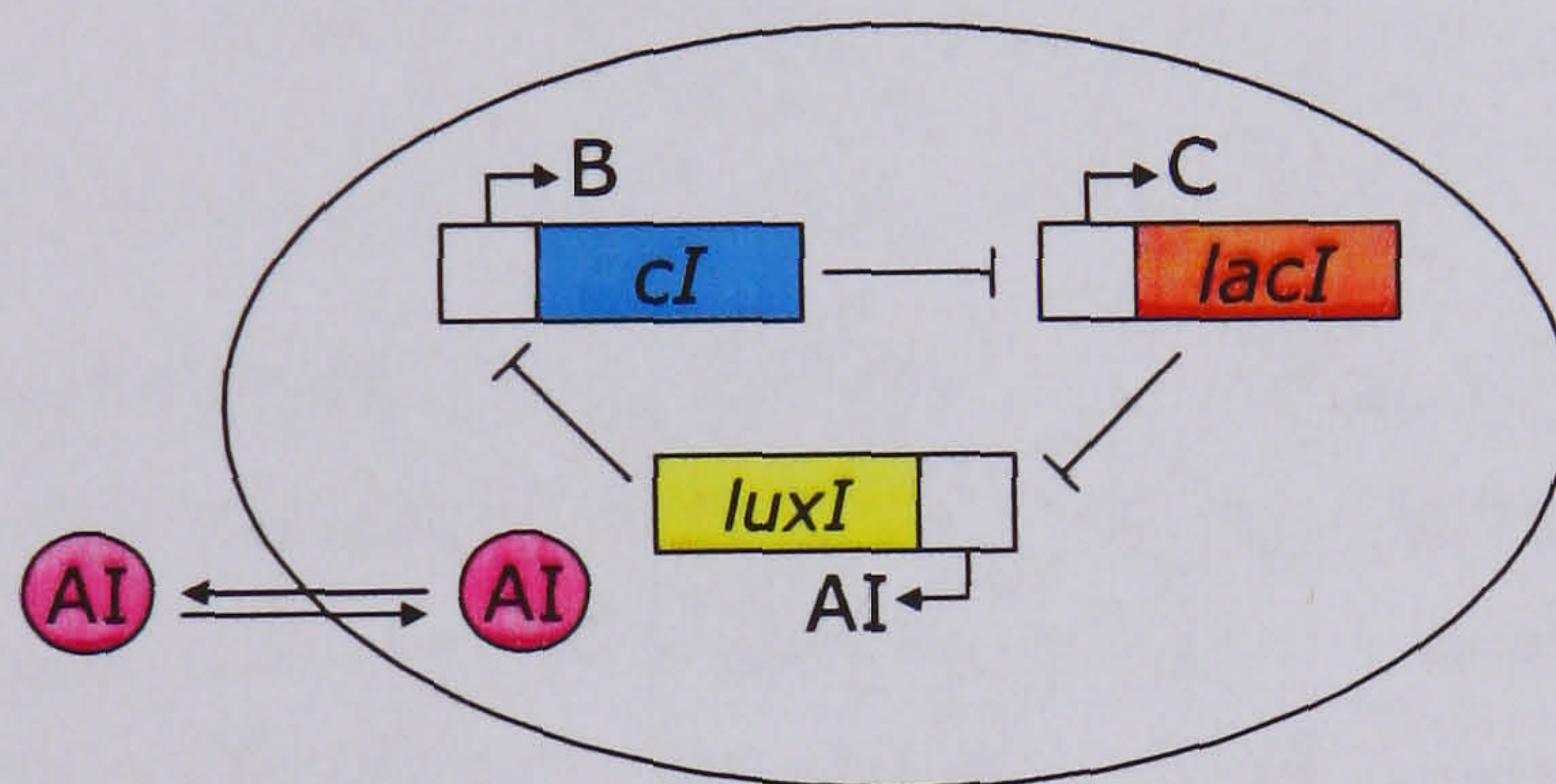


Figure 5.8: **The Repressilator.** Modified Repressilator to allow coupling between cells.

The Repressilator is presented through the following dynamical system, where the concentrations of $\{luxI, cI, lacI, AI, B, C\}$ are given by $\{x_1, \dots, x_6\}$:

$$\begin{aligned}
 \dot{x}_1 &= -x_1 + \frac{\alpha_1}{1 + x_6^2}, \\
 \dot{x}_2 &= -x_2 + \frac{\alpha_2}{1 + x_4^2}, \\
 \dot{x}_3 &= -x_3 + \frac{\alpha_3}{1 + x_5^2}, \\
 \dot{x}_4 &= \beta_4(x_1 - x_4), \\
 \dot{x}_5 &= \beta_5(x_2 - x_5), \\
 \dot{x}_6 &= \beta_6(x_3 - x_6).
 \end{aligned} \tag{5.40}$$

Note that, depending on parameter values, solutions of (5.40) tend either to a stable fixed

point or a stable periodic orbit [102].

We now establish conditions for the global complete synchronisation of coupled identical Repressilators. Consider a system of N coupled identical Repressilators in an all-to-all configuration. The dynamical system is given by (5.40) together with (5.19), where $D = \text{diag}([0 \ 0 \ 0 \ \frac{1}{N} \ 0 \ 0])$. The coupling constant κ is the diffusion rate of AI in and out of the cell. We assume that once protein AI leaves the cell, where it has been produced, it is distributed evenly among all cells. This is represented by factor $\frac{1}{N}$.

Note that the system given by (5.19) and (5.40) is positively forward invariant with respect to the positive orthant and its solutions are bounded. To see the latter, use the following Lyapunov function:

$$V(x) = \sum_{i=1}^N V_i(x), \quad V_i(x) = p^T x_i,$$

$$p^T = [1 \ 1 \ 1 \ \frac{1}{1 + \beta_{i_4}} \ \frac{1}{1 + \beta_{i_5}} \ \frac{1}{1 + \beta_{i_6}}],$$

$$x_i^T = [x_{i_1} \ x_{i_2} \ x_{i_3} \ x_{i_4} \ x_{i_5} \ x_{i_6}], \quad i \in \{1, \dots, N\}.$$

Since there exists a positive scalar η such that $\dot{V}(x) < 0$ if $p^T x_i > \eta$ for all i , boundedness follows. Moreover, the absorbing set is compact and connected in the nonnegative orthant. Now, we can use Theorem 5.2.3 to find a lower bound for $\kappa > 0$ which guarantees global complete synchronisation. Moreover, since solutions of the system given by (5.19) and (5.40) are bounded, the synchronised state corresponds to the union of either the stable fixed point or the stable periodic orbit that the individual Repressilator would approach when not coupled. We use YALMIP to see whether there exists a matrix $P > 0$ such that $PJ(x, \kappa) < 0$, for all $x \in \overline{\mathbb{R}}_+^n$, by increasing values of κ . Note that $J(x, \kappa)$ corresponds to $\frac{\partial \dot{x}}{\partial x} - N\kappa D$ (where \dot{x} is given by (5.40)) with $\alpha_{i_1} = \alpha_{i_2} = \alpha_{i_3} = 10$ and $\beta_{i_4} = \beta_{i_5} = \beta_{i_6} = 1$:

$$J(x, \kappa) = \begin{bmatrix} -1 & 0 & 0 & 0 & 0 & \frac{-20x_6}{(1+x_6^2)^2} \\ 0 & -1 & 0 & \frac{-20x_4}{(1+x_4^2)^2} & 0 & 0 \\ 0 & 0 & -1 & 0 & \frac{-20x_5}{(1+x_5^2)^2} & 0 \\ 1 & 0 & 0 & -1 - \kappa & 0 & 0 \\ 0 & 1 & 0 & 0 & -1 & 0 \\ 0 & 0 & 1 & 0 & 0 & -1 \end{bmatrix}.$$

We obtain that synchronisation is guaranteed if $\kappa \geq 145$. However, numerical results for the network of two identical Repressilators show that global complete synchronisation occurs

if $\kappa > 0.001$ (Figure 5.9). Unsurprisingly, the condition is conservative but it provides guaranteed global complete synchronisation. Moreover, note that if we consider a different coupling configuration then we have to amend κ ; that is we can guarantee global complete synchronisation only if $\kappa \geq \frac{145}{\gamma}$, where we know from graph-theory that $\gamma \leq 1$ (see also Figure 5.6).

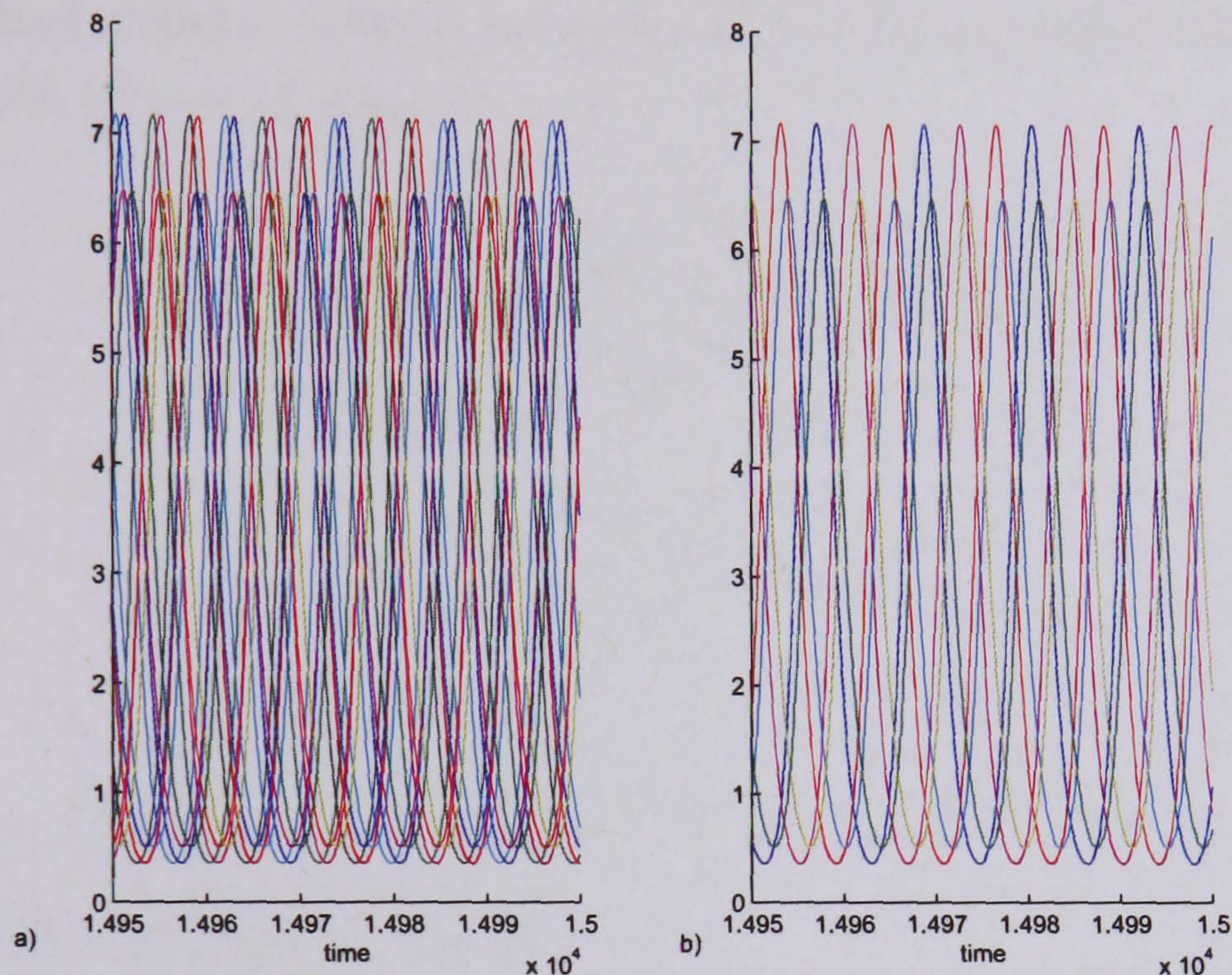


Figure 5.9: **Two coupled identical Repressilator.** (a) The coupling strength is $\kappa = 0.0001$ and the two coupled identical Repressilators do not synchronise. (b) The coupling strength is $\kappa = 0.001$ and the two coupled identical Repressilators completely synchronise.

The Repressilator, a synthetic oscillator, was designed to assist the study of more complex biological oscillators, particularly, when their behaviour is interconnected while in a culture. As synchronised behaviour has not been observed *in vitro* [93], the analysis in this section might provide the means to assist the design of the interconnection between cells that express the Repressilator circuit in order to guarantee synchronisation within the culture. In this section, we considered identical Repressilators only, in Section 5.4 we will extend our analysis to nonidentical Repressilators.

5.3 Constructing an observer

The notion of synchrony is closely related to the notion of observability. For instance, given a system H with state vector x and measurable outputs y , we feed y into an *observer* (or *state-estimator*) \hat{H} with state vector z and measurable outputs \hat{x} . They provide an estimate for x if $x - \hat{x} \rightarrow 0$ as $t \rightarrow \infty$. Let $\hat{x} = z$. Then, this is equivalent to complete synchronisation of x and z as time goes on (see also reference [45].) The following figure gives a schematic view of an observer:

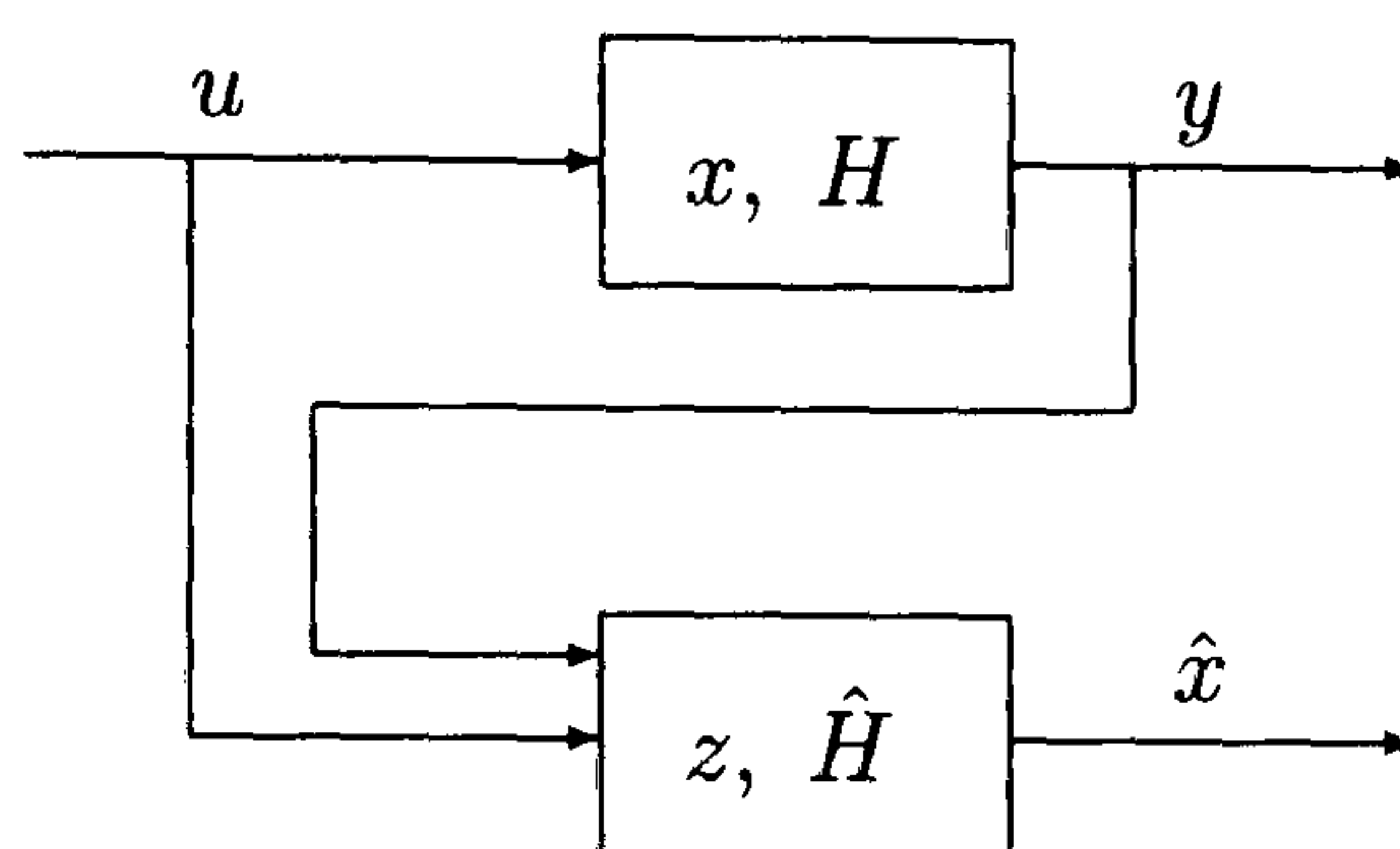


Figure 5.10: A schematic view of an observer.

Consider a biological system given by

$$\dot{x} = f(x) \quad (5.41)$$

with output y . Let $y = \kappa Dx$ be the input to the observer, which given by

$$\dot{z} = f(z) - \kappa Dz \quad (5.42)$$

with output z . Then, we obtain the following system:

$$\begin{aligned} \dot{x} &= f(x), \\ \dot{z} &= f(z) + \kappa D(x - z). \end{aligned} \quad (5.43)$$

Thus, the interconnection between (5.41) and (5.42) given by (5.43) can be written as

$$\begin{bmatrix} \dot{x} \\ \dot{z} \end{bmatrix} = \begin{bmatrix} f(x) \\ f(z) \end{bmatrix} + \kappa(C \otimes D) \begin{bmatrix} x \\ z \end{bmatrix}, \quad C = \begin{bmatrix} 0 & 0 \\ 1 & -1 \end{bmatrix}.$$

Now, if there exist matrices $D > 0$ and $P > 0$ and a constant $\kappa > 0$ such that (5.21) holds then the system is observable. ($N = 2$ and with $\gamma = \frac{1}{2}$: $U(C - \gamma U) \geq 0$.) This implies

that the search for κ can be implemented as:

$$\begin{array}{ll}
 \text{given} & f, D, \kappa \\
 \text{search for} & P \\
 \text{subject to} & P > 0, P \left(\frac{\partial f(x)}{\partial x} - \kappa D \right) < 0.
 \end{array} \tag{5.44}$$

Application to a simple gene regulation model

In the following, we apply above results to the gene regulatory system that controls the production of an enzyme from Section 5.1.1. For clarity, we restate here the set of differential equations representing the system, where we assume that the depletion rate of the final product is zero, $e = 0$:

$$\begin{aligned}
 \dot{x}_1 &= \frac{k}{1+x_3} - ax_1, \\
 \dot{x}_2 &= bx_1 - dx_2, \\
 \dot{x}_3 &= dx_2 - \frac{kx_3}{1+x_3} - ex_3.
 \end{aligned} \tag{5.45}$$

It possesses a unique positive equilibrium point

$$[x_1^*, x_2^*, x_3^*] = \left[\frac{k}{a+b}, \frac{b}{d} \frac{k}{a+b}, \frac{b}{a} \right],$$

whose instability guarantees oscillating behaviour, since solution trajectories are bounded (see Section 5.1.1). Moreover, the bounding set is compact and connected. Now, the Jacobian is given by

$$J = \begin{bmatrix} -a & 0 & \frac{-k}{(1+x_3)^2} \\ b & -d & 0 \\ 0 & d & \frac{-k}{(1+x_3)^2} \end{bmatrix}. \tag{5.46}$$

In order to find parameter regimes, in which oscillations occur (that is, the equilibrium point is unstable), we use the Routh-Hurwitz criterion (see (2.35)). It implies that $\text{Re}(\lambda) > 0$ if

$$(B - A^2)^2 > 4A^2ad > 0, \tag{5.47}$$

$$\frac{F^2}{2A}(B - A^2 - \sqrt{(B - A^2)^2 - 4A^2ad}) < k < \frac{F^2}{2A}(B - A^2 + \sqrt{(B - A^2)^2 - 4A^2ad}), \tag{5.48}$$

where $A = a + d$, $B = bd$, and $F = 1 + \frac{b}{a}$. For example, if inequality (5.47) holds – which is the case if b is sufficiently large – then there exists a k such that (5.48) also holds. Moreover, if $a = d$ then (5.47) holds if $b > 8a$ and (5.48) becomes

$$\frac{F^2}{4}(b - 4a - \sqrt{(b - 8a)b}) < k < \frac{F^2}{4}(b - 4a + \sqrt{(b - 8a)b}). \quad (5.49)$$

We wish to construct an observer for (5.45) and test its functionality for a case in which (5.45) exhibits oscillations. By inequality (5.49), this is the case if $a = d = 0.2$, $b = 2$, $e = 0$, and $k = 10$. Let $D = 0$ but for $D_{(i,i)} = 1$, $i = 1, 2, 3$. Using YALMIP, we obtain that the estimation error will decay exponentially to zero if, for example, $i = 1$ and $\kappa = 21.8$ or $i = 3$ and $\kappa = 2.6$. The time evolution of the estimation error is shown in Figure 5.11. Let us assume that we have perfect knowledge about all reaction rates. A potential application of our result is that by measuring concentrations of the final product x_3 one can deduce the level of mRNA (x_1), which might be far more difficult to measure directly [103].

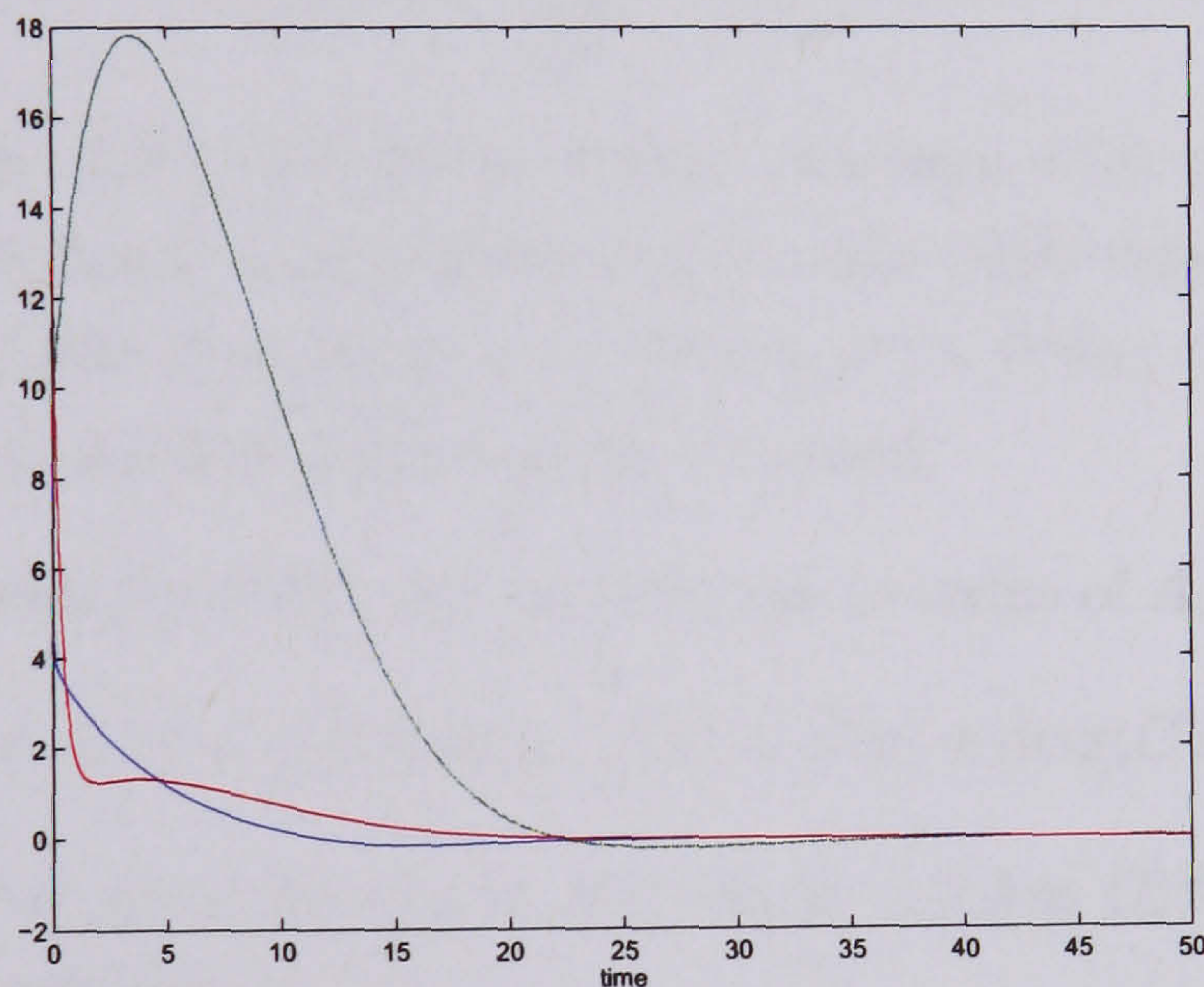


Figure 5.11: Estimation error. For $D_{(3,3)} = 1$ and $\kappa = 2.6$.

5.4 Frequency synchronisation of coupled nonidentical oscillators

Consider a network of nonidentical oscillators:

$$\dot{x} = \tilde{f}(x) + \kappa(C \otimes D)x, \quad (5.50)$$

where $D \in \overline{\mathbb{R}}_+^{n \times n}$, $x = [x_1 \dots x_N]^T$, $\tilde{f}(x) = [f_1(x_1) \dots f_N(x_N)]^T$, $x_i \in \mathcal{D} \subseteq \mathbb{R}^n$, $i \in \{1, \dots, N\}$. Here, $f_i \neq f_j$, $i \neq j$, however, we consider sign conserving parameter mismatch only; that is, $f_i(x_i) = f^*(x_i; a_i)$ for all i , where a_i is the parameter vector and $a_i^T a_j \gg 0$ for all i, j . In this section, we provide a proof for *frequency synchronisation*. Note that we allow any coupling topology as long as the coupling is linear and the associated graph is strongly connected. However, we require the existence of a periodic solution of (5.50).

Now, we introduce some additional definitions. We denote the adjacency matrix of the graph that encodes the coupling topology by A and the Laplacian matrix is $C = A - \text{diag}(A^T e)$ with $e = [1 \dots 1]^T$. We denote the period of the oscillator x_i as $\mathcal{P}(x_i)$. We say that two oscillators are frequency synchronised if their periods are equal. (See also [104] on frequency synchronisation.) Thus, two oscillators x_i and x_j are frequency-synchronised if $\mathcal{P}(x_i) = \mathcal{P}(x_j)$. In the following, $\frac{\partial \dot{x}_i}{\partial x_i} \equiv J_i(x_i, \kappa)$ and

$$P'_{i(k,\ell)}(x_i) = \sum_{j=1}^n \frac{\partial P_{i(k,\ell)}(x_i)}{\partial x_{i_j}} \dot{x}_{i_j}.$$

Lemma 5.4.1. *Assume that (5.50) has a bounded absorbing set \mathcal{B} and a periodic solution: $\bar{x}(t)$. If the coupling matrix C is irreducible and for all i there exists a constant κ^* and a matrix $P_i(x_i) > 0$ such that $P_i(x_i)J_i(x_i, \kappa^*) + \frac{1}{2}P'_i(x_i, \kappa^*) < 0 \forall x_i$, then $\mathcal{P}(\bar{x}_i) = \mathcal{P}(\bar{x}_j)$ for all i, j ; that is, the system will be frequency-synchronised.*

Proof. First, note that system (5.50) can be rewritten in terms of A , the adjacency matrix:

$$\dot{x} = \hat{f}(x) + \kappa(A \otimes D)x, \quad \hat{f}(x) = \tilde{f}(x) + \text{diag}(C)x.$$

The input from all other variables into \bar{x}_i is given by $\kappa((A \otimes D)\bar{x})_i = \kappa \sum_{j=1}^N A_{(i,j)} D \bar{x}_j$. Clearly, the period of this input is

$$\mathcal{P}(((A \otimes D)\bar{x})_i) = \max\{\mathcal{P}(A_{(i,1)} D \bar{x}_1), \dots, \mathcal{P}(A_{(i,j)} D \bar{x}_j), \dots, \mathcal{P}(A_{(i,N)} D \bar{x}_N)\}.$$

It follows from Theorem 3.1.8 that if \bar{x} is periodic, and for all i there exists a constant κ^* and a matrix $P_i(x_i) > 0$ such that $P_i(x_i)J_i(x_i, \kappa^*) + \frac{1}{2}P'_i(x_i, \kappa^*) < 0 \forall x_i$, then $\mathcal{P}(\bar{x}_i) = \mathcal{P}(((A \otimes D)\bar{x})_i) = \mathcal{P}_i$. Since C is irreducible, the associated directed graph is strongly connected and any two points are mutually reachable by means of directed paths [49]. This implies that, for any i, j , there exists at least one sequence of the form: $\{A_{(i,k)}, A_{(k,l)}, \dots, A_{(n,j)}, A_{(j,r)}, \dots, A_{(s,i)}\}$. Therefore, $\mathcal{P}_i \geq \mathcal{P}_k \geq \mathcal{P}_l \geq \mathcal{P}_m \geq \dots \geq \mathcal{P}_n \geq \mathcal{P}_j \geq \mathcal{P}_r \geq \dots \geq \mathcal{P}_s \geq \mathcal{P}_i$, which implies that $\mathcal{P}_i = \mathcal{P}_j$ ($\mathcal{P}(\bar{x}_i) = \mathcal{P}(\bar{x}_j)$), for all i, j . \square

Finally, if the entries to $J_i(x_i)$ are bounded then the search for a matrix $P_i(x_i) > 0$ such that $P_i(x_i)J_i(x_i, \kappa^*) + \frac{1}{2}P_i'(x_i, \kappa^*) < 0$ can be efficiently performed using semidefinite programming.

A network of coupled nonidentical van der Pol oscillators

Let us consider two coupled nonidentical van der Pol oscillators:

$$\begin{aligned}\dot{x}_{11} &= 3x_{12}, \\ \dot{x}_{12} &= -(1 + x_{11}^2)x_{12} - x_{11} + \kappa(x_{22} - x_{12}), \\ \dot{x}_{21} &= x_{22}, \\ \dot{x}_{22} &= -(1 + x_{21}^2)x_{22} - x_{21} + \kappa(x_{12} - x_{22}),\end{aligned}\tag{5.51}$$

Then, we cannot find constant matrices $P_i > 0$ such that $P_i J_i(x_i) < 0$ and $P_i D \geq 0$, $i = 1, 2$. Now, let us consider $\frac{\partial \dot{x}_i}{\partial x_j}$, $i \neq j$, to be some arbitrary but bounded input, where we obtain the bound from Section 4.1. Then, we can implement this condition into SOSTOOLS as described in Remark 3.4.1 (see also (5.57)). We find that frequency-synchronisation is guaranteed if $\kappa > 1$ and when the solution of the system is known to be periodic. Numerics indicate that frequency synchronisation indeed occurs at values of κ that are close to 1 (Figure 5.12).

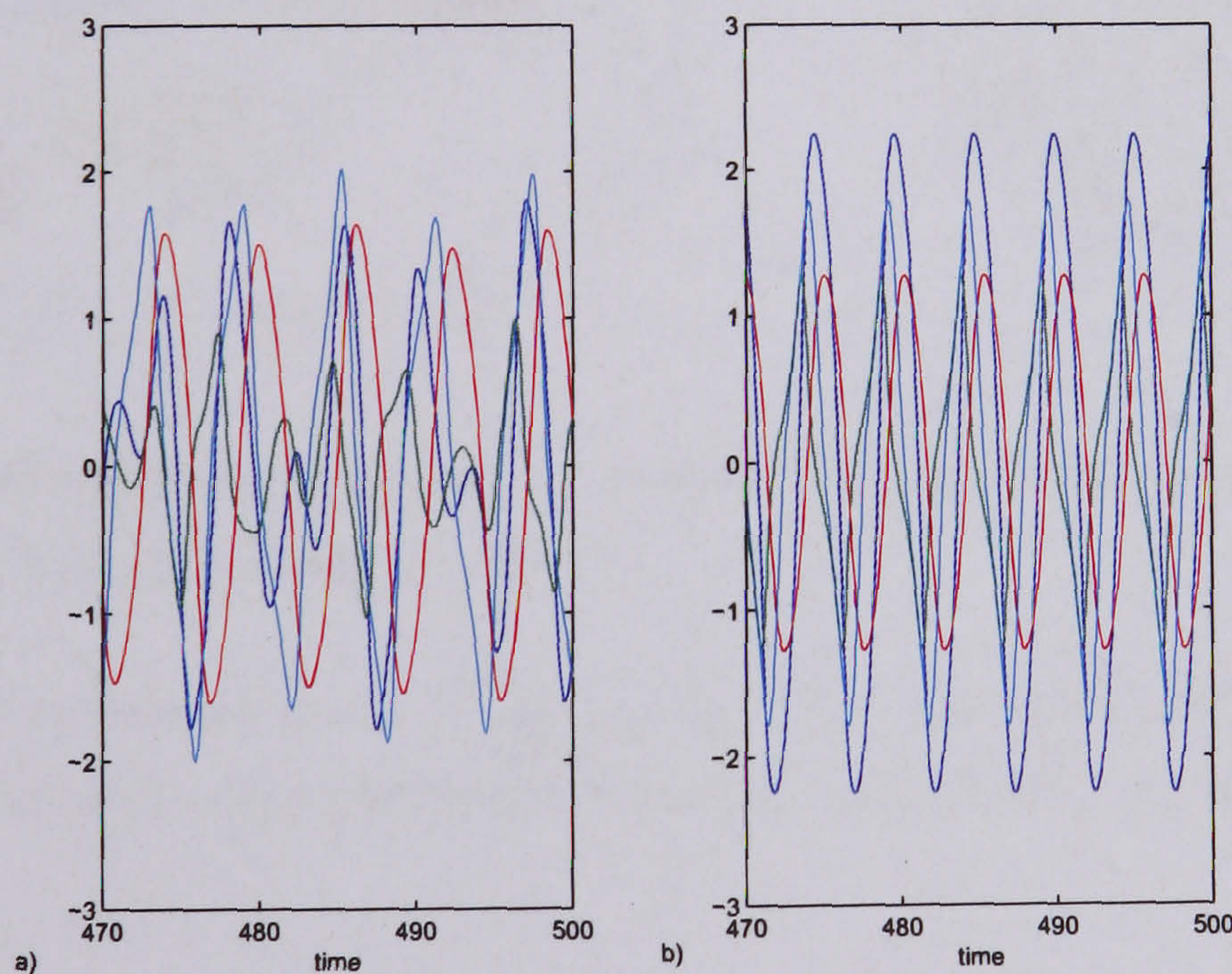


Figure 5.12: Two coupled nonidentical van der Pol oscillators. (a) For $\kappa = 0.4$, we do not observe synchronisation. (b) If $\kappa = 1.1$, we observe frequency synchronisation.

A network of coupled nonidentical Repressilators

Recall the Repressilator model from Section 5.2.3:

$$\begin{aligned}
 \dot{x}_1 &= -x_1 + \frac{\alpha_1}{1 + x_6^2}, \\
 \dot{x}_2 &= -x_2 + \frac{\alpha_2}{1 + x_4^2}, \\
 \dot{x}_3 &= -x_3 + \frac{\alpha_3}{1 + x_5^2}, \\
 \dot{x}_4 &= \beta_4(x_1 - x_4), \\
 \dot{x}_5 &= \beta_5(x_2 - x_5), \\
 \dot{x}_6 &= \beta_6(x_3 - x_6).
 \end{aligned}
 \tag{5.52}$$

Consider a system of ten coupled nonidentical Repressilators with all-to-all coupling (Figure 5.13), where $\alpha_{i_k} \neq \alpha_{j_k}$ and $\beta_{i_\ell} \neq \beta_{j_\ell}$, $k = 1, 2, 3$, $\ell = 4, 5, 6$, $i \neq j$, $i, j = 1, \dots, n$.

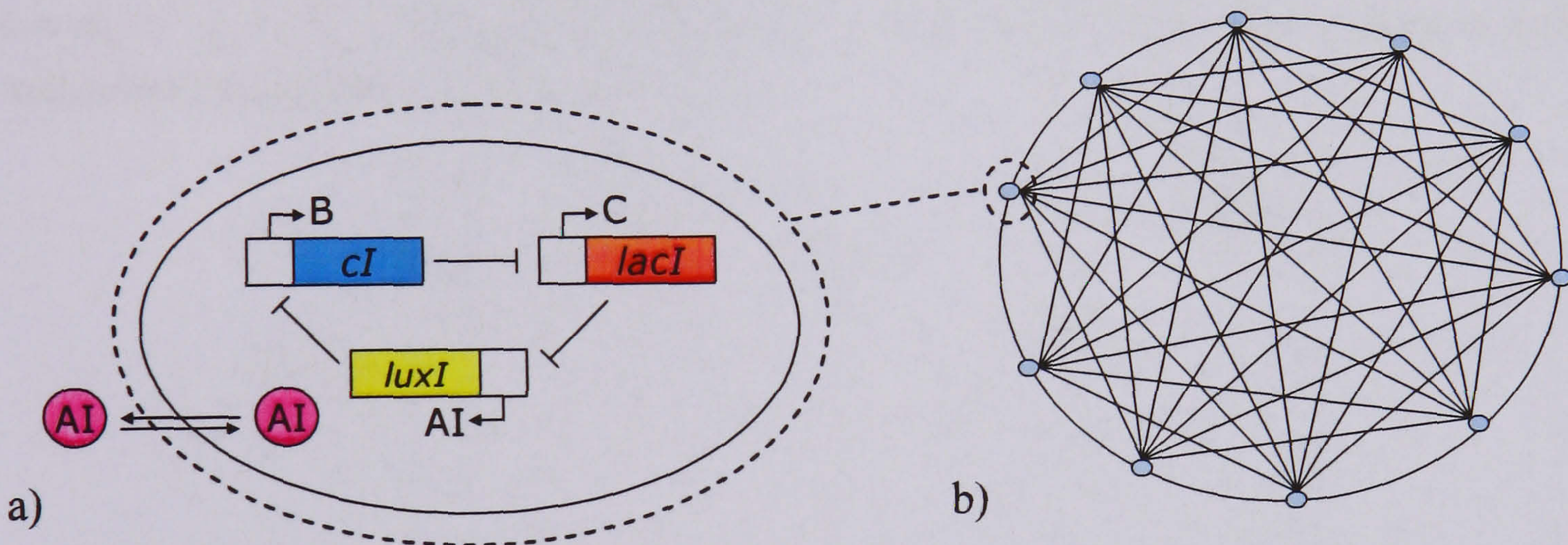


Figure 5.13: **Repressilator network.** a) Modified Repressilator circuit to allow coupling between cells. b) Coupling configuration ($N = 10$).

Note that the system given by (5.19) and (5.52) is forward invariant with respect to the positive orthant and thus, ultimately bounded; that is, it has an absorbing set \mathcal{B} that

attracts all solution trajectories. To see this, use the following Lyapunov Function,

$$V(x) = \sum_{i=1}^{10} V_i(x), \quad V_i(x) = p^T x_i,$$

$$p^T = [1 \ 1 \ 1 \ \frac{1}{1+\beta} \ \frac{1}{1+\beta_{i_5}} \ \frac{1}{1+\beta_{i_6}}],$$

$$\beta = \max\{\beta_{1_4}, \dots, \beta_{10_4}\},$$

$$x_i^T = [x_{i_1} \ x_{i_2} \ x_{i_3} \ x_{i_4} \ x_{i_5} \ x_{i_6}], \quad i \in \{1, \dots, 10\}.$$

Since there exists a positive scalar η such that $\dot{V}(x) < 0$ if $\|x\|_1 > \eta$, boundedness follows. Moreover, the absorbing set is compact and connected. Figure 5.14 presents numerical results for the network of ten coupled Repressilators showing that frequency synchronisation occurs if $\kappa \gtrsim 1.1$. Since solutions of the system given by (5.19) and (5.52) are bounded, we can use Lemma 5.4.1 to find a lower bound for κ which guarantees frequency synchronisation if the solution of the system given by (5.19) and (5.52) is periodic (or a fixed point). Let $\alpha_{i_1} = \alpha_{i_2} = \alpha_{i_3} = 10$ and $\beta_{i_4} = \beta_{i_5} = \beta_{i_6} = \beta_i$ for all i . Then, the Jacobian of each individual Repressilator is given by

$$J_i(x_i) = \begin{bmatrix} -1 & 0 & 0 & 0 & 0 & \frac{-20x_{i_6}}{(1+x_{i_6}^2)^2} \\ 0 & -1 & 0 & \frac{-20x_{i_4}}{(1+x_{i_4}^2)^2} & 0 & 0 \\ 0 & 0 & -1 & 0 & \frac{-20x_{i_5}}{(1+x_{i_5}^2)^2} & 0 \\ \beta_i & 0 & 0 & -\beta_i - \kappa(1 - \frac{1}{N}) & 0 & 0 \\ 0 & \beta_i & 0 & 0 & -\beta_i & 0 \\ 0 & 0 & \beta_i & 0 & 0 & -\beta_i \end{bmatrix}.$$

Note that $-6.5 \leq \frac{-20y}{(1+y^2)^2} \leq 0$. We use YALMIP to see whether, for all i , there exists a matrix $P_i > 0$ such that $P_i J_i(x_i) < 0$ and $P_i D \geq 0$, for all $x \in \overline{\mathbb{R}}_+^n$, for increasing values of κ . It is easy to verify that the largest lower bound of κ is associated with the largest β_i . Using this fact, for the parameters shown in Figure 5.14, we obtain that frequency synchronisation is guaranteed if $\kappa \geq 260.9$. Unsurprisingly, the condition is conservative but it provides guaranteed frequency-synchronisation when the solution of the system is known to be periodic.

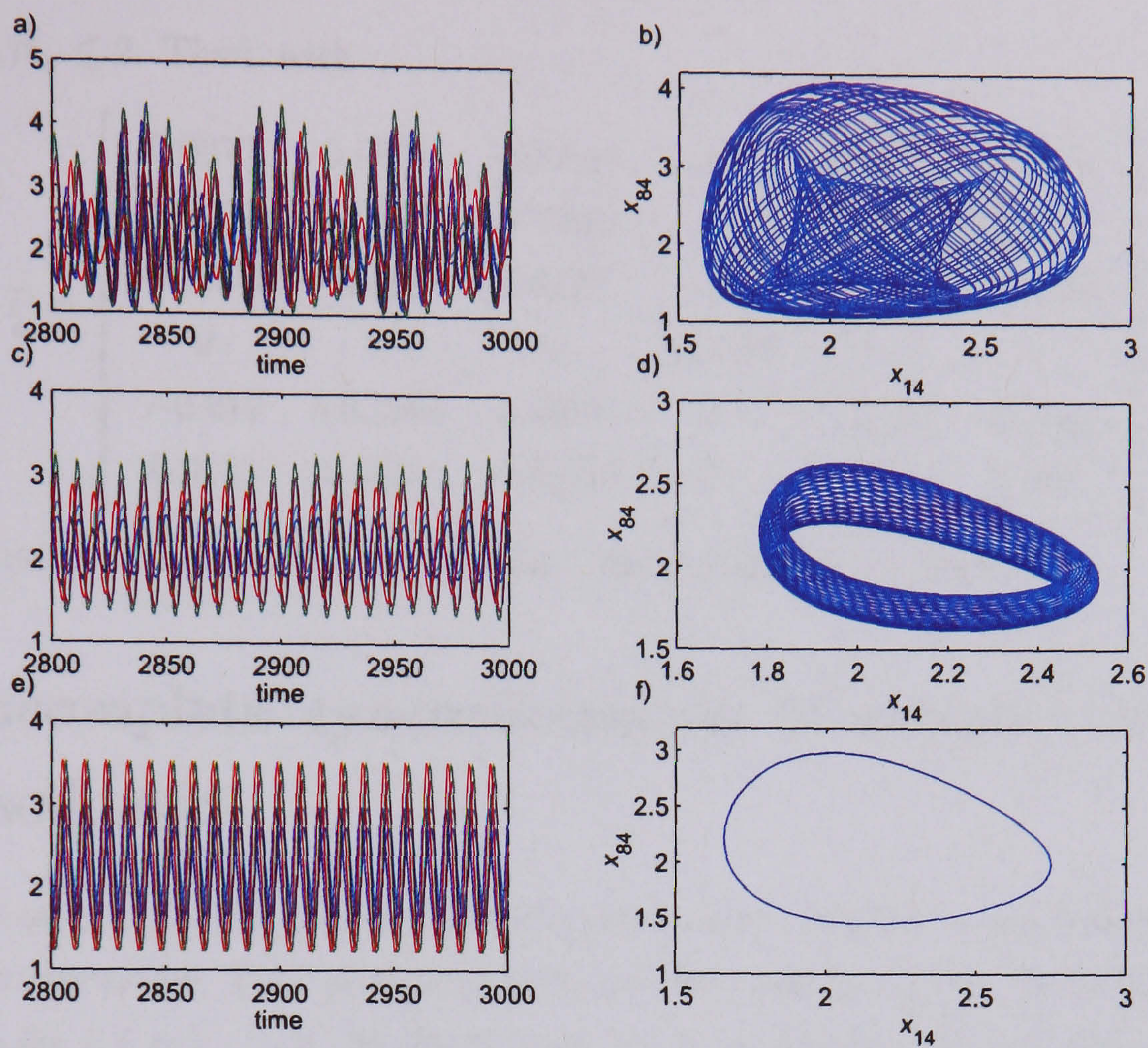


Figure 5.14: **Ten coupled nonidentical Repressilators.** The parameters are $\alpha_{i_1} = \alpha_{i_2} = \alpha_{i_3} = 10$, $\beta_{i_4} = \beta_{i_5} = \beta_{i_6} = \beta_i$ for all i , and $[\beta_1 \dots \beta_{10}] = [0.4666 \ 1.1125 \ 0.1234 \ 0.1264 \ 1.1014 \ 1.2476 \ 1.848 \ 1.82 \ 1.2292 \ 1.6002]$. The coupling strength in (a)-(b) is $\kappa = 0.7$; in (c)-(d) $\kappa = 1$; and in (e)-(f) $\kappa = 1.1$. In (a), (c) and (e), the variables x_{14} to x_{104} are shown. The phase space representations in (b) and (d) confirm that the different Repressilators are not frequency synchronised, as they show quasi-periodic orbits on torii, while the system in (e) is frequency synchronized.

Here, we obtained the value of κ which guarantees that a matrix $P_i > 0$ exists such that $P_i J_i(x_i) < 0$ for all i and all $x_i \in \mathcal{D}$ by checking for each individual β_i , $i = 1, \dots, n$. In general, to find the parameter combination that provides this value of κ is a combinatorial problem. However, one can perform a conservative search by allowing, for all i , an uncertainty in the parameters of $J_i(x_i) = J(x_i)$ and searching for a value of κ for which there exists a matrix $P > 0$ such that $PJ(x_i) < 0$ for all $x_i \in \mathcal{D}$. For instance, let

$1 \leq \beta_{i_4}, \beta_{i_5}, \beta_{i_6} \leq 2$. Then, with

$$P = \begin{bmatrix} 0.0077 & 0.0901 & -0.0035 & 0 & -0.019 & 0.0113 \\ 0.0901 & 12.7048 & -0.2691 & 0 & -6.2201 & 0.3376 \\ -0.0035 & -0.2691 & 0.4322 & 0 & 0.6011 & -0.2226 \\ 0 & 0 & 0 & 0.5196 & 0 & 0 \\ -0.019 & -6.2201 & 0.6011 & 0 & 11.3109 & -0.3963 \\ 0.0113 & 0.3376 & -0.2226 & 0 & -0.3963 & 0.355 \end{bmatrix}$$

it follows that the conditions in Lemma 5.4.1 are satisfied if $\kappa \geq 348.7$.

5.5 Incomplete synchronisation of coupled identical oscillators

As we have seen so far results that provide guaranteed complete synchronisation can be extremely conservative. They guarantee that the difference $x_i - x_j$ for all i, j will approach zero as $t \rightarrow \infty$, $i, j = 1, \dots, n$. In this section, we relax this requirement and require only that $|x_i - x_j|^T P |x_i - x_j| \leq \epsilon$ as $t \rightarrow \infty$, where $P > 0$ is a matrix and $\epsilon > 0$ is a constant. In other words, we do not require complete synchronisation.

Now, consider a network of identical oscillators with all-to-all coupling. For all i, j , we denote the difference between x_i and x_j by Y , $i, j = 1, \dots, n$; that is $x_i - x_j \equiv Y$. Assume that \dot{Y} can be written as

$$\dot{Y} = B(x_i, x_j, \kappa)Y = \tilde{B}(Y, \kappa)Y, \quad x_i, x_j \in \mathcal{D}, \quad \kappa \in \mathbb{R}_+. \quad (5.53)$$

Corollary 5.5.1. *For all i, j , if there exist constants $\epsilon, \kappa > 0$ and a matrix $P > 0$ such that, for all $x_i, x_j \in \mathcal{D}$, $P\tilde{B}(Y, \kappa) < 0$ if $Y^T P Y > \epsilon$ then there exists a t_0 such that $Y^T P Y \leq \epsilon$ for all $t > t_0$.*

Proof. The Lyapunov function $V(Y) = Y^T P Y$ will decrease until $Y^T P Y \leq \epsilon$ since $\dot{V}(Y) < 0$ if $Y^T P Y > \epsilon$. \square

Application to a simple gene regulation model

Consider the gene regulatory system that controls the production of an enzyme from the previous section. The dynamics of this system are represented by a system of differential

equations (5.45). Now, if we consider N coupled systems with $C = U$, $D = \text{diag}([1 \ 0 \ 0])$, and coupling constant κ then, for all i, j , the time evolution of $Y = x_i - x_j$ is given by:

$$\dot{Y} = \begin{bmatrix} -(a + \kappa) & 0 & -\frac{k}{(1+x_{i_3})(1+x_{j_3})} \\ b & -d & 0 \\ 0 & d & -\frac{k}{(1+x_{i_3})(1+x_{j_3})} - e \end{bmatrix} Y = B(x_{i_3}, x_{j_3}, \kappa)Y. \quad (5.54)$$

Note that $0 \leq \frac{1}{(1+x_{i_3})(1+x_{j_3})} \leq \frac{1}{1+|Y_3|}$. Thus, there exists a matrix function $\tilde{B}(\cdot)$ such that $\dot{Y} = \tilde{B}(Y_3, \kappa)Y$. Let the parameters of the system be $a = 0.2$, $d = 0.2$, $b = 2$, $e = 0.005$ and $k = 10$. In the following, we require that $P \geq 0$ and $P_{(3,3)} = 1$, and we wish to maximise $P_{(1,1)} + P_{(2,2)}$. (Clearly, one can choose a different objective function and, for example, minimise only one of the two summands.) Together with the requirements of Corollary 5.5.1 this poses a maximisation problem can be implemented as follows:

$$\begin{aligned} &\text{given} && B(Y_3), \kappa, \epsilon \\ &\text{maximise} && P_{(1,1)} + P_{(2,2)} \\ &\text{subject to} && P > 0, P_{(3,3)} = 1, P_{(i,j)} \geq 0, |Y_3| > \epsilon, P\tilde{B}(Y_3, \kappa) < 0. \end{aligned} \quad (5.55)$$

We use YALMIP to solve this problem. The following table summarises our results for $\epsilon = 0, 0.1, 3$:

ϵ	0			0.1			3		
κ	21.9			20.9			9.9		
P	4.644	0	0.045	5.155	0	0.047	8.262	0	0.12
	0	10.001	0	0	10.002	0	0	6.412	0.207
	0.045	0	1	0.047	0	1	0.12	0.207	1

Table 5.3: Incomplete synchronisation.

Here, $\epsilon = 0$ implies complete synchronisation. Note the tight bounds on Y_1 and Y_2 ; that is, for $\epsilon = 0.1$ ($Y_3^2 < 0.1$): $Y_1^2 < \frac{0.1}{5.2}$ and $Y_2^2 < 0.01$, and for $\epsilon = 3$ ($Y_3^2 < 3$): $Y_1^2 < \frac{3}{8.3}$ and $Y_2^2 < \frac{3}{6.4}$. Obviously, the results in the table serves merely as an illustration and the analysis can be extended. In summary, if we accept certificates that guarantee that differences between the coupled systems remain relatively small then these can be given for significantly lower values of the coupling constant κ .

5.6 Global complete synchronisation of identical oscillators with all-to-all coupling

In this section, we show that in the special case of a system of coupled identical oscillators with all-to-all coupling configuration and a single weight constant the coupling strength, it is possible to extend previous results. In Section 5.6.1, we provide a lemma which is equivalent to Theorem 5.2.3 but allows us to consider a nonconstant matrix $P(x) > 0$. We then extend this result to obtain conditions that guarantee global complete synchronisation for coupled identical discrete-time dynamical systems. In Section 5.6.2, we provide novel sufficient conditions for global complete synchronisation of coupled identical oscillators as an alternative to the ones presented in Section 5.6.1. They are based on the so called Bendixson's Criterion for higher dimensions which we have presented in Section 3.2.

5.6.1 Sufficient conditions based on contraction theory

In Section 5.2, we require a constant matrix $P > 0$ to fulfill certain conditions to guarantee global complete synchronisation of coupled identical oscillators. In this section, because we assume all-to-all coupling, we can consider a nonconstant matrix $P(x) > 0$. This result was anticipated by Jean-Jacques E. Slotine in [45]. We exemplify the result through a network of coupled van der Pol oscillators.

The following lemma is an extension of Theorem 5.2.3. It holds only if $C = U$ (all-to-all coupling) but allows for a nonconstant matrix $P(z) \in \mathbb{R}^{n \times n}$, $z \in \mathcal{D}$. A similar result is given in [105] with a different proof. Using modern computational tools, this makes it possible for us to obtain sufficient conditions for synchronisation in cases in which they could not be obtained for a constant P (see example below). In the following,

$$P'_{(i,j)}(y) = \sum_{k=1}^n \frac{\partial P_{(i,j)}(y)}{\partial y_k} (f_k(y) - (\kappa N D y)_k).$$

Lemma 5.6.1. *Consider the coupling scheme given by (5.19). Let $x_i \in \mathcal{D}$ and \mathcal{D} be convex. If $C = U$ and there exists a nonconstant symmetric matrix $P(z) > 0$ such that*

$$P(z_i)J(x_i)|_{x_i=z_i} - \kappa N P(z_i)D + \frac{1}{2}P'(z_i) < 0 \quad (5.56)$$

for all $z_i \in \mathcal{D}$ then (5.19) completely synchronises as $t \rightarrow \infty$.

Proof. Note that if $C = U$ then the following holds, where X is given by (5.25):

$$\dot{X} = (\tilde{J} - \kappa ND)X, \quad \tilde{J} = \begin{bmatrix} 0 & 0 & \dots & 0 \\ 0 & J(x_2)|_{x_2=z_2} & \dots & 0 \\ \vdots & \vdots & \ddots & \vdots \\ 0 & 0 & \dots & J(x_N)|_{x_N=z_N} \end{bmatrix}.$$

Consider the Lyapunov function given by

$$V(X) = \frac{1}{2}X^T \tilde{P}(z)X > 0, \quad X \neq 0, \quad \tilde{P}(z) = \begin{bmatrix} P(z_1) & 0 & 0 \\ 0 & \ddots & 0 \\ 0 & 0 & P(z_N) \end{bmatrix}.$$

It follows that

$$\dot{V}(X) = X^T \left(\tilde{P}(z)\tilde{J} - \kappa N\tilde{P}(z)D + \frac{1}{2}\tilde{P}'(z) \right) X.$$

Hence, $\dot{V}(X) < 0$ if (5.56) holds, which implies that (5.19) completely synchronises as $t \rightarrow \infty$. \square

Now, condition (5.56) comprises a feasibility problem that we implement in SOSTOOLS as:

$$\begin{array}{ll} \text{given} & x_i \in \mathcal{D}, f(x_i), N, D, \kappa, \delta > 0 \\ \text{search for} & P(x_i) \\ \text{subject to} & v^T(P(x_i) - \delta I)v, v^T \left(P(x)D + \frac{1}{2}\bar{P}'(x_i) \right) v \text{ are SOS } \forall v \in \mathbb{R}^n \\ & -v^T \left(P(x_i)(J(x_i) - N\kappa D) + \frac{1}{2}P'(x_i) + \delta I \right) v \text{ is SOS } \forall v \in \mathbb{R}^n, \end{array} \quad (5.57)$$

where

$$P'_{(j,\ell)}(x_i) = \sum_{k=1}^n \frac{\partial P_{(j,\ell)}(x_i)}{\partial x_{i_k}} (f_k(x_i) - (\kappa NDx_i)_k),$$

and

$$\bar{P}'_{(j,\ell)}(x) = \sum_{k=1}^n \frac{\partial P_{(j,\ell)}(x_i)}{\partial x_{i_k}} (Dx_i)_k.$$

Note that we have included the requirement of Remark 5.0.1.

A network of coupled identical van der Pol oscillators

In [30], it was shown that in a network of coupled van der Pol oscillators representing individual heart cells, one group of coupled oscillators could represent the right atrium called sino-atrial node. This cell aggregate generates the normal cardiac rhythm. In addition, there is another pacemaker, the atrio-ventricular node, which takes over when the former fails to perform well. As discussed in [30], this node could be represented by the other group and both groups interact with each other. Investigating conditions for synchrony of the two heart cell aggregates is of major importance as unsynchronised behaviour is associated with cardiac dysrhythmia, a life threatening heart disease. The mathematical framework presented in this chapter and exemplified below provides valuable information about conditions for which synchronised behaviour between heart cells is guaranteed. Moreover, therapeutic interventions use beta blockers and antiarrhythmic agents which affect only the atrio-ventricular node. The analysis presented below can be used to see the effects on the synchrony of the whole system (arguably, the heart).

Now, consider an all-to-all coupling scheme for a network of coupled identical van der Pol oscillators. The individual oscillator with $k = -1$ is described by:

$$\begin{aligned}\dot{x}_1 &= x_2 \\ \dot{x}_2 &= (1 - x_1^2)x_2 - x_1,\end{aligned}\tag{5.58}$$

The Jacobian of an individual oscillator is given by

$$J_v = \begin{bmatrix} 0 & 1 \\ -(2x_1x_2 + 1) & 1 - x_1^2 \end{bmatrix}.$$

The equations for the coupled system are given by (5.58) together with (5.19), where $C = U$ and $D = \text{diag}([0 \ 1])$.

Let us assume that the coupled system has a compact, convex and positively invariant set. Moreover, the origin is an unstable equilibrium point of the coupled system. To see this, consider the Lyapunov function $V(x) = x^T x$; in the vicinity of the origin $\dot{V}(x) > 0$. Thus, the unique synchronised state corresponds to the limit cycle that is the union of the limit cycles of the individual uncoupled oscillators. Now, in order to apply the result of Lemma 5.6.1, we use SOSTOOLS to search for a matrix $P(x) > 0$ that guarantees complete synchronisation of the coupled system. Moreover, we are interested to see whether the value of κ decreases as we increase the order of the polynomial functions which are entries to

$P(x)$. The results are as follows (note that $P(x)$ is a sum of squares only if the polynomials are of even order [92]):

- For polynomials of order 0, a constant matrix $P(x) = P > 0$ and a constant $\kappa > 0$ such that (5.56) holds was not found.
- For polynomials of order 2, a matrix $P(x) > 0$ and a constant $\kappa > 0$ such that (5.56) holds was not found.
- For polynomials of order 4, inequality (5.56) holds if $\kappa N > 1$. Note that this case corresponds to the van der Pol oscillator with $\dot{x}_2 = (-k^* - x_1^2)x_2 - x_1$, $1 - \kappa \equiv k^* > 0$. For $\kappa = 1.1$:

$$P_{(1,1)}(x) = 1.748 + 1.102x_1^2 - 1.379x_1x_2 + 1.473x_2^2 + 1.321x_1^4 \\ + 0.452x_1^2x_2^2 - 0.037x_1x_2^3 + 0.002x_2^4,$$

$$P_{(1,2)}(x) = 0.056 + 1.506x_1^2 - 0.935x_1x_2 + 0.145x_2^2 - 0.101x_1^3x_2 \\ + 0.028x_1^2x_2^2 - 0.001x_1x_2^3,$$

$$P_{(2,2)}(x) = 1.761 + 1.211x_1^2 - 0.460x_1x_2 + 0.064x_2^2 + 0.085x_1^4 - 0.019x_1^3x_2 \\ + 0.002x_1^2x_2^2.$$

- Additional increases in polynomial order fail to lower the value of κ for which (5.56) holds. This was expected since $N\kappa < 1$ corresponds to the case when the fixed point of the van der Pol oscillator with $\dot{x}_2 = (-k^* - x_1^2)x_2 - x_1$, $k^* < 0$. Therefore, a $P(x)$ such that (5.56) holds cannot exist for $N\kappa < 1$.

For $N = 2$, numerical results show that complete synchronisation occurs if $\kappa \geq 0.017$ (see, for example, Figure 5.15). Unsurprisingly, our condition is conservative (the numerical value is about 30 times lower) but it provides guaranteed complete synchronisation.

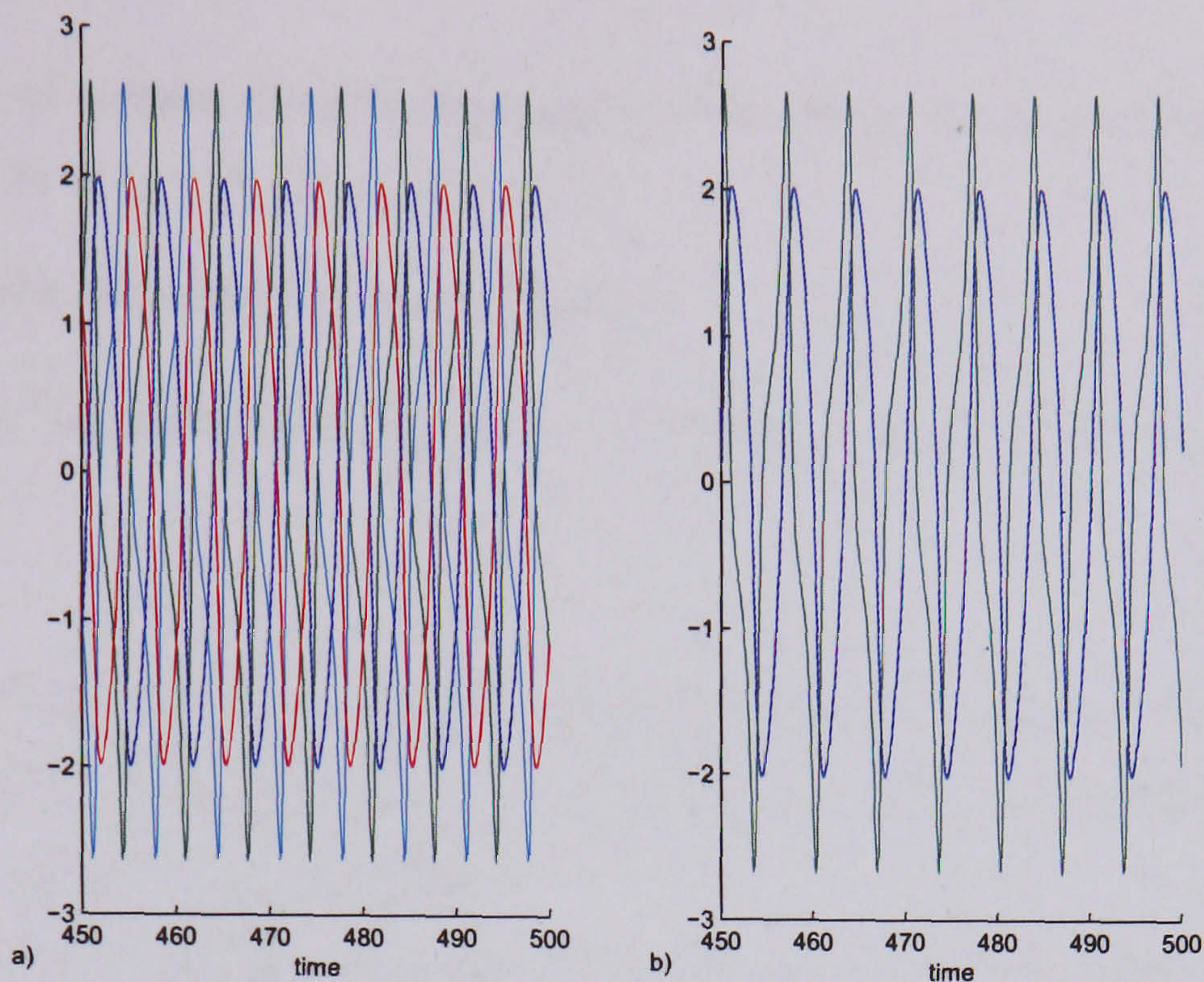


Figure 5.15: **Two coupled identical van der Pol oscillators.** (a) The coupling strength is $\kappa = 0.01$ and the two coupled identical van der Pol oscillators do not synchronise. (b) The two coupled identical van der Pol oscillators completely synchronise for $\kappa = 0.02$.

Sufficient conditions of discrete-time dynamical systems

Here, we provide conditions that guarantee global complete synchronisation for coupled identical discrete-time dynamical systems with all-to-all coupling configuration. In what follows, $-U$ is the Laplacian Matrix of the completely connected graph and matrix D is the output matrix of the variables that are used in the coupling.

Theorem 5.6.2. *Let $U \in \mathbb{R}^{N \times N}$ be given by (5.17). Consider*

$$x(k+1) = \tilde{f}(x(k)) + \kappa(U \otimes D)x(k), \quad k = 1, 2, \dots, \quad (5.59)$$

where $D \in \overline{\mathbb{R}}_+^{n \times n}$, $x = [x_1 \dots x_N]^T$, $\tilde{f}(x) = [f(x_1) \dots f(x_N)]^T$, $x_i \in \mathcal{D} \subseteq \mathbb{R}^n$, $i \in \{1, \dots, N\}$. Furthermore, let

$$g(x_i) = f(x_i) - N\kappa D x_i. \quad (5.60)$$

Then, if there exists a symmetric and positive matrix $P(y) > 0$ such that for all $x_i, y \in \mathcal{D}$ and all i

$$\frac{\partial g(x_i)}{\partial x_i} P(y) \frac{\partial g(x_i)}{\partial x_i} < P(y), \quad (5.61)$$

then the network of coupled discrete-time dynamical systems given by (5.59) synchronises in the sense that $x_i - x_j \rightarrow 0, \forall i, j$, as $t \rightarrow \infty$.

Proof. Consider the following Lyapunov function:

$$V(x) = -x^T(U \otimes P(y))x = \sum_{i < j} (x_i - x_j)^T P(y) (x_i - x_j) > 0 \text{ if } x_i \neq x_j, \forall i, j.$$

Thus,

$$\begin{aligned} \Delta V(x) &= x^T(U \otimes P(y))x - [\tilde{f}(x) + \kappa(U \otimes D)x]^T(U \otimes P(y))[\tilde{f}(x) + \kappa(U \otimes D)x] \\ &= x^T(U \otimes P(y))x - \tilde{f}(x)(U \otimes P(y))\tilde{f}(x)^T - 2x^T \kappa(U^2 \otimes D^T P(y))\tilde{f}(x) \\ &\quad - x^T \kappa(U^3 \otimes D^T P(y)D)x \\ &= x^T(U \otimes P(y))x - \tilde{f}(x)(U \otimes P(y))\tilde{f}(x)^T + 2x^T \kappa N(U \otimes D^T P(y))\tilde{f}(x) \\ &\quad - x^T \kappa N^2(U \otimes D^T P(y)D)x \\ &= x^T(U \otimes P(y))x - [\tilde{f}(x) - N\kappa Dx]^T(U \otimes P(y))[\tilde{f}(x) - N\kappa Dx] \\ &= \sum_{i < j} (g(x_i) - g(x_j))^T P(y) (g(x_i) - g(x_j)) - (x_i - x_j)^T P(y) (x_i - x_j) \quad (5.62) \end{aligned}$$

It follows from (5.61) and the mean value theorem (Theorem 3.1.1) that (5.62) < 0 if $x_i \neq x_j$, which implies that (5.59) synchronises in the sense that $x_i - x_j \rightarrow 0, \forall i, j$, as $t \rightarrow \infty$. \square

5.6.2 Sufficient conditions based on the Bendixson's Criterion for higher dimensions

In this section, we provide novel sufficient conditions for global complete synchronisation of coupled identical oscillators as an alternative to the ones presented so far. They are based on the so called Bendixson's Criterion for higher dimensions that we have presented in Section 3.2. We believe that there is much scope for further relaxation of conditions for synchronisation by expanding the result of this section.

Recall Theorem 3.2.1: If the origin is the unique equilibrium point of $\dot{x} = f(x)$ in $\mathcal{B} \subseteq \mathbb{R}^n$ and there exists a nonsingular and real $\binom{n}{2} \times \binom{n}{2}$ matrix A such that

$$\frac{1}{2}P'(x) + P(x) \left(\frac{\partial f(x)}{\partial x} \right)^{[2]} < 0, \forall x \in \mathcal{B}, \quad (5.63)$$

then the origin is globally asymptotically stable in \mathcal{B} . Here,

$$P'_{(i,j)}(x) = \sum_{k=1}^n \frac{\partial P_{(i,j)}(x)}{\partial x_k} f_k(x),$$

\mathcal{B} is a compact and simply connected invariant set containing the origin and $\left(\frac{\partial f(x)}{\partial x}\right)^{[2]}$ is the second additive compound of $\left(\frac{\partial f(x)}{\partial x}\right)$. Searching for a constant matrix $P > 0$ such that (5.63) holds can be efficiently performed using YALMIP by solving the following feasibility problem:

$$\begin{array}{ll} \text{given} & f(x) \\ \text{search for} & P \\ \text{subject to} & P > 0, P \left(\frac{\partial f(x)}{\partial x}\right)^{[2]} < 0. \end{array} \quad (5.64)$$

Now, consider a system of N coupled identical systems given by (5.19) with all-to-all coupling. If $\mathcal{B} \subseteq \mathbb{R}^n$ is convex then

$$\dot{X}_i = J(x_i)X_i - N\kappa D X_i, \quad (5.65)$$

where $J(x_i) = \frac{\partial f(x_i)}{\partial x_i} \Big|_{x_i=z_i}$, $X_i = x_i - x_1$, $x_1, x_i, z_i \in \mathcal{B}$, $i = 2, \dots, N$. This leads to the following theorem:

Theorem 5.6.3. *If there exists a matrix $P(z_i) > 0$ and a coupling strength κ^* such that*

$$\frac{1}{2}P'(z_i) + P(z_i)(J(x_i) - N\kappa^* D)^{[2]} < 0 \quad (5.66)$$

then the following holds for X_i whose evolution with is given by (5.65): $X_i \rightarrow 0$ as $t \rightarrow \infty$ for all i .

Here,

$$P'_{(i,j)}(y) = \sum_{k=1}^n \frac{\partial P_{(i,j)}(y)}{\partial y_k} ((J(x_i) - N\kappa^* D)y)_k.$$

Note that Theorem 5.6.3 implies that the system of N all-to-all coupled identical systems given by (5.19) together with (5.65) completely synchronises.

Remark 5.6.4. Let $P = I$ and $D \geq 0$ be diagonal. Moreover, let (5.56) hold; that is, $J(x_i) - N\kappa^* D < 0$ and thus, $\lambda_i < 0$ for all i , $i = 1, \dots, n$, where λ_i are the eigenvalues of

$$J(x_i) + J(x_i)^T - 2N\kappa^* D.$$

Now, note that condition (5.66) is equivalent to $\sup\{\lambda_i + \lambda_j\} < 0$, $i, j = 1, \dots, n$, which clearly holds if (5.56) holds but also if there exists a $\lambda_i > 0$ such that $\lambda_i < -\lambda_j$ for all j , $j \neq i$. Thus, for $P = I$, inequality (5.66) connotes a more relaxed requirement than inequality (5.56). Furthermore, it is reasonable to assume that this is true in general. (It is indeed in all cases presented in the next section.)

In the light of Remark 5.0.1, in the following we require that $PD^{[2]} \geq 0$ such that if (5.66) holds for κ^* then it holds for all $\kappa \geq \kappa^*$.

Coupled van der Pol oscillators

Consider N coupled identical van der Pol oscillators:

$$\begin{aligned}\dot{x}_{i_1} &= x_{i_2} \\ \dot{x}_{i_2} &= (1 - x_{i_1}^2)x_{i_2} - x_{i_1},\end{aligned}\tag{5.67}$$

where $i = 1, \dots, N$. Let $D = \text{diag}([0 \ 1])$. Note that if $J \in \mathbb{R}^{2 \times 2}$ then $J^{[2]} = J_{(1,1)} + J_{(2,2)}$. Thus, $J^{[2]} = (1 - x_{i_1}^2) - N\kappa$, which implies that complete synchronisation is guaranteed if

$$\kappa > \frac{1}{N}.\tag{5.68}$$

In the case of two coupled identical van der Pol oscillators with all-to-all coupling, inequality (5.68) translates to $\kappa > 0.5$. This is the same value as the one obtained in Section 5.2.3.

Now, consider $D = \text{diag}([1 \ 0])$. Then, again $J^{[2]} = (1 - x_{i_1}^2) - N\kappa$ and thus, complete synchronisation is guaranteed if $\kappa > \frac{1}{N}$. However, when implementing the condition of Theorem 5.2.3 computationally in SOSTOOLS, we obtain no solution for polynomial entries to matrix $P(x) > 0$ up to order twelve. Thus, by applying Theorem 5.6.3, we can guarantee synchronisation for this case if $\kappa > \frac{1}{N}$, although we could not do so before.

Coupled biological oscillator

Consider a network of coupled identical biological oscillators:

$$\begin{aligned}\dot{x}_{i_1} &= \frac{10}{1 + x_{i_3}} - 0.2x_{i_1}, \\ \dot{x}_{i_2} &= 2x_{i_1} - 0.2x_{i_2}, \\ \dot{x}_{i_3} &= 0.2x_{i_2} - \frac{10x_{i_3}}{1 + x_{i_3}} - ex_{i_3},\end{aligned}\tag{5.69}$$

with coupling constant κ , all-to-all coupling and $D = \text{diag}([1 \ 0 \ 0])$. Numerics indicate that complete synchronisation occurs for $\kappa \geq 0.0005$. Figure 5.16 shows the behaviour of two coupled oscillators.

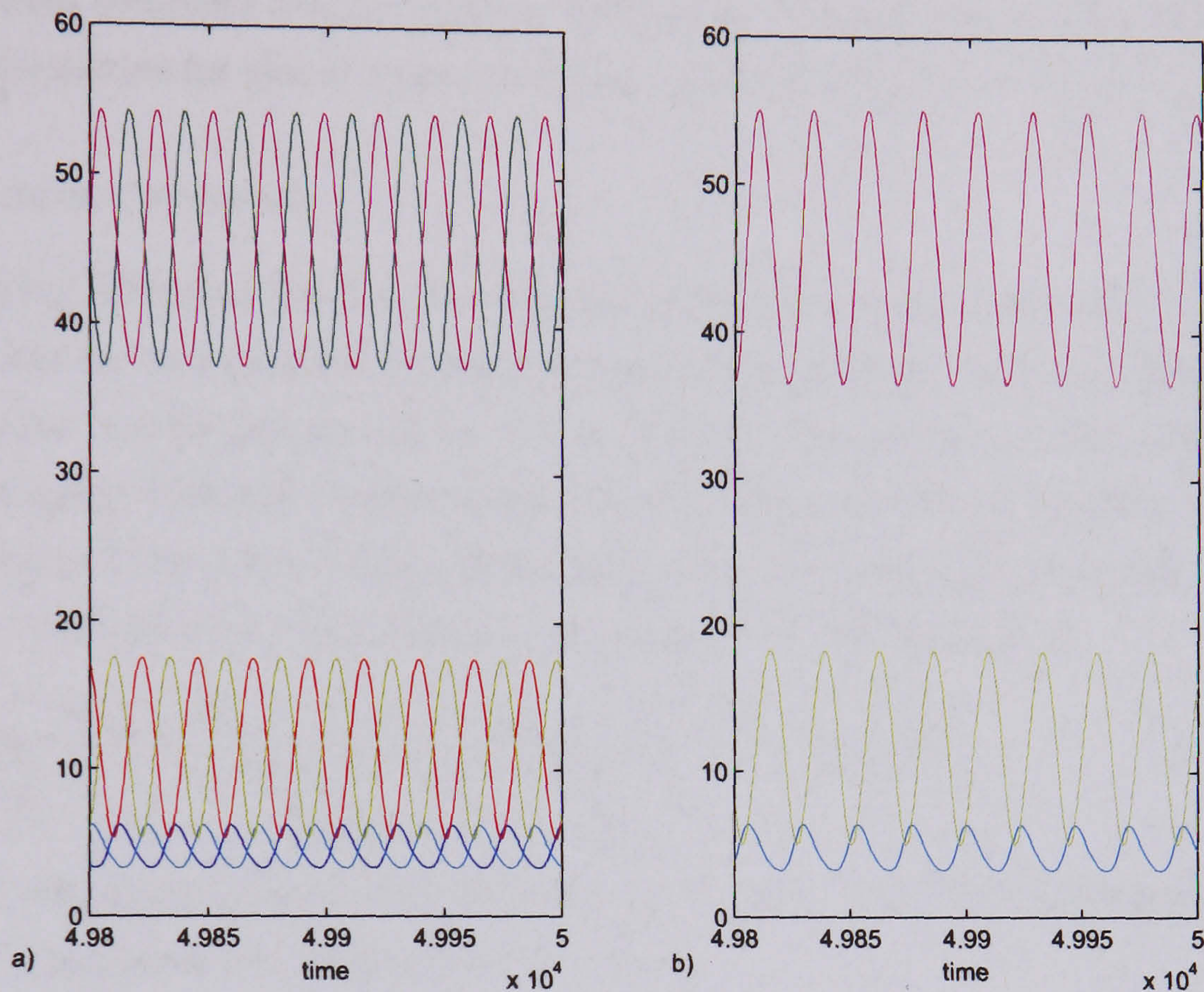


Figure 5.16: **Two coupled identical biological oscillators.** We consider the following initial conditions: $[94.424 \ 83.856 \ 25.843 \ 4.29 \ 0.589 \ 57.442]$. (a) For $\kappa = 0.0004$, we do not observe complete synchronisation. (b) For $\kappa = 0.0005$, we observe complete synchronisation.

Using YALMIP to search for a constant matrix P and constant κ such that the condition of Theorem 5.2.3 is fulfilled, we find that complete synchronisation is guaranteed for $\kappa N = 21.9$ if $e = 0.005$. Note that if $e = 0$, Theorem 5.2.3 fails us, because a κ such that (5.23) holds cannot exist, as at $x_{i_3} = \infty$ the Jacobian becomes singular.

Let J correspond to the Jacobian of (5.69). Then, the second additive compound of $J - N\kappa D$ is:

$$\begin{bmatrix} -0.4 - N\kappa & 0 & \frac{10}{(1+x_{i_3})^2} \\ 0.2 & -0.2 - N\kappa - \frac{10}{(1+x_{i_3})^2} - e & 0 \\ 0 & 2 & -0.2 - \frac{10}{(1+x_{i_3})^2} - e \end{bmatrix}.$$

Using YALMIP to search for a constant matrix $P > 0$ and constant $\kappa > 0$ such that (5.66) holds, we find that complete synchronisation occurs for $\kappa N = 0.195$ when $e = 0.005$ and $\kappa N = 0.202$ when $e = 0$. Thus, in the first case, we have lowered the value of κ that guarantees complete synchronisation more than 100-fold; and in the second, we have provided a guarantee for global complete synchronisation which we could not obtain before.

Coupled Lorenz systems

When applying Theorem 5.6.3 to the Lorenz system discussed perviously in this thesis, we obtain that for two coupled identical systems with all-to-all coupling, global complete synchronisation can be guaranteed for $\kappa \geq \kappa^* = 55.8$. The following table summarises our results for coupled identical Lorenz systems and it also provides an excellent opportunity to display some of the achievements of the research work presented this thesis (considering that, so far, only the first result could be obtained from the literature):

	reference [34]	Theorem 5.2.3	Theorem 5.6.3	numerics
κ^*	525	222.6	55.8	4

Table 5.4: Comparison between the different approaches to obtain the minimal value of κ ($= \kappa^*$) that guarantees complete synchronisation.

In summary, we could improve the result from the literature nearly ten-fold and obtain now a value of κ^* which is less than fourteen times larger than the value we observe in numerical trials.

5.7 Conclusion

In Section 5.1, we have presented results that provide conditions which guarantee that a periodic input to a biological system will create a response with the same period. We illustrated our result with applications to a gene regulatory system that we sought to manipulate, and to the heart driven by an external pacemaker. In Section 5.2, we have provided a sufficient condition for global complete synchronisation. These certificates are hard to obtain. Using the methods presented in Chapter 3, we have shown how they can be obtain computationally and how this can improve the result even for cases for which certificates were obtained analytically. We could minimise the value of the coupling strength,

κ , by searching for a matrix $P > 0$ that provides optimal κ as opposed to using a fixed P . For example, in the literature, one finds $P = I$, which does not necessarily provides the lowest value of κ (for instance, see reference [34]). We could improve results on κ also by considering nonlinear bounds (instead of only linear) which we implemented in SOSTOOLS. In section 5.4, we presented analytical results that guarantee that systems with periodic behaviour will all frequency synchronise when coupled one to each other. A key aspect is that we considered nonidentical oscillators, for which only few analytical results exist in the literature. We illustrated our results with applications to systems from biology and biochemistry. For example, these results could aid the synthetic biologist in the design of genetic circuits. The result of Section 5.1 allows to design a circuit that will entrain to external periodic inputs. The results of Section 5.2 and Section 5.4 indicate when cells that express a circuit that leads to periodic behaviour and are coupled through an interaction network will all synchronise. In Section 5.6.1, we provided conditions for the global complete synchronisation of discrete-time systems. In Section 5.6.2, we provided novel results that guarantee complete synchronisation and can also be implemented computationally. The required condition on the system are more relaxed and thus, lead to lower values of κ that guarantee synchronisation. For instance, in one example we could improve results 100-fold. Moreover, we also obtained conditions for global complete synchronisation in cases for which other methods failed. The subject-matter of the last section can be further explored and is considered a fruitful area for future research.

Finally, we would like to note that in the literature (for example, see [36,93]), one also finds a coupling scheme of the following form:

$$\begin{aligned}\dot{x} &= f(x) + v\kappa e^T(I_{Nn} \otimes D) \\ \dot{v} &= e^T(I_{Nn} \otimes D)x, \quad x \in \mathbb{R}^{Nn}, v \in \mathbb{R}.\end{aligned}$$

It is called *mean-field coupling*; here, v denotes the mean field. Note that none of the results in this chapter can be applied in this case as the coupling term $v\kappa e^T(I_{Nn} \otimes D)$ disappears, when one considers the difference equation $x_i - x_j$. However, numerics show that coupling of this kind is considerably less robust than the coupling configuration assumed in this thesis; particularly, they show that for mean-field coupling, whether coupled nonidentical oscillators synchronise depends greatly on the range of the parameter mismatch. Larger ranges are void of synchronisation. It is debatable, whether mean-field coupling constitutes a more realistic assumption for system modelling. However, from the point of view of system synthesis it is clearly less practical.

Chapter 6

Conclusions

6.1 Summary

In this thesis, we have extended Martin Feinberg's CRNT, a mathematical analysis framework for chemical reaction networks that does not require knowledge about parameter values (reaction rates). For instance, in Chapter 2, we have considered chemical reaction networks in crowded environments such as the cell. Therefore, their kinetics do not necessarily obey the law of mass action, which assumes that reactions take place at constant temperature in a homogenous and well mixed solution. We have provided a theorem based solely on structural properties of the network that guarantees uniqueness and local asymptotic stability of a positive equilibrium point. Thereafter, we have showed that the solutions of a dynamical system that represents a chemical reaction network that is weakly reversible (that is, has a specific connectivity structure) are bounded. Hence, by checking structural properties of the graph of the reaction network, this result provides a qualitative criterion, which is completely independent of reaction rate values and the deficiency of the system. Moreover, the result can also be used to characterise certain bifurcations from stationary to oscillatory (periodic, quasi-periodic or chaotic) behaviour as exemplified in Section 2.4.1.

In Chapter 4, we have provided a technique to obtain invariant sets of dynamical systems. These are relevant sets as they trap the dynamics of the system if they include the initial condition. This implies that we can restrict our attention to an invariant set when analysing the system if the set includes the initial conditions. We have also provided a practical means, based on results by Peter Giesl, to prove the existence of exponentially

stable periodic solutions of polynomial dynamical systems. We have then applied the method to the van der Pol system.

In Chapter 5, we have first presented results that provide conditions which guarantee that a periodic input to a biological system will create a response with the same period. We have shown how these results might be used in the design of medical devices and medication. First, we have sought to manipulate a gene regulatory system. It has been our goal that it should react to medication with the same frequency as the intake. We have been able to specify the strength of the medication in order to achieve this and the reaction rates that should be targeted to guarantee efficiency. Another application of our result is how to determine the strength of an external pacemaker, which drives the heart, that guarantees entrainment and absence of dysrhythmia. The other major results of the chapter are:

- We have reformulated known results on conditions that guarantee complete synchronisation of coupled identical oscillators in order to make them computationally implementable. To this end, we have taken advantage of recent computational developments in semidefinite programming. Thus, we have been able to minimise the coupling strength that guarantees complete synchronisation.
- We have extended these results to frequency synchronisation. We have provided a novel condition that guarantees that coupled nonidentical oscillators will frequency synchronise and showed how to implement this condition computationally. A key aspect is that we have considered nonidentical oscillators, for which only few analytical results exist in the literature.
- We have provided novel results for all-to-all coupling, based on the Bendixson's Criterion for higher dimensional dynamical systems, that guarantee complete synchronisation and can also be implemented computationally. The required conditions on the system are more relaxed and thus, can lead to lower values of the coupling strength that guarantees complete synchronisation and also to certificates for global complete synchronisation in cases for which other methods failed.

We have applied our results to models of coupled van der Pol oscillators representing individual heart cells and of coupled Repressilators. Synchrony in the heart is thought to be essential to avoid some life threatening conditions. The Repressilator is an artificially

designed biological oscillator in *E. coli*. It consists of three genes, which synthesise proteins that inhibit the transcription of each other in a cyclic way. It is used to shed light into the behaviour of more complex naturally occurring genetic oscillatory circuits. Synchronised behaviour in cultures of cells expressing the Repressilator circuit and that can interact through quorum sensing have not been observed so far. We have shown mathematically how to obtain the coupling strength, which is related to the density of the outer medium, that guarantees complete and frequency synchronisation. Finally, what unifies the work presented in Chapter 2 and Chapter 5 is that in both we have provided means to identify robustness of certain qualitative behaviour of a biological system to changes in parameters.

6.2 Discussion and future research

Martin Feinberg's CRNT requires weak reversibility of a chemical reaction network to guarantee existence of a unique positive equilibrium point for systems of deficiency zero or one and stability for systems of deficiency zero. Weak reversibility is also required in the novel results presented in Chapter 2 in order to guarantee boundedness of solution trajectories independently of the deficiency. A fruitful area of research would be to investigate whether other, potentially less strict, graph-theoretical properties can provide the same or similar results.

In the examples presented in Chapter 2, we have observed only periodic behaviour. Moreover, when we have introduced migration terms to the Lotka-Volterra model (Section 2.4) and thus, made the corresponding chemical reaction network weakly reversible previously nonperiodic behaviour of the system became periodic. Therefore, an interesting question is whether weak reversibility of a chemical reaction network excludes nonperiodic behaviour.

We believe that there is great potential for several key extensions of the work presented in this thesis:

- The results presented in Section 5.6.2 provide a promising start for further research into conditions for synchronisation of coupled oscillators based on the Bendixson Criterion for systems of order ≥ 2 . Particularly, we have considered a all-to-all coupling only to obtain conditions that guarantee global complete synchronisation of coupled identical dynamical system. Moreover, a theorem that provides conditions

that guarantee the entrainment of a dynamical system to a periodic external drive is missing (and for that matter, conditions that guarantee frequency synchronisation of coupled nonidentical oscillators).

- To obtain conditions that guarantee global complete synchronisation of coupled identical dynamical system, we have considered symmetric coupling topologies given by matrix C only. A fruitful area of research would be to consider asymmetric zero row sum matrices (see for example [106]).
- In Section 5.4, we have provided conditions on the individual subsystems of the coupled system that guarantee frequency synchronisation. However, the result requires that the system possesses a periodic solution. Clearly, it would defeat the purpose of the work presented in this thesis, if one would have to analyse the whole system. However, it is possible that the existence of a periodic solution can be deduced from properties of the individual systems and the coupling topology alone. A promising venue to explore are theorems on bounds of the Hausdorff dimension of attracting sets [76–78, 107, 108].
- Until today the Markus-Yamabe conjecture (Conjecture 3.1.7) was not disproved for bounded polynomial systems [109]. Proving the conjecture for bounded polynomial systems would provide conditions that might lead to lower values of κ^* that guarantees synchronisation and might provide solutions to some of the problems mentioned above.
- Finally, it would be great to see the results of this work applied directly to biological systems by working closely with experimentalists. Payoffs would arise from potentially reduced costs and time in the development of devices that are designed to drive a biological system and of medications that are supposed to synchronised coupled biological oscillators, as the criteria provided in this thesis could provide guidelines (see Sections 5.1.1, 5.1.2, 5.3 and 5.6.1).

Appendix A

```
% system variables
syms v1 v2 x1 x2; vars=[v1;v2;x1;x2];

% declaring them as vectors of monomials
v=monomials([v1;v2],1); x=monomials([x1;x2],1);

% van der Pol equation
k=-1;
f1=x2;
f2=-(k+x1^2)*x2-x1;

f=monomials([f1;f2],1);

% the system's Jacobian
J=jacobian([f1;f2]);

% initiation
prog = sosprogram(vars);
```



```

% The symmetric matrix N (to be searched)
VEC1 = monomials([x1; x2],[0 2 4]);
[prog,N11] = sospolyvar(prog,VEC1,'wscoeff');
[prog,N12] = sospolyvar(prog,VEC1,'wscoeff');
[prog,N22] = sospolyvar(prog,VEC1,'wscoeff');
N=[N11 N12; N12 N22];
% and its directional derivative NN
NN11=[diff(N11,x1) diff(N11,x2)]*f;
NN12=[diff(N12,x1) diff(N12,x2)]*f;
NN22=[diff(N22,x1) diff(N22,x2)]*f;
NN=[NN11 NN12; NN12 NN22];

% condition N>0
prog=sosineq(prog, v'*(N-0.0001*eye(size(N)))*v);

%creating polynomial function with unknown coefficients
VEC2 = monomials([x1; x2],[0 2 4]); VEC3 = monomials([v1; v2],[2]);
[prog,alpha] = sospolyvar(prog,VEC2,'wscoeff');
[prog,p1] = sospolyvar(prog,VEC3,'wscoeff');
[prog,p2] = sospolyvar(prog,VEC3,'wscoeff');

% condition p1,p2>=0
prog=sosineq(prog,p1); prog=sosineq(prog,p2);

% boundaries of invariant set
% outer boundary
B0=-3.7+78.361*x1^2-11.679*x1*x2+...
% inner boundary
BI=-4-4.281*x1*x2+4.93*x1^2+2.213*x2^2...

```



```

% requiring that  $v'(J*N-1/2*NN)*v-\alpha*(v'*f*f'*v)<0$  in the invariant set
prog=sosineq(prog, v'*(1/2*NN-J*N)*v +alpha*(v'*f*f'*v)
            -p1*BI +p2*B0 -0.0001*v'*eye(size(N))*v);

% calling solver
[prog,info] = sossolve(prog);

% getting N
N11 = sosgetsol(prog,N11)
N12 = sosgetsol(prog,N12)
N22 = sosgetsol(prog,N22)

```


Appendix B

```
% declaring variables
zeta = sdpvar(1); P = sdpvar(3,3);

% system's jacobian, where zeta = 1/(1+x3)^2
kappa = 21.8; A = [-0.25-kappa 0 -10*zeta; 2 -0.2 0; 0 0.2 -10*zeta-0.005];

% setting requirements
R = set(P > 0.001) + set((A'*P+P*A) < 0) + set(0<= zeta <=1)
  + set(P*diag([1 0 0])+diag([1 0 0])*P >= 0) + set(uncertain(zeta));

% solving
[info] = solvesdp(R)

% getting P
P = double(P)
```


Bibliography

- [1] L. H. Hartwell, J. J. Hopfield, S. Leibler, and A. W. Murray. From molecular to modular cell biology. *Nature*, 402:C47–C52, 1999.
- [2] C. V. Rao, D. M. Wolf, and A. P. Arkin. Control, exploitation and tolerance of intracellular noise. *Nature*, 420:231–237, 2002.
- [3] D. A. Lauffenburger. Cell signaling pathways as control modules: Complexity for simplicity? *PNAS*, 97(10):5031–5033, 2000.
- [4] Y. Lazebnik. Can a biologist fix a radio? Or, what I learned while studying apoptosis. *Cancer Cell*, 2:179–182, 2002.
- [5] J. D. Murray. *Mathematical Biology*. Springer-Verlag, New York, 1990.
- [6] R. Badii and A. Politi. *Complexity: Hierarchical structures and scaling in physics*. Cambridge University Press, Cambridge, UK, 1999.
- [7] M. Barahona and L. M. Pecora. Synchronization in Small-World Systems. *Physical Review Letters*, 89(5):1–4, 2002.
- [8] J. E. Bailey. Complex biology with no parameters. *Nature Biotechnology*, 19:503–504, 2001.
- [9] M. Feinberg. Chemical reaction network structure and the stability of complex isothermal reactors—I. The deficiency zero and deficiency one theorems. *Chem. Eng. Sci.*, 42(10):2229–2268, 1987.
- [10] T. G. Buchman. The community of the self. *Nature*, 420:246–251, 2002.

- [11] R. Milo, S. Shen-Orr, S. Itzkovitz, N. Kashtan, D. Chklovskii, and U. Alon. Network Motifs: Simple Buildings Blocks of Complex Networks. *Science*, 298:824–827, 2002.
- [12] U. Alon. Biological Networks: The Tinkerer as an Engineer. *Science*, 301:1866–1867, 2003.
- [13] J. Stelling. Mathematical models in microbial systems biology. *Current Opinion in Microbiology*, 7:513–518, 2004.
- [14] M. Feinberg. Lectures on chemical reaction networks. Mathematics Research Centre, University of Wisconsin, 1979.
- [15] B. N. Kholodenko and H. V. Westerhoff. The macroworld versus the microworld of biochemical regulation and control. *Trends in Biochemical Sciences*, 20(2):52–54, 1995.
- [16] J. Gunawardena. Chemical reaction network theory for in-silico biologists. Bauer Center for Genomics Research, Harvard University, Cambridge, MA 02138, USA, 2003.
- [17] G. Craciun, Y. Tang, and M. Feinberg. Understanding bistability in complex enzyme-driven reaction networks. *PNAS*, 103(23):8697–8702, 2006.
- [18] S. Schnell and T. E. Turner. Reaction kinetics in intracellular environments with macromolecular crowding: simulations and rate laws. *Progress in Biophysics & Molecular Biology*, 85:235–260, 2004.
- [19] H. R. Horton, L. A. Moran, R. S. Ochs, J. D. Rawn, and K. G. Scrimgeour. *Principles of Biochemistry*. Prentice-Hall, Upper Saddle River, NJ 07458, 2002.
- [20] S. H. Strogatz. *Sync: rhythms of nature, rhythms of ourselves*. Allen Lane, London, UK, 2003.
- [21] A. Pikovsky, M. Rosenblum, and J. Kurths. *Synchronization: A universal concept in nonlinear sciences*. Cambridge University Press, Cambridge, UK, 2003.
- [22] P. Mohanty. Nano-oscillators get it together. *Nature*, 437:325–326, 2005.
- [23] I. M. Beeton. *The Book of Household Management*. 1861.

- [24] www.euclock.org.
- [25] S. M. Reppert and D. R. Weaver. Coordination of circadian timing in mammals. *Nature*, 418:935–941, 2002.
- [26] C. H. Johnson. As time glows by in bacteria. *Nature*, 430:23–24, 2004.
- [27] D. Scanlan. Cyanobacteria: ecology, niche adaptation and genomics. *Microbiology Today*, 28:128–130, 2001.
- [28] Y. Ouyang, C. R. Andersson, T. Kondo, S. S. Golden, and C. H. Johnson. Resonating circadian clocks enhance fitness in cyanobacteria. *PNAS*, 95:8660–8664, 1998.
- [29] B. E. H. van Oort, N. J. C. Tyler, M. P. Gerkema, L. Folkow, A. S. Blix, and K.-A. Stokkan. Circadian organization in reindeer. *Nature*, 438:1095–1096, 2005.
- [30] A. M. dos Santos, S. R. Lopes, and R. L. Viana. Rhythm synchronization and chaotic modulation of coupled Van der Pol oscillators in a model for the heartbeat. *Physica A*, 338:335–355, 2004.
- [31] L. Glass, M. R. Guevara, A. Shrier, and R. Perez. Bifurcation and chaos in a periodically stimulated cardiac oscillator. *Physica D*, 7:89–101, 1983.
- [32] S. H. Strogatz. From Kuramoto to Crawford: exploring the onset of synchronization in populations of coupled oscillators. *Physica D*, 143:1–20, 2000.
- [33] L. M. Pecora and T. L. Carroll. Master Stability Functions for Synchronized Coupled Systems. *Physical Review Letters*, 80:2109–2112, 1998.
- [34] V. N. Belykh, I. V. Belykh, and M. Hasler. Connection graph stability method for synchronized coupled chaotic systems. *Physica D*, 195:159–187, 2004.
- [35] C. W. Wu. Synchronization in networks of nonlinear dynamical systems coupled via a directed graph. *Nonlinearity*, 18:1057–1064, 2005.
- [36] D. Gonze, S. Bernard, C. Waltermann, A. Kramer, and H. Herzog. Spontaneous Synchronization of Coupled Circadian Oscillators. *Biophysical Journal*, 89:120–129, 2005.

- [37] M. B. Elowitz and S. Leibler. A synthetic oscillatory network of transcriptional regulators. *Nature*, 403(20):335–338, 2000.
- [38] B. C. Goodwin. Oscillatory behavior in enzymatic control processes. *Advances in Enzyme Regulation*, 3:425–438, 1965.
- [39] P. Ruoff and L. Rensing. The Temperature-Compensated Goodwin Model Simulates Many Circadian Clock Properties. *J. Theor. Biol.*, 179:275–285, 1996.
- [40] P. Ruoff, M. Vinsjevik, C. Monnerjahn, and L. Rensing. The Goodwin Oscillator: On the Importance of Degradation Reactions in the Circadian Clock. *Journal of Biological Rhythms*, 14(6):469–479, 1999.
- [41] P. Ruoff, M. Vinsjevik, C. Monnerjahn, and L. Rensing. The Goodwin Model: Simulating the Effect of Light Pulses on the Circadian Sporulation Rhythm of *Neurospora Crassa*. *J. Theor. Biol.*, 209:29–42, 2001.
- [42] P. Giesl. Unbounded Basins of Attraction of Limit Cycles. *Acta Math. Univ. Comenianae*, LXXII(1):81–110, 2003.
- [43] P. Giesl. On the Basin of Attraction of Limit Cycles in Periodic Differential Equations. *Journal for Analysis and its Applications*, 23(3):547–576, 2004.
- [44] P. Giesl. Necessary conditions for a limit cycle and its basin of attraction. *Nonlinear Analysis*, 56:643–677, 2004.
- [45] W. Lohmiller and J.-J. E. Slotine. On contraction analysis for nonlinear systems. *Automatica*, 34(6):683–696, 1998.
- [46] J. M. Guberman. *Mass Action Networks and the Deficiency Zero Theorem*. BSc thesis, Harvard University, 2003.
- [47] K. Gatermann and B. Huber. A Family of Sparse Polynomial Systems Arising in Chemical Reaction Systems. *Journal Symbolic Computation*, 33:275–305, 2002.
- [48] R. Abraham, J. E. Marsden, and T. Ratiu. *Manifolds, tensor analysis, and applications*. Addison-Wesley, London, UK, 1983.

- [49] F. Harary. A graph theoretic approach to matrix inversion by partitioning. *Numerische Mathematik*, 4:128–135, 1962.
- [50] H. K. Khalil. *Nonlinear Systems*. Prentice-Hall, Upper Saddle River, New Jersey, 3rd edition, 2000.
- [51] J. M. Buick. *Lattice Boltzmann Methods in Interfacial Wave Modelling*. PhD thesis, The University of Edinburgh, 1997.
- [52] D. Shear. An Analog of the Boltzmann H-Theorem (a Liapunov Function) for Systems of Coupled Chemical Reactions. *J. Theoret. Biol.*, 16:212–228, 1967.
- [53] F. Horn and R. Jackson. General mass action kinetics. *Arch. Rational Mech. Anal.*, 47:81–116, 1972.
- [54] E. Batchelor and M. Goulian. Robustness and the cycle of phosphorylation and dephosphorylation in a two-component regulatory system. *PNAS*, 100(2):691–696, 2003.
- [55] D. Erle. Nonoscillation in closed reversible chemical systems. *Journal of Mathematical Chemistry*, 27(4):293–302, 2000.
- [56] M. Feinberg. The Existence and Uniqueness of Steady States for a Class of Chemical Reaction Networks. *Arch. Rational Mech. Anal.*, 132:311–370, 1995.
- [57] R. Thomas and M. Kaufman. Multistationarity, the basis of cell differentiation and memory. I. Structural conditions of multistationarity and other nontrivial behavior. *Chaos*, 11(1):170–179, 2001.
- [58] C. Soulé. Graphic requirements for multistationarity. *ComplexUs*, 1:123–133, 2003.
- [59] R. Thomas. Circular causality. *IEE Proc. Syst. Biol.*, 153(4):140–153, 2006.
- [60] M. A. Savageau. Development of fractal kinetic theory for enzyme-catalysed reactions and implications for the design of biochemical pathways. *BioSystems*, 47:9–36, 1998.
- [61] T. W. McKeithan. Kinetic proofreading in T-cell receptor signal transduction. *PNAS*, 92:5042–5046, 1995.

- [62] E. D. Sontag. Structure and Stability of Certain Chemical Networks and Applications to the Kinetic Proofreading Model of T-Cell Receptor Signal Transduction. *IEEE Transactions on Automatic Control*, 46(7):1028–1047, 2001.
- [63] M. C. F. Chaves. *Observer Design for a Class of Nonlinear Systems, with Applications to Biochemical Networks*. PhD thesis, Rutgers, The State University of New Jersey, 2003.
- [64] I. D. Chueshov. *Introduction to the Theory of Infinite-Dimensional Dissipative Systems*. ACTA Scientific Publishing House, Kharkiv, Ukraine, 2002.
- [65] F. Horn. Necessary and sufficient conditions for complex balancing in chemical kinetics. *Archive for Rational Mechanics and Analysis*, 49(3):172–186, 1972.
- [66] M. Feinberg. Complex Balancing in General Kinetic Systems. *Archive for Rational Mechanics and Analysis*, 49(3):187–194, 1972.
- [67] A. Berman and R. J. Plemmons. *Nonnegative matrices in the mathematical sciences*. Academic Press, London, UK, 1979.
- [68] F. M. C. Vieira and P. M. Bisch. Oscillations and multiple steady states in active membrane transport models. *Eur. Biophys. J.*, 23:277–287, 1994.
- [69] R. M. May and W. J. Leonard. Nonlinear Aspects of Competition Between Three Species. *SIAM Journal on Applied Mathematics*, 29(2):243–253, 1975.
- [70] D. C. Lewis. Metric properties of differential equations. *American Journal of Mathematics*, 71:294–312, 1949.
- [71] J. Jouffroy. Some ancestors of contraction analysis. *Proc. IEEE Conf. Dec. Contr.*, 2005.
- [72] B. Stenström. Dynamical systems with a certain local contraction property. *Math. Scand.*, 11:151–155, 1962.
- [73] L. Markus and H. Yamabe. Global stability criteria for differential systems. *Osaka Math. J.*, 12:305–317, 1960.

- [74] J. P. La Salle. The Stability of Dynamical Systems. *CBMS-NSF Regional Conference Series in Applied Mathematics*, 25:., 1976.
- [75] A. Cima, A. van den Essen, A. Gasull, E. Hubbers, and F. Mañosas. A Polynomial Counterexample to the MarkusYamabe Conjecture. *Advances in Mathematics*, 131(2):453–457, 1997.
- [76] R. A. Smith. Some applications of Hausdorff dimension inequalities for ordinary differential equations. *Proc. Roy. Soc. Edinburgh Sect. A*, 104:235–259, 1986.
- [77] Y. Li and J. S. Muldowney. On Bendixson’s criterion. *Journal of Differential Equations*, 106:27–93, 1993.
- [78] J. S. Muldowney. Compound matrices and ordinary differential equations. *Rocky Mountain J. Math.*, 120:857–872, 1990.
- [79] M. Y. Li and J. S. Muldowney. A Geometric Approach to Global-Stability Problems. *SIAM J. Math. Anal.*, 27(4):1070–1083, 1996.
- [80] L. Vandenberghe and S. Boyd. Semidefinite programming. *SIAM Review*, 38(1):49–95, 1996.
- [81] S. Boyd and L. Vandenberghe. *Convex Optimization*. Cambridge University Press, Cambridge, UK, 2004.
- [82] P. A. Parrilo. Semidefinite programming relaxations for semialgebraic problems. *Math. Program., Ser. B*, 96:293–320, 2003.
- [83] J. Löfberg. YALMIP: A Toolbox for Modeling and Optimization in MATLAB. In *Proceedings of the CACSD Conference*, Taipei, Taiwan, 2004. Available from <http://control.ee.ethz.ch/~joloef/yalmip.php>.
- [84] J. F. Sturm. Using SeDuMi 1.02, a MATLAB toolbox for optimization over symmetric cones. *Optimization Methods and Software*, 11-12:625–653, 1999. Available at <http://fewcal.kub.nl/sturm/software/sedumi.html>.
- [85] G. Blekherman. There are significantly more nonnegative polynomials than sums of squares. *arXiv:math/0309130v1*, 2003.

- [86] S. Prajna, A. Papachristodoulou, and P. A. Parrilo. SOSTOOLS: Sum of squares optimization toolbox for MATLAB. Available from <http://www.cds.caltech.edu/sostools> and <http://www.aut.ee.ethz.ch/~parrilo/sostools>. 2002.
- [87] A. Papachristodoulou. *Scalable Analysis of Nonlinear Systems Using Convex Optimization*. PhD thesis, California Institute of Technology, Pasadena, California, 2005.
- [88] E. N. Lorenz. Deterministic Nonperiodic Flow. *Journal of the Atmospheric Sciences*, 20:130–141, 1963.
- [89] R. A. FitzHugh. Impulses and physiological states in theoretical models of nerve membrane. *Biophys. J.*, 1:445–466, 1961.
- [90] P. G. Drazin. *Nonlinear Systems*. Cambridge University Press, Cambridge, United Kingdom, 1994.
- [91] H. R. Wilson. Simplified Dynamics of Human and Mammalian Neocortical Neurons. *J. theor. Biol.*, 200:375–388, 1999.
- [92] E. M. Aylward, P. A. Parrilo, and J.-J. E. Slotine. Stability and Robustness Analysis of Nonlinear Systems via Contraction Metrics and SOS Programming. *arXiv:math/0603313v1*, 2006.
- [93] J. Garcia-Ojalvo, M. B. Elowitz, and S. H. Strogatz. Modeling a synthetic multicellular clock: Repressilators coupled by quorum sensing. *PNAS*, 101(30):10955–10960, 2004.
- [94] Jay Dunlap. An End in the Beginning. *Science*, 280:1548–1549, 1998.
- [95] J. K. Hale. Diffusive Coupling, Dissipation, and Synchronization. *Journal of Dynamics and Differential Equations*, 9(1):1–52, 1997.
- [96] C. W. Wu. Synchronization in an array of chaotic systems coupled via a directed graph. *IEEE International Symposium on Circuits and Systems*, 6:6046–6049, 2005.
- [97] I. Belykh, V. Belykh, K. Nevidin, and M. Hasler. Persistent clusters in lattices of coupled nonidentical chaotic systems. *Chaos*, 13(1):165–178, 2003.

- [98] U. Miekkala. Graph properties for splitting with grounded laplacian matrices. *BIT*, 33:485–495, 1993.
- [99] A. Jadbabaie, N. Motee, and M. Barahona. On the stability of the kuramoto model of coupled nonlinear oscillators. *Proceeding of the 2004 American Control Conference*, pages 4296–4301, 2004.
- [100] H. S. Thurston. On the Characteristic Equations of Products of Square Matrices. *The American Mathematical Monthly*, 38(6), 1931.
- [101] D. Li, J. Lu, X. Wu, and G. Chen. Estimating the ultimate bound and positively invariant set for the Lorenz system and a unified chaotic system.
- [102] S. Müller, J. Hofbauer, L. Endler, C. Flamm, S. Widder, and P. Schuster. A generalized model of the repressilator. *J. Math. Biol.*, 53:905–937, 2006.
- [103] B. B. Kaufmann and A. v. Oudenaarden. Stochastic gene expression: from single molecules to the proteome. *Current opinion in genetics and development*, 17:107–112, 2007.
- [104] R. Brown and L. Kocarev. A unifying definition of synchronization for dynamical systems. *Chaos*, 10(2):344–349, 2000.
- [105] W. Wang and J.-J. E. Slotine. On partial contraction analysis for coupled nonlinear oscillators. *Biological Cybernetics*, 92:38–53, 2005.
- [106] I. Belykh, V. Belykh, and M. Hasler. Generalized connection graph method for synchronization in asymmetrical networks. *Physica D*, 224:42–51, 2006.
- [107] M. Y. Li and J. S. Muldowney. Lower Bounds for the Hausdorff Dimension of Attractors. *Journal of Dynamics and Differential Equations*, 7(3):457–469, 1995.
- [108] A. Yu. Pogromsky and H. Nijmeijer. New results for estimation of hausdorff dimension. In *IEEE International Symposium on Circuits and Systems*, Geneva, Switzerland, 2000.
- [109] G. Meisters. A biography of the Markus-Yamabe conjecture. *A talk given at the conference: Aspects of Mathematics-Algebra, Geometry and Several Complex Variables*, The University of Hong Kong, 1996.